

DISSERTATION

DEVELOPMENT OF AN ASYMMETRIC NHC-CATALYZED CASCADE REACTION AND  
STUDIES TOWARDS THE ASYMMETRIC AMINOMETHYLATION OF ENALS

Submitted by

Kerem Ozboya

Department of Chemistry

In partial fulfillment of the requirements

For the Degree of Doctor of Philosophy

Colorado State University

Fort Collins, Colorado

Spring 2015

Doctoral Committee:

Advisor: Tomislav Rovis

Charles Henry  
Andrew McNally  
Alan Kennan  
Julia Inamine

Copyright by Kerem Ozboya 2015

All Rights Reserved

## ABSTRACT

### DEVELOPMENT OF AN ASYMMETRIC NHC-CATALYZED CASCADE REACTION AND STUDIES TOWARDS THE ASYMMETRIC AMINOMETHYLATION OF ENALS

A cascade reaction is developed to form complex cyclopentanones using an asymmetric Michael/Benzoin sequence. This reaction employs simple aliphatic aldehydes and ketoesters in conjunction with a chiral amine catalyst and a chiral NHC catalyst. Further investigation reveals a surprising interplay between these two catalysts. This relationship is manifested in a pseudo-dynamic kinetic resolution, which is responsible for the high diastereoselectivity observed.

Subsequent work details the discovery of the aminomethylation of enals using NHC catalysis. This reaction utilizes an iminium source as well as cinnamaldehyde derivatives to form gamma-amino butyrate derivatives. Rendering this reaction asymmetric has proven a challenge, despite extensive effort to resolve these issues. In the course of these studies, an unexpected NHC-catalyzed Morita-Baylis-Hillman reaction was observed. Optimal conditions for this reaction were established, proving access to useful amino-enals.

In an effort to design suitable catalysts for the asymmetric aminomethylation reaction, a strategy for the late-stage manipulation of NHC catalysts was developed. Key to this strategy is the 'protection' of the triazolium salt by reduction to the triazoline. An aryl C-Br bond is then exploited for cross-coupling reactions, building a small library of new catalysts. The triazolium salt is then recovered by oxidation with a trityl salt.

## ACKNOWLEDGEMENTS

The completion of my PhD took a tremendous amount of work, and it would not have been possible without the help of many people. First I thank my PI, Prof. Tomislav Rovis. Thank you for the opportunity to join your lab (even despite my GPA). I am also grateful for your patience, understanding, motivation, and support during my graduate career. I also thank my graduate committee for serving such important roles even with busy schedules of your own, especially Prof. Kennan and McNally who agreed to join my committee at the last minute.

My coworkers in the Rovis lab are possibly the most amazing people on the planet. Any success I have had at CSU is completely due to my coworkers, from their intellectual discussions to irrelevant revelry. I must thank Kevin Oberg and Todd Hyster for countless scientific discussions as well as for general support and inspiration. Several people helped to proofread this dissertation, and so I thank Kyle, Nick, Darrin, and Todd for their help. I am also lucky to have friends outside the Rovis group (Travis, Doug, Erin, Paul, Eric) as well as great friends back in California (Jeff, Thao, Terrence) who have been a tremendous source of support.

I must thank my previous manager from Roche, Dr. Stephen Lynch.

And of course I must thank my wonderful family. They have been incredibly supportive and patient during these last few years, and I am eternally thankful for their generosity. Thank you all.

## TABLE OF CONTENTS

ABSTRACT.....	ii
ACKNOWLEDGEMENTS.....	iii
CHAPTER 1: BACKGROUND OF <i>N</i> -HETEROCYCLIC CARBENE CATALYSIS.....	1
1.1 BENZOIN DISCOVERY.....	1
1.2 STETTER REACTION.....	2
1.3 BENZOIN REACTION.....	8
1.4 REDOX CHEMISTRY.....	10
CHAPTER 2: ASYMMETRIC MICHAEL/BENZOIN CASCADE FOR THE SYNTHESIS OF ENANTIOENRICHED CYCLOPENTANONES.....	14
2.1 INTRODUCTION TO CASCADE REACTIONS.....	14
2.2 REACTION DEVELOPMENT.....	19
2.3 SCOPE OF REACTION.....	25
2.4 MECHANISTIC INSIGHT.....	28
2.5 APPLICATIONS TOWARD THE SYNTHESIS OF NATURAL PRODUCTS.....	36
CHAPTER 3: ASYMMETRIC AMINOMETHYLATION OF ENALS BY NHC CATALYSIS.....	40
3.1 HOMOENOLATE BACKGROUND.....	40
3.2 REACTION OPTIMIZATION.....	44
3.3 ASYMMETRIC HOMOENOLATE/MANNICH REACTION.....	47
3.4 NHC CATALYZED AZA-MORITA-BAYLIS-HILMAN.....	53
CHAPTER 4: STRATEGY FOR THE LATE-STAGE MANIPULATION OF TRIAZOLIUM-BASED CATALYSTS.....	58

4.1 SIGNIFICANCE OF CATALYST DESIGN .....	58
4.2 MODIFICATION OF AMINOINDANOL SCAFFOLD .....	61
4.3 OXIDATION BY TRITYL SALTS TO FORM TRIAZOLIUMS .....	65
4.4 CROSS-COUPLING AS STRATEGY FOR LATE-STAGE MODIFICATION .....	68
REFERENCES .....	76
APPENDIX 1: EXPERIMENTAL AND SPECTRAL DATA FOR CHAPTER 2 .....	81
APPENDIX 2: X-RAY CRYSTAL STRUCTURE DATA FOR CHAPTER 2 .....	123
APPENDIX 3: EXPERIMENTAL AND SPECTRAL DATA FOR CHAPTER 3 .....	131
APPENDIX 4: EXPERIMENTAL AND SPECTRAL DATA FOR CHAPTER 4 .....	165
APPENDIX 5: X-RAY CRYSTALLOGRAPHY DATA FOR CHAPTER 4 .....	218
APPENDIX 6: TRENDS IN REACTION SELECTIVITY BETWEEN HOMOENOLATE VS AZA-MORITA-BAYLISS-HILMAN REACTIVITY .....	228

## CHAPTER 1

### BACKGROUND OF *N*-HETEROCYCLIC CARBENE CATALYSIS

#### 1.1 *Benzoin Discovery*

In the 1830's, Justus von Liebig and Friedrich Wöhler undertook studies of the properties of bitter almond oil.<sup>1</sup> The oil was extracted from bitter wild almonds, which are the highly poisonous progenitors of the modern domesticated almond. During the course of their studies, they noticed formation of a new compound: benzoin (**5**, Figure 1.1). The source of this phenomenon is due to one of the key constituents of bitter almond oil: amygdalin (**1**). This compound easily fragments to release sugars (**4**), benzaldehyde (**2**), and cyanide (**3**). Liebig's student, Nikolay Zinin, further studied this unusual reaction. Zinin proved that the combination of benzaldehyde and only a catalytic amount of cyanide is needed for this reaction to proceed.

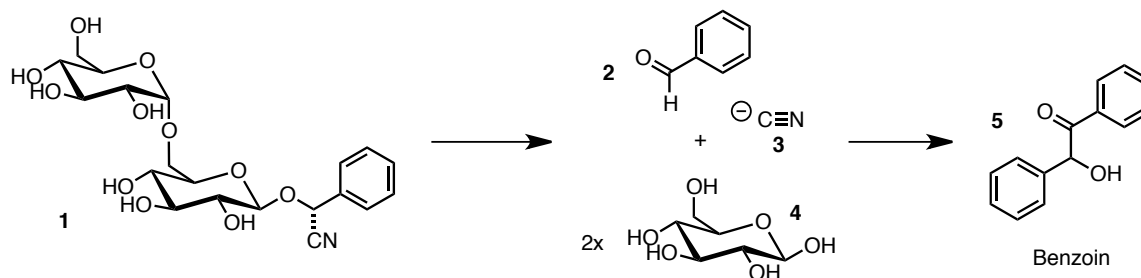


**Figure 1.1**

In 1943, Ugai and coworkers discovered that this transformation could be catalyzed by a thiazolium catalyst derived from thiamine.<sup>2</sup> Shortly after, Breslow proposed a mechanism for this reaction.<sup>3</sup> This was modeled after work published by Lapworth in 1903.<sup>4</sup> The first step is deprotonation of the thiazolium pre-catalyst to form

stabilized N-heterocyclic carbene **II** (Figure 1.2). The catalytic cycle begins with the nucleophilic addition of the carbene catalyst onto benzaldehyde to form intermediate **III**. Proton transfer leads to the formation of the en-diaminol **IV**, commonly referred to as the “Breslow Intermediate.” This intermediate then adds into a second equivalent of benzaldehyde. Proton transfer leads to intermediate **VI**, which then collapses to release benzoin **5** and the carbene catalyst **II**.

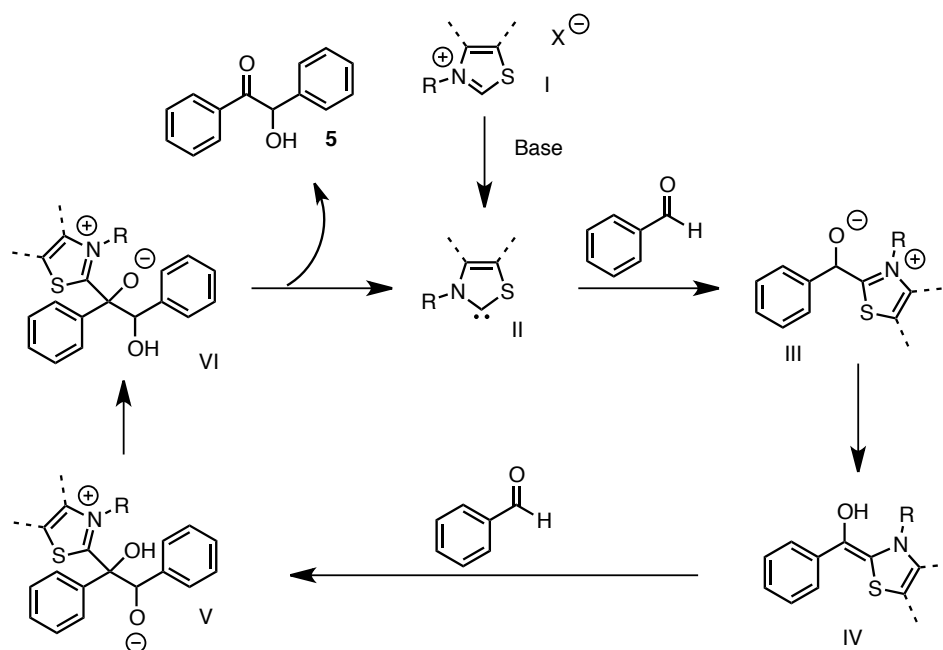
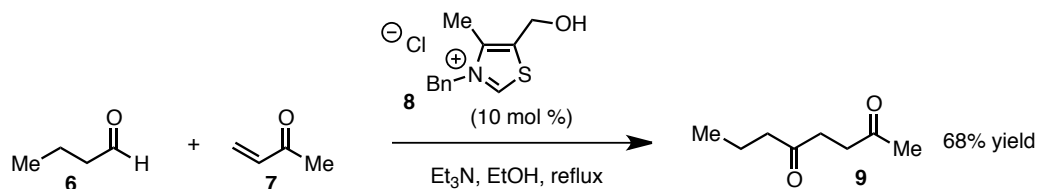


**Figure 1.2**

### 1.2 Stetter Reaction

The most intriguing feature of the benzoin reaction is the catalytic formation of the acyl anion equivalent. Formation of a transient nucleophile from an electrophilic species and its associated reactions is often termed *Umpolung*.<sup>5</sup> The next question was whether this nucleophilic intermediate can add to other electrophiles. One of the first answers to this question was work done by Stetter. In 1973, he reported the coupling of

an aldehyde and an enone to yield a 1,4-dicarbonyl compound using either cyanide or a thiazolium-based carbene as a catalyst (Scheme 1.1).<sup>6</sup> This serves as a solution in the synthesis of this challenging motif.

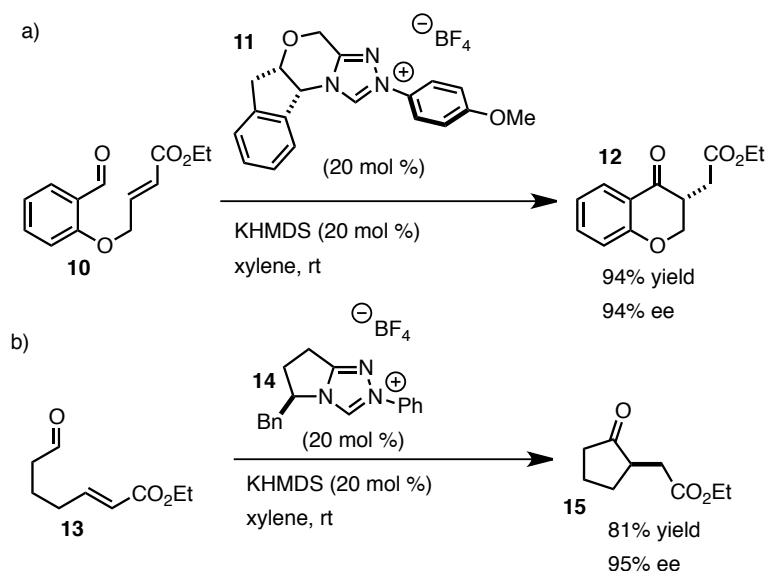


### Scheme 1.1

A key difference between the benzoin reaction and the Stetter reaction is that the former is occasionally reversible while the latter is not.<sup>7</sup> In addition, several groups observe that the benzoin product is often formed faster than the Stetter product, but the dimer is eventually consumed while the ratio of Stetter product increases.<sup>8</sup> In certain instances, it is possible to use a benzoin product as a source of the acyl-anion precursor.<sup>9</sup>

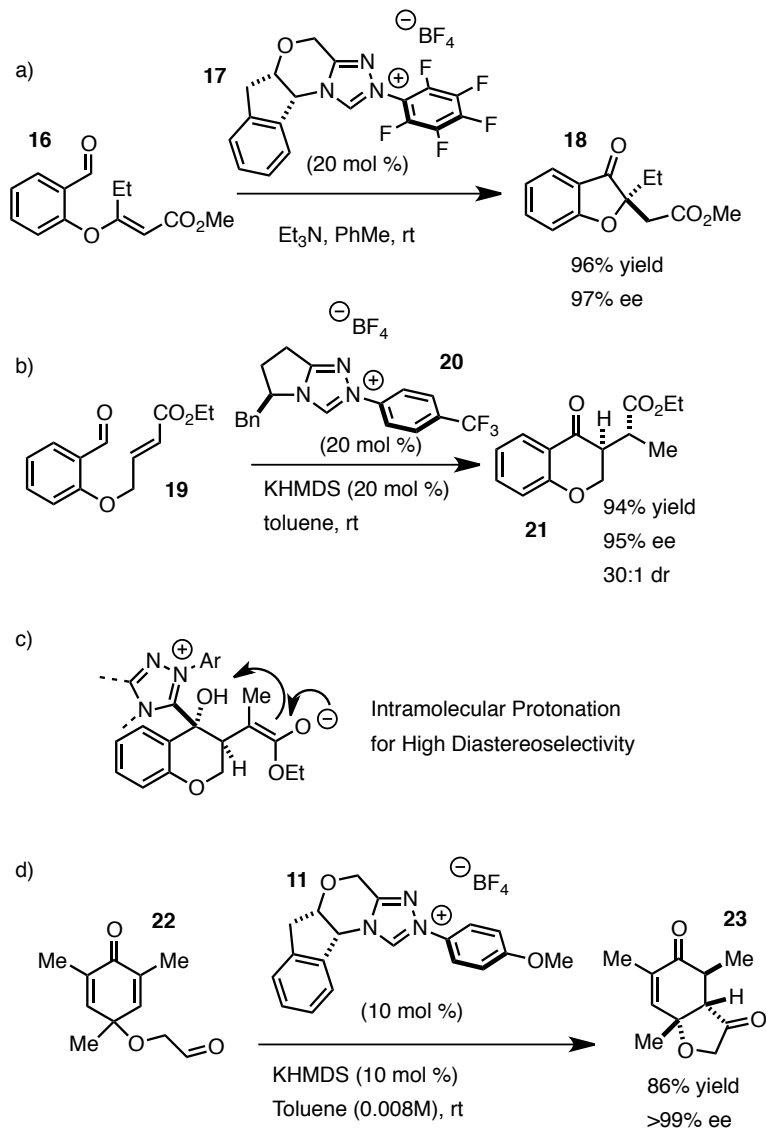
Besides enones, Stetter showed that enoates, acrylonitriles, and several other Michael acceptors are competent in the reaction.<sup>10</sup> However, he also described many limitations. Substitution at the  $\alpha$ -carbon seems to be well tolerated. In contrast, he reported only limited success with  $\beta$ -substituted Michael acceptors. The nature of the aldehyde is not as stringent, with aryl and aliphatic aldehydes shown to be suitable acyl-anion donors. It should be noted that the use of NHC catalysts often lead to milder conditions when compared to the cyanide based conditions.

The Rovis group has made a significant impact with the development of the asymmetric intramolecular Stetter reaction,<sup>11</sup> based on a substrate designed by Ciganek (Scheme 1.2a).<sup>12</sup> Key to the success of this reaction was the design of novel triazolium precatalyst **11**. Based on an aminoindanol developed at Merck,<sup>13</sup> this catalyst maintains a rigid backbone that proves excellent at inducing asymmetry. The chromanone product **12** is formed in both high yields and high enantioselectivity. This initial work was expanded to include aldehydes with aliphatic backbones as well (Scheme 1.2b). Triazolium precatalyst **14** based on phenylalanine is employed in this case.



### Scheme 1.2

In addition, higher substitution on the olefin is tolerated. With  $\beta$ -substitution, products that bear an enantioenriched quaternary carbon are formed (Scheme 1.3a).<sup>14</sup> These quaternary centers are difficult to form asymmetrically, so this provides

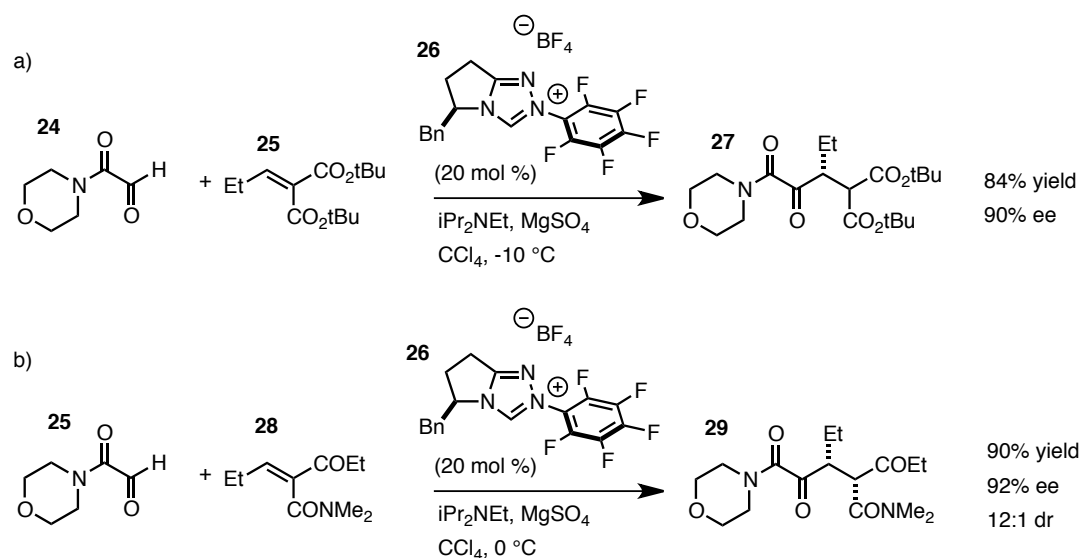


### Scheme 1.3

a convenient route to this system. Substitution at the  $\alpha$ -carbon is also tolerated (Scheme 1.3b). This motif allows formation of a second stereocenter, and this is formed in high diastereoselectivity.<sup>15</sup> This high selectivity can be explained by an intramolecular protonation event (Scheme 1.3c). This effectively translates chirality from the catalyst to the distant stereocenter. Similar strategies were used in the

desymmetrization of cyclohexadienones **22** (Scheme 1.3d).<sup>16</sup> This motif allows for the rapid construction of three contiguous stereocenters.

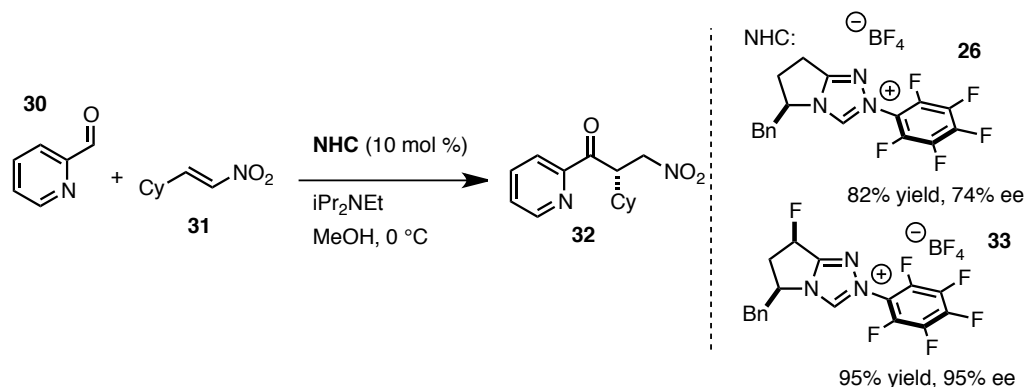
Enders and coworkers first reported an asymmetric intermolecular Stetter reaction with chalcones as substrates.<sup>17</sup> In the Rovis group, glyoxamides were pursued due to their success as donors as described by Stetter.<sup>18</sup> For the electrophile, alkylidene malonates were selected for their high reactivity (Scheme 1.4a). This reaction proved successful with the use of phenylalanine derived triazolium precatalyst **26**.<sup>19</sup> High yields and enantioselectivity are maintained with a diversity of alkyl-substituted malonates. This system was later extended to alkylidene ketoamides **28** (Scheme 1.4b).<sup>20</sup> As the use of tertiary amides inhibits epimerization, these products are formed in both high enantio- and diastereoselectivity.



## Scheme 1.4

Heteroaryl aldehydes were next explored as donors for the asymmetric Stetter reaction with nitroalkenes as the Michael acceptor (Scheme 1.5). Catalyst design proved crucial to improve yield and stereoselectivity.<sup>21</sup> Precatalysts based upon amino-

acids (**26**), only provided moderate selectivity. Introduction of a fluorine in the backbone of catalyst **33** significantly improves selectivity. The impact caused by this group on enantioselectivity while being distant from the active site of the catalyst was initially puzzling. An explanation for this effect was a strong puckering of the 5-membered ring, which is observed by X-Ray crystallography. This could arise from a strong hyperconjugation effect between an electron-rich C-H bond and the activated  $\sigma^*$  orbital of the C-F bond. Alternatively, the  $\sigma^*$  of the C-F bond could interact and direct the ionic nitro moiety of the Michael acceptor.<sup>22</sup>

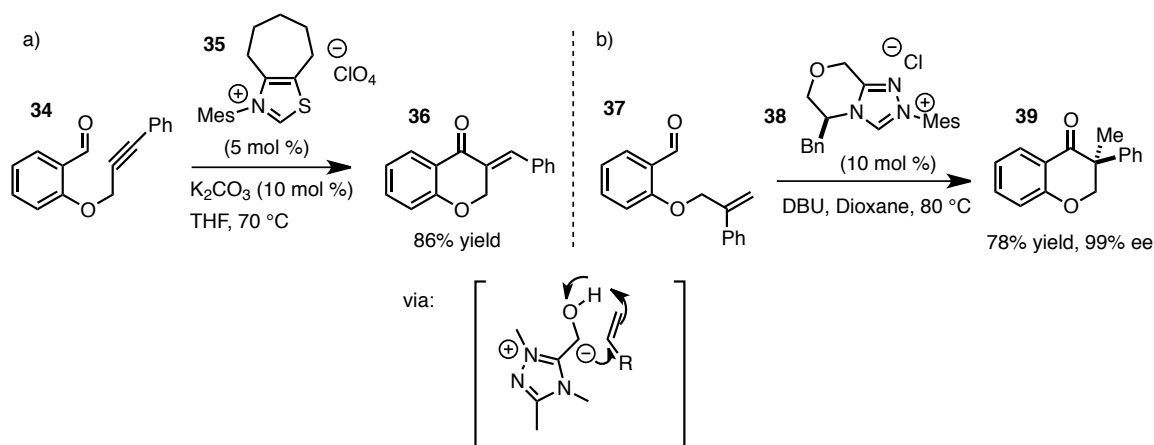


### Scheme 1.5

This same catalyst motif was used successfully again in the development of further intermolecular Stetter reactions. New aldehyde donors include enals<sup>23</sup> and aliphatic aldehydes.<sup>24</sup> In addition, this catalyst was also employed by the Gravel group in the intermolecular Stetter between heteroaryl aldehydes with keto-esters.<sup>25</sup>

Glorius and coworkers have shown that unactivated alkenes<sup>26</sup> and alkynes<sup>27</sup> can make excellent electrophiles (Scheme 1.6). Tethered alkenes and alkynes lead to cyclohexanones in excellent yield, without the need for an electron-withdrawing group

on the alkene. We propose a ‘retro-Cope elimination’ is responsible for this transformation. They have further developed this reaction to intermolecular variants. They demonstrate that cyclopropenes are excellent substrates.<sup>28</sup> Additionally, they report that certain styrenes are also competent partners leading to ketone products.<sup>29</sup>



**Scheme 1.6**

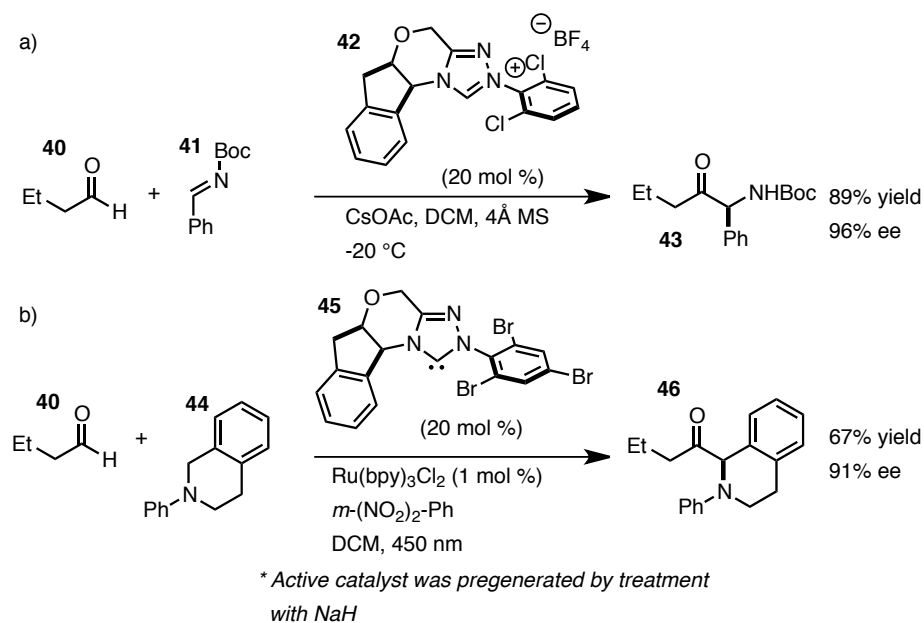
### 1.3 Benzoin Reaction

There remains significant challenges associated with the benzoin reaction, including selectivity between homobenzoin vs cross-benzoin, reversibility of the benzoin reaction, and facile epimerization of the products. Despite these issues, there has been considerable accomplishments in this area by several groups including Enders<sup>30</sup> and Gravel.<sup>31</sup>

Suzuki and coworkers have successfully employed asymmetric intramolecular benzoin reactions in the synthesis of natural products.<sup>32</sup> They utilize a modification of the aminoindanol scaffold pioneered by the Rovis group (not shown).<sup>33</sup> The desired compounds are formed in excellent yields and enantioselectivity.

One strategy to promote cross-selectivity is to use the ‘aza-benzoin.’ This ultimately leads to the formation of amino-ketones selectively. The first reports of this came from the López-Calahorra lab in 1988<sup>34</sup> and Merck Process in 2001.<sup>35</sup> In 2012, DiRocco and Rovis reported a similar aza-benzoin using a specialized triazolium salt **42** (Scheme 1.7a).<sup>36</sup> Compounds were isolated in high yields and enantioselectivity.

Iminiums are also suitable as electrophiles, and DiRocco and Rovis demonstrated



### Scheme 1.7

that these could be formed catalytically through the use of photoredox catalysis

(Scheme 1.7b).<sup>37</sup> There are several important aspects that should be made explicit.

First, this reaction serves as an excellent example of cooperative catalysis, with both catalysts working independent from each other. There appears to be no detrimental effect between the NHC and the Ru(bpy)<sub>3</sub> photosensitizer. Second, they elucidated that an ‘aza-Breslow’ intermediate is formed between the iminium and NHC catalyst.<sup>38</sup>

This serves as a resting state for the catalyst, and the active NHC is released with mild

acid. Third, this remains one of the few examples of asymmetric reactions that involve photoredox catalysis.

### 1.4 Redox Chemistry

In the 2000's, several groups reported an unusual transformation when  $\alpha$ -reducible aldehydes are used as an acyl-anion donor. Rather than seeing nucleophilic behavior at the aldehydic carbon (e.g. benzoin or Stetter), what is observed is an oxidation of the aldehyde as well as a reduction at the  $\alpha$ -carbon.<sup>39</sup> This unexpected redox pathway can be explained by multiple possible reaction pathways after the formation of the acyl-anion equivalent (Figure 1.3). When a leaving group is at

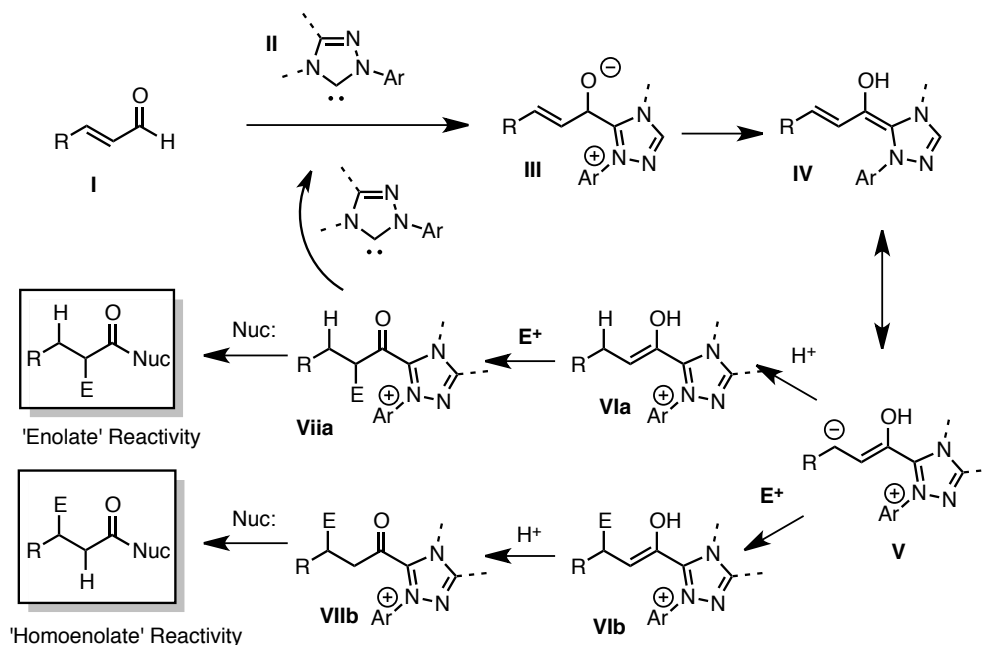
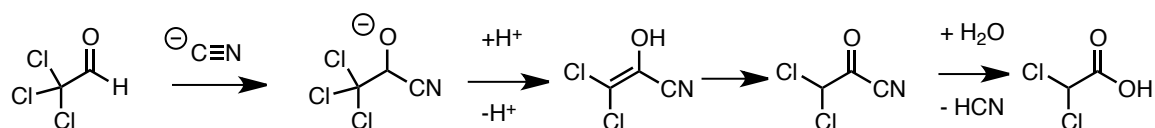


**Figure 1.3**

the  $\alpha$ -carbon (e.g. a chloride, epoxide), this group can be eliminated by the Breslow intermediate **IV**. The enol equivalent generated can undergo protonation (or alkylation) to form an 'acyl-azolium' intermediate (**VIIa** or **VIIb**). This serves as an activated ester

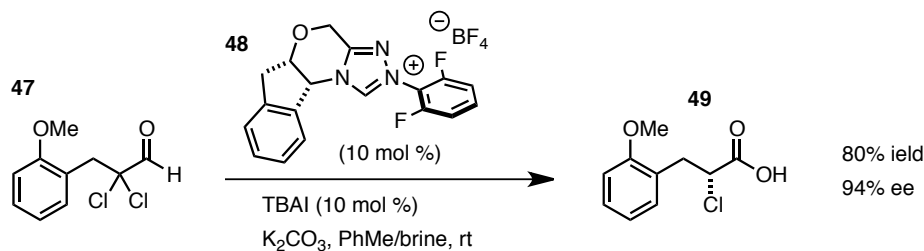
equivalent, and is easily displaced to release the NHC catalyst and a new ester or amide.

In 1873, Wallach observed this transformation with the conversion of trichloroacetaldehyde to a dichloroacetate using a cyanide catalyst.<sup>40</sup> This remains the earliest example of this type of mechanism (Scheme 1.8).



**Scheme 1.8**

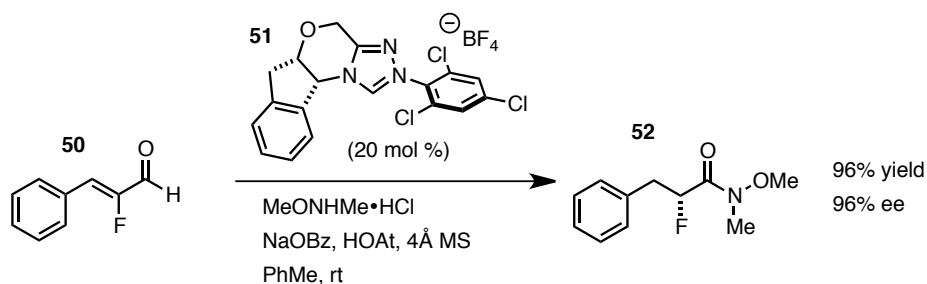
Using a chiral NHC catalyst, the Rovis group was successful in eliminating a single chloride from a dichlorinated aldehyde (Scheme 1.9). The chiral enolate equivalent then protonates stereoselectively, and after displacement of the catalyst by water, provides enantioenriched  $\alpha$ -chloro-acids.<sup>41</sup>



**Scheme 1.9**

In addition, the Breslow intermediate formed from enals can impart nucleophilicity at the  $\beta$ -carbon, often called an “extended Breslow” Intermediate (**V** in Figure 1.3).

Following a similar pathway as before, an ester equivalent can easily be formed. This strategy can allow for the formation of enantioenriched  $\alpha$ -fluoro amides as demonstrated by Wheeler, Vora, and Rovis (Scheme 1.10).<sup>42</sup>

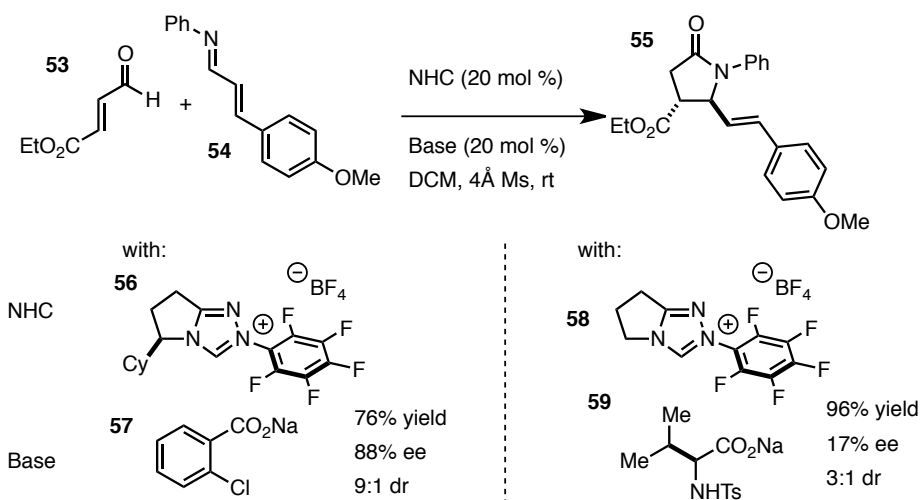


### Scheme 1.10

Rovis and coworkers further used this chemistry to form  $\gamma$ -lactams in high enantioselectivity and diastereoselectivity from enals and imines (Scheme 1.11).<sup>43</sup>

Scheidt and coworkers reported a similar transformation, but arrive at the alternate diastereomer.<sup>44</sup> Zhao and Rovis noticed the use of achiral NHC **58** and chiral

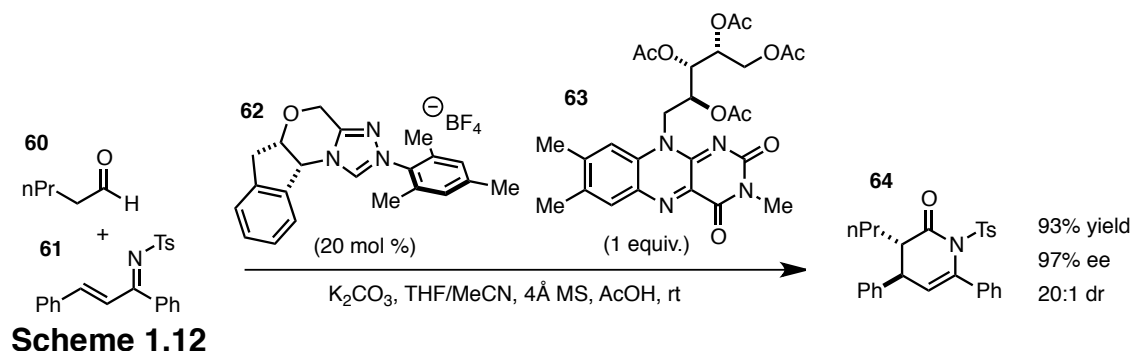
carboxylate base **59** can impart moderate enantioselectivity. The chiral acid formed in this reaction can activate the imine, thus leading to this stereoselectivity.



### Scheme 1.11

Similar to work done with chloro-aldehydes, enals can form chiral enolate equivalents after protonation. Whereas we had previously catalyzed an asymmetric protonation at the alpha position, one can extend this to other electrophiles. Bode

employed this strategy for the formation of delta-lactones.<sup>45</sup> Rovis and coworkers applied this methodology to the synthesis of  $\delta$ -lactams (Scheme 1.12).<sup>46</sup>



Recent work by White and Rovis describes the homoenolate addition of enals with nitroolefins to form acyclic systems.<sup>47</sup> A more in-depth explanation of this area will be found in Chapter 3.

Hopefully this introduction has provided a brief insight into recent advances with NHC-based organocatalysis. The key feature of this chemistry is the inversion of polarity of electrophilic aldehydes. Through catalyst development, a myriad of new chemical transformations have been uncovered, including reactivity at both the aldehydic carbon and  $\beta$ -carbon. The following chapters will further describe several new contributions to this growing field.

## CHAPTER 2

### ASYMMETRIC MICHAEL/BENZOIN CASCADE FOR THE SYNTHESIS OF ENANTIOENRICHED CYCLOPENTANONES

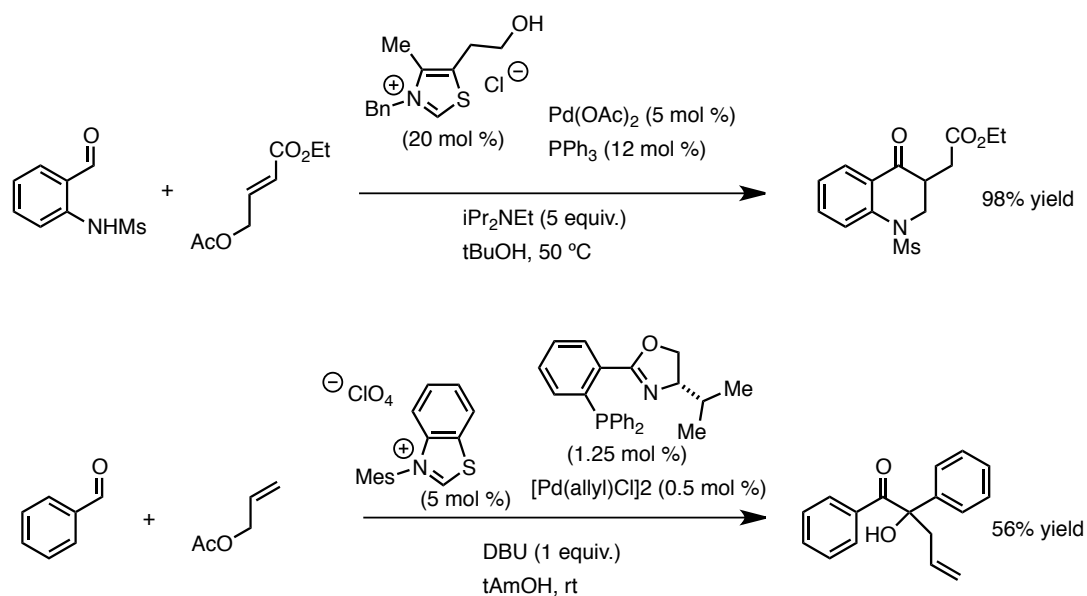
#### 2.1 *Introduction to Cascade Reactions*

Of all the catalysts that our group has designed and created, the most utilized are the catalysts bearing an *N*-pentafluorophenyl group.<sup>48</sup> The impact of this highly electron-deficient substituent can be explained by its pKa.<sup>49</sup> The acidity of the C-H bond of the triazolium is increased, meaning that it can be deprotonated by a weak base. This leads to a higher proportion of active catalyst available. Additionally, it is our belief this leads to an increased acidity of the NHC-aldehyde adduct. This translates to easy and facile formation of the requisite Breslow intermediate with weak bases (see Chapter 1).<sup>50</sup> While this can lead to highly efficient reactions, there is another attribute that is often overlooked. The ability for NHC-catalysis to exist under mild conditions can allow for other synthetic transformations to occur. The best example for this strategy is cascade catalysis.

While there are many competing names for this process (e.g. cascade, domino, tandem), we define cascade catalysis as a reaction containing two or more independent catalytic cycles.<sup>51</sup> This strategy has been popular in recent years for its many advantages. By combining multiple catalytic processes in one flask, one can generate elaborate and complicated compounds from simple starting materials. Cascade

reactions avoid extra workups and purification, which not only conserves time and resources, but also is essential if an intermediate is unstable to isolation. As such, there are many excellent examples of this work in the literature.<sup>52</sup>

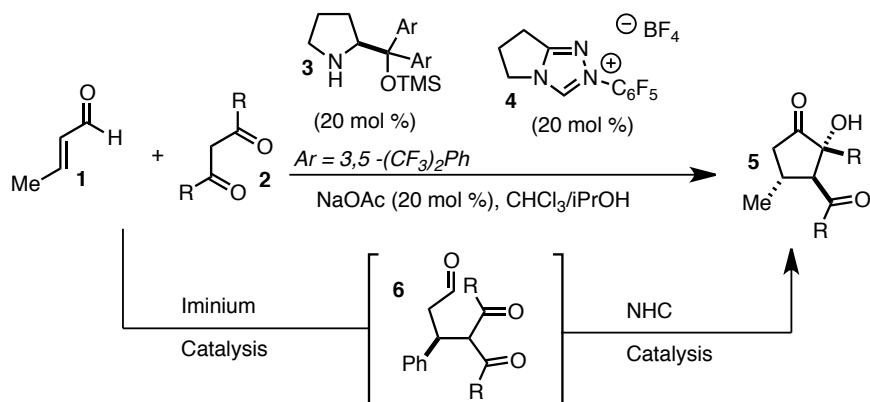
Our group grew interested in using NHC catalysts in cascade reactions. There has been some precedent that this is feasible, such as the work of Hamada<sup>53</sup> and Glorius<sup>54</sup> combining NHC and Pd catalysis (Scheme 2.1). In addition, Glorius has provided an example with NHC and base catalysis.<sup>55</sup> There are also examples of cascade reactions where the NHC is responsible for multiple transformations.<sup>56</sup> We focused our research on the synthesis of enantioenriched compounds using NHC/organocatalysis cascade reactions.



### Scheme 2.1

Stephen Lathrop reported our initial finding. He discovered a cascade reaction that combines asymmetric iminium catalysis with a diastereoselective benzoin cyclization.<sup>57</sup> This process leads to complex cyclopentanones **5** from an enal (**1**) and

1,3-dicarbonyl nucleophile **2** (Scheme 2.2). This occurs via formation of an iminium intermediate from the amine catalyst and the enal. This activated species undergoes conjugate addition from the acetyl-acetate derivative. Release of the amine catalyst provides aldehyde intermediate **6**. This aldehyde is intercepted by the NHC catalyst and undergoes a benzoin cyclization with the ketone to form a cyclopentanone.

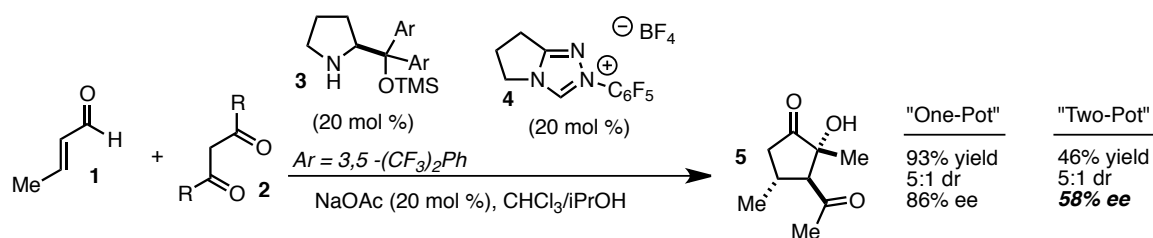


## Scheme 2.2

There are two important attributes that should be mentioned. Lathrop showed that sodium acetate is an effective base. This is useful, as the acetic acid generated as a byproduct is important for turnover of the amine catalyst. However, acetic acid has also shown to be excellent as a useful additive for NHC catalysis and has since become commonly found in recent reports.<sup>58</sup>

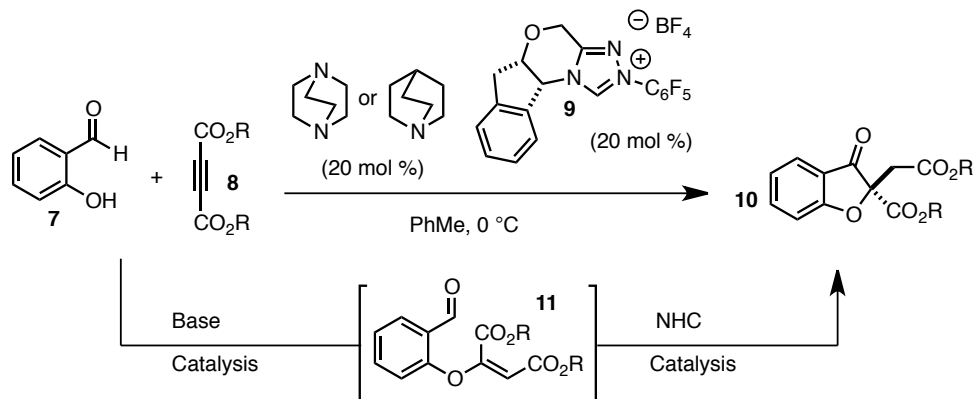
The second observation is that this is a 'one-pot' reaction. In cascade reactions reported by other groups, it is common for the second catalyst to be added later.<sup>59</sup> Sometimes there is a solvent exchange as well. Lathrop's reaction is interesting in that not only *can* this cascade be run with all reagents present, but also that it *must* be run with all reagents present. When this reaction is carried out as two separate reactions

(the 'two-pot' reaction), Lathrop observes a diminished yield and diastereoselectivity (Scheme 2.3). Unexpectedly, he noticed a significant drop in enantioselectivity. To investigate this phenomenon, he conducted mechanistic studies. The result of this work indicates that the first step of the reaction, the conjugate addition, is reversible. The benzoin cyclization quickly consumes this intermediate, preventing complete racemization.



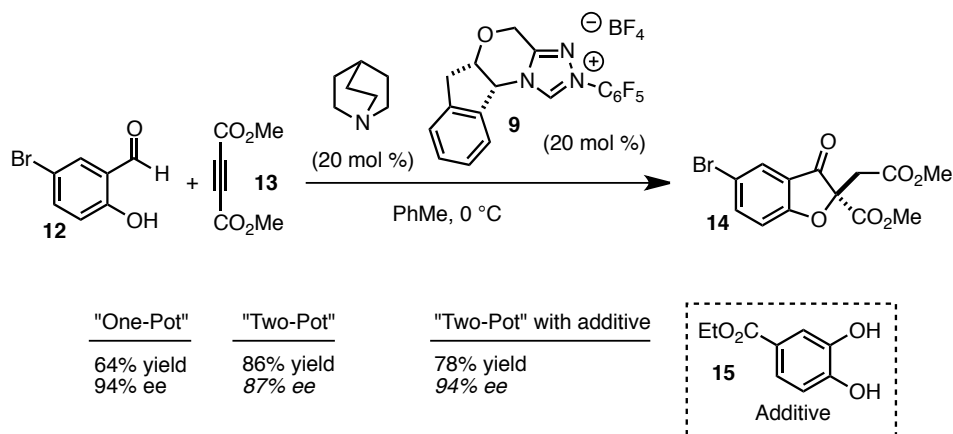
**Scheme 2.3**

The next question to consider was if other modes of organocatalysis are compatible with NHC's. The use of base catalysis between salicylaldehyde and propiolates can lead to an intermediate that is suitable for an intramolecular Stetter reaction. Claire Filloux studied and developed this reaction, leading to an elegant reaction system (Scheme 2.4).<sup>60</sup> This reaction forms enantioenriched benzofuranones **10** from salicylaldehydes (**7**) and electron-deficient alkynes (**8**). She employs either quinuclidine or DABCO as a base catalyst and chiral triazolium **9** as an NHC source. This process not only allows for the asymmetric formation of benzofuranones, but also an excellent method for the generation of stereodefined tetra-substituted carbons.



### Scheme 2.4

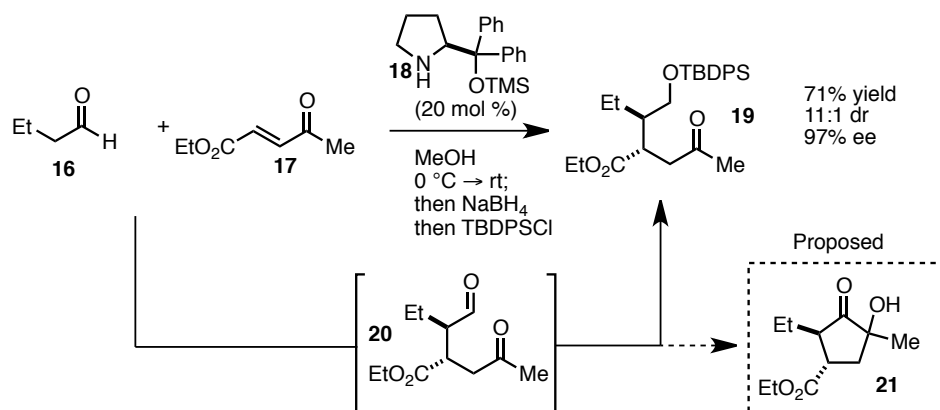
There are some features worth mentioning regarding Filloux's work. Besides alkynes, she demonstrated that allenes are suitable surrogates. Additionally, she conducted a 'two-pot' reaction, similar to Lathrop's work. In these experiments, Filloux noticed a drop in yield from this study (Scheme 2.5).



### Scheme 2.5

After further investigation, she determined that the salicylaldehyde starting material also functions as an additive for the Stetter reaction, most likely from the phenol moiety. In fact, she improves the reaction significantly when catechol **15**,<sup>61</sup> also containing a phenol group, is used as an additive.

Lathrop reasoned that an intermediate similar to aldehyde **6** in his earlier work can be obtained using enamine chemistry rather than iminium catalysis. He drew inspiration from work published by Ma and coworkers.<sup>62</sup> They reported an asymmetric addition of aliphatic aldehydes to activated enones using chiral amine catalyst **18** (Scheme 2.6). After a reductive workup and silylation, they isolate keto-alcohol products in high enantio- and diastereoselectivity. Their initial product (**20**), before reduction by sodium borohydride, bears the same backbone as the intermediate seen in Lathrop's work. In theory, interception of this intermediate by benzoin cyclization would allow formation of new cyclopentanones **21** and a new cascade reaction can be developed.

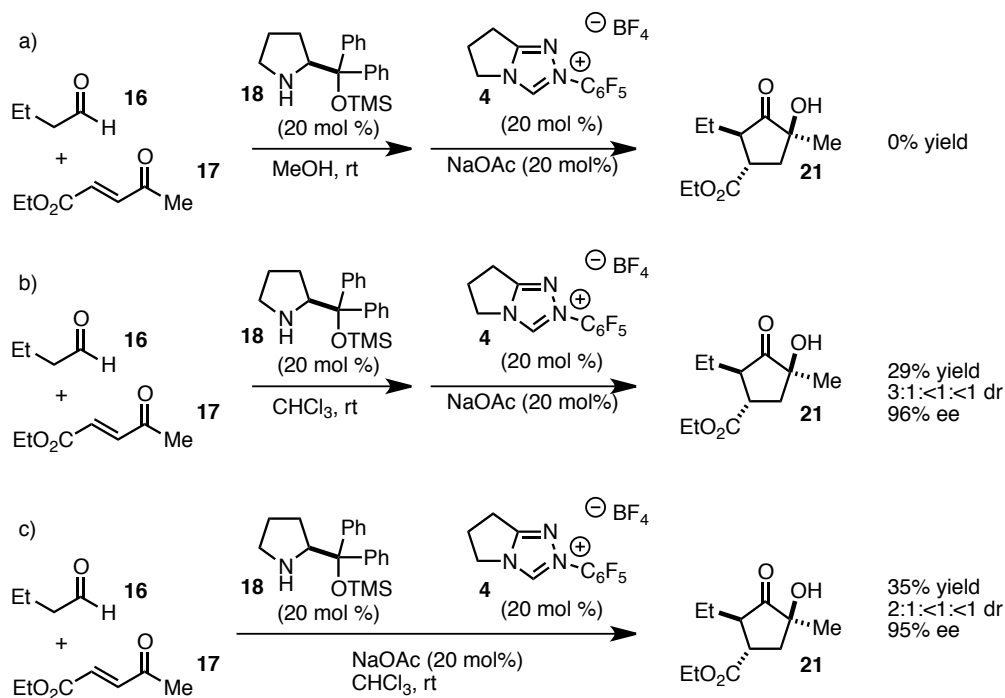


**Scheme 2.6**

## 2.2 Reaction Development

A new project was started to determine if this pathway was feasible. As a safe approach, we initially reproduced Ma's protocol and added the NHC catalyst and base later. While formation of the desired intermediate was smooth, the benzoin reaction did not proceed (Scheme 2.7a). Upon suggestion by coworkers, the solvent was switched from methanol (Ma's conditions) to chloroform (Lathrop's conditions). This was

fortuitous, as we were able to isolate the desired compound (Scheme 2.7b). This initial hit was very exciting, as the compound was generated in high enantioselectivity, moderate diastereoselectivity, and in modest yield. However, we were delighted that there is no detriment with the inclusion NHC pre-catalyst **4** from the outset of the reaction, making this a ‘one-step, one-pot’ reaction. It was decided to focus on improving the yield of the reaction (Scheme 2.7c).

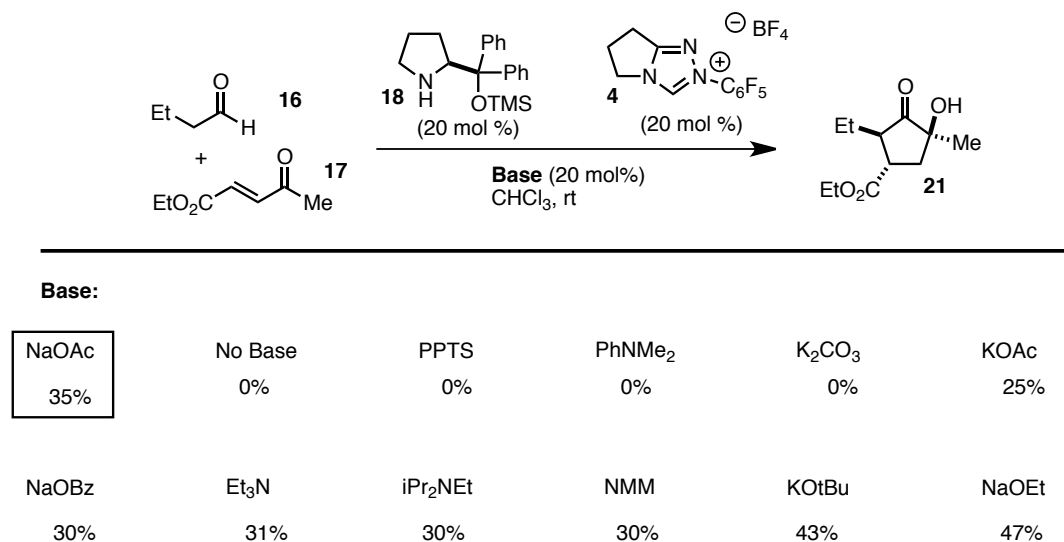


### Scheme 2.7

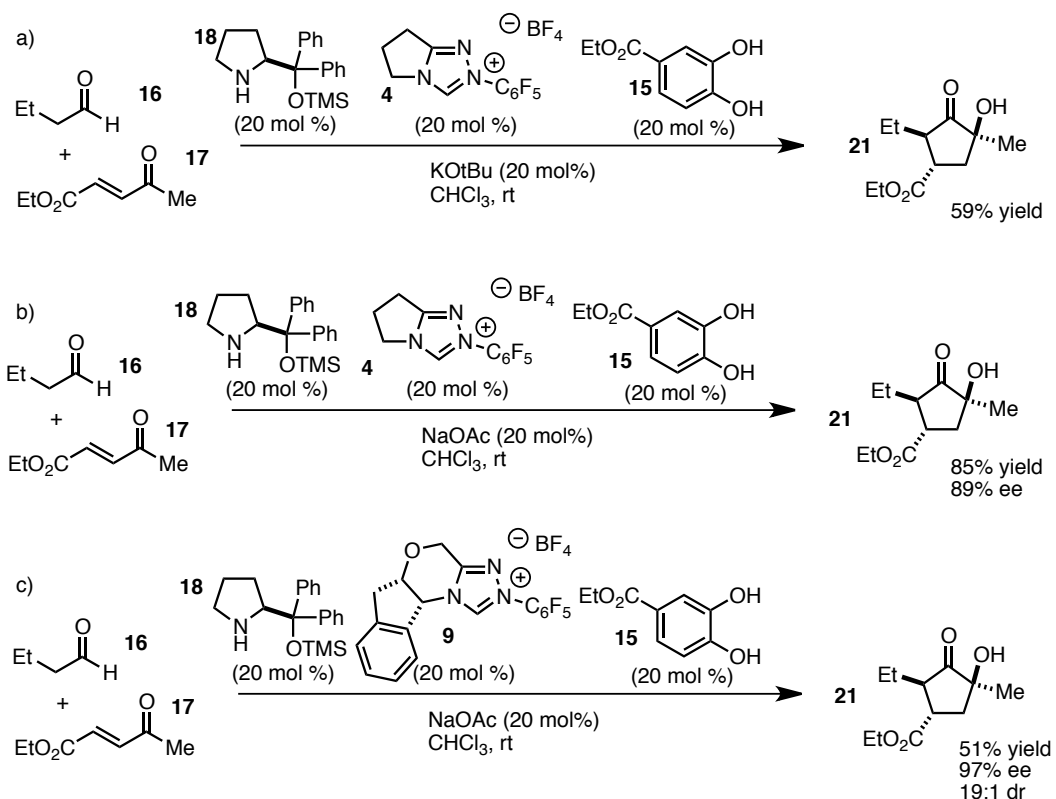
Different bases were then screened in an effort to increase the yield of the reaction. While several bases were completely ineffective, several matched the capability of sodium acetate (Table 2.1). These include amine bases such as triethylamine, *N,N*-diisopropylethylamine, and *N*-methylmorpholine. There is also a slight improvement with alkoxide bases, with potassium *t*-butoxide and sodium ethoxide

showing increased yields. However, these results were far below expectations, so more options to improve the reaction was explored.

**Table 2.1**

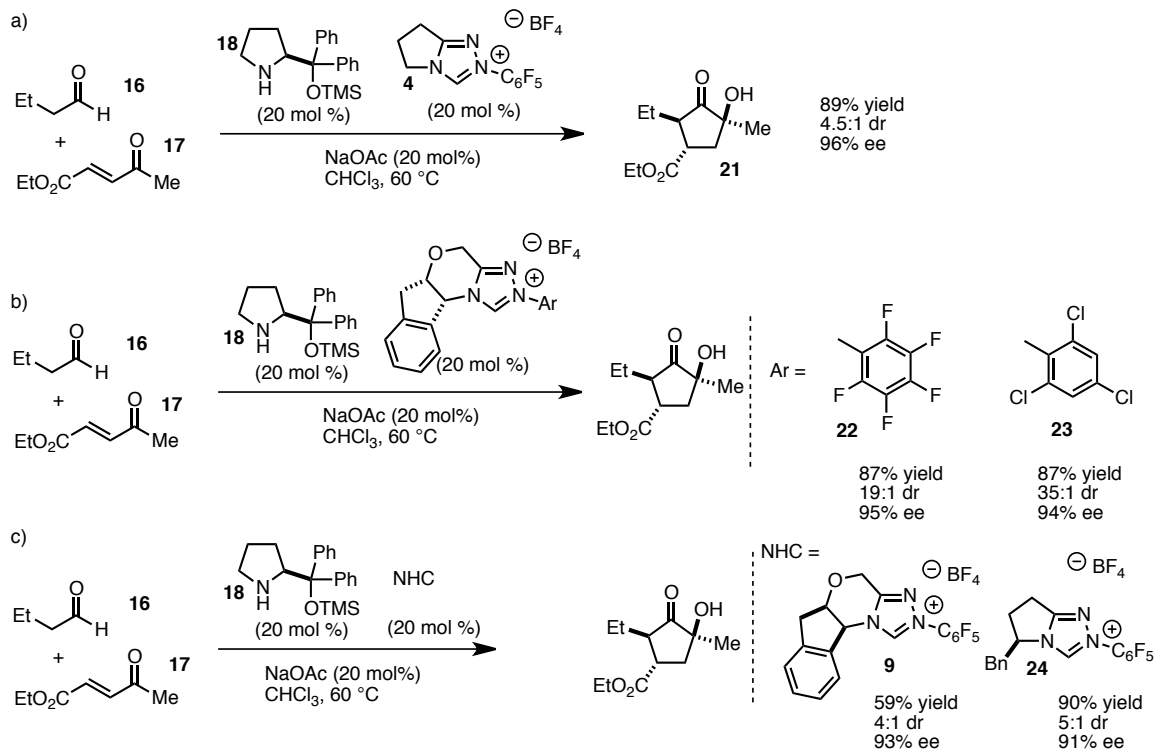


There was concern that perhaps the initial step of the reaction, the amine-catalyzed conjugate addition of the aldehyde with the enone, was responsible for the poor results. Literature has shown that a catechol additive can lead to significantly improved results in this type of reaction.<sup>63</sup> In fact, our group has shown that catechol derivatives are superb additives for various NHC-catalyzed transformations.<sup>13a</sup> Catechol derivative **15** developed by Chi and Gellman was therefore employed in this reaction.<sup>13b</sup> We observe dramatic improvements in yield when an achiral NHC catalyst is used, especially with sodium acetate as base (Scheme 2.8b). Thrilled with this result, this reaction was carried out with chiral NHC catalyst **9**. Exceptional diastereoselectivity is achieved with this combination, but diminished yields are once again observed (Scheme 2.8c).



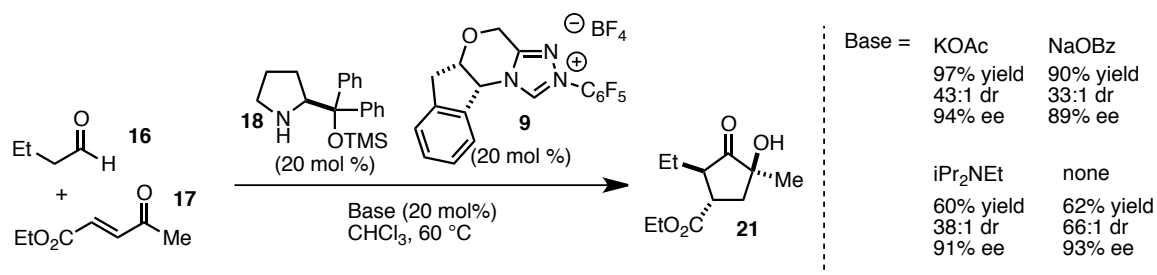
## Scheme 2.8

Following advice by my colleague Phillip Wheeler, this reaction was run under heated conditions. By heating this reaction to 60 °C, high conversion to the desired product is achieved (Scheme 2.9a). We were delighted that high enantioselectivity is maintained (94% ee). However, diastereoselectivity remains poor, with a ratio of 9:2. This is resolved when a chiral NHC is used, resulting in a 19:1 dr (Scheme 2.9b). This is accomplished without any loss in enantioselectivity or yield. Choice of NHC catalyst is crucial though. A bulkier aryl group leads to even higher diastereoselectivity. The antipode of the catalyst leads to a 4:1 dr, and a separate chiral scaffold provides similar poor results (Scheme 2.9c).



### Scheme 2.9

With heat as a useful additive in this reaction, a base screen was revisited. Bases that gave similar results to sodium acetate at room temperature also provide superb results at the elevated temperature (Scheme 2.10). Other carboxylate bases are also advantageous in improving the diastereoselectivity, whereas the amine base (diisopropylethylamine) forms product in lower yield. We also tested the reaction without a carboxylate base, with the hypothesis that the amine catalyst is also capable of deprotonating the triazolium salt. Not only is this true, but it is accompanied by a dramatic improvement in diastereoselectivity, with the product formed in a 66:1 dr with 93% ee. Unfortunately, the yield is diminished at 62%.



**Scheme 2.10**

The proposed mechanism is shown in Figure 2.1. Condensation of the amine catalyst **18** with butanal **16** forms the reactive enamine **I**. This then undergoes Michael addition with the enone **17** to form **II**. Hydrolysis of the iminium releases the amine catalyst and the aldehyde intermediate **20**. This aldehyde is intercepted by the NHC catalyst and forms the requisite Breslow

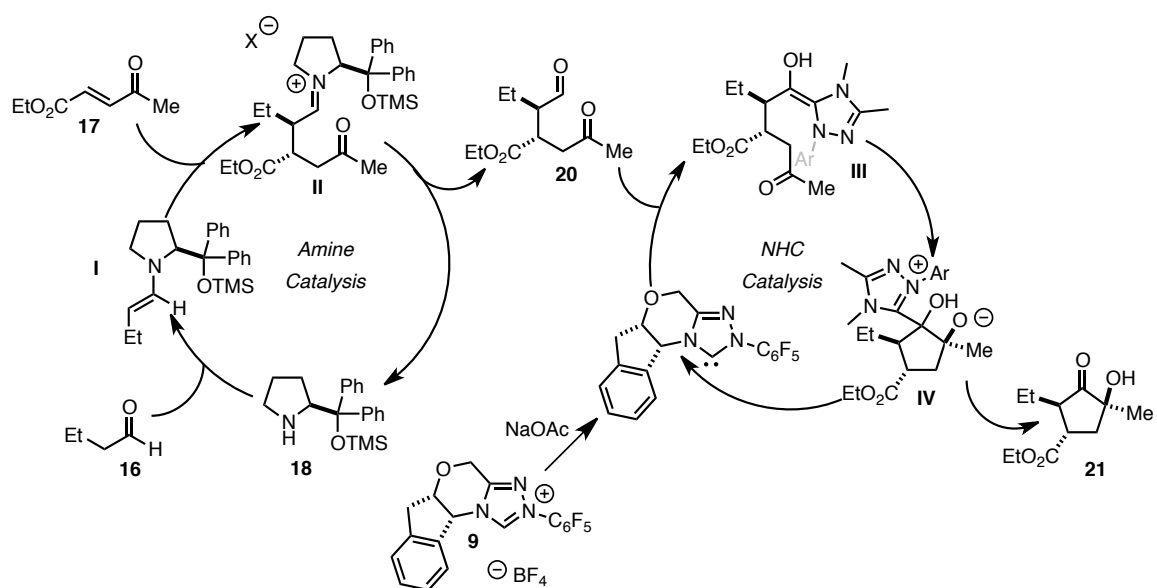


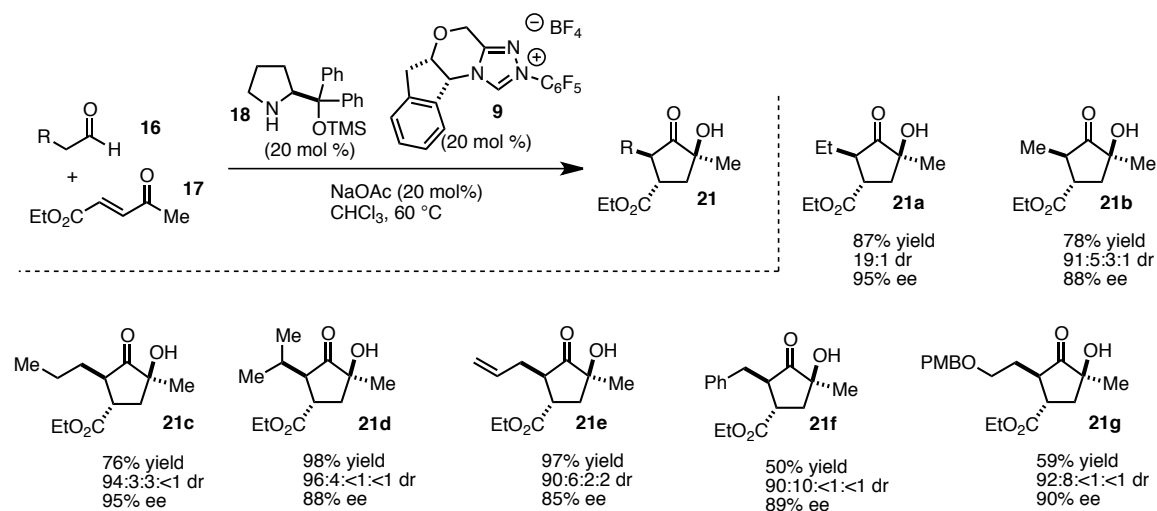
**Figure 2.1**

intermediate **III**. This then adds onto the tethered ketone to form the cyclized intermediate **IV**. Proton transfers, followed by ejection of the NHC catalyst, forms the cyclopentanone product **21**.

## 2.3 Scope of Reaction<sup>64</sup>

With suitable conditions that provide high yield, diastereoselectivity, and enantioselectivity, it was deemed prudent to explore the scope of this reaction. Variation of the aldehyde donor was initially explored (Table 2.2). Similar to butanal, other straight-chain aldehydes are suitable substrates (**21b-c**). Isovaleraldehyde, which bears a branched group, lead to complications. Notably, formation of Stetter product was observed.<sup>65</sup> We inferred that the first catalytic

**Table 2.2**

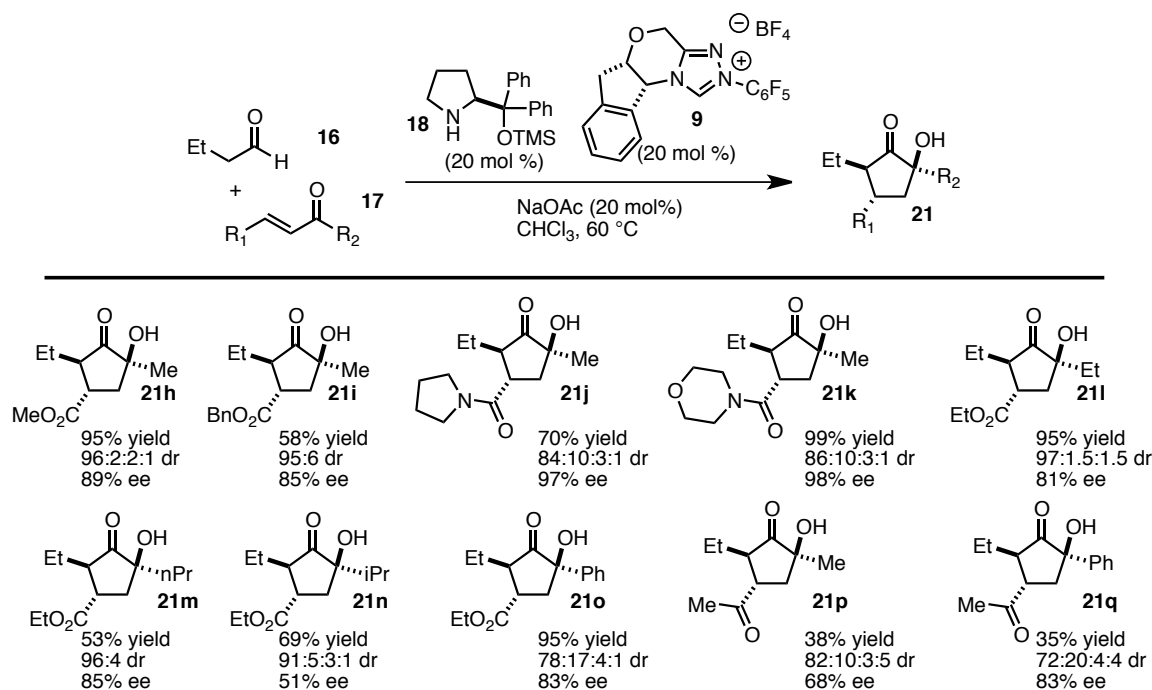


cycle might have been slowed by this bulkier aldehyde. By withholding the triazolium salt until complete consumption of starting materials (monitored by TLC), the desired cyclopentanone is formed (**21d**). Larger aldehydes are also tolerated, but in lower yields and diastereoselectivity (**21e-g**).

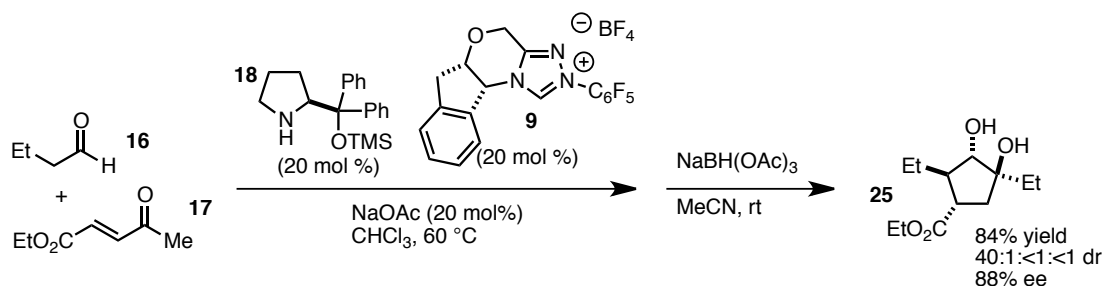
Variation of the enone was then explored (Table 2.3). Replacing the ethyl ester moiety with a methyl ester was successful (**21h**). The benzyl ester is also competent, but in a lower yield (**21i**). Whereas secondary amides were ineffective, tertiary amides

are well tolerated (**21j-k**). While diastereoselectivity is moderate (about 9:1 dr), enantioselectivity is superb. We also explored variation of the ketone group. Both ethyl- and propyl- ketones can be used in this reaction (**21l-m**). The bulkier isopropyl-ketone does not provide product with our standard conditions (**21n**). However, when the smaller achiral catalyst **4** is employed, formation of the desired cyclopentanone is achieved. A phenyl-ketone group is also effective, in good yield and enantioselectivity but in lower diastereoselectivity (**21o**). Diketones are also competent, albeit in lower yields and stereoselectivity (**21p-q**). This is likely due to their higher reactivity, and side reactions are more prevalent with these systems. In the case of an unsymmetrical diketone, only one regioisomer is formed for compound. This indicates that the enamine intermediate undergoes addition onto the more electron-deficient carbon.

**Table 2.3**



We were curious if further transformations can be affected onto this system. One key feature of these compounds is the  $\alpha$ -hydroxy-ketone. This system is an excellent substrate for a directed reduction of the carbonyl. Treatment of this compound with sodium triacetoxyborohydride in acetonitrile at room temperature provides the expected *trans*-diol **25** (Scheme 2.11). Luckily, this product can be obtained in ‘one-pot.’ After complete formation of cyclopentanone is observed by TLC, the reaction is cooled to room temperature. Addition of acetonitrile and sodium triacetoxyborohydride provides the diol product in 84% yield, 88% ee, and a 40:1 dr.



### Scheme 2.11

Absolute configuration was determined by X-ray crystallography. The ester of the cyclopentanone product **21i** was hydrogenated to the free acid, and the ammonium salt was generated from a chiral phenethylamine. This salt was recrystallized from ethyl acetate. The relationship of the alcohol and alkyl groups was determined from this crystal. Kevin Oberg’s work was essential for solving this crystal structure (Figure 2.2).

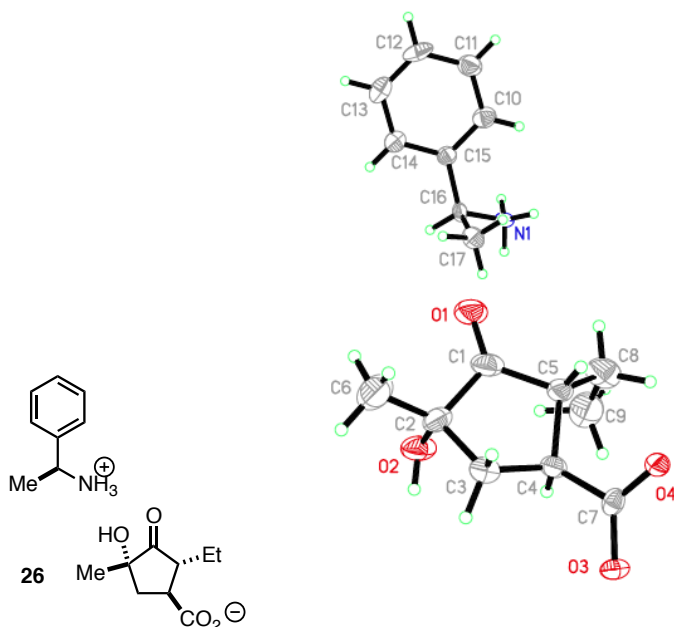
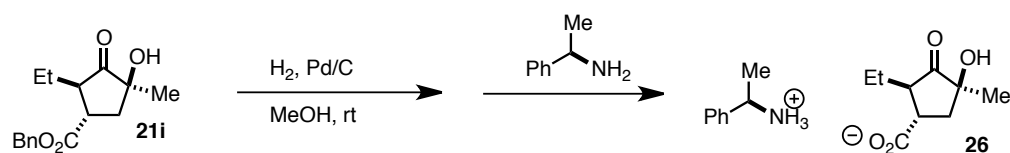
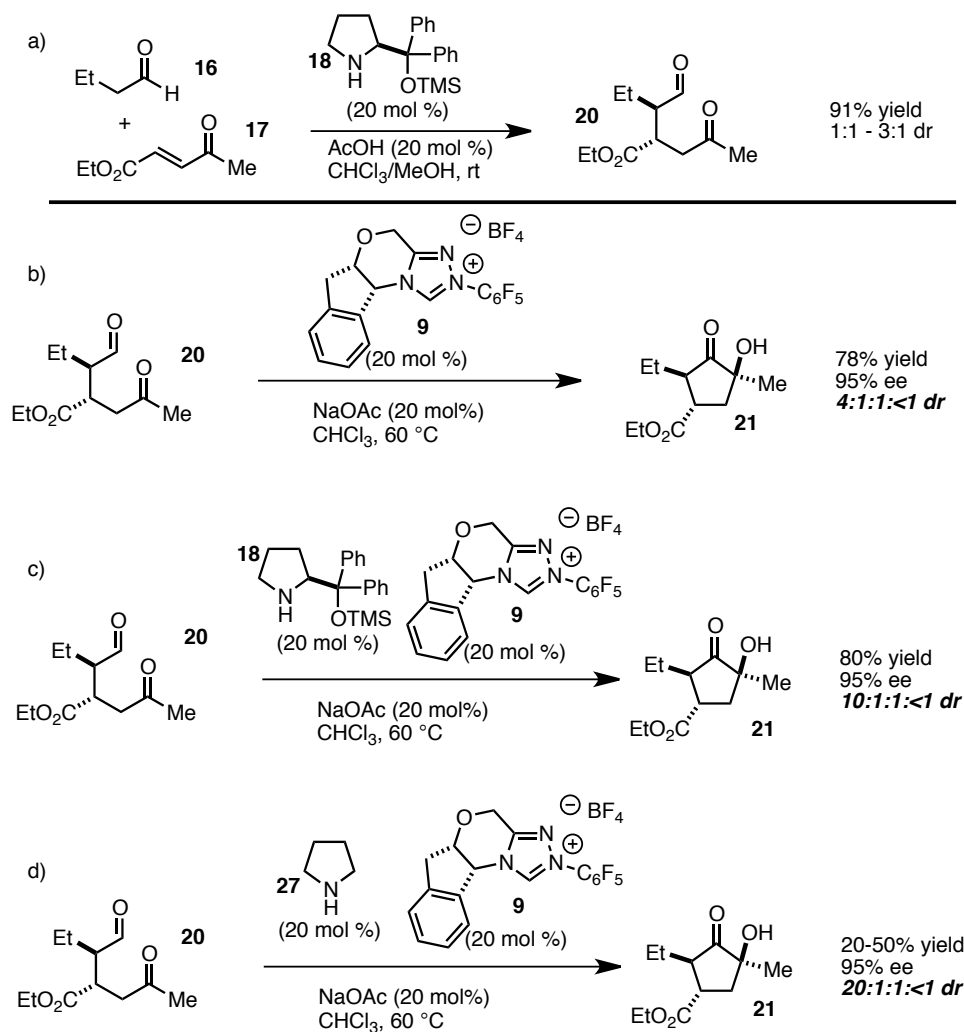


**Figure 2.2**

#### 2.4 Mechanistic Insight

As mentioned earlier, Lathrop and Filloux noticed an astonishing requirement for both catalytic cycles to be present to achieve their excellent results. Their ‘one-pot’ protocol was essential for success. We were curious if this relationship was present in this reaction as well. To explore, the first catalytic cycle was conducted in absence of the triazolium salt. The intermediate aldehyde **20** was isolated in low dr (often between 1:1 to 3:1 dr). This aldehyde was then exposed to the triazolium salt and acetate base (Scheme 2.12). The expected cyclopentanone was isolated in similar yield and enantioselectivity to products from the ‘one-pot’ protocol. This contrasts to what was observed in Lathrop’s and Filloux’s work. Surprisingly, a significant drop is seen in

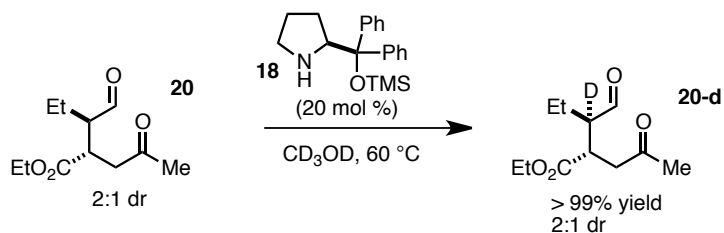
diastereoselectivity (4:1 dr instead of 19:1 dr). Intriguing as this is, we conducted further experiments. The benzoin catalytic cycle was repeated again, but with the amine catalyst also added. This combination improves the diastereoselectivity to 10:1 (Scheme 2.12c). The chirality of the amine is not even essential: the use of pyrrolidine (**27**) in place of the chiral catalyst increased the dr to 20:1 (Scheme 2.12d). However, pyrrolidine also initiates decomposition of the product as well as multiple side-products.



**Scheme 2.12**

These results were quite unexpected. A dramatic improvement in diastereoselectivity is observed when a chiral NHC is used instead of an achiral catalyst (see Scheme 2.9). This naturally led to the belief that the high diastereoselectivity is formed during the benzoin cyclization, catalyzed by the chiral NHC catalyst. However, these ‘two-pot’ experiments seem to refute this hypothesis. There also seems to be an essential role for the amine catalyst in the second catalyst. This seems contradictory, as the amine catalyzed reaction provides the intermediate aldehyde **20** in low dr, but is somehow responsible for the high dr of the finished compound.

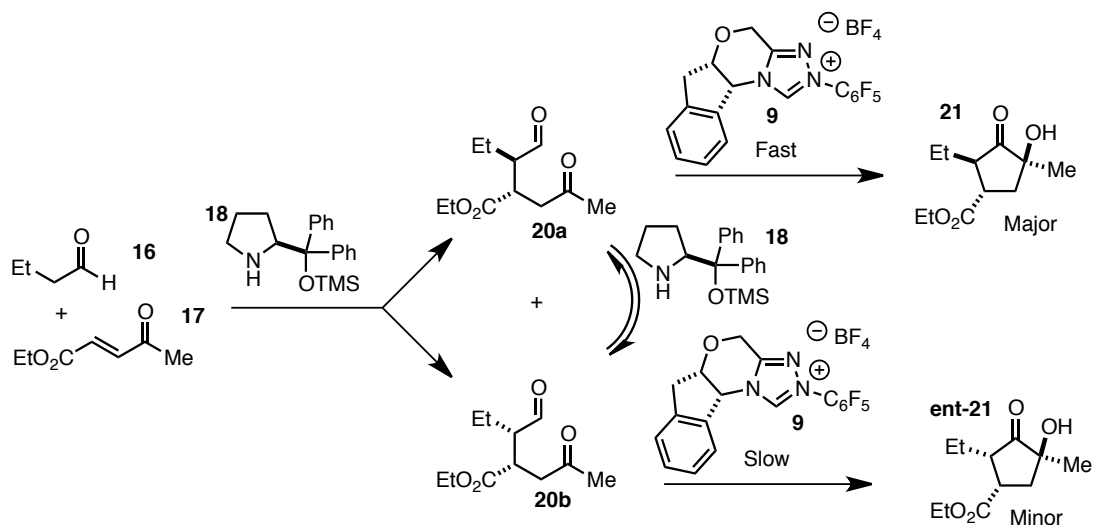
We proposed several different hypotheses to explain these findings. One experiment provided useful insight and guidance for our investigation. When the aldehyde intermediate is exposed to the amine catalyst in the presence of deuterated methanol, complete deuteration is seen at the  $\alpha$ -carbon of the aldehyde (Scheme 2.13). It should be noted that this experiment is flawed, as a methanolic environment is highly different from the regular reaction conditions.



### Scheme 2.13

Nevertheless, this observation led us to consider this carbon as the center for the diastereoselectivity. With this as a basis, we proposed a new catalytic model for this reaction (Scheme 2.14). We assume that the benzoin cyclization is slow while the amine-catalyzed conjugate addition is fast. We theorized that the amine catalyst also

epimerizes the  $\alpha$ -carbon of the intermediate aldehyde quickly as well. One diastereomer of this aldehyde (20a) is then favored for the benzoin cyclization. The unfavored diastereomer is then converted to the favorable one by this epimerization.



**Scheme 2.14**

While this proposal was interesting, more evidence was needed beyond the deuteration experiment. Following the suggestions of my colleagues Harit Vora and Todd Hyster, this reaction was monitored by  $^1\text{H}$  NMR. For the sake of simplification, we focused on the transformation of the aldehyde intermediate to product. This intermediate was isolated in low diastereoselectivity (3:1). Monitoring the entire spectra would be prohibitively complicated, so attention was paid solely to the consumption of the aldehyde peaks. First, the intermediate aldehyde was combined with the triazolium salt and sodium acetate in deuterated chloroform at 60 °C. NMR spectroscopy clearly shows consumption of one diastereomer over the other (Fig 2.3).

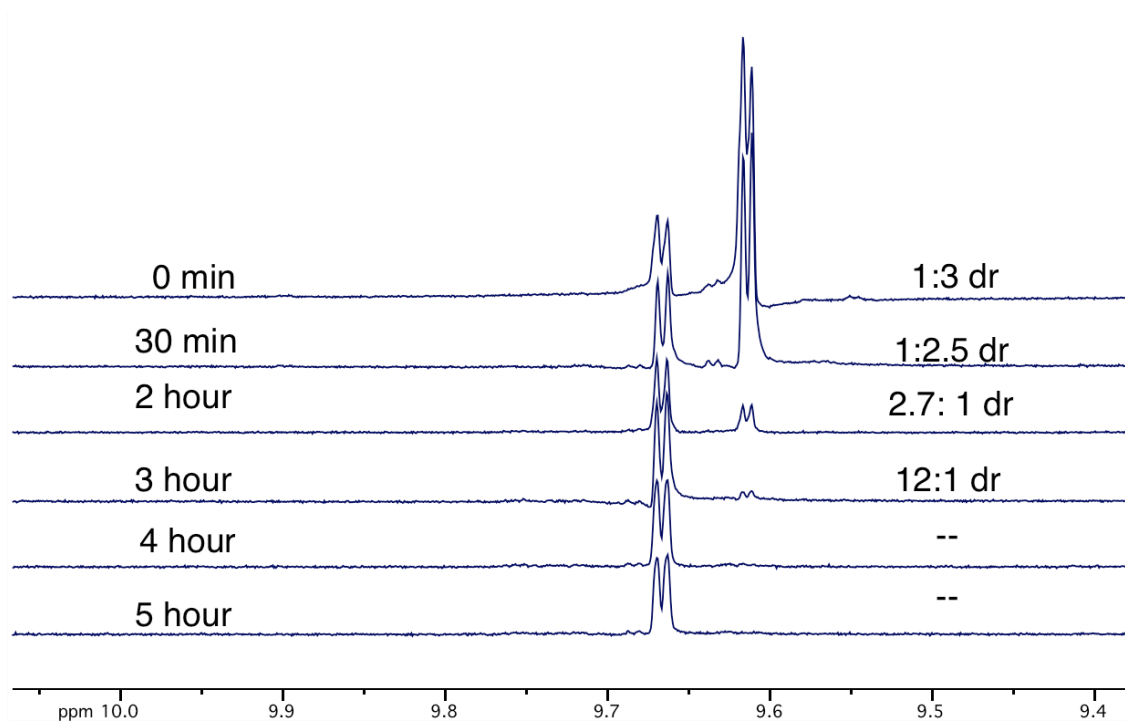
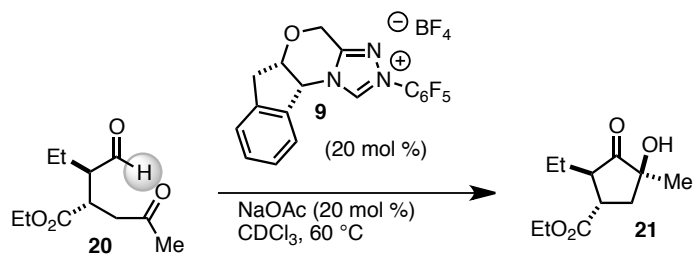


**Figure 2.3**

A second experiment was conducted which combined the aldehyde intermediate with both catalysts and sodium acetate (Fig 2.4). In contrast to the previous experiment, signals from both diastereomers persist in the reaction. It also appears that both diastereomers are being consumed.

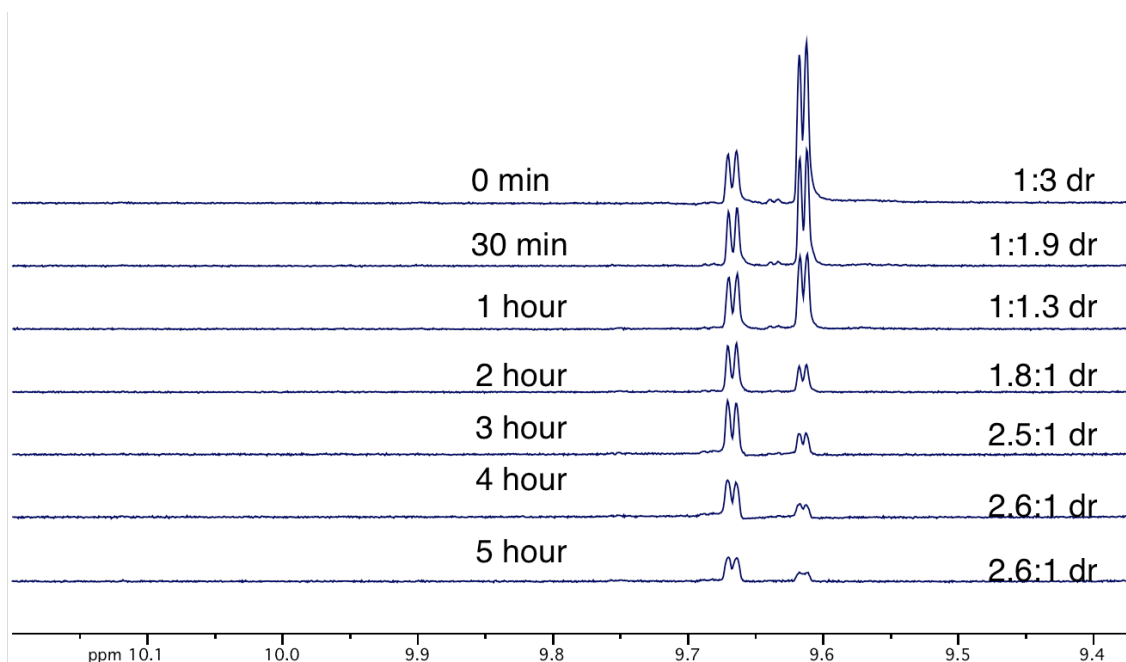
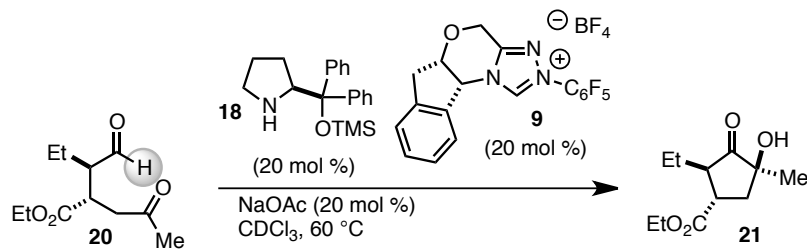


**Figure 2.4**

Lastly, the amine catalyst is added to the reaction mixture of the first NMR experiment (Fig 2.5). While one aldehyde diastereomer was completely consumed in this experiment, addition of the amine leads to the reemergence of both diastereomers. This observation provides strong evidence for the revised mechanism.

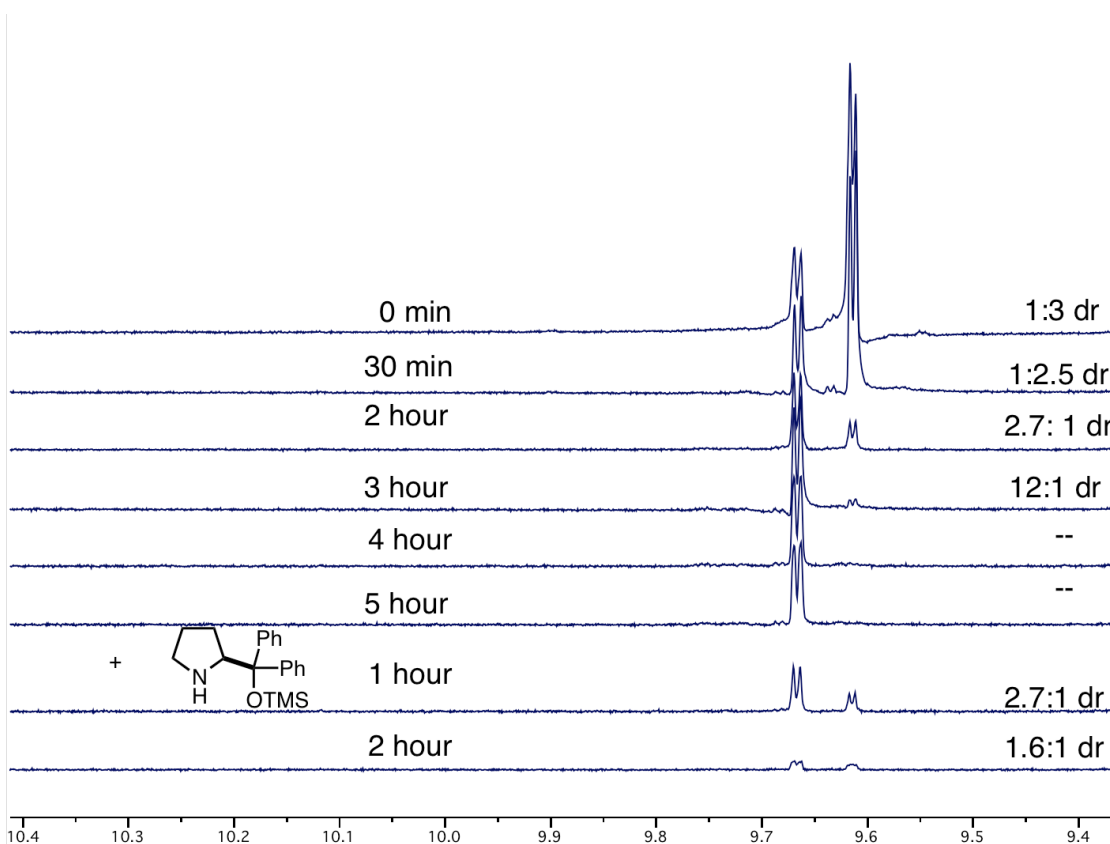
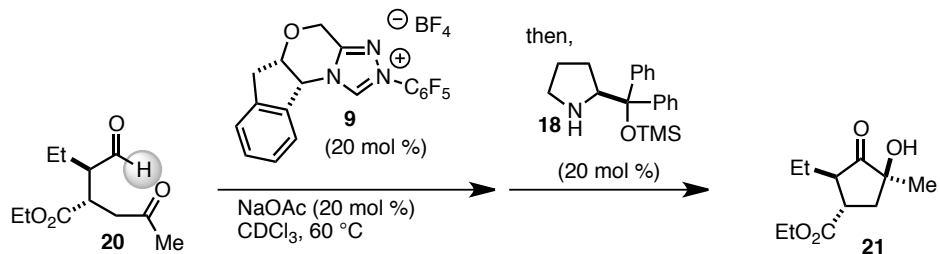


**Figure 2.5**

This relationship can be considered a pseudo-‘Dynamic Kinetic Resolution (DKR).’ A true DKR converts a racemic mixture of starting material to one enantiomer of product. Normally, a DKR reaction has to differentiate between two enantiomers of equal energy. Our reaction selects between two possible diastereomers, which are inherently of different energy. Exposure of a cyclopentanone formed in low diastereoselectivity to the optimal NHC catalyst, amine catalyst, or combination showed

no improvement. This indicates that the final step of this reaction is irreversible. Thus, the diastereoselectivity observed is from a kinetic process, not a thermodynamic one.

With the correct structure and mechanism determined, we sought to rationalize the observed stereochemistry. The stereochemistry  $\alpha$  to the ester is explained by the chiral amine catalyst, and so this must translate to the selectivity for the next two stereocenters. We also deduced that the  $\alpha$ -carbon selectivity is formed between the first and second catalytic cycle, and is dependent on the structure of the NHC catalyst. Previous work in our group has demonstrated the importance of internal 'proton shuttles' for NHC catalysis.<sup>66</sup> Often, this is a heteroatom found in the substrate that aids in deprotonation to form the Breslow intermediate. We were curious if a carbonyl in the intermediate can also serve this role. This intermediate has two carbonyls as potential proton shuttles: the ester and the ketone. A transition state with the ketone as proton shuttle has the two substituents in an anti conformations, as what is seen in the product (I, Fig. 2.6). This seven-membered transition state also orients the carbonyl oxygen at a larger angle, optimal for deprotonation of the pre-Breslow intermediate. This theory can explain the observed configuration.

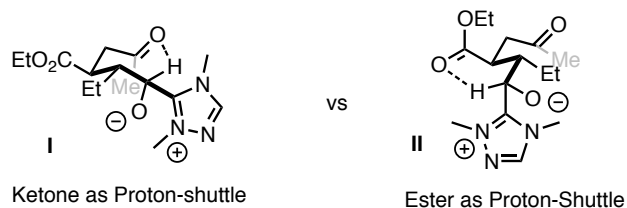


**Figure 2.6**

However, this model lacks any explanation for the influence of catalyst structure in diastereoselectivity. At this time, there is insufficient evidence to build a complete

rationale for the observed selectivity. For example, it is still unknown if either NHC addition into the aldehyde or formation of the Breslow intermediate is reversible.

With the mechanism more clearly understood, we were curious if there is a strategy to 'tune' the stereoselectivity. Our idea was with proper choice of NHC catalyst, another diastereomer could be favored. A perfect example of this is demonstrated by Carreira and coworkers.<sup>67</sup> The right combination of a chiral amine catalyst with a chiral Ir catalyst allows specific access to one of four isomers. I initially explored the use of the antipode of the successful catalyst, but this led only to a diminished diastereomeric ratio, and not an inverted one. Another chiral scaffolds also failed to show any inversion of this intermediate.

## ***2.5 Applications Toward the Synthesis of Natural Products.***

Complex cyclopentanes are a motif found in many biologically active molecules (Fig 2.7). For example, the cores of marine natural products massadine<sup>68</sup> and palau'amine<sup>69</sup> bear a fully substituted cyclopentane. Both these compounds share an elaborated cyclopentane core, with 5-contiguous stereocenters. They also possess a unique  $sp^3$  C-Cl bond that is not common in many alkaloids. Cyclopentanes are also present in several terrestrial-based natural products. This includes Crescentin IV, a small natural product isolated from the Calabash tree.<sup>70</sup> Even though it lacks significant bioactivity, it is most likely a precursor to several other iridoid products that are medicinally interesting.

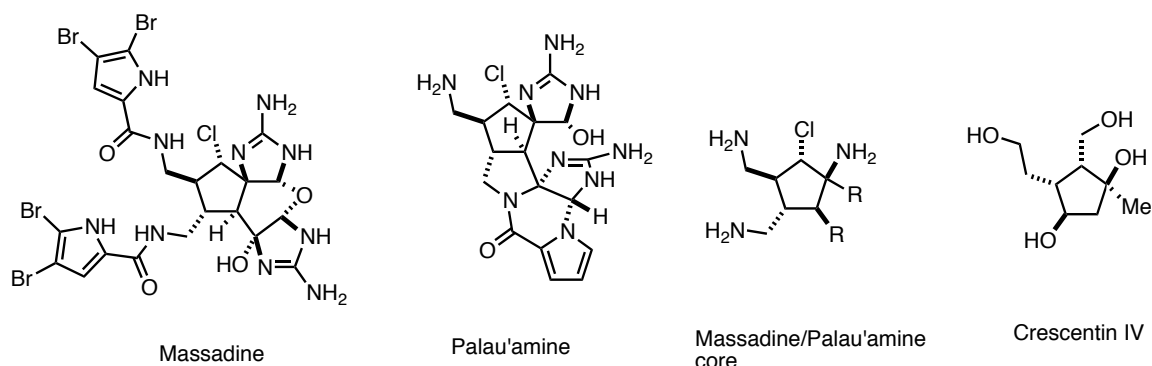
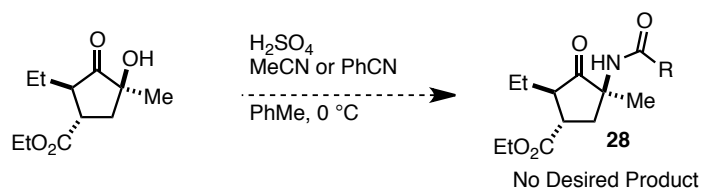


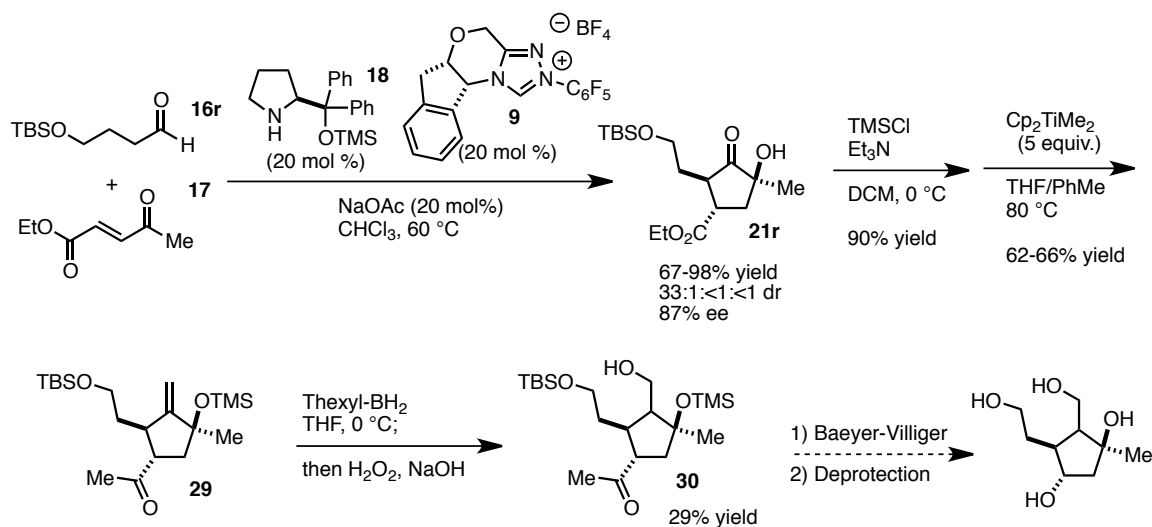
**Figure 2.7**

The syntheses of massadine, palau'amine, and similar compounds have elicited a fair amount of attention from the synthetic community. Much of the work has been in the construction of the densely substituted cyclopentane core. We were curious if our cascade reaction could provide a quick synthesis to this system. However, there are some key differences that need to be addressed. These natural products contain a tertiary amine, which is not present in our products. There are possible routes to introduce this functionality. For example, replacement of the methyl ketone of the Michael acceptor with an imine should lead to similar products. However, all attempts at this proposed reaction were unsuccessful. We then envisioned that this compound could be reached by a Ritter reaction with the tertiary alcohol of the final compound. While initial approaches did not lead to the desired amine, this would be an effective strategy.



**Scheme 2.15**

We initially ventured to synthesize Crescentin IV using this methodology. Synthetically, it bears a cyclopentane core that can be easily accessed through this methodology. Two major obstacles were present: 1) conversion of the ketone group to a hydroxymethyl substituent, and 2) conversion of the ester moiety to a hydroxyl group. Manipulation of the ketone would be straightforward, employing a methylenation of the carbonyl (either by Wittig or with the Petasis reagent) followed by a diastereoselective hydroboration (followed by oxidation). Replacement of the ester group proved challenging. Initial ideas employed the formation of an acyl-peroxide. These are known to be unstable, and after decarboxylation, will leave an acyloxy group. After critical thinking, we determined both of these issues can be resolved by the use of excess Petasis reagent. Not only would this olefinate the ketone moiety, but also the carbonyl of the ester. Mild hydrolysis would reveal the exocyclic methyl ketone. Hydroboration of the newly formed alkene would install the hydroxymethyl group, and a simple Baeyer-Villiger would form the requisite C-O bond.



**Scheme 2.16**

Initial work lead to a cascade product with a protected propanol group, similar to the natural product (**21r**, Scheme 2.16). Treatment of this product to the Petasis reagent was successful, forming the enol ether in 20% yield. Hydrolysis led to the methyl ketone in a 57% yield (not shown). Optimization shows that protection of the tertiary alcohol improves the reaction, and addition of silica gel to the reaction mixture allows for the *in situ* hydrolysis of the enol ether to form **29** in up to 66% yield. Initial studies show that thexyl-borane is capable of the hydroboration of the alkene to form alcohol **30**. At the time, the determination of diastereoselectivity proved difficult. It was also at this time that we decided to discontinue this synthesis. The concurrent determination of the crystal structure revealed that the orientation of the tertiary alcohol formed was incongruent with Crescentin IV, and the synthesis of this compound was abandoned.

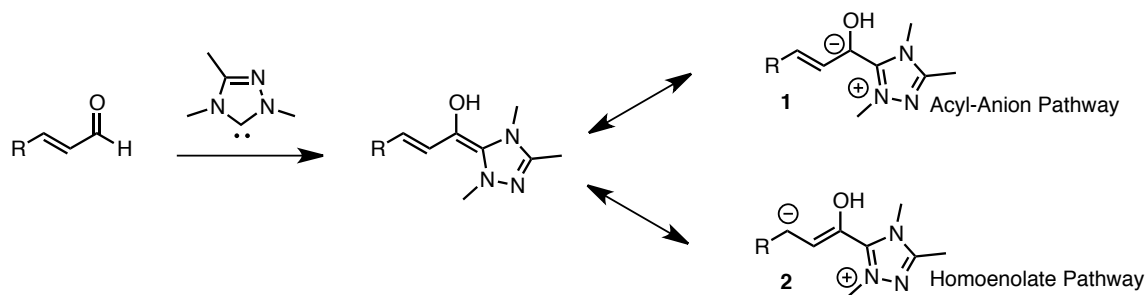
In conclusion, a cascade reaction was developed for the synthesis of complex cyclopentanones in high stereoselectivity. This reaction compliments our previously established work. In addition, our work revealed a unique synergistic cooperation between the amine catalyst and the NHC catalyst. We believe that elaboration of these products could lead to the cores of several bioactive compounds.

## CHAPTER 3

### ASYMMETRIC AMINOMETHYLATION OF ENALS BY NHC CATALYSIS

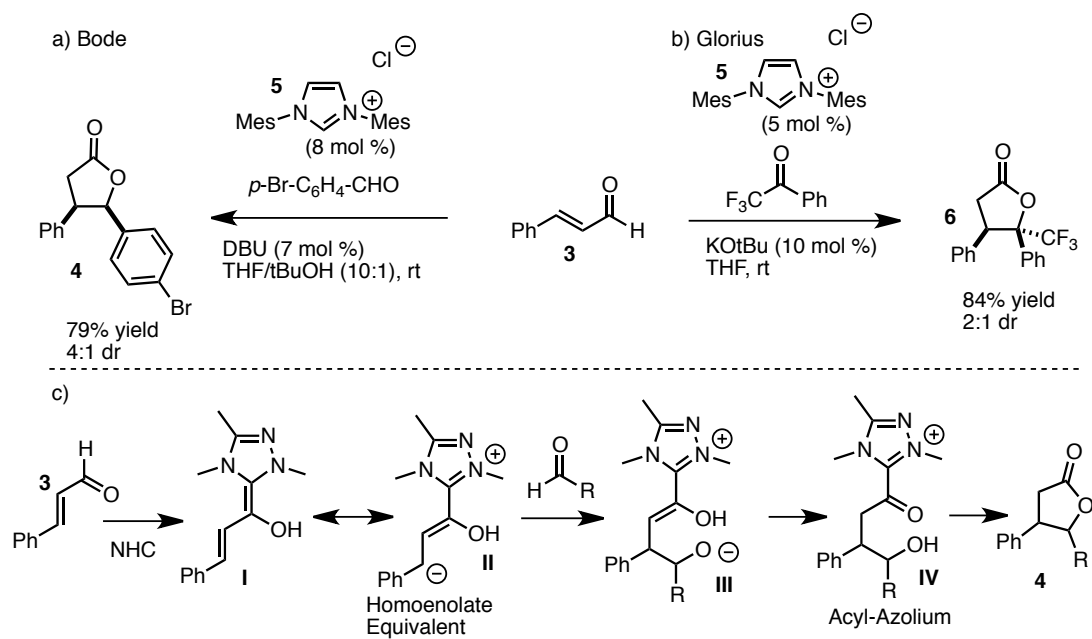
#### 3.1 Homoenate Background

Formation of the Breslow Intermediate is key for observing Umpolung reactivity. This intermediate is formed via the addition of an NHC to an aldehyde. With enals, however, complications arise as the acyl anion is now allylic. Consequently, nucleophilicity can be observed  $\beta$  to the aldehyde (Scheme 3.1). As such, this is termed as ‘homoenate’ reactivity.<sup>71</sup>



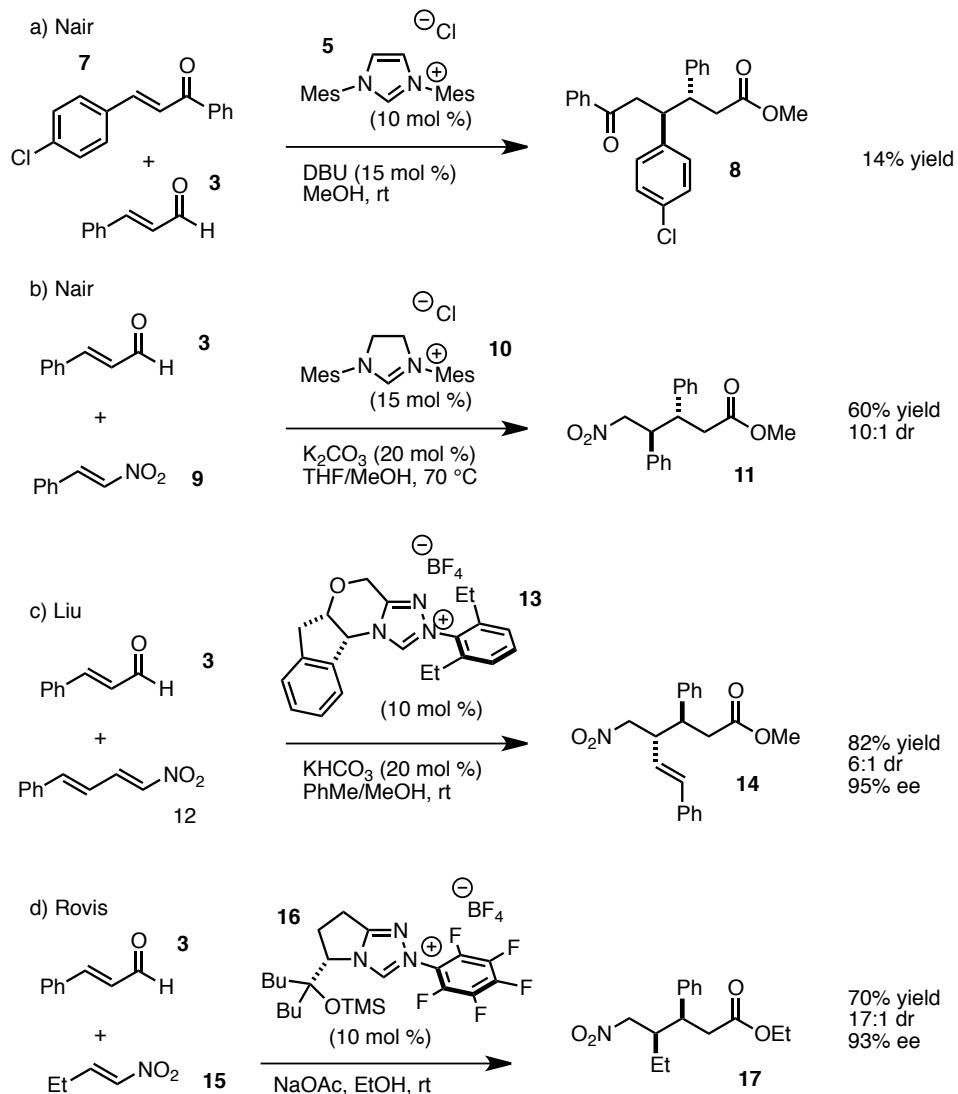
**Scheme 3.1**

Bode<sup>72</sup> and Glorius<sup>73</sup> concurrently reported an example of this with the formation of a  $\gamma$ -lactone that arises from cinnamaldehyde and aryl aldehydes (Scheme 3.2). In this reaction, the enal/NHC adduct undergoes nucleophilic addition with either an aldehyde or ketone at the homoenate position to form adduct **III**. Proton transfers lead to acyl-azolium intermediate **IV**, which undergoes a cyclization to form a lactone **4** or **6**.



### Scheme 3.2

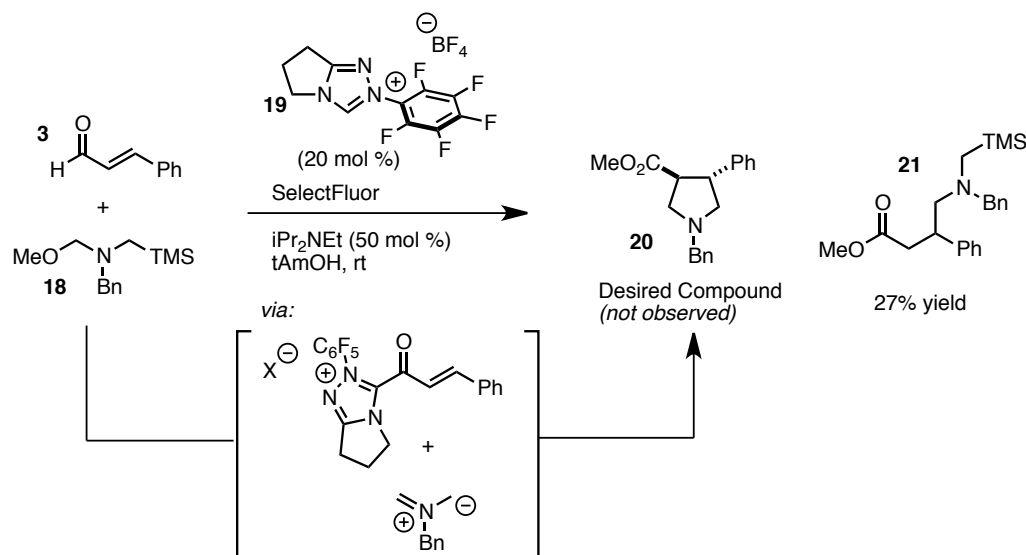
This technology has led to efficient, practical syntheses of a variety of different carbocycles and heterocycles.<sup>71</sup> Recently, there has been a push to develop reactions that form acyclic products. Nair and coworkers reported initial work coupling enals with chalcones to form straight-chain products (though this was observed as a side product).<sup>74</sup> This was followed by further work employing nitro-olefins as substrates.<sup>75</sup> This was expanded with reports of an asymmetric variant from the Liu group<sup>76</sup> and a highly enantio- and diastereoselective procedure from the Rovis group.<sup>77</sup>



### Scheme 3.3

Our initial proposal intended for the catalytic formation of an acyl azolium intermediate by oxidative methods, leading to an activated olefin susceptible to cycloaddition chemistry. This strategy has been utilized by the Lupton lab to form cyclic systems.<sup>78</sup> We envisioned that a [3+2] cycloaddition between enal **3** and iminium precursor **18** would form pyrrolidine **20**. Unfortunately, only a side-product was observed. Elucidation by NMR indicates the side-product is a  $\gamma$ -aminobutyrate

compound **21**, which seems to arise from the homoenolate addition of the cinnamaldehyde and the iminium (Scheme 3.4).



**Scheme 3.4**

This was a fortuitous discovery, as this presents a simple strategy to construct substituted  $\gamma$ -aminobutyrate. The backbone resembles GABA (**22**, Fig 3.1), an essential mammalian neurotransmitter. Derivatives of this compound often display potent bioactivity, and have found use in medical applications.

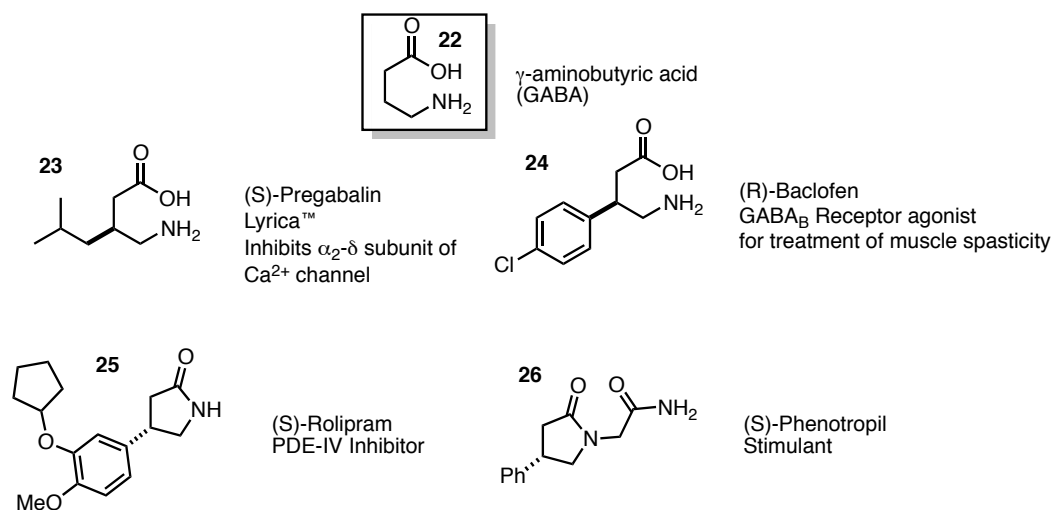
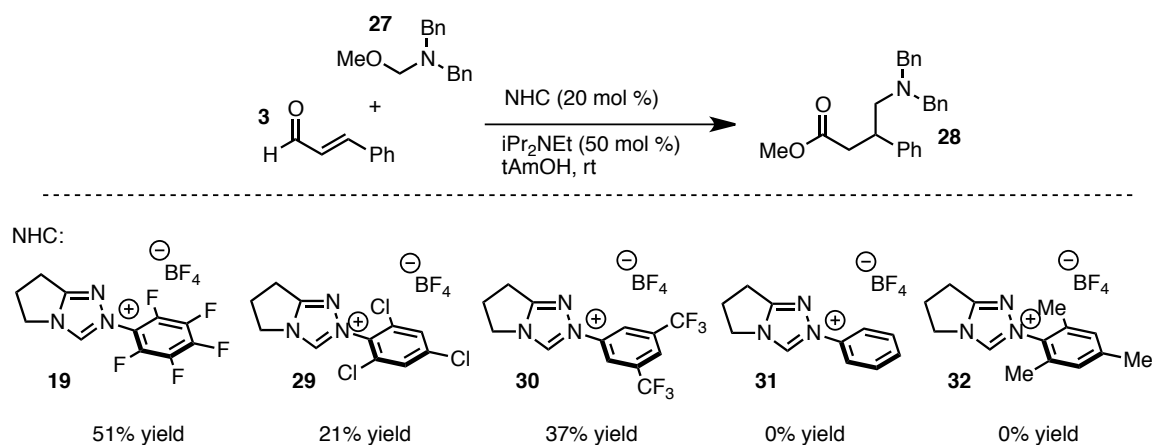


**Figure 3.1**

### 3.2 Reaction Optimization

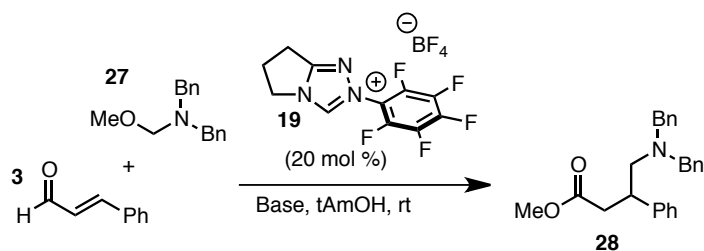
Attracted by the opportunity to quickly access GABA derivatives, we sought to optimize the reaction. A screen of our achiral catalysts revealed that electron-deficient catalysts give satisfactory results, whereas the electron rich *N*-phenyl (**23**) and mesityl (**24**) catalysts yielded no desired product (Table 3.1).

**Table 3.1**



While initial results were positive, the impact of the base was explored (Table 3.2). A full equivalent of base was found to be optimal. Carboxylate

**Table 3.2**



Entry	Base	x (mol %)	yield (%)	Entry	Base	x (mol %)	yield (%)
1	iPr <sub>2</sub> NEt	20	35	7	CsOAc	100	19
2	iPr <sub>2</sub> NEt	100	74	8	LiOAc	100	49
3	iPr <sub>2</sub> NEt	150	50	9	NaOPiv	100	50
4	iPr <sub>2</sub> NEt (+ AcOH)	100	52	10	CsOPiv	100	15
5	NaOAc	100	57	11	DBU	100	0
6	KOAc	100	45	12	K <sub>2</sub> CO <sub>3</sub>	100	0

bases were also effective, with acetates and pivalates providing good yields. However, certain counterions (Li or Cs) lead to side-reactions and lower than expected yield. Stronger bases, such as DBU and  $K_2CO_3$ , provided no product.

Solvent choice has a significant impact on the availability of the iminium precursor. NMR experiments indicate that in tAmOH, a diamino-acetal is formed, which is a less reactive iminium precursor compared to the *N,O*-acetal (Fig 3.2).<sup>79</sup> In contrast, in ethanol or methanol, the parent *N,O*-acetal remains intact. Exchange of the alkoxy groups is also observed between the parent acetals and solvent. The use of organic cosolvents, such as THF, toluene, or DCM, promoted formation of the hydrocinnamates. This is the product of simple protonation of the homoenolate intermediate, which is often termed 'proteo-redox'.<sup>80</sup>

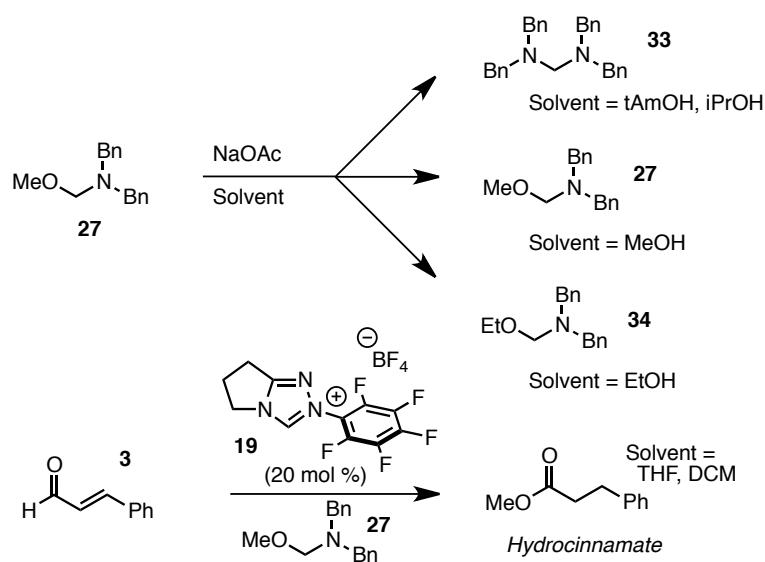
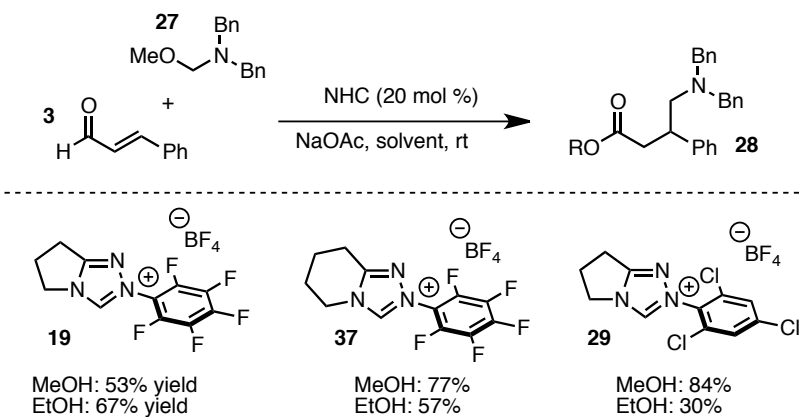


**Figure 3.2**

With methanol and ethanol as excellent solvents at preserving the acetal, several catalysts were rescreened to gauge further improvement in yield. The use of the trichloro-phenyl catalyst is optimal for this reaction. This result corresponds with

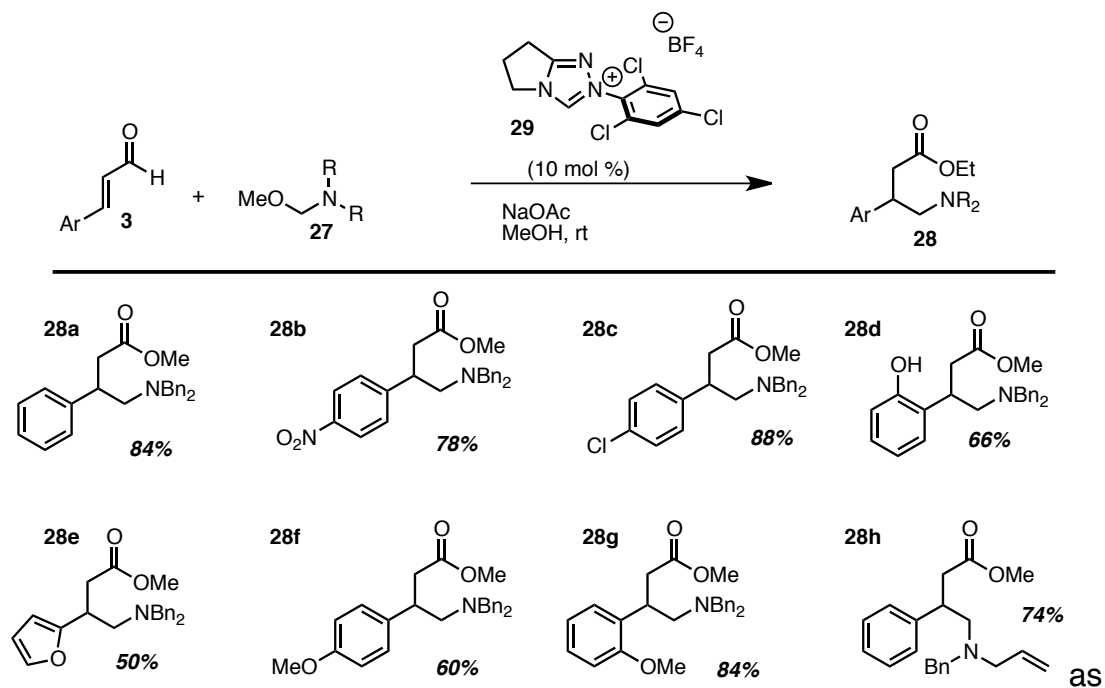
observations made by my colleague Nick White who proposed increasing the steric bulk in the catalyst can inhibit acyl-anion reactivity and promote homoenolate chemistry.

**Table 3.3**



With suitable conditions, the scope of the racemic reaction was explored (Table 3.4). Electron-deficient enals are tolerated in this reaction (**36b** and **36c**) as well as electron-rich enals (**36d**, **f-g**).

**Table 3.4**



Heterocycles show mixed results, with furan demonstrating success (**36e**) whereas 2-pyridyl leads to no desired product (not shown). Variation of the amine is tolerated, allowing for different deprotection strategies (**36h**).

### 3.3 Asymmetric Homoenate/Mannich Reaction

We sought to render this reaction asymmetric. When t-amyl alcohol was used, none of our typical NHC catalysts induced asymmetry (Fig 3.4a). The initial hypothesis was that the increased steric bulk of the chiral catalysts impeded catalyst turnover by methanol and interrupted the catalytic cycle.

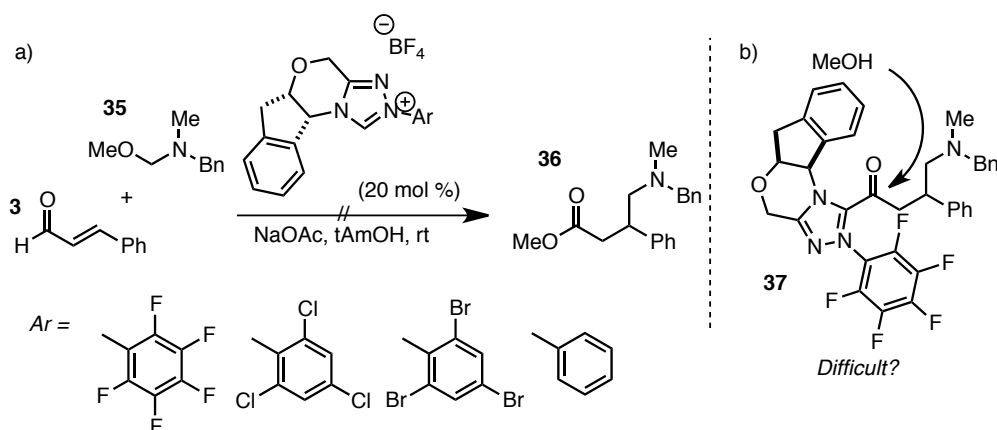
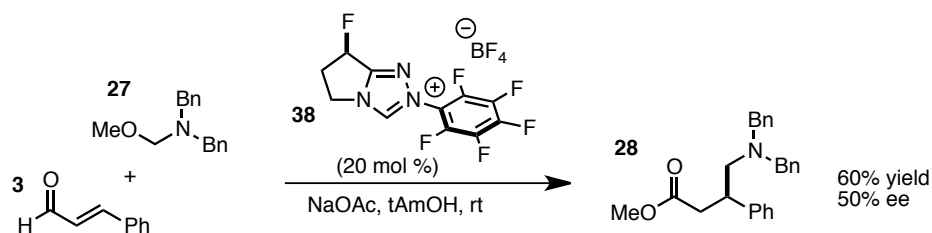


**Figure 3.4**

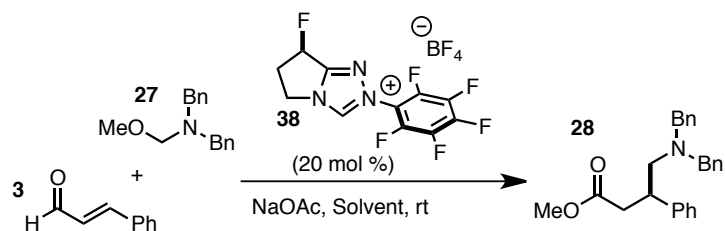
One solution to this issue is to decrease the size of the catalyst. We decided to test catalyst **38** developed by my colleague, Daniel DiRocco, for the asymmetric Stetter reaction.<sup>81</sup> This bears a single, remote fluorine-containing stereocenter, effectively making this the same size as an achiral catalyst. This catalyst provides product in 60% yield and an astonishing 50% ee (Scheme 3.4).



### Scheme 3.4

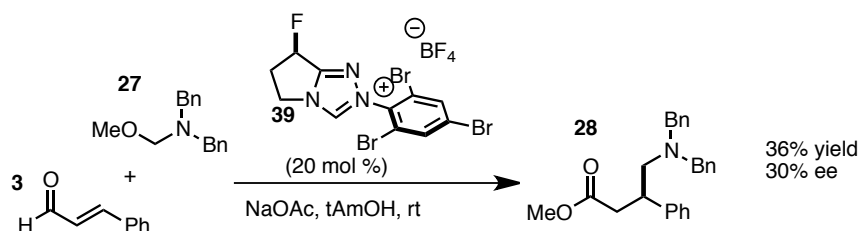
This enantioselectivity was much higher than expected due to the small steric impact of the fluoride that is distant from the active site of the catalyst. We then sought to improve the stereoselectivity of this reaction. Using cosolvents such as THF or  $\text{CHCl}_3$  provided no product, only hydrocinnamate products (Table 3.5). Toluene as cosolvent improved enantioselectivity slightly to 55% ee. Methanol effectively erases any enantioselectivity. Reduction in reaction temperature also lowers yield and enantioselectivity.

**Table 3.5**



Entry	Solvent	yield (%)	ee (%)
1	1:1 tAmOH/THF	0	--
2	1:1 tAmOH/ $\text{CHCl}_3$	0	--
3	1:1 tAmOH/PhMe	65	55
4	1:1 tAmOH/MeOH	63	4
5	tAmOH (0 °C)	34	6

Regarding catalyst design, the introduction of the N-tribromophenyl group (**39**) led to a decrease in selectivity (Scheme 3.5). While interesting, there were no promising trends with this catalyst, and alternative strategies were explored.



### Scheme 3.5

Maintaining the hypothesis the catalyst turnover was problematic with the larger chiral catalyst, a change of solvent was explored. An HTE (High Throughput Experimentation) screen with several aminoindanol based catalysts was tested against three different alcohol solvents and eight different bases. To our delight, these catalysts are effective in the reaction (Figure 3.3).

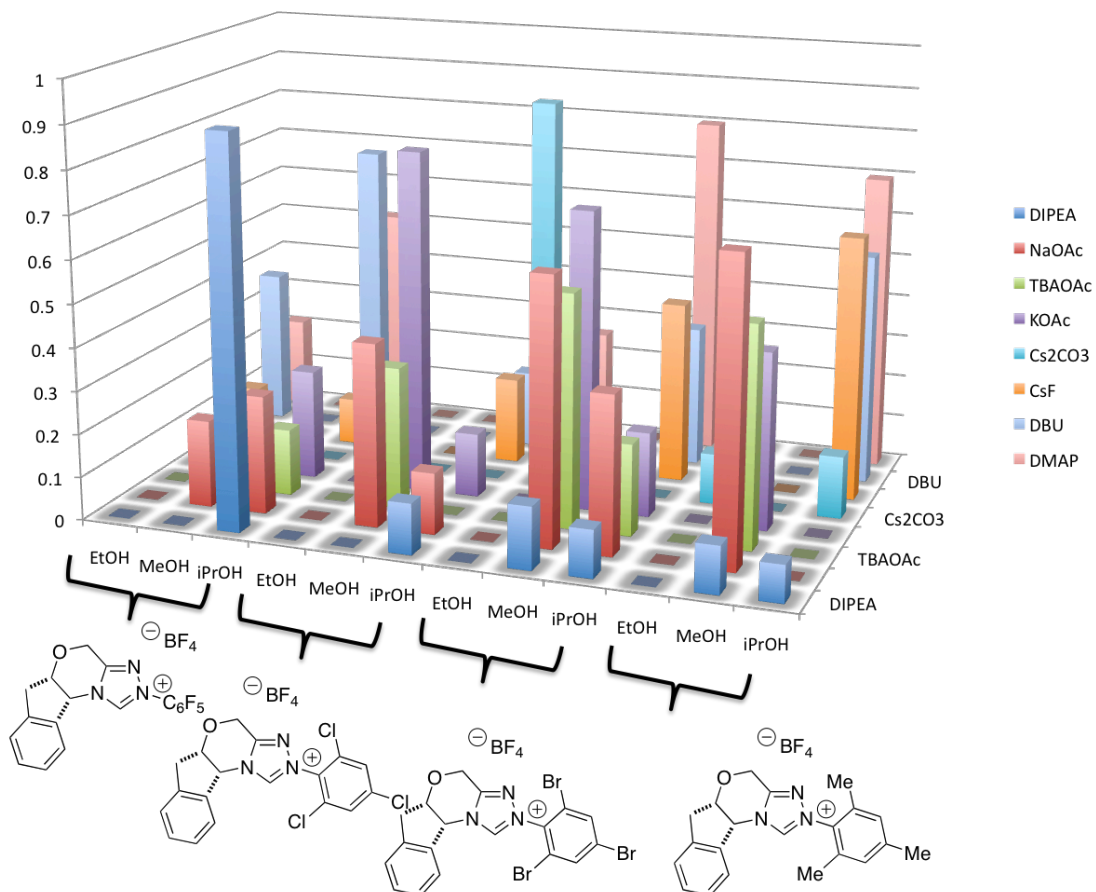
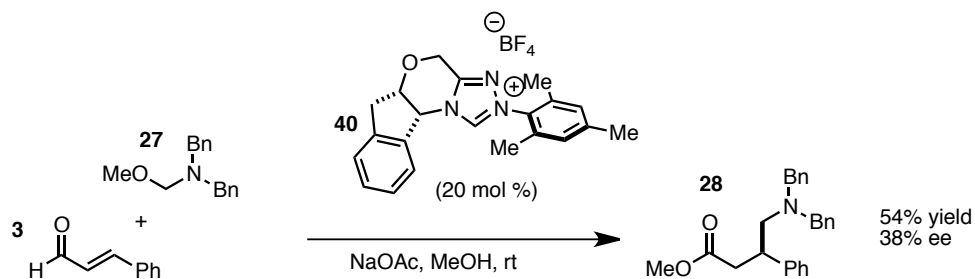


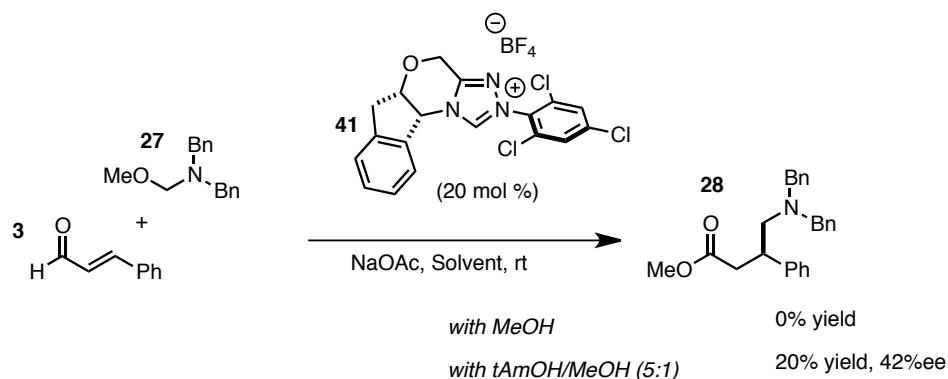
**Figure 3.3**

Scaling up the reaction using the catalyst **33** in methanol reveals formation of product in 54% yield and 38% ee (Scheme 3.6).



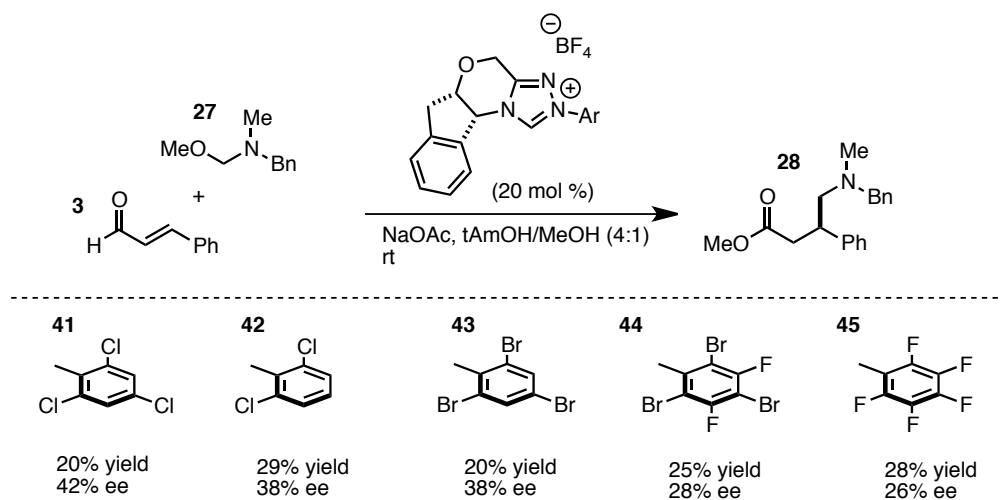
**Scheme 3.6**

Curiously, this system was unsuitable for other catalysts. However, using a mixture of *t*-amyl alcohol and methanol allows for bulky, electron-deficient catalysts to be utilized (Scheme 3.7). Unfortunately, results remain mediocre (Table 3.6).



### Scheme 3.7

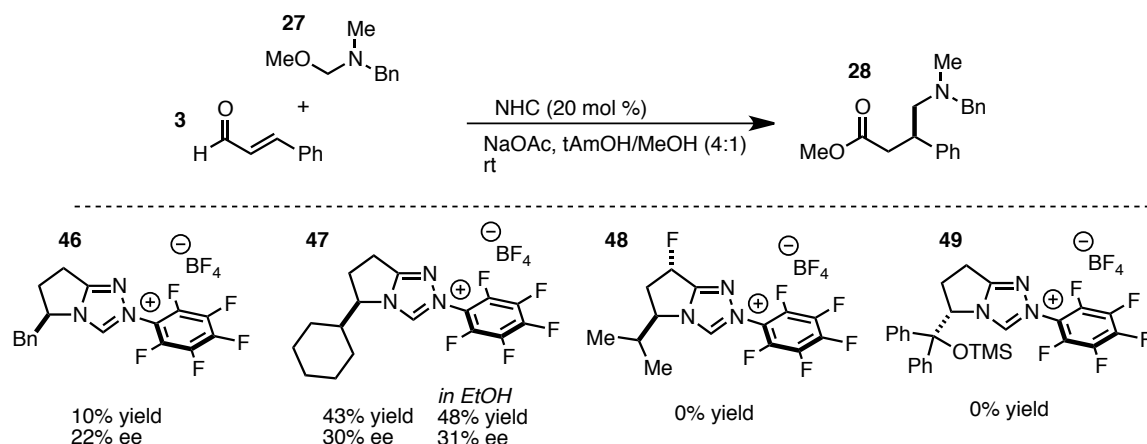
Table 3.6



NHC catalysts bearing a bicyclic backbone are also effective in this reaction (Table 3.7). Benzyl substituted catalyst **46** formed the desired product in low yields. The cyclohexyl substituted catalyst **47** showed improved reactivity, with similar results with EtOH as the solvent. However, not all catalyst scaffolds failed to yield any desired products. Catalyst **48** promoted formation of side-products. Also catalyst **49**, which

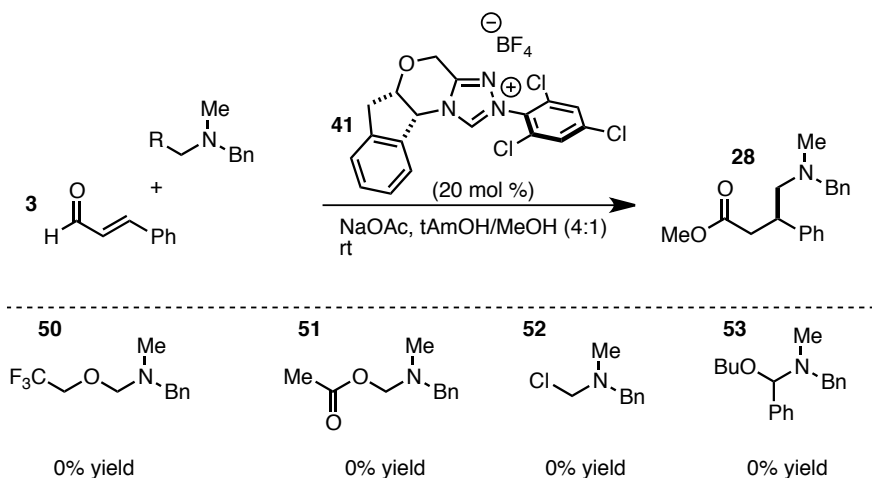
favors homoenolate reactivity in our work with nitroolefins,<sup>77</sup> does not lead to product formation in this reaction.

**Table 3.7**



The nature of the iminium precursor was also explored (Table 3.8). Activated aminals proved to be highly reactive and unstable, while the substituted iminium **53** was unreactive as a substrate.

**Table 3.8**



Even though some progress has been made, a general solution for rendering this reaction asymmetric has not been discovered as of yet. Changes in reaction conditions

reveal no promising trends, so the best direction seems to be in the design of new catalysts. Chapter 4 will provide detail in these efforts. However, at this time a suitable catalyst has yet to be discovered.

### 3.4 NHC Catalyzed Aza-Morita-Baylis-Hilman

A persistent challenge encountered in this chemistry is reaction selectivity. During the course of these studies, products formed from side reactions were isolated in varying amounts. The hydrocinnamate product (**54**), derived from the protonation of the homoenolate equivalent, is one side-product that was expected (Figure 3.5).

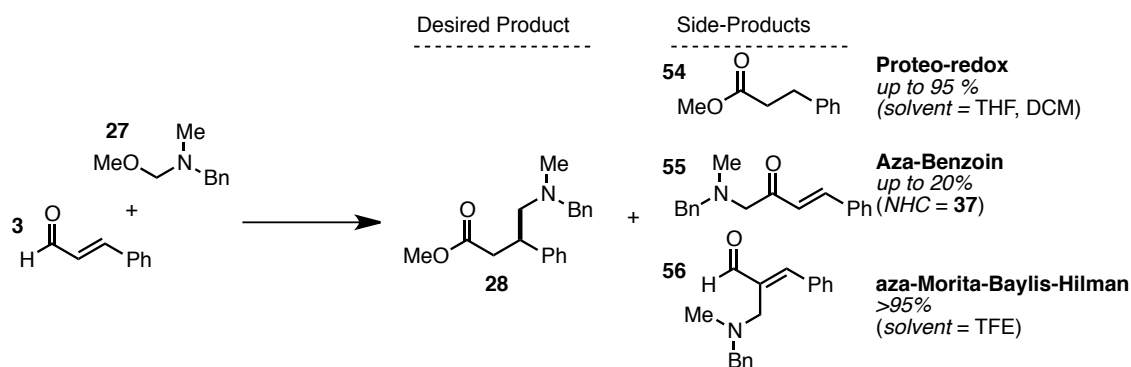
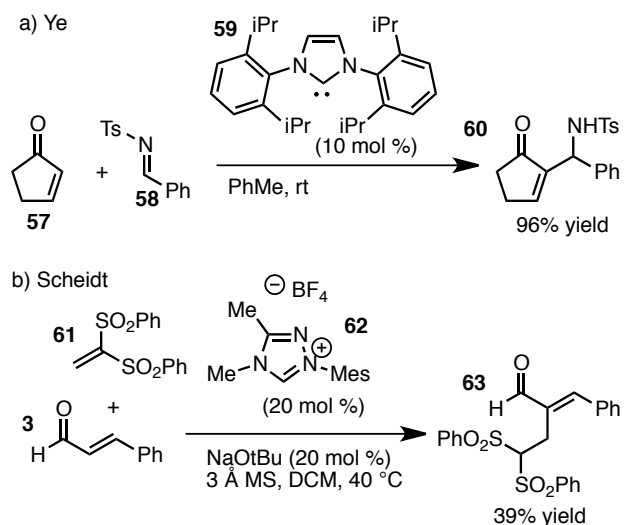


**Figure 3.5**

In addition, an aza-benzoin product (**55**) is occasionally formed in the course of this reaction. This is most often seen with the use of catalyst **37**. This is not a surprising result, as similar products were reported by López-Calahorra.<sup>82</sup>

An unexpected result was the formation of the aza-Morita-Baylis-Hilman adduct **56**. While there has been extensive work with this reaction, reports using NHC catalysis are quite rare. Song Ye reported a similar transformation using an imidazolium catalysis

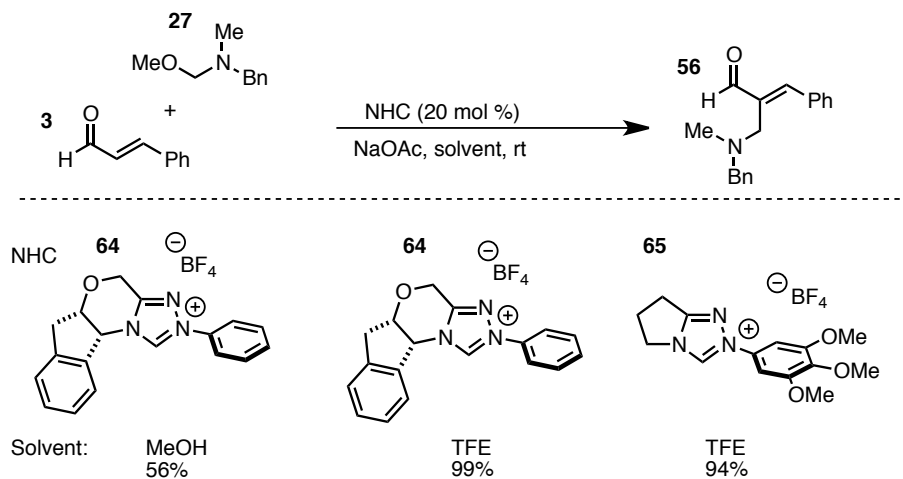
between cyclic enones and tosyl-imines (Scheme 3.7a).<sup>83</sup> In a related reaction, Scheidt and coworkers reported an NHC catalyzed Rauhut-Currier reaction with enals and bis(sulfonyl)alkenes (Scheme 3.7b).<sup>84</sup> With few examples reported, we decided to explore this reaction further.



### Scheme 3.7

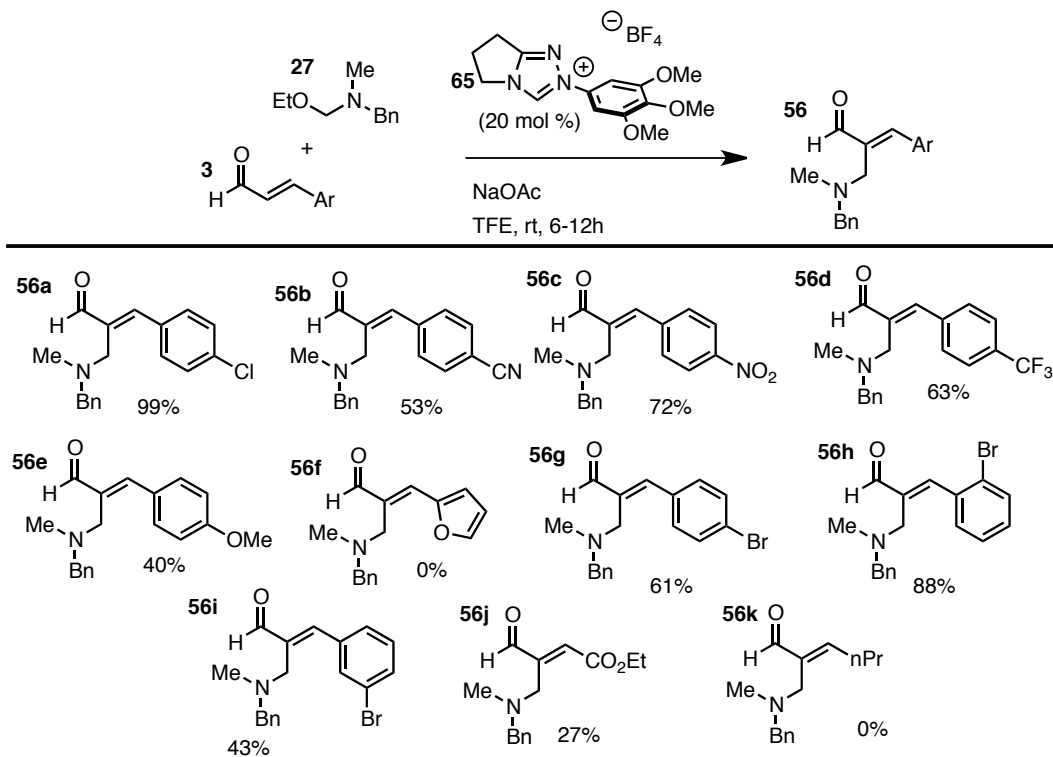
With the help of a talented undergraduate student, Adam Golos, the reaction was optimized. The initial hit for the reaction was with chiral catalyst **64** with an *N*-phenyl group (Table 3.9). While the yields were adequate, this catalyst demonstrated increased selectivity for this product. With trifluoroethanol as solvent, the yield of the reaction is drastically improved. However, we found it superfluous to use a chiral NHC catalyst to form achiral products. Various achiral catalysts were screened, and catalyst **65** with a 3,4,5-trimethoxyphenyl group proved optimal.

**Table 3.9**



With suitable conditions at hand, Golos worked on elucidating the scope of the reaction (Table 3.10). Electron-deficient enals make excellent substrates, with cyano-cinnamaldehyde being the exception (**56b-d**).

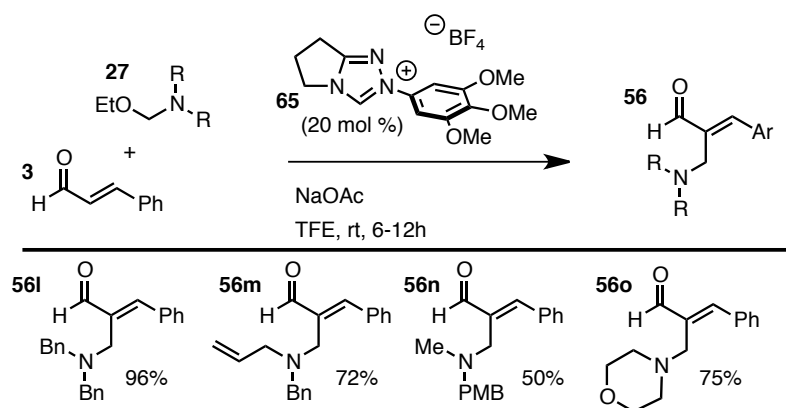
**Table 3.10**



Electron-rich enals are not well tolerated, and a furyl group shuts down reactivity(**56e-f**). In terms of substitution, *o*-bromo-cinnamaldehyde (**56h**) performs better than *p*-bromocinnamaldehyde (**56g**), while the *m*-substitution is not well tolerated (**56i**). A butenoate substrate provides the expected product **56j**, albeit in low yields. This is notable as this enal is not a suitable substrate in the homoenolate chemistry. Alkyl-substituted enals are not converted to product.

Substitution of the amine with various protecting groups is tolerated (Table 3.11). The dibenzylamine and allyl benzylamine lead to product formation in high conversion (**56l-m**). The use of a morpholine based acetal is also effective (**56o**), allowing for the incorporation of heterocycles.

**Table 3.11**



In conclusion, our work has revealed new synthetic access to  $\gamma$ -aminobutyrate through a homoenolate/Mannich reaction. This route provides access to a biologically relevant group of compounds. As of yet, we have not discovered conditions to form these compounds in high stereoselectivity. With further work and time, this goal can

certainly be achieved. In addition, we have revealed a rare case of an aza-Morita-Baylis-Hilman reaction using NHC catalysis.

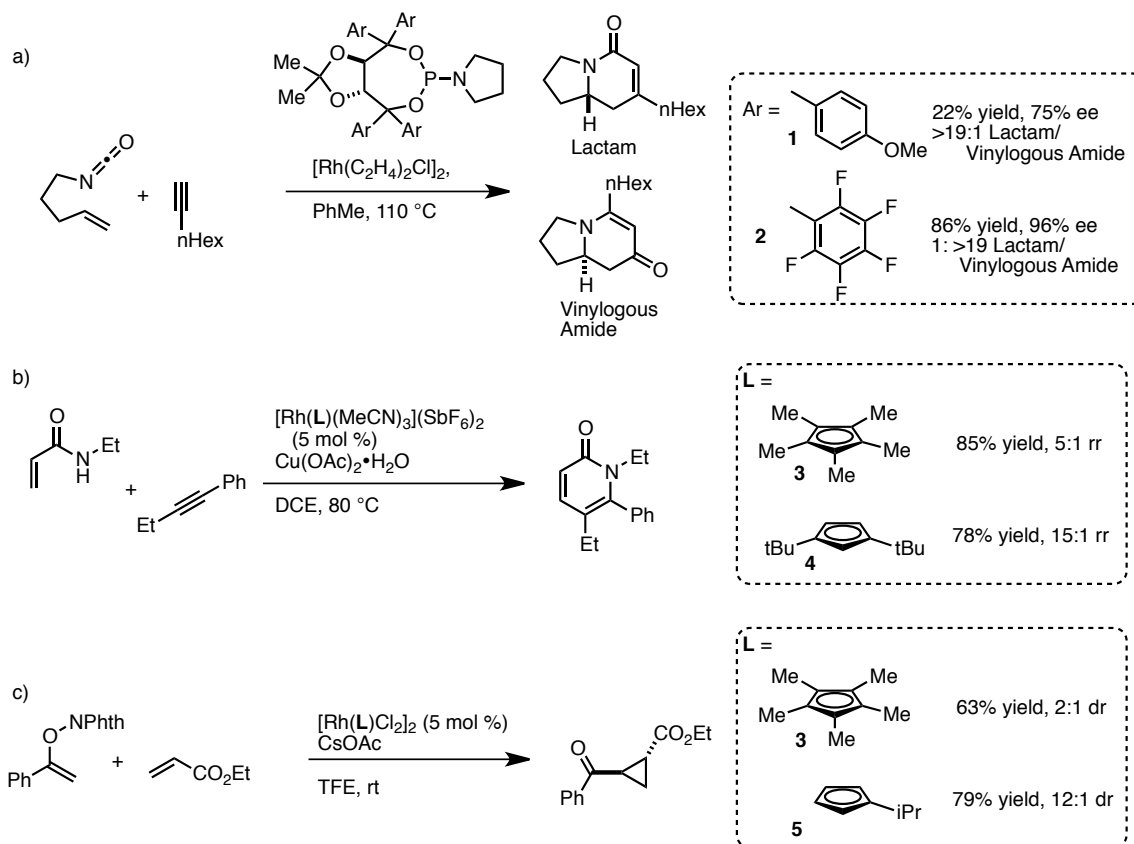
CHAPTER 4  
STRATEGY FOR THE LATE-STAGE MANIPULATION OF TRIAZOLIUM-BASED  
CATALYSTS

**4.1** *Significance of Catalyst Design*

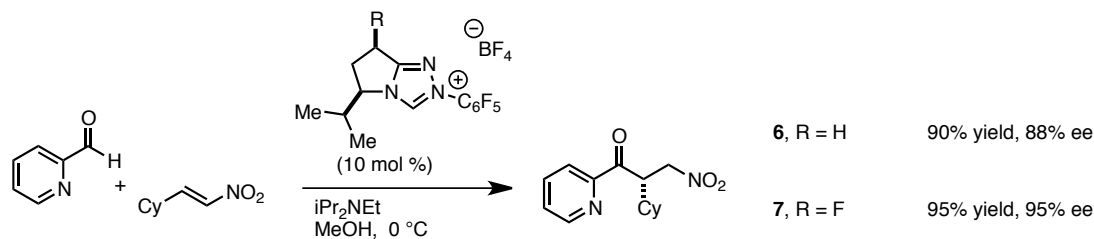
In our group's work in Rhodium catalysis, we see strong impact from the selection of ligand, and catalyst design has emerged as a strong tradition. For example, in the Rh-catalyzed [2+2+2] cycloaddition, the use of the perfluorinated phosphoramidite ligand **2** shows enhanced selectivity (Scheme 4.1a).<sup>85</sup> In the Rh(III)-catalyzed formation of pyridones from acrylamides, there is a substantial enhancement of regioselectivity with a bis(*t*-butyl) substituted Cp ligand **4** is used instead of pentamethyl Cp **3** (Scheme 4.1b).<sup>86</sup> The same is observed in recent work describing the Rh-catalyzed cyclopropanation of acrylates (Scheme 4.1c).<sup>87</sup> As such, catalyst design is considered critical for reaction success.

Design and modification of N-heterocyclic carbene catalysts has also led to significant improvements in reaction performance. One example is work accomplished by my colleague Daniel DiRocco in his work with the asymmetric intermolecular Stetter reaction with nitroalkenes (Scheme 4.2). He designed NHC catalyst **7** that bears a single fluoride on the backbone, distant from the active site.<sup>88</sup> The single modification leads to significant improvements in enantioselectivity. Lessons learned from this

achievement were critical for the success of future asymmetric intermolecular Stetter reactions, both by our group and others.<sup>89</sup>



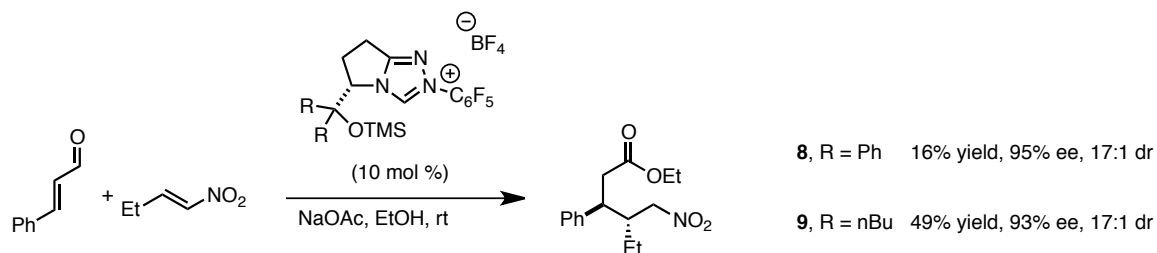
**Scheme 4.1**



**Scheme 4.2**

In the development of the asymmetric homoenolate addition of enals with nitroalkenes, Nicholas White explored catalyst modification to improve selectivity (Scheme 4.3).<sup>90</sup> His work revealed that pyroglutamate-derived catalysts were the most promising. While the reported diphenyl-catalyst **8** provided good results, he explored modification as a way to

enhance selectivity. Indeed, the dibutyl-catalyst **9** was key to the success of this reaction.



**Scheme 4.3**

In NHC catalysis, our group employs two classes of catalysts: amino-acid based and aminoindanol based (Figure 4.1).<sup>91</sup> The NHC catalysts derived from amino-acids have proven to be a reliable scaffold due to the variety of chiral amino-acids, both natural and synthetic, that can serve as starting material for catalyst synthesis. Inherently, a diversity of catalysts can be rapidly constructed.

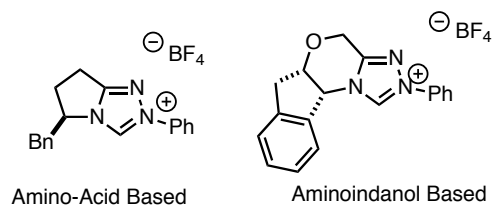


**Figure 4.1**

The aminoindanol scaffold, for the time being, has proven difficult to modify. The enantioenriched aminoindanol (Fig 4.2) is a key structural compound of the HIV drug indinavir<sup>92</sup> (trade name: Crixivan). With large amounts of this compound available, the enantioenriched aminoindanol can also be found in other catalysts. These include in PHOX ligands,<sup>93</sup> BOX ligands,<sup>94</sup> as well as chiral thiourea catalysts.<sup>95</sup> While popular, there are only a few examples of modification of this motif.

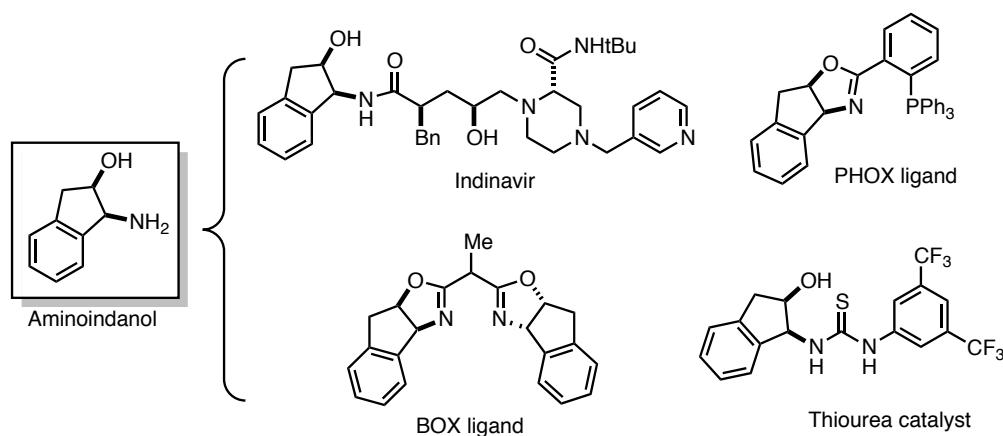
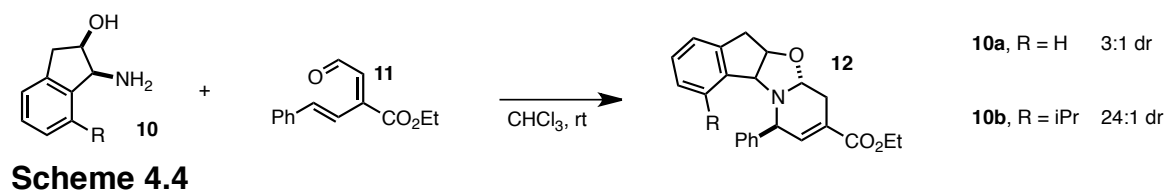


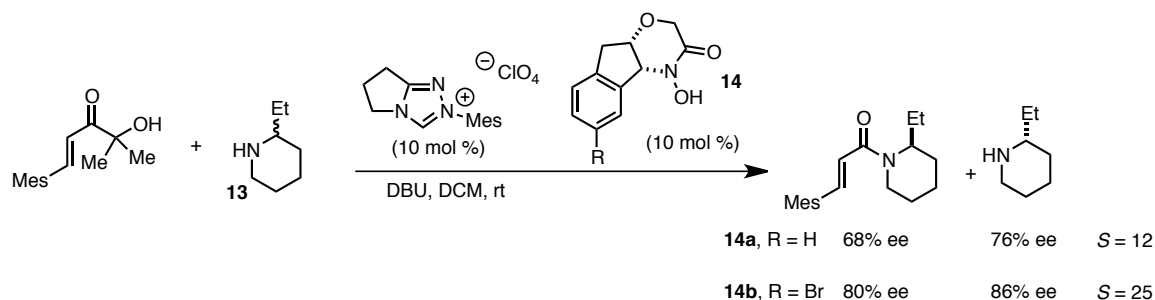
**Figure 4.2**

#### 4.2 Modification of Aminoindanol Scaffold

One example is work reported by the Katsumara group.<sup>96</sup> Their work is concerned with the development of an asymmetric 6 $\pi$  cyclization as a method to form enantioenriched piperidines (**12**, Scheme 4.4). Crucial to this reaction was the use of the chiral aminoindanol **10** as an auxiliary. Initial work with auxiliary **10a** produced compounds in a 3:1 dr. As a route to improve this, they explored installing alkyl groups to the C-7 site of the aminoindanol. This dramatically improves diastereoselectivity to an impressive 40:1 dr with **10b**. It should be noted, however, that the synthesis of these modified amino-indanols can be lengthy, involving between 9-11 steps. This provides a substantial barrier in supplying more derivatives.

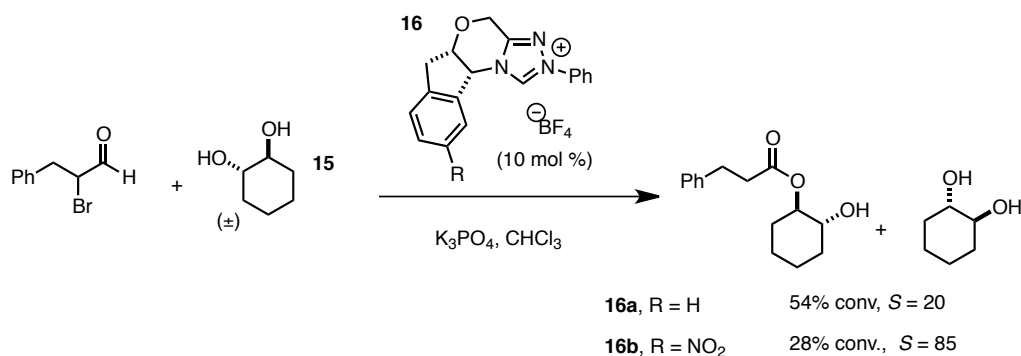


Work by Bode and coworkers provide another great example. In the kinetic resolution of chiral secondary amines, they employ chiral hydroxamic acid co-catalyst **14** derived from the aminoindanol (Scheme 4.5).<sup>97</sup> An improvement in *S*-factor is observed with a catalyst bearing a bromide at C-6 (**14b**). Dibromination, on the other hand leads to no improvement in selectivity. In addition, these aminoindanol variants are fairly simple to produce: electrophilic bromination under acidic conditions yields the 6-substituted bromide selectively from the parent lactam.



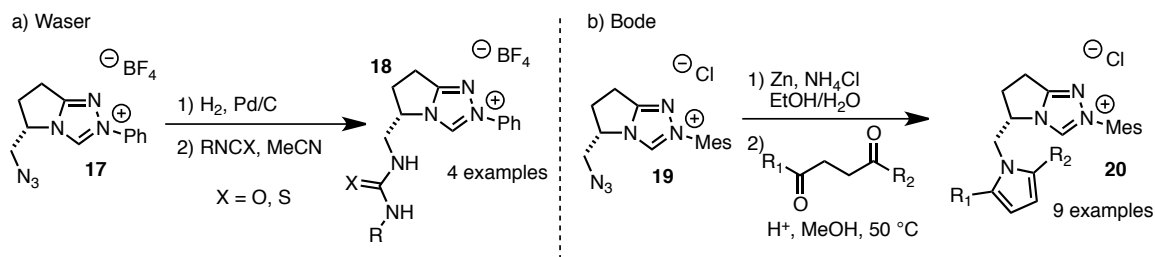
**Scheme 4.5**

Besides electrophilic bromination, the aminoindanol scaffold is susceptible to nitration at the 6-position as well. This was exploited by Takasu and Yamada for the synthesis of nitrated aminoindanol derivatives **16** (Scheme 4.6).<sup>98</sup> The material was taken on to construct a triazolium salt used for the kinetic resolution of meso-diols **15**. The nitrated-aminoindanol is not completely unprecedented, as a group from Eli Lilly used this scaffold for the synthesis of an M1 agonist.<sup>99</sup> However, they use a parent nitro-indanone as starting material in contrast to the late stage installation demonstrated by Takasu and Yamada.



#### Scheme 4.6

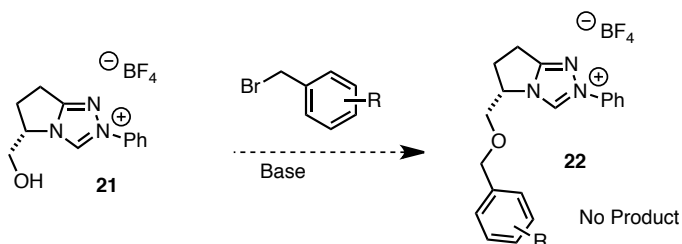
In the course of research at CSU, we were curious about methods for late-stage modification of our triazolium salts. This was inspired by work of Waser and Bode (Scheme 4.7). Waser reported the late stage modification of a triazolium salt **17** by careful reduction of a tethered azide.<sup>100</sup> The primary amine formed is then captured by a thioisocyanate to form a pendant thiourea side chain. In a similar fashion, Bode used a similar starting strategy to arrive at triazolium **19** bearing a primary amine,<sup>101</sup> which is then condensed with various 1,4-diketones to quickly access a variety of catalysts with pyrrole side chains (**20**).



#### Scheme 4.7

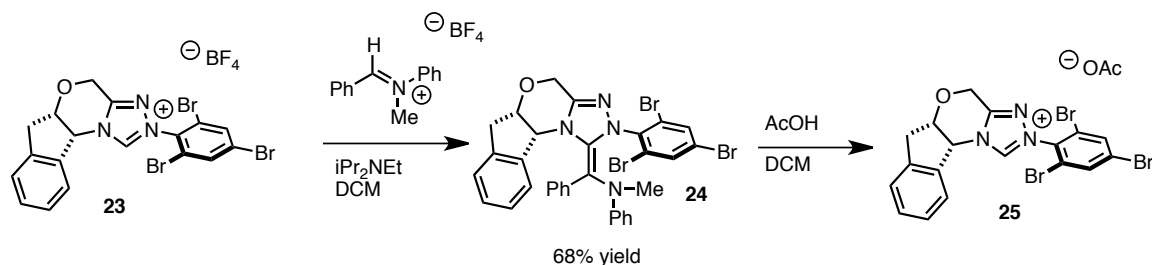
Concurrently, we explored ways for the late stage modification of catalysts as well. However, basic conditions lead to the deprotonation of the triazolium and can often lead to side reactions. Our initial efforts in the alkylation of alcohol-containing

catalysts met with failure (Scheme 4.8). A method to ‘protect’ the triazolium from basic conditions would allow for easy modification, and so we sought methods that can serve as a way to protect the catalyst.



**Scheme 4.8**

One such idea came during the discovery of the ‘aza-Breslow’ intermediate. DiRocco encountered this adduct in his work in the aza-benzoin reaction.<sup>102</sup> Exposure of a triazolilylidene with an iminium leads to the formation of compound **24** (Scheme 4.9). Furthermore, this formation is reversible, and the free NHC **25** can be liberated by acidic conditions. With easy formation and recovery, this showed promise as a way to protect the triazolium. Unfortunately, isolation of stable aza-Breslow intermediate is limited to a few specific systems.



**Scheme 4.9**

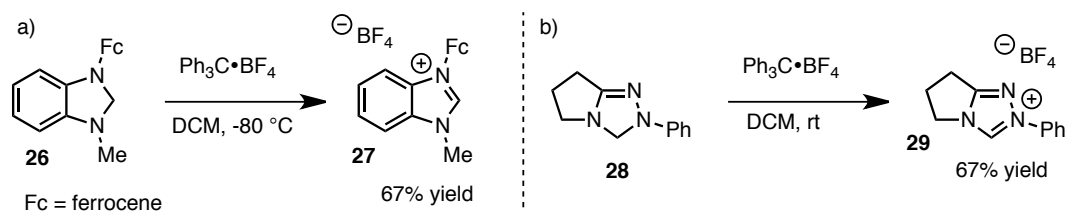
We imagined that reducing the triazolium to the triazolene would access intermediates that would tolerate basic conditions. Reduction by Pd-catalyzed hydrogenation did not yield the desired product, so boron based reagents were then

explored. Sodium borohydride ( $\text{NaBH}_4$ ) is an effective reagent, but conditions proved harsh and yields are low. By running the reaction at  $0\text{ }^\circ\text{C}$  in a 10:1 ratio of DCM/EtOH (or DCM/ $\text{H}_2\text{O}$ ), the product can be isolated cleanly (see Table 4.1). Dependent on the purity of the starting material, the reduction proceeds cleanly and no further purification is needed. For milder conditions, sodium triacetoxyborohydride ( $\text{NaBH}(\text{OAc})_3$ ) can be used as well, but this is limited to electron-deficient catalysts (i.e.: catalysts bearing an *N*-pentafluorophenyl group). Plenio and coworkers employed this strategy in their modification of imidazolinium-based catalysts.<sup>103</sup>

#### 4.3 Oxidation by Trityl Salts to Form Triazoliums

With a method to convert triazoliums to triazolines, we then explored conditions for the reverse reaction. Bildstein and coworkers described the synthesis of benzimidazolines bearing an *N*-ferrocenyl group and an *N*-Methyl group.<sup>104</sup> This is then oxidized to the benzimidazolium salt **27** by exposure to triphenylcarbenium (aka trityl) tetrafluoroborate (Scheme 4.10a). We were curious if this strategy would work to form triazoliums. To our delight, exposure of the triazoline **28** to trityl  $\text{BF}_4$  at room temperature in DCM led to clean conversion to the desired triazolium **29** (Scheme 4.10b). A method was then sought to separate the triphenylmethane side-product from the triazolium. This can be accomplished by addition of diethyl ether to the reaction. The triazolium salt precipitates as a powdery solid, and filtration separates the product from any waste material. In contrast to our traditional catalyst synthesis, where

formation of a workable solid can sometimes be elusive, this approach reliably provides the catalyst as a free flowing solid.

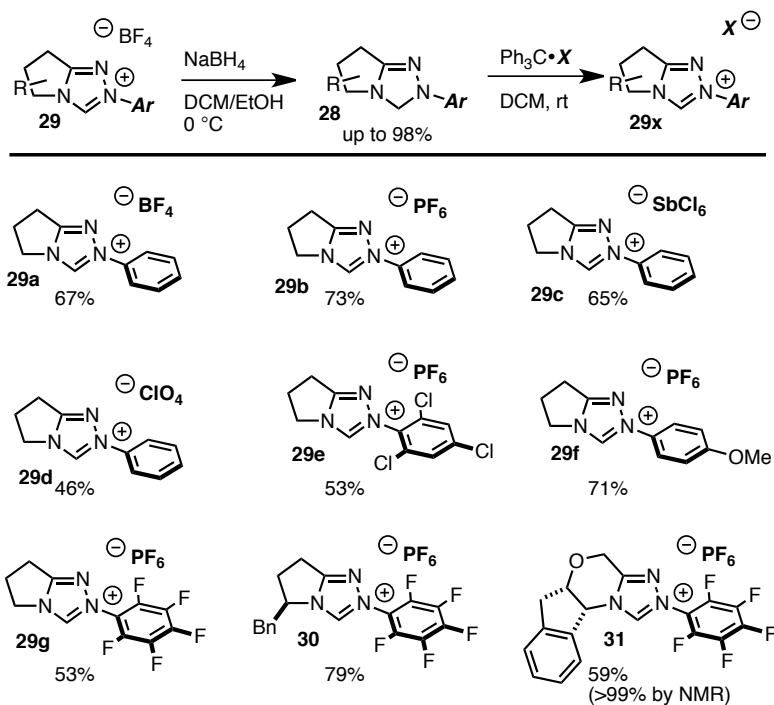


### Scheme 4.10

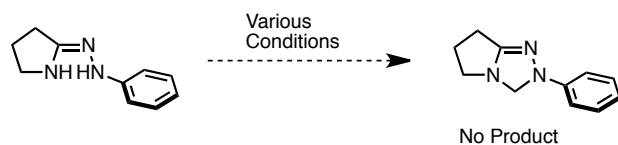
We then screened this method with various triazolines. This reaction works well with electron-rich, electron-deficient, and bulky substrates (Table 4.1). Additionally, the method can be used to introduce new counterions, such as hexafluorophosphate (**29b**) and hexachloroantimonate (**29c**). Chiral substrates (**30** and **31**) also are competent in this reaction.

A direct synthesis of triazolines, side-stepping the reduction of a triazolium, would be a welcome advantage for this method.<sup>105</sup> Similar to what Bildstein reported, we imagine that formation of a hydrazide followed by cyclization with formaldehyde would yield the triazoline.<sup>106</sup> Unfortunately, attempts with cyclization were unsuccessful and only starting material was isolated (Scheme 4.11). Under more forcing conditions, the hydrazide simply hydrolyzes and the amide precursor is recovered.

**Table 4.1**



Other C1 sources were explored, including diiodomethane,<sup>107</sup> dibromomethane, dimethoxymethane, and the Glorius reagent (chloromethyl pivalate),<sup>108</sup> but no desired product was formed. It was at this time that a visiting graduate student, Milind Jadhav of the University of Camerino, continued in the search for conditions to synthesize a triazoline. Despite intense effort, he also was unable to find suitable conditions (Scheme 4.11).

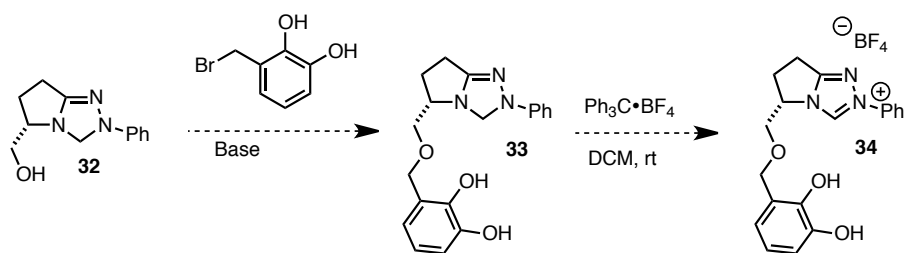


**Scheme 4.11**

One issue that manifested itself during this work was the lability of triazolines. Under acidic conditions, these products decompose. The electronics of the *N*-aryl group seem to have the biggest impact in this property. Phenyl and methoxy-phenyl substituted triazolines decompose upon exposure to silica gel, and the methoxy-phenyl variant can degrade at room temperature after several days. Electron-deficient analogs tend to show increased stability, and can tolerate column chromatography with silica gel. With this in mind, purification of triazolines is usually accomplished with basic alumina as the solid phase. Similar observations were described by Plenio and coworkers in their work with imidazoliniums. In their report, symmetrical imidazolines are accessed by condensation with formaldehyde, but unsymmetrical analogs proved difficult. They thus formed the imidazolium salt and reduced to the desired compound, which is the route we selected.

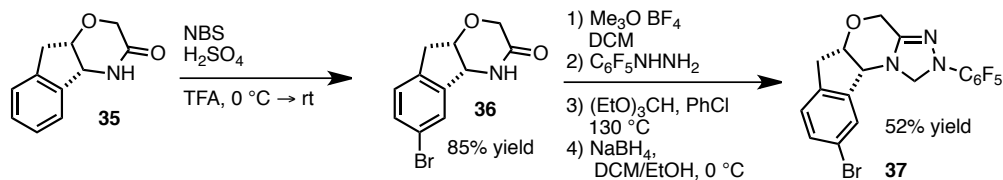
#### ***4.4 Cross-Coupling as Strategy for Late-Stage Modification***

Our initial strategy involved alkylation of an NHC catalyst. A triazoline with a free hydroxyl group can be accessed from pyroglutamic acid. Our aim was to attach an additive at this position. Previous work has demonstrated some key additives that improve various NHC catalyzed reactions, specifically carboxylic acids and catechol.<sup>109,110</sup> My colleague, Phil Goldblatt, explored the syntheses of these compounds (Scheme 4.12). However, this chapter will focus on the manipulation of the aminoindanol scaffold.



### Scheme 4.12

The brominated lactam, as reported by Bode, could provide opportunity for downstream modification. Bromination of the amide precursor formed the precursor **36** (Scheme 4.13). The material is carried forward through traditional catalyst synthesis,<sup>113</sup> then reduced with NaBH<sub>4</sub> and purified by column chromatography (Scheme 4.13). This provides product **37** as a clean solid that is easy to work with.



### Scheme 4.13

We decided the aryl bromide would serve as an excellent substrate for a Suzuki-Miyaura cross-coupling.<sup>111</sup> This would be useful method for the introduction of aryl groups to this scaffold. To fully appreciate this, it is worth examining an X-ray crystal structure obtained of the aminoindanol-based catalyst (Fig 4.3).<sup>112</sup> The aryl group of the aminoindanol portion is almost perpendicular to the triazole ring. This arrangement is

effective in imparting enantioselectivity in acyl-anion chemistry, as seen in successful cases of asymmetric benzoin and Stetter reactions (see Chapter 1). However, with the emergence of homoenolate chemistry with NHC catalysis, this conformation might have little effect in setting the more distant stereocenter. Installing large substituents on the aminoindanol could be a remedy.

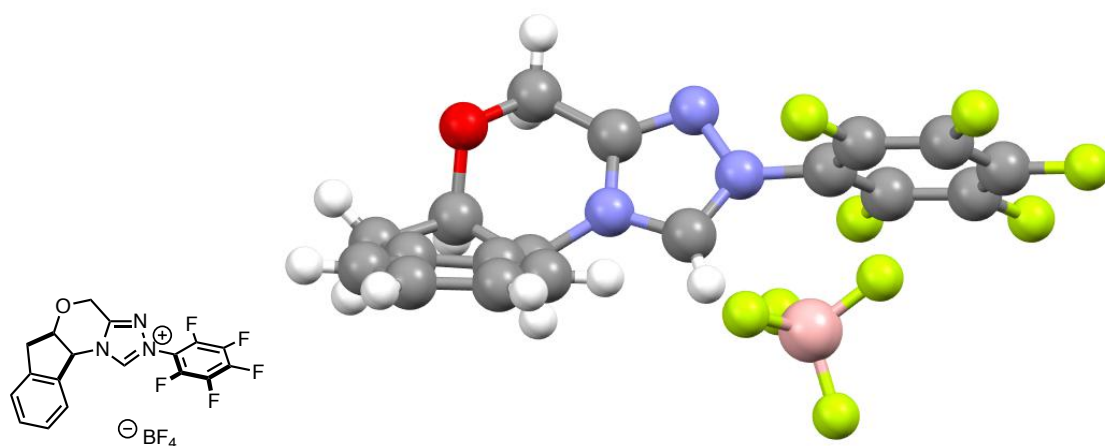


**Figure 4.3**

To determine optimal conditions for the Suzuki coupling, High-Throughput Experimentation (HTE) was employed. HPLC results from the HTE experiment show two promising set of conditions (Fig 4.4). While sodium hydroxide (NaOH) proved to be a false positive, the potassium phosphate ( $\text{K}_3\text{PO}_4$ ) hit gave promising results. When this reaction was conducted at the bench, the desired compound was isolated in 63% yield using  $\text{PdCl}_2(\text{PPh}_3)_2$  with  $\text{K}_3\text{PO}_4$  in THF/ $\text{H}_2\text{O}$ .

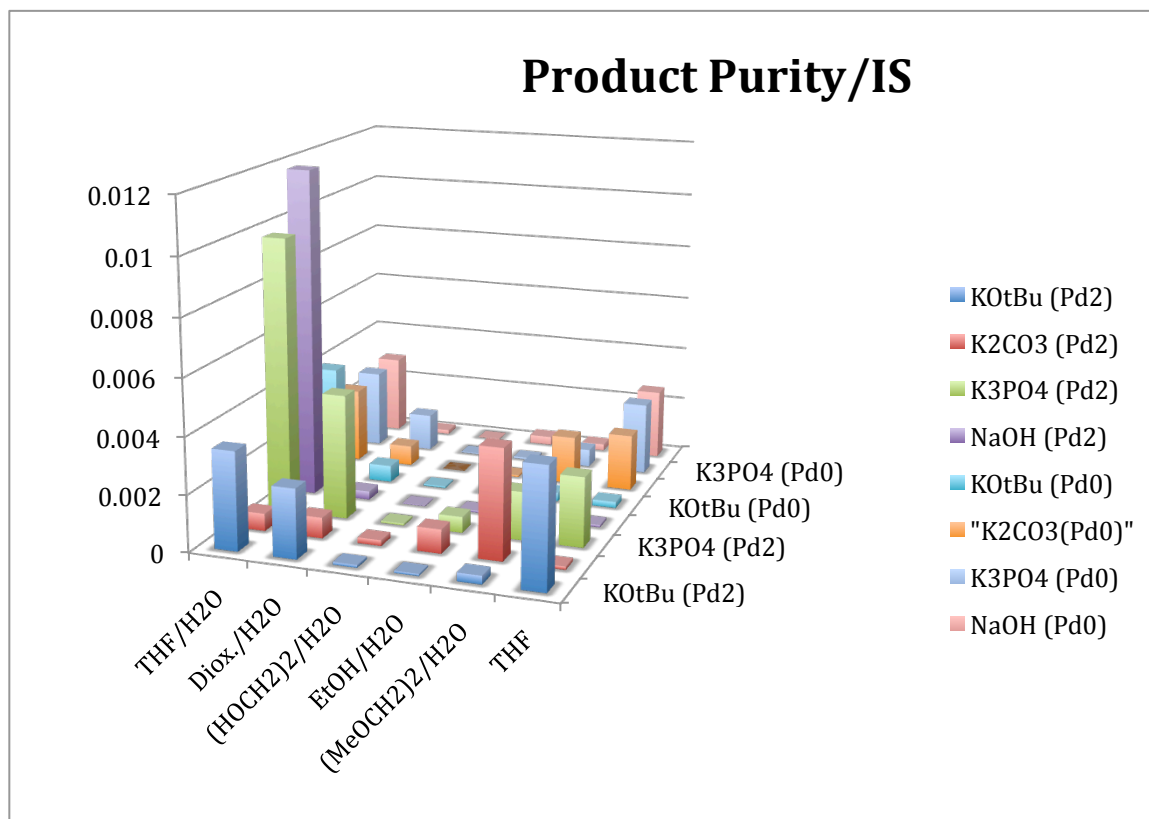
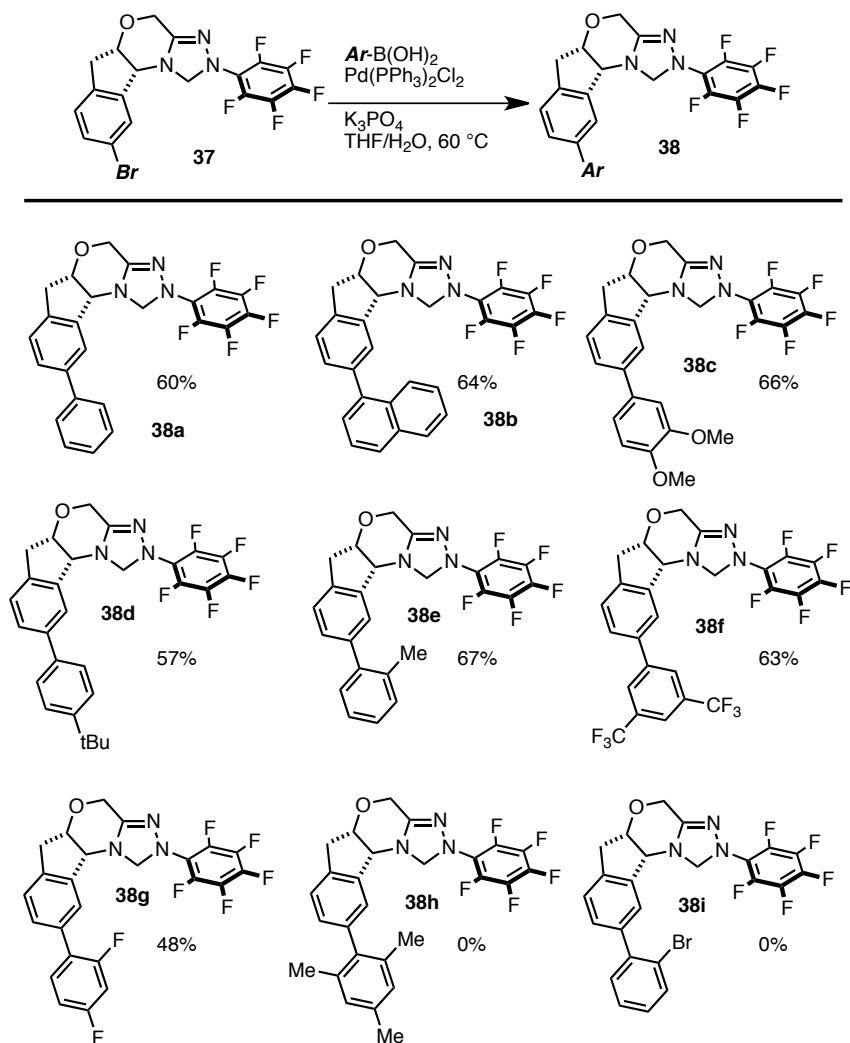


**Figure 4.4**

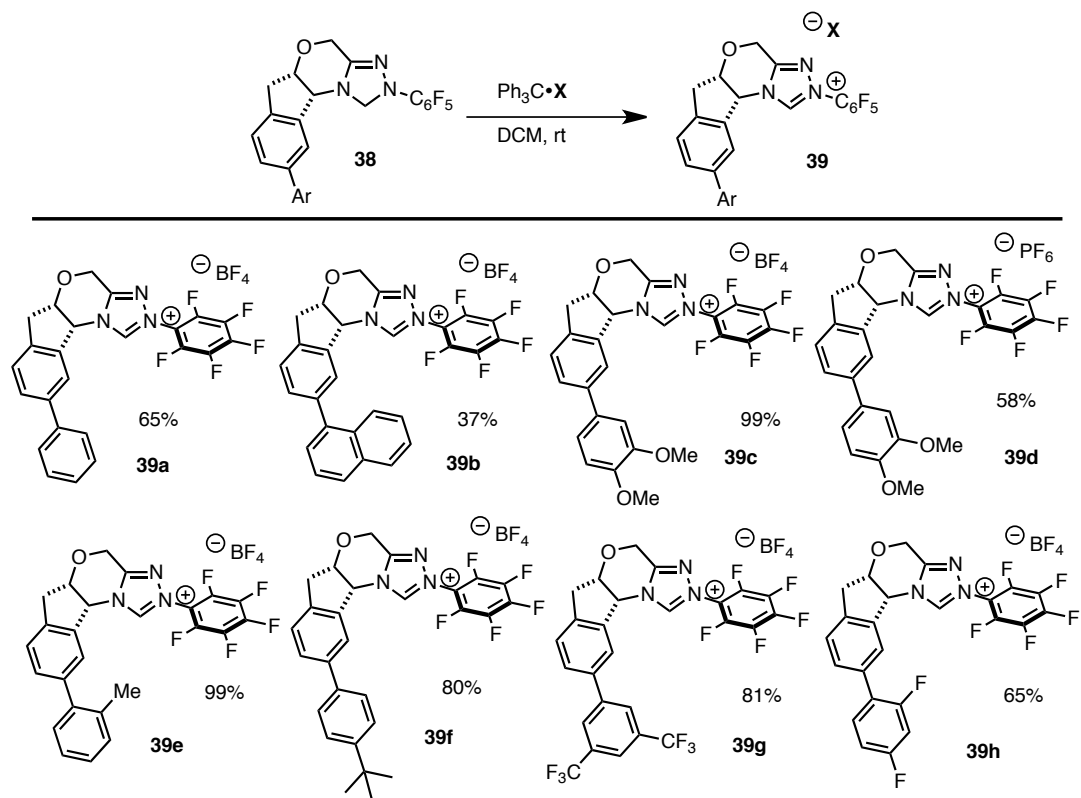
With optimal conditions discovered, we set out to synthesize a variety of elaborated triazolines (Table 4.2). Electron-rich aryl boronic acids are superb as substrates, whereas electron-deficient partners give product in diminished yields. Even some bulky aromatic species are tolerated. There is a limit, however, as very bulky and very electron-deficient aryl-boronic acids fail to yield desired product (**38h** and **38i**).

**Table 4.2**

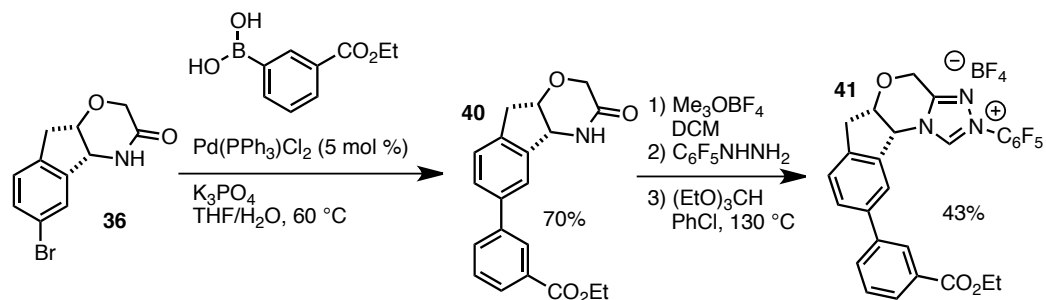


With elaborated triazolines at hand, we tested if trityl salt mediated oxidation will work on these substrates. To our delight, this reoxidation does work to provide the desired triazoliums (Table 4.3).

**Table 4.3**



For a shorter synthesis, cross-coupling can be performed on the bromo-lactam precursor **36** followed by traditional catalyst synthesis to form **41** (Scheme 4.14).<sup>113</sup>

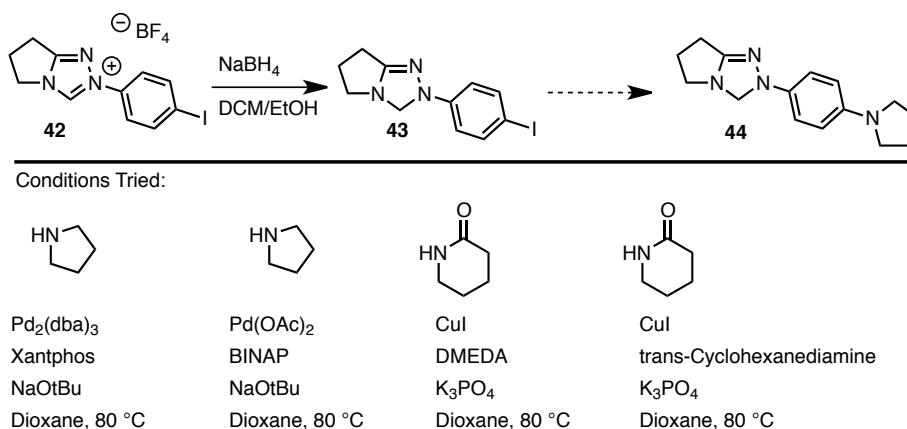


**Scheme 4.14**

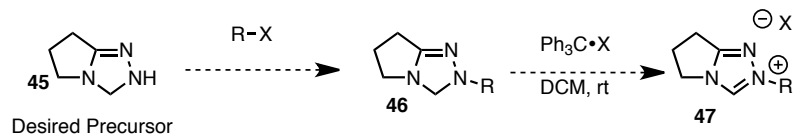
We were curious if cross-coupling can occur on the *N*-Aryl group as well. The use of *p*-iodophenylhydrazine as starting material introduces a C-I bond that can be manipulated in similar fashion. We also decided to attempt a C-N cross-coupling as a

way to introduce highly electron-releasing substituents onto the *N*-aryl group of the triazolium catalysts (Table 4.4). NHC catalysts that contain highly electron-donating groups on the arene often possess unique capabilities.<sup>114</sup> However, the parent hydrazines are highly unstable, so an alternative synthetic strategy would prove useful. Unfortunately, no desired products were formed: the triazolium substrate **42** is unstable, and decomposes under attempted literature conditions.<sup>115</sup>

**Table 4.4**



A future direction for this project would be the development of a simple triazolene precursor. If simple *N*-H variant **45** can be accessed, this can serve as a substrate for diversification by simple alkylation or arylation (Scheme 4.15). Oxidation to the triazolium would provide a convenient route to many different NHC catalysts. This strategy would avoid two major pitfalls in catalyst synthesis: 1) usage of unstable aryl hydrazines, and 2) difficult cyclization to form the triazole core. However, a practical synthesis of the precursor needs to be explored.



### Scheme 4.15

In summary, a useful strategy for the diversification of aminoindanol-based NHC catalysts has been described. This will serve in the exploration of new catalysts in the discovery and optimization of new organocatalyzed reactions.

## REFERENCES

- <sup>1</sup> Wöhler, F.; Liebig, J. *Annalen der Pharmacie* **1832**, 249-282.
- <sup>2</sup> Ugai, T.; Tanaka, R.; Dokawa, T. *J. Pharm. Soc. Jpn.* **1943**, *63*, 296-300.
- <sup>3</sup> Breslow, R. *J. Am. Chem. Soc.* **1958**, *80*, 3719-3726.
- <sup>4</sup> Lapworth, A. *J. Chem. Soc.* **1903**, *83*, 995-1005.
- <sup>5</sup> Seebach, D. *Angew. Chem. Int. Ed.* **1979**, *18*, 239-258.
- <sup>6</sup> a) Stetter, H.; Schreckenber, M. *Angew. Chem. Int. Ed. Engl.* **1973**, *12*, 81. b) Stetter, H. *Angew. Chem. Int. Ed. Engl.* **1976**, *15*, 639-647.
- <sup>7</sup> Enders, D.; Han, J.; Henseler, A. *Chem. Commun.* **2008**, *34*, 3989-3991.
- <sup>8</sup> a) see ref 7. b) Bugaut, X.; Liu, F.; Glorius, F. *J. Am. Chem. Soc.* **2011**, *133*, 8130-8133.
- <sup>9</sup> a) Chiang, P.-C.; Rommel, M.; Bode, J. W. *J. Am. Chem. Soc.* **2009**, *131*, 8714-8718. b) Wanner, B.; Mahatthananchai, J.; Bode, J. W. *Org. Lett.* **2011**, *13*, 5378-5381. c) Binanzer, M.; Hsieh, S.-Y.; Bode, J. W. *J. Am. Chem. Soc.* **2011**, *133*, 19698-19701. d) Hsieh, S.-Y.; Binanzer, M.; Kreituss, I.; Bode, J. W. *Chem. Commun.* **2012**, *48*, 8892-8894.
- <sup>10</sup> Stetter, H.; Kuhlmann, H. *Org. React.* **1991**, *40*, 407-496.
- <sup>11</sup> Kerr, M. S.; Read de Alaniz, J.; Rovis, T. *J. Am. Chem. Soc.* **2002**, *124*, 10298-10299.
- <sup>12</sup> Ciganek, E. *Synthesis* **1995**, 1311
- <sup>13</sup> Vacca, J. P.; Dorsery, B. D.; Schleif, W. A.; Levin, R. B.; McDaniel, S. L.; Darke, P. L.; Zugay, J.; Quintero, J. C.; Blahny, O. M.; Roth, E.; Sardana, V. V.; Schlabach, A. J.; Graham, P. I.; Condra, J. H.; Gotlib, L.; Holloway, M. K.; Lin, J.; Chen, I.-W.; Vastag, K.; Ostovic, D.; Anderson, P. S.; Emini, E. A.; Huff, J. R. *Proc. Natl. Acad. Sci. U.S.A.* **1994**, *91*, 4096.
- <sup>14</sup> Kerr, M. S.; Rovis, T. *J. Am. Chem. Soc.* **2004**, *126*, 8876-8877.
- <sup>15</sup> Read de Alaniz, J.; Rovis, T. *J. Am. Chem. Soc.* **2005**, *127*, 6284-6289.
- <sup>16</sup> Liu, Q.; Rovis, T. *J. Am. Chem. Soc.* **2006**, *128*, 2552-2553.
- <sup>17</sup> Enders, D.; Han, J.; Henseler, A. *Chem. Commun.* **2008**, 3989-3991.
- <sup>18</sup> see ref. 10
- <sup>19</sup> Liu, Q.; Perreault, S.; Rovis, T. *J. Am. Chem. Soc.* **2008**, *130*, 14066-14067.
- <sup>20</sup> Liu, Q.; Rovis, T. *Org. Lett.* **2009**, *11*, 2856-2859.
- <sup>21</sup> DiRocco, D. A.; Oberg, K. M.; Dalton, D. M.; Rovis, T. *J. Am. Chem. Soc.* **2009**, *131*, 10872-10874.
- <sup>22</sup> Um, J. M.; DiRocco, D. A.; Noey, E. L.; Rovis, T.; Houk, K. N. *J. Am. Chem. Soc.* **2011**, *133*, 11249-11254.
- <sup>23</sup> DiRocco, D. A.; Rovis, T. *J. Am. Chem. Soc.* **2011**, *133*, 10402-10405.
- <sup>24</sup> DiRocco, D. A.; Noey, E. L.; Houk, K. N.; Rovis, T. *Angew. Chem. Int. Ed.* **2012**, *51*, 2391-2394.
- <sup>25</sup> Sánchez-Larios, E.; Thai, K.; Bilodeau, F.; Gravel, M. *Org. Lett.* **2011**, *13*, 4942-4945.
- <sup>26</sup> Piel, I.; Steinmetz, M.; Hirano, K.; Fröhlich, R.; Grimme, S.; Glorius, F. *Angew. Chem. Int. Ed.* **2011**, *50*, 4983-4987.

- <sup>27</sup> Biju, A. T.; Wurz, N. E.; Glorius, F. *J. Am. Chem. Soc.* **2010**, *132*, 5970-5971.
- <sup>28</sup> Bugaut, X.; Liu, F.; Glorius, F. *J. Am. Chem. Soc.* **2011**, *133*, 8130-8133.
- <sup>29</sup> Schedler, M.; Wang, D.-S.; Glorius, F. *Angew. Chem. Int. Ed.* **2013**, *52*, 2585-2589.
- <sup>30</sup> Enders, D.; Kallfass, U. *Angew. Chem. Int. Ed. Engl.* **2002**, *41*, 1743-1745.
- <sup>31</sup> Langdon, S. M.; Wilde, M. M. D.; Thai, K.; Gravel, M. *J. Am. Chem. Soc.* **2014**, *136*, 7539-7542.
- <sup>32</sup> Takikawa, H.; Hachisu, Y.; Bode, J. W.; Suzuki, K. *Angew. Chem. Int. Ed.* **2006**, *45*, 3492-3494.
- <sup>33</sup> Takikawa, H.; Suzuki, K. *Org. Lett.* **2007**, *9*, 2713-2716.
- <sup>34</sup> Castells, J.; López-Calahorra, F.; Bassedas, M.; Urrios, P. *Synthesis* **1988**, 314-315.
- <sup>35</sup> Murry, J. A.; Frantz, D. E.; Soheili, A.; Tillyer, R.; Grabowski, E. J. J.; Reider, P. J. *J. Am. Chem. Soc.* **2001**, *123*, 9696-9697.
- <sup>36</sup> DiRocco, D. A.; Rovis, T. *Angew. Chem. Int. Ed.* **2012**, *51*, 5904-5906.
- <sup>37</sup> DiRocco, D. A.; Rovis, T. *J. Am. Chem. Soc.* **2012**, *134*, 8094-8097.
- <sup>38</sup> DiRocco, D. A.; Oberg, K. M.; Rovis, T. *J. Am. Chem. Soc.* **2012**, *134*, 6143-6145.
- <sup>39</sup> a) Reynolds, N. T.; Read de Alaniz, J.; Rovis, T. *J. Am. Chem. Soc.* **2004**, *126*, 9518-9519. b) Chow, K. Y.-K.; Bode, J. W. *J. Am. Chem. Soc.* **2004**, *126*, 8126-8127. c) Sohn, S. S.; Rosen, E. L.; Bode, J. W. *J. Am. Chem. Soc.* **2004**, *126*, 14370-14371. d) Burstein, C.; Glorius, F. *Angew. Chem. Int. Ed.* **2004**, *43*, 6205-6208.
- <sup>40</sup> a) Wallach, O. *Ber. Dtsch. Chem. Ges.* **1873**, 6 b) Kötz, A. *J. Prakt. Chem.* **1913**, *88*, 531-532.
- <sup>41</sup> a) Reynolds, N. T.; Rovis, T. *J. Am. Chem. Soc.* **2005**, *127*, 16406-16407. b) also see 39a
- <sup>42</sup> Wheeler, P.; Vora, H. U.; Rovis, T. *Chem. Sci.* **2013**, *4*, 1674-1679.
- <sup>43</sup> Zhao, X.; DiRocco, D. A.; Rovis, T. *J. Am. Chem. Soc.* **2011**, *133*, 12466-12469.
- <sup>44</sup> Raup, D. E. A.; Cardinal-David, B.; Holte, D.; Scheidt, K. A. *Nat. Chem.* **2010**, *2*, 766-767.
- <sup>45</sup> Kaeobamrung, J.; Mahatthananchai, J.; Zheng, P.; Bode, J. W. *J. Am. Chem. Soc.* **2010**, *132*, 8810-8812.
- <sup>46</sup> Zhao, X.; Ruhl, K. E.; Rovis, T. *Angew. Chem. Int. Ed.* **2012**, *51*, 12330-12333.
- <sup>47</sup> White, N. A.; DiRocco, D. A.; Rovis, T. *J. Am. Chem. Soc.* **2013**, *135*, 8504-8507.
- <sup>48</sup> Kerr, M. S.; Rovis, T. *J. Am. Chem. Soc.* **2004**, *126*, 8876-8877.
- <sup>49</sup> Massey, R. S.; Collett, C. J.; Lindsay, A. G.; Smith, A. D.; O'Donoghue, A. C. *J. Am. Chem. Soc.* **2012**, *134*, 20421-20432.
- <sup>50</sup> Collett, C. J.; Massey, R. S.; Maguire, O. R.; Batsanov, A. S.; O'Donoghue, A. C.; Smith, A. D. *Chem. Sci.* **2013**, *4*, 1514-1522.
- <sup>51</sup> For some recent reviews, see: a) Grondal, C.; Jeanty, M.; Enders, D. *Nat. Chem.* **2010**, *2*, 167-178. b) Pellissier, H. *Tetrahedron* **2013**, *69*, 7171-7210. c) Pellissier, H. *Adv. Synth. Catal.* **2012**, *354*, 237-294. d) Albrecht, L.; Jiang, H.; Jørgensen, K. A. *Angew. Chem. Int. Ed.* **2011**, *50*, 8492-8509. e) Patil, N. T.; Shinde, V. S.; Gajula, B. *Org. Biomol. Chem.* **2012**, *10*, 211-224. d) Allen, A. E.; MacMillan, D. W. C. *Chem. Sci.* **2012**, *3*, 633-658.
- <sup>52</sup> Some excellent examples include: a) Huang, Y.; Walji, A. M.; Larsen, C. H.; MacMillan, D. W. C. *J. Am. Chem. Soc.* **2005**, *127*, 15051-15053. b) Zhou, J.; List, B. *J. Am. Chem. Soc.* **2007**, *129*, 7498-7499. c) Wang, Y.; Han, R.-G.; Zhou, Y.-L.; Yang, S.;

Xu, P.-F.; Dixon, D. J. *Angew. Chem. Int. Ed.* **2009**, *48*, 9834-9838. d) Belot, S.; Vogt, K. A.; Besnard, C.; Krause, N.; Alexakis, A. *Angew. Chem. Int. Ed.* **2009**, *48*, 8923-8926. e) Simmons, B.; Walji, A. M.; MacMillan, D. W. C. *Angew. Chem. Int. Ed.* **2009**, *48*, 4349-4359. f) Quintard, A.; Alexakis, A.; Mazet, C. *Angew. Chem. Int. Ed.* **2011**, *50*, 2354-2358.

<sup>53</sup> Nemoto, T.; Fukuda, T.; Hamada, Y. *Tetrahedron Lett.* **2006**, *47*, 4365-4368.

<sup>54</sup> Lebeuf, R.; Hirano, K.; Glorius, F. *Org. Lett.* **2008**, *10*, 4243-4246.

<sup>55</sup> Biju, A. T.; Wurz, N. E.; Glorius, F. *J. Am. Chem. Soc.* **2010**, *132*, 5970-5971.

<sup>56</sup> Padmanaban, M.; Biju, A. T.; Glorius, F. *Org. Lett.* **2011**, *13*, 5624-5627.

<sup>57</sup> Lathrop, S. P.; Rovis, T. *J. Am. Chem. Soc.* **2009**, *131*, 13628-13630. For related work, see: Jacobsen, C. B.; Jensen, K. L.; Udmark, J.; Jørgensen, K. A. *Org. Lett.* **2011**, *13*, 4790-4793.

<sup>58</sup> a) Liu, G.; Wilkerson, P. D.; Toth, C. A.; Xu, H. *Org. Lett.* **2012**, *14*, 858-861. b) Li, J.-L.; Sahoo, B.; Daniliuc, C.-G.; Glorius, F. *Angew. Chem. Int. Ed.* **2014**, Early View, DOI: 10.1002/anie.201405178. c) Fu, Z.; Sun, H.; Chen, S.; Tiwari, B.; Li, G.; Chi, Y. R. *Chem. Commun.* **2013**, *49*, 261-263.

<sup>59</sup> For example, see: Jiang, H.; Elsner, P.; Jensen, K. L.; Falcicchio, A.; Marcos, V.; Jørgensen, K. A. *Angew. Chem. Int. Ed.* **2009**, *48*, 6844-6848.

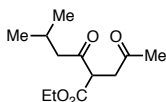
<sup>60</sup> Filloux, C. M.; Lathrop, S. P.; Rovis, T. *Proc. Natl. Acad. Sci. USA* **2010**, *107*, 20666-20671.

<sup>61</sup> a) DiRocco, D. A.; Rovis, T. *J. Am. Chem. Soc.* **2011**, *133*, 10402-10405. b) Peelen, T. J.; Chi, Y.; Gellman, S. H. *J. Am. Chem. Soc.* **2005**, *127*, 11598-11599. c) Fang, X.; Chen, X.; Lv, H.; Chi, Y. R. *Angew. Chem. Int. Ed.* **2011**, *50*, 11782-11785.

<sup>62</sup> Wang, J.; Ma, A.; Ma, D. *Org. Lett.* **2008**, *10*, 5425-5428.

<sup>63</sup> see ref 58, 59, and also: a) Campbell, M. J.; Johnson, J. S. *J. Am. Chem. Soc.* **2009**, *131*, 10370-10371. b) Chen, K.; Baran, P. S. *Nature* **2009**, *459*, 824-828.

<sup>64</sup> Ozboya, K. E.; Rovis, T. *Chem. Sci.* **2011**, *2*, 1835-1838.



<sup>65</sup> Stetter product formed:

<sup>66</sup> Moore, J. L.; Silvestri, A. P.; Read de Alaniz, J.; DiRocco, D. A.; Rovis, T. *Org. Lett.* **2011**, *13*, 1742-1745.

<sup>67</sup> a) Krautwald, S.; Sarlah, D.; Schafroth, M. A.; Carreira, E. M. *Science* **2013**, *340*, 1065-1068. b) Krautwald, S.; Schafroth, M. A.; Sarlah, D.; Carreira, E. M. *J. Am. Chem. Soc.* **2014**, *136*, 3020-3023.

<sup>68</sup> Su, S.; Seiple, I. B.; Young, I. S.; Baran, P. S. *J. Am. Chem. Soc.* **2008**, *130*, 16490-16491.

<sup>69</sup> a) Seiple, I. B.; Su, S.; Young, I. S.; Lewis, C. A.; Yamaguchi, J.; Baran, P. S. *Angew. Chem. Int. Ed.* **2010**, *49*, 1095-1098. b) Seiple, I. B.; Su, S.; Young, I. S.; Nakamura, A.; Yamaguchi, J.; Jørgensen, L.; Rodriguez, R. A.; O'Malley, D. P.; Gaich, T.; Köck, M.; Baran, P. S. *J. Am. Chem. Soc.* **2011**, *133*, 14710-14726.

<sup>70</sup> Kaneko, T.; Ohtani, K.; Kasai, R.; Yamasaki, K.; Duc, N. M. *Phytochemistry* **1997**, *46*, 907-910.

<sup>71</sup> Nair, V.; Menon, R. S.; Biju, A. T.; Sinu, C. R.; Paul, R. R.; Jose, A.; Sreekumar, V. *Chem. Soc. Rev.* **2011**, *40*, 5336-5346.

- <sup>72</sup> Sohn, S. S.; Rosen, E. L.; Bode, J. W. *J. Am. Chem. Soc.* **2004**, *126*, 14370-14371.
- <sup>73</sup> Burstein, C.; Glorius, F. *Angew. Chem. Int. Ed.* **2004**, *43*, 6205-6208.
- <sup>74</sup> Nair, V.; Babu, B. P.; Vellalath, S.; Varghese, V.; Raveendran, A. E.; Suresh, E. *Org. Lett.* **2009**, *11*, 2507-2510.
- <sup>75</sup> Nair, V.; Sinu, C. R.; Babu, B. P.; Varghese, V.; Jose, A.; Suresh, E. *Org. Lett.* **2009**, *11*, 5570-5573.
- <sup>76</sup> Maji, B.; Ji, L.; Wang, S.; Vedachalam, S.; Ganguly, R.; Liu, X.-W. *Angew. Chem. Int. Ed.* **2012**, *51*, 8276-8280.
- <sup>77</sup> White, N. A.; DiRocco, D. A.; Rovis, T. *J. Am. Chem. Soc.* **2013**, *135*, 8504-8507.
- <sup>78</sup> This was inspired by work from the Lupton group. See: a) Pandiancherri, S.; Ryan, S. J.; Lupton, D. W. *Org. Biomol. Chem.* **2012**, *10*, 7903-7911. b) Ryan, S. J.; Candish, L.; Lupton, D. W. *J. Am. Chem. Soc.* **2011**, *133*, 4694-4697.
- <sup>79</sup> When this is used as starting material, no conversion to desired product is observed.
- <sup>80</sup> Chan, A.; Scheidt, K. A. *Org. Lett.* **2005**, *7*, 905-908.
- <sup>81</sup> DiRocco, D. A.; Oberg, K. M.; Dalton, D. M.; Rovis, T. *J. Am. Chem. Soc.* **2009**, *131*, 10872-10874.
- <sup>82</sup> Castells, J.; López-Calahorra, F.; Bassedas, M.; Urrios, P. *Synthesis* **1988**, 314-315.
- <sup>83</sup> He, L.; Jian, T.-Y.; Ye, S. *J. Org. Chem.* **2007**, *72*, 7466-7468. Also see: Chen, X.-Y.; Xia, F.; Ye, S. *Org. Biomol. Chem.* **2013**, *11*, 5722-5726.
- <sup>84</sup> Atienza, R. L.; Scheidt, K. A. *Aust. J. Chem.* **2011**, *64*, 1158-1164.
- <sup>85</sup> Dalton, D. M.; Rappé, A. K.; Rovis, T. *Chem. Sci.* **2013**, *4*, 2062-2070. Also see: a) Keller-Friedman, R.; Oberg, K. M.; Dalton, D. M.; Rovis, T. *Pure Appl. Chem.* **2010**, *82*, 1353-1364. b) Dalton, D. M.; Oberg, K. M.; Yu, R. T.; Lee, E. E.; Perreault, S.; Oinen, M. E.; Pease, M. L.; Malik, G.; Rovis, T. *J. Am. Chem. Soc.* **2009**, *131*, 15717-15728.
- <sup>86</sup> Hyster, T. K.; Rovis, T. *Chem. Sci.* **2011**, *2*, 1606-1610.
- <sup>87</sup> Piou, T.; Rovis, T. *J. Am. Chem. Sci.* 2014 ASAP doi: 10.1021/ja506579t
- <sup>88</sup> DiRocco, D. A.; Oberg, K. M.; Dalton, D. M.; Rovis, T. *J. Am. Chem. Soc.* **2009**, *131*, 10872-10874.
- <sup>89</sup> Please see: a) DiRocco, D. A.; Rovis, T. *J. Am. Chem. Soc.* **2011**, *133*, 10402-10405. b) DiRocco, D. A.; Noey, E. L.; Houk, K. N.; Rovis, T. *Angew. Chem. Int. Ed.* **2012**, *51*, 2391-2394. c) Sánchez-Larios, E.; Thai, K.; Bilodeau, F.; Gravel, M. *Org. Lett.* **2011**, *13*, 4942-4945.
- <sup>90</sup> White, N. A.; DiRocco, D. A.; Rovis, T. *J. Am. Chem. Soc.* **2013**, *135*, 8504-8507.
- <sup>91</sup> a) Rovis, T. *Chem. Lett.* **2008**, *37*, 2-7. b) Read de Alaniz, J.; Kerr, M. S.; Moore, J. L.; Rovis, T. *J. Org. Chem.* **2008**, *73*, 2033-2040.
- <sup>92</sup> Vacca, J. P.; Dorsery, B. D.; Schleif, W. A.; Levin, R. B.; McDaniel, S. L.; Darke, P. L.; Zugay, J.; Quintero, J. C.; Blahny, O. M.; Roth, E.; Sardana, V. V.; Schlabach, A. J.; Graham, P. I.; Condra, J. H.; Gotlib, L.; Holloway, M. K.; Lin, J.; Chen, I.-W.; Vastag, K.; Ostovic, D.; Anderson, P. S.; Emini, E. A.; Huff, J. R. *Proc. Natl. Acad. Sci. U.S.A.* **1994**, *91*, 4096.
- <sup>93</sup> For a recent example, see: Behenna, D. C.; Mohr, J. T.; Sherden, N. H.; Marinescu, S. C.; Harned, A. M.; Tani, K.; Seto, M.; Ma, S.; Novák, Z.; Krout, M. R.; McFadden, R. M.; Roizen, J. L.; Enquist, Jr. J. A.; White, D. E.; Levine, S. R.; Petrova, K. V.; Iwashita, A.; Virgil, S. C.; Stoltz, B. M. *Chem. Eur. J.* **2011**, *17*, 14199-14223.

- <sup>94</sup> For a recent example, see: Xiong, H.; Xu, H.; Liao, S.; Xie, Z.; Tang, Y. *J. Am. Chem. Soc.* **2013**, *135*, 7851-7854.
- <sup>95</sup> For a recent example, see: Sibi, M. P.; Ito, K. *J. Am. Chem. Soc.* **2007**, *129*, 8064-8065.
- <sup>96</sup> a) Tanaka, T.; Katsumura, S. *J. Am. Chem. Soc.* **2002**, *124*, 9660-9661. b) Kobayashi, T.; Tanaka, K.; Miwa, J.; Katsumura, S. *Tetrahedron: Asymmetry* **2004**, *15*, 185-188. c) Liu, S. Y.; Katsumura, S. *Chin. Chem. Lett.* **2009**, *20*, 1204-1206. d) Kobayashi, T.; Hasegawa, F.; Hirose, Y.; Tanaka, K.; Mori, H.; Katsumura, S. *J. Org. Chem.* **2012**, *77*, 1812-1832.
- <sup>97</sup> Hsieh, S.-Y.; Binanzer, M.; Kreituss, I.; Bode, J. W. *Chem. Commun.* **2012**, *48*, 8892-8894.
- <sup>98</sup> Kuwano, S.; Harada, S.; Kang, B.; Oriez, R.; Yamaoka, Y.; Takasu, K.; Yamada, K.-i. *J. Am. Chem. Soc.* **2013**, *135*, 11485-11488.
- <sup>99</sup> Hansen, M. M.; Borders, S. S. K.; Clayton, M. T.; Heath, P. C.; Kolis, S. P.; Larsen, S. D.; Linder, R. J.; Reutzler-Edens, S. M.; Smith, J. C.; Tameze, S. L.; Ward, J. A.; Weigel, L. O. *Org. Proc. Res. Dev.* **2009**, *13*, 198-208.
- <sup>100</sup> Brand, J. P.; Osuna Siles, J. I.; Waser, J. *Synlett* **2010**, 881-884.
- <sup>101</sup> Zheng, P.; Gondo, C. A.; Bode, J. W. *Chem. Asian. J.* **2011**, *6*, 614-620.
- <sup>102</sup> DiRocco, D. A.; Oberg, K. M.; Rovis, T. *J. Am. Chem. Soc.* **2012**, *134*, 6143-6145.
- <sup>103</sup> Egert, M.; Walther, S.; Plenio, H. *Eur. J. Org. Chem.* **2014**, 4362-4369.
- <sup>104</sup> Bildstein, B.; Malaun, M.; Kopacka, H.; Ongania, K.-H.; Wurst, K. *J. Organomet. Chem.* **1999**, *572*, 177-187.
- <sup>105</sup> For an example, see: a) Colotta, V.; Catarzi, D.; Varano, F.; Filacchioni, G.; Martini, C.; Trincavelli, L.; Lucacchini, A. *Bioorg. Med. Chem.* **2003**, *11*, 3541-3550. b) Abd Allah, S. O.; Ead, H. A.; Kassab, N. A.; Zayed, M. M. *J. Heterocyclic Chem.* **1983**, *20*, 189-190.
- <sup>106</sup> Jafarpour, L.; Stevens, E. D.; Nolan, S. P. *J. Organomet. Chem.* **2000**, *606*, 49-54. Also ref. 21
- <sup>107</sup> a) Calder, I. C.; Spotswood, T. M.; Sasse, W. H. F. *Tetrahedron Lett.* **1963**, *2*, 95. b) Calder, I. C.; Sasse, W. H. F. *Aust. J. Chem.* **1965**, *18*, 1819.
- <sup>108</sup> Würtz, S.; Glorius, F. *Acc. Chem. Res.* **2008**, *41*, 1523.
- <sup>109</sup> See ref: 90a, 93
- <sup>110</sup> Liu, G.; Wilkerson, P. D.; Toth, C. A.; Xu, H. *Org. Lett.* **2012**, *14*, 858-861.
- <sup>111</sup> a) Miyaura, N.; Suzuki, A. *Chem. Rev.* **1995**, *95*, 2457. b) Martin, R.; Buchwald, S. L. *Acc. Chem. Res.* **2008**, *41*, 1461.
- <sup>112</sup> Structure Elucidation accomplished by John Chu (CSU)
- <sup>113</sup> Vora, H. U.; Lathrop, S. P.; Reynolds, N. T.; Kerr, M. S.; Read de Alaniz, J.; Rovis, T. *Org. Synth.* **2010**, *87*, 350.
- <sup>114</sup> Schedler, M.; Fröhlich, R.; Daniliuc, C.-G.; Glorius, F. *Eur. J. Org. Chem.* **2012**, 4164-4171.
- <sup>115</sup> a) Surry, D. S.; Buchwald, S. L. *Chem. Sci.* **2011**, *2*, 27-50. b) Ziegler, D. T.; Muñoz-Molina, J. M.; Bissember, A. C.; Peters, J. C.; Fu, G. C. *J. Am. Chem. Soc.* **2013**, *135*, 13107-13112.

## APPENDIX 1

### Experimental And Spectral Data for Chapter 2

#### General Methods:

All reactions were carried out under an atmosphere of argon with magnetic stirring.

HPLC grade Chloroform preserved with pentane was purchased from Fisher Scientific.

Column chromatography was performed on SiliCycle®SilicaFlash® P60, 40-63 $\mu$ m 60A.

Thin layer chromatography was performed on SiliCycle® 250 $\mu$ m 60A plates.

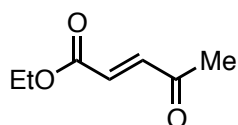
Visualization was accomplished with UV light or p-anisaldehyde stain followed by heating. This stain is highly recommended, with starting material typically staining orange, intermediate as brown, and final product as a dark blue.

<sup>1</sup>H NMR spectra were obtained on Varian 300 or 400 MHz spectrometers at ambient temperature. Data is reported as follows: chemical shift in parts per million ( $\delta$ , ppm) from CDCl<sub>3</sub> (7.26 ppm) multiplicity (s = singlet, bs = broad singlet, d = doublet, t = triplet, q = quartet, and m = multiplet), coupling constants(Hz).

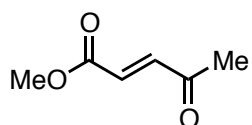
<sup>13</sup>C NMR was recorded on Varian 300 or 400 MHz spectrometers (at 75 or 100 MHz) at ambient temperature. Chemical shifts are reported in ppm from CDCl<sub>3</sub> (77.2 ppm)

Varian CP-3800 Gas Chromatograph was used to determine diastereomeric and enantiomeric ratios. For the achiral column, Varian CP-Sil 8CB (15m X 0.25mm) was used. For the chiral column, Chiraldex BDM-1 was used, unless otherwise stated.

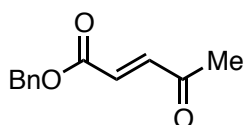
Aldehyde substrates were purchased from Sigma-Aldrich and subsequently distilled.



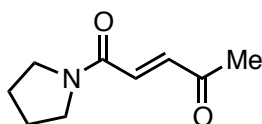
**17a**



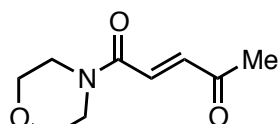
**17h**



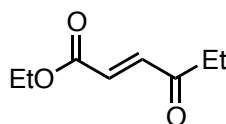
**17i**



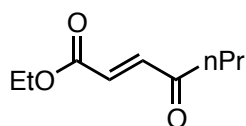
**17j**



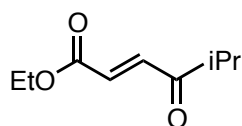
**17k**



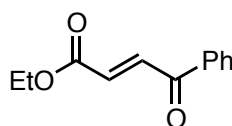
**17l**



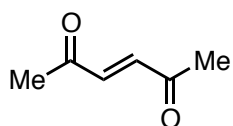
**17m**



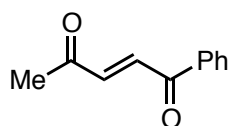
**17n**



**17o**



**17p**



**17q**

Ketoesters were prepared according to literature precedent:

**17a**,<sup>1</sup> **17h**,<sup>2</sup> **17i**,<sup>3</sup> **17j-17k**,<sup>4</sup> **17l-17p**,<sup>1</sup> **17q**.<sup>5</sup>

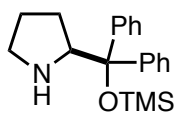
<sup>1</sup> Runcie, K. A.; Taylor, R. J. K. *Chem. Commun.* **2002**, 974-975

<sup>2</sup> Schuda, P. F.; Ebner, C. B.; Potlock, S. J. *Synthesis*, **1987**, 1055-1057.

<sup>3</sup> Gérard, S.; Raoul, M.; Sapi, J. *Eur. J. Org. Chem.* **2006**, 2440-2445.

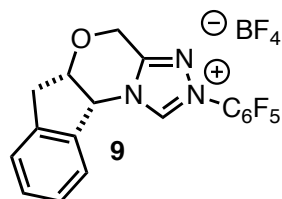
<sup>4</sup> Zigterman, J. L.; Woo, J. C. S.; Walker, S. D.; Tedrow, J. S.; Borths, C. J.; Bunel, E. E.; Faul, M. *M. J. Org. Chem.* **2007**, *72*, 8870-8876.

<sup>5</sup> Yu, J.-Q.; Corey, E. J. *J. Am. Chem. Soc.* **2003**, *125*, 3232-3233.



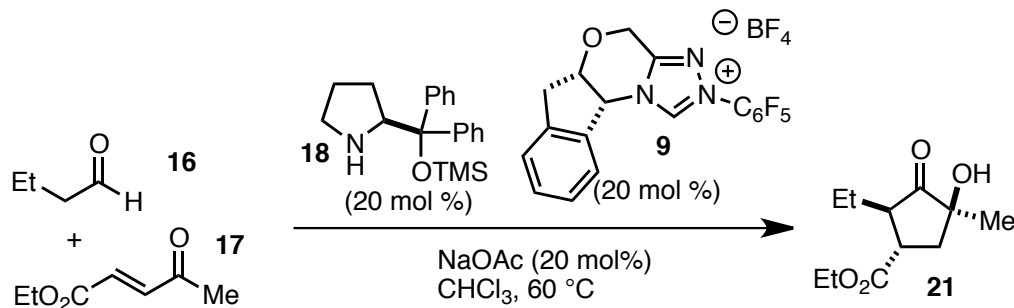
**18**

Amine catalyst **18** was prepared by literature reported method.<sup>6</sup>



**9**

Triazolium catalyst **9** was prepared by literature reported method.<sup>7</sup>



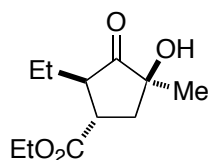
### General procedure for synthesis of **21a**:

25 mg (0.17 mmol) of Keto-Ester **17a** is added to an oven-dried 10mL round bottom flask. 11mg (0.2 equiv., 0.03 mmol) of amine catalyst **18** and 14 mg (0.2 equiv., 0.03 mmol) of triazolium **9** are then added. 1 ml of CHCl<sub>3</sub> is added and argon is bubbled into the mixture. 20 μl (1.2-1.5 equiv, 0.2 mmol) of butyraldehyde (**16a**) is then added, followed by 2.5mg (0.2 equiv, 0.03 mmol) of NaOAc. The reaction is outfitted with a reflux condenser and stir bar, and heated to 60 °C for 12 hours. Reaction is monitored

<sup>6</sup> Marigo, M.; Wabnitz, T. C.; Fielenbach, D.; Jørgensen, K. A. *Angew. Chem. Int. Ed.* **2005**, *44*, 794-797.

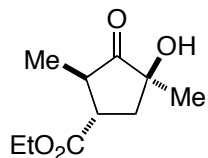
<sup>7</sup> Vora, H. U.; Lathrop, S. P.; Reynolds, N. T.; Kerr, M. S.; Read de Alaniz, J.; Rovis, T. *Org. Synth.* **2010**, *87*, 350-361.

by silica gel TLC. Upon completion, the reaction is cooled to room temperature and filtered through a small plug (1 in) of silica gel, washing with DCM then EtOAc. The solution is concentrated and purified by column chromatography, eluting with 10% EtOAc/DCM to 50% EtOAc/Hexanes through silica gel. Fractions were collected and concentrated to provide the desired product.



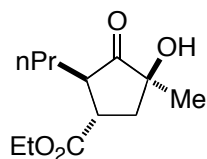
**(1S,2R,4S)-ethyl 2-ethyl-4-hydroxy-4-methyl-3-oxocyclopentanecarboxylate (21a)**

R<sub>f</sub> = 0.3 (10% Ethyl Acetate/Dichloromethane); 28 mg (72%), 94% ee, 19:1:<1:<1 dr  
[α]<sub>D</sub><sup>21</sup> = -40.83 (c = 0.0024 g/ml, CHCl<sub>3</sub>) **GC Analysis** CP-Sil 8CB column at 110 °C, 1 ml/min. Major: 12.07min. Minor: 12.95 min, 13.84 min, 15.14 min. BDM-1 column at 130 °C, 1 ml/min. Major: 24.35 min. Minor: 23.81 min. **<sup>1</sup>H NMR:** (300 MHz; CDCl<sub>3</sub>): δ<sub>H</sub> 4.16-4.23 (2 H, q), 2.98 (1 H, d, *J* 7.2), 2.33 (1 H, ddd, *J* = 13.7, 7.2 and 0.3), 1.94 (1 H, d, *J* = 10.5), 1.63 (1 H, d, *J* = 7.3), 1.33 (3 H, d, *J* = 0.8), 1.25-1.33 (3 H, t, *J* = 7.2), 0.92 (3 H, td, *J* = 7.5 and 0.8). **<sup>13</sup>C NMR:** (100 MHz, CDCl<sub>3</sub>) δ 216.7, 174.8, 75.7, 60.9, 51.7, 42.3, 39.3, 23.0, 22.1, 14.1, 10.8. **IR** (NaCl, neat): 3465, 2971, 2937, 2878, 1733, 1519, 1447, 1378, 1298, 1234, 1177. **HRMS:** (ESI-) calcd for C<sub>12</sub>H<sub>20</sub>O<sub>4</sub>, 227.1289. Found 227.1291.



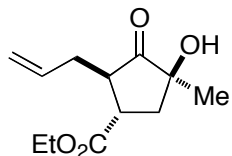
**(1S,2R,4S)-ethyl 4-hydroxy-2,4-dimethyl-3-oxocyclopentanecarboxylate (21b)**

R<sub>f</sub> = 0.3 (10% Ethyl Acetate/Dichloromethane); 28 mg (78%), 88% ee, 24:1.5:1 dr [α]<sub>D</sub><sup>21</sup> = -101.82 (c = 0.0011 g/ml, CHCl<sub>3</sub>) **GC Analysis** CP-Sil 8CB column at 110 °C, 1 ml/min. Major: 7.54 min. Minor: 8.22, 9.46 min. BDM-1 column at 130 °C, 1 ml/min. Major: 17.33 min. Minor: 16.82 min. **<sup>1</sup>H NMR:** (300 MHz, CDCl<sub>3</sub>) δ 4.20 (q, 2H), 2.84 (q, 1H), 2.61 (m, 1H), 2.34 (dd, 1H), 1.94 (t, 1H), 1.35 (s, 3H), 1.29 (s, 3H), 1.24 (t, 3H). **<sup>13</sup>C NMR:** (100 MHz, CDCl<sub>3</sub>) δ 217.4, 174.5, 61.2, 46.07, 45.4, 39.3, 23.5, 14.4, 13.9. **IR** (NaCl, neat): 3436, 2980, 2938, 1732, 1520, 1450, 1376, 1181. **HRMS:** (ESI-) calcd for C<sub>11</sub>H<sub>26</sub>O<sub>4</sub>, 213.1249. Found 213.1256.



**(1S,2R,4S)-ethyl 4-hydroxy-4-methyl-3-oxo-2-propylcyclopentanecarboxylate(21c)**

R<sub>f</sub> = 0.3 (10% Ethyl Acetate/Dichloromethane); 31 mg (76%), 95% ee, 33:1:1 dr [α]<sub>D</sub><sup>21</sup> = -56.97 (c = 0.0033 g/ml, CHCl<sub>3</sub>) **GC Analysis** CP-Sil 8CB column at 110 °C, 1 ml/min. Major: 19.66 min. Minor: 20.77, 22.00 min. BDM-1 column at 100 °C, 2 ml/min. Major: 112.04 min. Minor: 113.74 min. **<sup>1</sup>H NMR:** (300 MHz, CDCl<sub>3</sub>) δ 4.20 (q, 2H), 2.95 (q, 1H), 2.66 (m, 1H), 2.33 (dd, 1H), 1.92 (m, 1H), 1.72 (m, 1H), 1.49 (m, 1H), 1.33 (s, 3H), 1.28 (t, 3H), 0.90 (t, 3H). **<sup>13</sup>C NMR:** (100 MHz, CDCl<sub>3</sub>) δ 217.3, 175.1, 61.2, 50.2, 43.4, 39.7, 31.9, 23.2, 20.1, 14.4, 14.2. **IR** (NaCl, neat): 3448, 2964, 1734, 1377, 1178, 1038, 756 cm<sup>-1</sup>. **HRMS:** (ESI-) calcd for C<sub>12</sub>H<sub>20</sub>O<sub>4</sub>, 227.1289. Found 227.1291.



**(1S,2R,4S)-ethyl 2-allyl-4-hydroxy-4-methyl-3-oxocyclopentanecarboxylate (21e)**

R<sub>f</sub> = 0.39 (10% Ethyl Acetate/Dichloromethane); 37 mg (97%), 85% ee, 15:1:0.2:0.2 dr,

[α]<sub>D</sub><sup>21</sup> = -67.23 (c = 0.0047 g/ml, CHCl<sub>3</sub>) **GC Analysis:** CP-Sil 8CB at 110 °C, 1 ml/min.

Major 16.70 min. Minor: 18.16 min, 20.74 min, 21.11 min. HPLC Analysis: ChiralPak IA

column at 97% Hexanes/iPrOH, 1 ml/min. Major: 14.346 min. Minor: 12.338 min. <sup>1</sup>H

**NMR:** (300 MHz, CDCl<sub>3</sub>): δ 5.73-5.61 (m, 1H), 5.12-5.00 (m, 2H), 4.20-4.13 (m, 2H),

2.98 (td, *J* = 10.3, 7.2 Hz, 1H), 2.77 (ddd, *J* = 10.2, 7.3, 4.8 Hz, 1H), 2.56-2.50 (m, 1H),

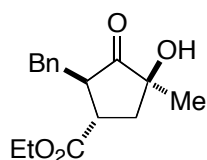
2.33 (dtd, *J* = 13.6, 6.8, 1.9 Hz, 2H), 1.91 (ddd, *J* = 13.7, 10.4, 0.4 Hz, 1H), 1.33 (d, *J* =

0.7 Hz, 3H), 1.33-1.24 (m, 3H). <sup>13</sup>C **NMR:** (100 MHz, CDCl<sub>3</sub>): δ 216.0, 174.5, 134.3,

117.7, 75.6, 60.9, 49.9, 42.2, 39.3, 33.4, 23.0, 14.1 **IR** (NaCl, neat): 3457, 2979, 2930,

1734, 1641, 1520, 1444, 1378, 1227, 1179 cm<sup>-1</sup>. **HRMS:** (APCI+) Calc'd for C<sub>12</sub>H<sub>18</sub>O<sub>4</sub>,

227.1278. Found 227.1276.



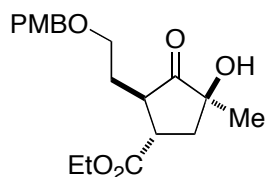
**(1S,2R,4S)-ethyl 2-benzyl-4-hydroxy-4-methyl-3-oxocyclopentanecarboxylate (21f)**

R<sub>f</sub> = 0.21 (5% Ethyl Acetate/Dichloromethane); 25 mg (50%), 89% ee, 9:1:0.2:0.2 dr,

[α]<sub>D</sub><sup>21</sup> = -126.92 (c = 0.0013 g/ml, CHCl<sub>3</sub>) **HPLC Analysis** Chiracel IC at 95%

Hexanes/iPrOH. Major 13.36 min. Minor: 11.36 min <sup>1</sup>H-**NMR** (300 MHz; CDCl<sub>3</sub>): δ 7.32-

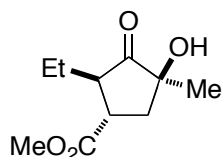
7.14 (m, 5H), 3.98-3.83 (m, 2H), 3.19 (dd,  $J = 13.7, 4.5$  Hz, 1H), 3.04-2.89 (m, 2H), 2.81 (dd,  $J = 13.7, 7.2$  Hz, 1H), 2.30-2.23 (m, 1H), 1.91-1.83 (m, 2H), 1.33 (s, 3H), 1.15-1.11 (t,  $J = 7.0$  Hz, 3H).  $^{13}\text{C NMR}$ : (100 MHz,  $\text{CDCl}_3$ ):  $\delta$  215.9, 174.6, 138.3, 129.55, 128.55, 126.72, 75.8, 61.1, 52.5, 42.8, 39.7, 35.4, 23.1, 14.2. **IR** (NaCl, neat): 3442, 2980, 1732, 1496, 1454, 1377, 1178, 1045. **HRMS**: (APCI+) Calc'd for  $\text{C}_{16}\text{H}_{19}\text{O}_4$ , 275.1289. Found 275.1292.



**(1S,2R,4S)-ethyl 4-hydroxy-2-(2-((4-methoxybenzyl)oxy)ethyl)-4-methyl-3-oxocyclopentanecarboxylate (21g)**

R<sub>f</sub> = 0.31 (5% Ethyl Acetate/Dichloromethane); 37mg (59%), 90% ee, 9:1:0.2:0.2 dr,  $[\alpha]_{\text{D}}^{21} = -42.61$  ( $c = 0.0023$  g/ml,  $\text{CHCl}_3$ ) **HPLC Analysis** Chiracel IC at 95%

Hexanes/*i*ProH. Major 13.64 min. Minor: 16.34 min  $^1\text{H-NMR}$  (300 MHz;  $\text{CDCl}_3$ ):  $\delta$  7.23 (d,  $J = 8.5$  Hz, 2H), 6.86 (d,  $J = 8.7$  Hz, 2H), 4.36 (d,  $J = 4.0$  Hz, 2H), 4.13 (dd,  $J = 11.6, 7.1$  Hz, 3H), 3.80 (s, 3H), 3.55 (td,  $J = 4.8, 2.1$  Hz, 2H), 3.09 (d,  $J = 7.2$  Hz, 1H), 2.78 (s, 1H), 2.38-2.34 (m, 1H), 2.04 (d,  $J = 5.4$  Hz, 3H), 1.88 (dd,  $J = 13.7, 10.6$  Hz, 2H), 1.31 (s, 3H), 1.23 (t,  $J = 7.1$  Hz, 3H).  $^{13}\text{C NMR}$ : (100 MHz,  $\text{CDCl}_3$ ):  $\delta$  216.5, 191.3, 180.5, 174.5, 159.1, 130.0, 129.2, 113.8, 113.7, 72.4, 67.1, 60.9, 55.2, 47.7, 42.7, 39.8, 29.0, 22.7, 14.1 **IR** (NaCl, neat): 3445, 2936, 1730, 1611, 1514, 1444, 1376, 1301, 1247, 1174. **HRMS**: (ESI-) Calc'd for  $\text{C}_{19}\text{H}_{25}\text{O}_6$ , 349.1657. Found 349.1663.



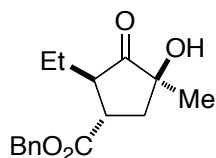
**(1S,2R,4S)-methyl 2-ethyl-4-hydroxy-4-methyl-3-oxocyclopentanecarboxylate**

**(21h)**

Rf= 0.24 (10% Ethyl Acetate/Dichloromethane); 38 mg (97%), 89% ee, 33:1:1:nd dr

$[\alpha]_D^{21} = -62.32$  (c = 0.0043 g/ml,  $\text{CHCl}_3$ ) **GC Analysis** CP-Sil 8CB column at 110 °C, 1 ml/min. Major: 8.33 min. Minor: 8.98, 9.51 min. BDM-1 column at 130 °C, 1 ml/min.

Major: 18.72 min. Minor: 18.31 min.  **$^1\text{H NMR}$** : (300 MHz,  $\text{CDCl}_3$ )  $\delta$  3.7 (s, 3H), 2.99 (q, 1H), 2.62 (m, 1H), 2.32 (dd, 1H), 1.93 (m, 1H), 1.77 (m, 1H), 1.63 (m, 2H), 1.33 (s, 3H), 0.91 (t, 3H).  **$^{13}\text{C NMR}$** : (100 MHz,  $\text{CDCl}_3$ )  $\delta$  216.3, 175.6, 52.4, 52.1, 42.4, 39.6, 23.1, 22.2, 10.9. **IR** 3456, 2970, 1737, 1439, 1377, 1170, 1032. **HRMS**: (ESI-) Calc'd for  $\text{C}_{10}\text{H}_{16}\text{O}_4$ , 199.0976. Found 199.0979.

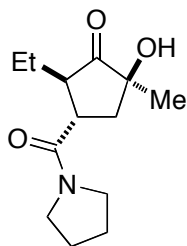


**(1S,2R,4S)-benzyl 2-ethyl-4-hydroxy-4-methyl-3-oxocyclopentanecarboxylate (21i)**

Rf= 0.31 (10% Ethyl Acetate/Dichloromethane); 24 mg (58%), 85% ee, 17:1 dr  $[\alpha]_D^{21} = -65.38$  (c = 0.0013 g/ml,  $\text{CHCl}_3$ ) **GC Analysis** CP-Sil 8CB column at 140 °C, 3 ml/min.

Major: 17.98 min. Minor: 19.92 min. HPLC Analysis : Chiralcel IC column 95:5

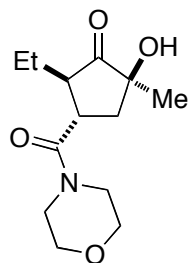
Hexanes/Isopropanol, 1ml/min. Major: 11.03 min. Minor: 9.89 min. **<sup>1</sup>H NMR:** (300 MHz, CDCl<sub>3</sub>) δ 7.36 (bs, 5H), 5.18 (s, 2H), 3.06 (q, 1H), 2.65 (m, 1H), 2.32 (dd, 1H), 1.94 (m, 1H), 1.62 (m, 2H), 1.32 (s, 3H), 0.89 (t, 3H). **<sup>13</sup>C NMR:** (100 MHz, CDCl<sub>3</sub>) δ 216.7, 174.9, 135.8, 128.8, 128.6, 128.4, 67.0, 51.9, 42.6, 39.5, 23.1, 22.3, 11.0. **IR** (NaCl, neat): 3448, 3034, 2969, 2935, 2878, 1734, 1455, 1385 cm<sup>-1</sup>. **HRMS:** (ESI-) calcd for C<sub>16</sub>H<sub>19</sub>O<sub>4</sub>, 275.1289. Found 275.1292.



**(2*S*,4*S*,5*R*)-5-ethyl-2-hydroxy-2-methyl-4-(pyrrolidine-1-carbonyl)cyclopentanone (21j)**

R<sub>f</sub> = 0.27 (50% Ethyl Acetate/Dichloromethane); 30 mg (70%), 97% ee, 8:1:0.3:0.1 dr, [α]<sub>D</sub><sup>21</sup> = -40.0 (c = 0.0017 g/ml, CHCl<sub>3</sub>) **GC Analysis** CP-Sil 8CB at 140 °C, 3 ml/min.

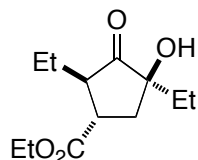
Major: 12.52 min. Minor: 10.08min, 9.59 min.,. BDM1 column at 170 °C, 3ml/min. Major: 20.23 min. Minor: 19.75 min. **<sup>1</sup>H NMR:** (300 MHz, CDCl<sub>3</sub>) δ 3.52 (quint, *J* = 6.6 Hz, 4H), 3.08 (m, 1H), 2.94 (m, 1H), 2.25 (dd, *J* = 6.9 Hz, 1H), 1.97-1.81 (m, 5H), 1.71 (m, 2H), 1.54 (m, 1H), 1.34 (s, 3H), 0.89 (t, *J* = 7.5 Hz, 3H). **<sup>13</sup>C NMR:** (100 MHz, CDCl<sub>3</sub>) δ 217.8, 172.3, 52.4, 46.8, 46.3, 42.1, 39.5, 26.2, 24.5, 23.4, 21.9, 11.3 **IR** (NaCl, neat): 3354, 2969, 2876, 1746, 1622, 1518, 1452, 1343, 1255, 1229, 1165cm<sup>-1</sup>. **HRMS:** (ESI+) Calcd for C<sub>13</sub>H<sub>22</sub>NO<sub>3</sub>, 240.1594. Found 240.1596.



**(2S,4S,5R)-5-ethyl-2-hydroxy-2-methyl-4-(morpholine-4-carbonyl)cyclopentanone**

**(21k)**

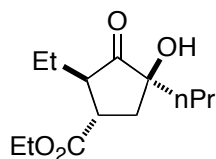
Rf= 0.30 (100% Ethyl Acetate); 37 mg (99%), 98% ee, 9:1:0.4:0.1 dr,  $[\alpha]_D^{21} = -44.23$  (c = 0.0052 g/ml, CHCl<sub>3</sub>) **GC Analysis** CP-Sil 8CB at 140 °C, 3 ml/min. Major: 14.49 min. Minor: 12.83min, 12.01 min, 12.45 min. BDM1 column at 160 °C, 3ml/min. Major: 41.07 min. Minor: 40.48 min. **<sup>1</sup>H NMR:** (300 MHz, CDCl<sub>3</sub>) δ 3.68 (m, 8H), 3.17 (m, 1H), 3.01 (m, 1H), 2.19 (dd, J = 6.9, 13.5 Hz, 1H), 1.81 (m, 2H), 1.55 (m, 1H), 1.33 (s, 3H), 0.89 (t, J = 7.5 Hz, 3H) **<sup>13</sup>C NMR:** (100 MHz, CDCl<sub>3</sub>) δ 217.0, 191.3, 172.0, 75.84, 66.9, 51.8, 45.9, 42.6, 39.8, 39.5, 23.1, 21.7, 11.1 **IR** (NaCl, neat): 3383, 2966, 1745, 1638, 1438, 1240, 1117 cm<sup>-1</sup>. **HRMS:** (ESI+) Calcd for C<sub>13</sub>H<sub>22</sub>NO<sub>3</sub>, 240.1594. Found 240.1596.



**(1S,2R,4S)-ethyl 2,4-diethyl-4-hydroxy-3-oxocyclopentanecarboxylate (21l)**

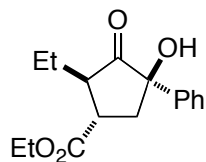
Rf= 0.21 (10% Ethyl Acetate/Dichloromethane); 42 mg (76%), 81% ee, 55:1:1 dr  $[\alpha]_D^{21} = -56.82$  (c = 0.0022 g/ml, CHCl<sub>3</sub>) **GC Analysis** CP-Sil 8CB at 110 °C, 1 ml/min. Major: 20.19 min. Minor: 22.52, 24.50 min. BDM-1 column at 130 °C, 1 ml/min. Major: 35.16

min. Minor: 34.54 min. **<sup>1</sup>H NMR**: (300 MHz, CDCl<sub>3</sub>) δ 4.20 (q, 2H), 2.94 (q, 1H), 2.61 (m, 1H), 2.21 (dd, 1H), 1.99 (m, 1H), 1.78 (m, 1H), 1.60 (m, 3H), 1.29 (t, 3H), 0.92 (t, 3H). **<sup>13</sup>C NMR**: (100 MHz, CDCl<sub>3</sub>) δ 217.3, 175.2, 61.2, 52.6, 42.4, 36.7, 29.6, 21.9, 14.4, 11.1, 7.8. **IR** (NaCl, neat): 3467, 2970, 2938, 2880, 1734, 1518, 1462, 1378, 1231, 1179, 1035, 995, 947 cm<sup>-1</sup>. **HRMS**: (ESI-) calcd for C<sub>12</sub>H<sub>20</sub>O<sub>4</sub>, 227.1289. Found 227.1292.



**(1S,2R,4S)-ethyl 2-ethyl-4-hydroxy-3-oxo-4-propylcyclopentanecarboxylate (21m)**

R<sub>f</sub> = 0.24 (10% Ethyl Acetate/Dichloromethane); 19 mg (53%), 85% ee, 16:1 dr [α]<sub>D</sub><sup>21</sup> = -70.0 (c = 0.0008 g/ml, CHCl<sub>3</sub>) **GC Analysis** CP-Sil 8CB at 110 °C, 1 ml/min. Major: 32.66min. Minor: 35.76 min. BDM-1 column at 130 °C, 1 ml/min. Major: 55.68 min. Minor: 54.01 min. **<sup>1</sup>H NMR**: (300 MHz, CDCl<sub>3</sub>) δ 4.20 (q, 2H), 2.95 (q, 1H), 2.60 (m, 1H), 2.20 (dd, 1H), 2.02 (m, 1H), 1.79 (m, 1H), 1.60 (m, 3H), 1.50 (m, 2H) 1.29 (t, 3H), 0.92 (m, 6H). **<sup>13</sup>C NMR**: (100 MHz, CDCl<sub>3</sub>) δ 217.2, 175.1, 61.2, 52.5, 42.5, 38.9, 37.2, 21.9, 16.9, 14.6, 14.4, 11.1. **IR** (NaCl, neat): 3437, 2957, 2865, 1720, 1462, 1377, 1232, 1191 cm<sup>-1</sup>. **HRMS**: (ESI-) calcd for C<sub>13</sub>H<sub>21</sub>O<sub>4</sub>, 241.1445. Found 241.1442.



**(1*S*,2*R*,4*R*)-ethyl 2-ethyl-4-hydroxy-3-oxo-4-phenylcyclopentanecarboxylate (21o)**

R<sub>f</sub> = 0.71 (10% Ethyl Acetate/Dichloromethane); 39 mg (95%), 83% ee, 4.4:1:<1:<1 dr

[α]<sub>D</sub><sup>21</sup> = -62.50 (c = 0.002 g/ml, CHCl<sub>3</sub>) **GC Analysis** CP-Sil 8CB at 170 °C, 2 ml/min.

Major: 6.40min. Minor: 6.50, 7.96, 7.86 min. **HPLC Analysis** : Chiralcel IC column 95:5

Hexanes/Isopropanol, 1ml/min. Major: 9.43 min. Minor: 10.13 min. **<sup>1</sup>H NMR**: (300 MHz,

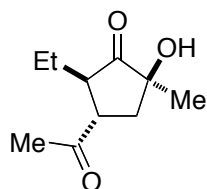
CDCl<sub>3</sub>) δ 7.35 (bs, 5H), 4.15 (m, 2H), 3.13 (q, 1H), 2.83 (m, 1H), 2.60 (dd, 1H), 2.30 (m,

0.5H), 1.74 (m, 1H), 1.27 (q, 3H), 0.98 (t, 3H). **<sup>13</sup>C NMR**: (100 MHz, CDCl<sub>3</sub>) δ 215.7,

174.7, 141.2, 128.7, 128.2, 125.6, 61.3, 53.9, 42.8, 42.0, 22.0, 14.4, 11.0. **IR** (NaCl,

neat): 3442, 3062, 2973, 2938, 2878, 1733, 1496, 1448, 1376 cm<sup>-1</sup>. **HRMS**: (ESI+)

calcd for C<sub>16</sub>H<sub>20</sub>O<sub>4</sub>Na, 299.1254. Found 299.1256.



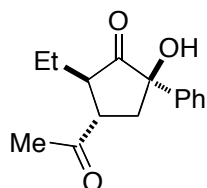
**(2*S*,4*S*,5*R*)-4-acetyl-5-ethyl-2-hydroxy-2-methylcyclopentanone (21p)**

R<sub>f</sub> = 0.3 (10% Ethyl Acetate/Dichloromethane); 24mg (58%), 68% ee, 9:1:0.4:0.6 dr,

[α]<sub>D</sub><sup>21</sup> = -56.0 (c = 0.0025g/ml, CHCl<sub>3</sub>) **GC Analysis** [CP-Sil 8CB] at 110 °C, 1 ml/min.

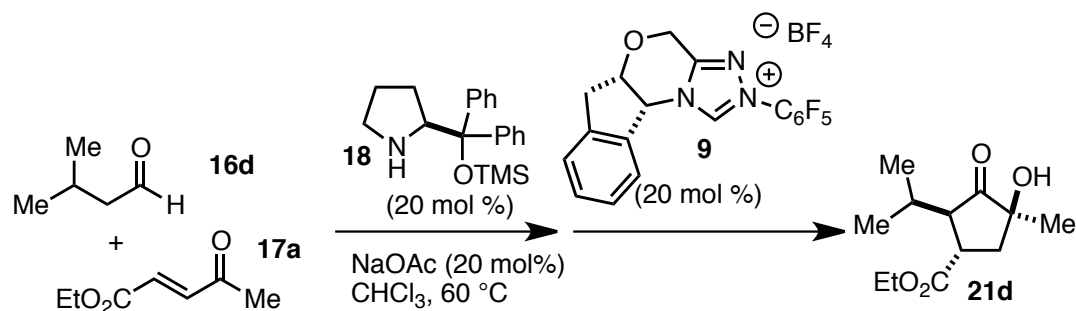
Major: 6.96. Minor: 7.37 min, 8.05 min, 8.38 min. **HPLC Analysis**: Chiralcel IC column at

98% Hexanes/Isopropanol, 1ml/min. Major: 33.32 min. Minor: 27.89 min. **<sup>1</sup>H NMR:** (300 MHz; CDCl<sub>3</sub>): δ 3.17 (td, *J* = 10.2, 7.4 Hz, 1H), 2.78-2.71 (m, 1H), 2.36 (dd, *J* = 13.5, 7.4 Hz, 1H), 2.27 (s, 3H), 2.01-2.00 (m, 1H), 1.77-1.66 (m, 2H), 1.62-1.52 (m, 2H), 1.31 (s, 3H), 0.88 (t, *J* = 7.5 Hz, 3H). **<sup>13</sup>C NMR:** (100 MHz, CDCl<sub>3</sub>): δ 217.1, 208.9, 75.9, 49.9, 49.8, 39.4, 29.5, 22.9, 22.1, 11.0 **IR** (NaCl, neat): 3442, 2971, 2931, 1741, 1702, 1437, 1386, 1267, 1226, 1162 cm<sup>-1</sup>. **HRMS:** (ESI-) calcd for C<sub>10</sub>H<sub>15</sub>O<sub>3</sub>, 183.1027. Found 183.1027.



**(2*R*,4*S*,5*R*)-4-acetyl-5-ethyl-2-hydroxy-2-phenylcyclopentanone (21q)**

R<sub>f</sub> = 0.12 (10% Ethyl Acetate/Dichloromethane); 12mg (35%), % ee, 4:1:0.4:0.6 dr, [α]<sub>D</sub><sup>21</sup> = -104 (c = 0.003g/ml, CHCl<sub>3</sub>) **GC Analysis:** CP-Sil 8CB at 170 °C and 3 ml/min. Major: 25.108 min. Minor: 26.679 min, 30.489 min, 35.243 min. **HPLC Analysis** Chiracel IC column at 95% Hexanes/*i*PrOH, 1 ml/min. Major: 11.248 min. Minor 12.768 min. **<sup>1</sup>H NMR:** (300 MHz; CDCl<sub>3</sub>): δ 7.41-7.27 (m, 5H), 3.33 (td, *J* = 11.0, 6.7 Hz, 1H), 2.95 (dt, *J* = 10.9, 5.6 Hz, 1H), 2.66-2.56 (m, 2H), 2.32-2.24 (m, 3H), 2.02 (ddd, *J* = 13.6, 11.5, 2.0 Hz, 1H), 1.86-1.76 (m, 1H), 1.74-1.64 (m, 1H), 1.64-1.57 (m, 1H), 0.96-0.88 (m, 3H). **<sup>13</sup>C NMR:** (100 MHz, CDCl<sub>3</sub>) δ 215.9, 208.4, 140.9, 128.5, 128.0, 125.2, 80.2, 52.3, 49.8, 41.9, 29.7, 21.7, 11.0 **IR** (NaCl, neat): 3410, 3061, 3029, 2966, 2934, 2877, 2252, 1956, 1744, 1708, 1600, 1518, 1495, 1448, 1367, 1217 cm<sup>-1</sup>.

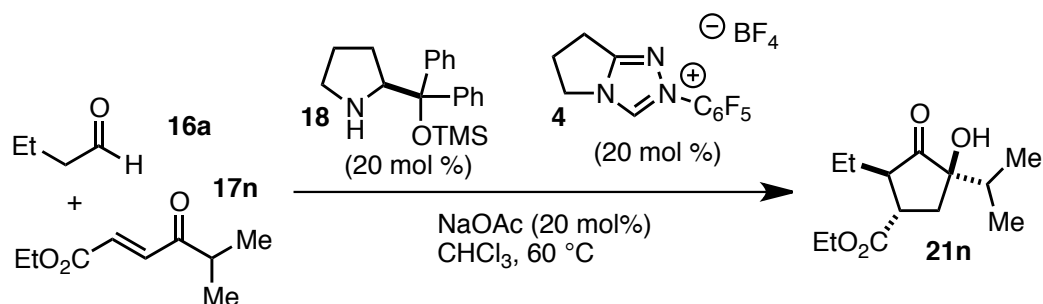


**(1*S*,2*R*,4*S*)-ethyl 4-hydroxy-2-isopropyl-4-methyl-3-oxocyclopentanecarboxylate  
(21d)**

In a 5 ml round bottom flask, 25 mg of **2a** (0.17 mmol) was combined with 10 mg of **3** (0.2 equiv, 0.03 mmol) and 1.7  $\mu$ l of AcOH (0.2 equiv., 0.03 mmol) and dissolved in 1 ml of chloroform. The reaction was stirred at 60 °C for 3 hours. The reaction was cooled to room temperature and 14 mg of **6** (0.2 equiv., 0.03 mmol) and 5 mg of sodium acetate (0.4 equiv., 0.06 mmol) were added. The reaction was stirred at 60 °C for an additional 4 hours. The reaction was cooled to room temperature and filtered through a plug of silica gel, washing with DCM then EtOAc. The filtrate was concentrated and purified by column chromatography, eluting with 10% EtOAc/DCM to 50% EtOAc/Hexanes through silica gel. Isolated a yellow oil.

R<sub>f</sub> = 0.35 (10% Ethyl Acetate/Dichloromethane); 49 mg (90%), 88% ee, 24:1:0.1 dr, [α]<sub>D</sub><sup>21</sup> = -66.96 (c = 0.0046 g/ml, CHCl<sub>3</sub>) **GC Analysis** CP-Sil 8CB column at 90 °C, 2 ml/min. Major: 24.48 min. Minor: 26.62 min, 27.69 min. BDM1 column at 130 °C, 2ml/min. Major: 18.48 min. Minor: 17.71 min. **<sup>1</sup>H NMR:** (300 MHz, CDCl<sub>3</sub>) δ 4.20 (q, *J* =

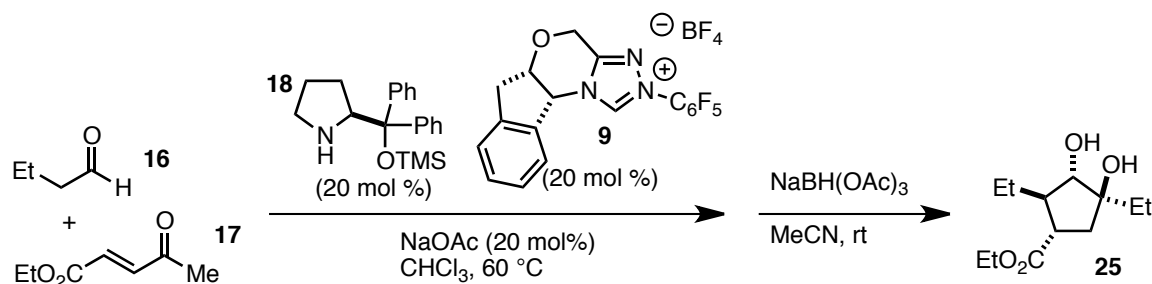
6.9, 2H), 3.08 (q,  $J = 7.5$ , 1H), 2.72 (dd,  $J = 3.9, 9.9$ , 1H), 2.92 (dd,  $J = 7.5, 13.8$ , 1H), 2.25 (m, 1H), 1.90 (m, 2H), 1.31 (s, 3H), 1.29 (t,  $J = 7.2$ , 3H), 0.97 (d,  $J = 6.9$ , 3H), 0.91 (d,  $J = 6.9$ , 3H).  $^{13}\text{C NMR}$ : (100 MHz,  $\text{CDCl}_3$ )  $\delta$  216.7, 175.7, 61.2, 56.7, 39.9, 39.6, 27.9, 22.9, 20.3, 18.8, 14.3 **IR** (NaCl, neat): 3472, 2967, 2876, 1735, 1519, 1466, 1378, 1338, 1239, 1177  $\text{cm}^{-1}$ . **HRMS**: (ESI-) Calcd for  $\text{C}_{12}\text{H}_{19}\text{O}_4$ , 227.1289. Found 227.1291.



**(1*S*,2*R*,4*R*)-ethyl 2-ethyl-4-hydroxy-4-isopropyl-3-oxocyclopentanecarboxylate (21n)**

In a 5 ml round bottom flask, combined 25 mg of **2o** (0.15 mmol) with 10 mg of **3** (0.2 equiv., 0.03 mmol) and 11 mg of **5** (0.2 equiv., 0.03 mmol). Dissolved in 1 ml of  $\text{CHCl}_3$  and bubbled Ar into the reaction mixture for 1 minute. Added 20  $\mu\text{l}$  of butyraldehyde (**1a**, 1.5 equiv., 0.22 mmol) and 2.5 mg of NaOAc (0.2 equiv., 0.03 mmol). Stirred at 80  $^\circ\text{C}$  for 4 hours. Cooled to room temperature and filtered through a plug of silica gel, washing with DCM then EtOAc. Concentrated the filtrate and purified by column chromatography, eluting with 10% EtOAc/DCM through 50% EtOAc/Hexanes through silica gel. Isolated a yellow solid (mixture of diastereomers).

R<sub>f</sub> = 0.3 (10% Ethyl Acetate/Dichloromethane); 25 mg (69%), 51% ee, 18:1:0.1:0.7 dr, [α]<sub>D</sub><sup>21</sup> = -44.50 (c = 0.004 g/ml, CHCl<sub>3</sub>) **GC Analysis** CP-Sil 8CB at 110 °C, 1 ml/min. Major: 27.97min. Minor: 28.35 min, 30.41 min, 32.16 min. BDM1 column at 130 °C, 2ml/min. Major: 26.85 min. Minor: 27.55 min. **<sup>1</sup>H NMR:** (300 MHz, CDCl<sub>3</sub>) δ 4.21 (q, *J* = 7.2, 2H), 2.93 (q, *J* = 7.2, 1H), 2.54 (q, *J* = 5.7, 1H), 2.01 (m, 3H), 1.83 (m, 2H), 1.60 (m, 1H), 1.29 (t, *J* = 6.9, 3H), 0.98 (d, *J* = 6.9, 3H), 0.90 (t, *J* = 7.5, 3H), 0.83 (d, *J* = 6.9, 3H). **<sup>13</sup>C NMR:** (100 MHz, CDCl<sub>3</sub>) δ 217.6, 175.2, 81.4, 61.2, 53.9, 42.2, 33.4, 33.3, 21.5, 17.7, 16.2, 14.4, 10.9 **IR** (NaCl, neat): 3467, 2967, 2878, 1735, 1466, 1377, 1233, 1180 cm<sup>-1</sup>. **HRMS:** (ESI-) calcd for C<sub>13</sub>H<sub>21</sub>O<sub>4</sub>, 241.1445. Found 241.1444.

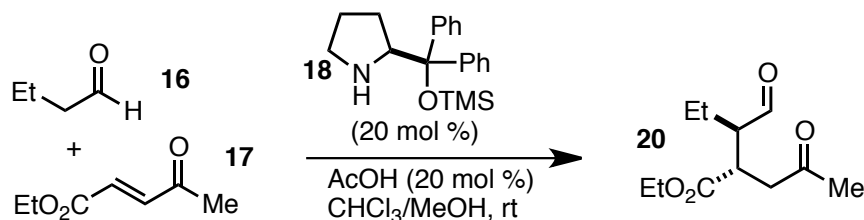


**(1*S*,2*R*,3*S*,4*S*)-ethyl 2-ethyl-3,4-dihydroxy-4-methylcyclopentanecarboxylate (7)**

In a 5 ml round bottom flask, 25 mg (0.17 mmol) of **2a** was combined with 10 mg of **3** (0.2 equiv., 0.03 mmol) and 14 mg of **6** (0.2 equiv., 0.03 mmol). This mixture was taken up in CHCl<sub>3</sub> and bubbled with Ar for 1 minute. 18 μl of butyraldehyde (**1a**, 1.2 equiv., 0.2 mmol) and 2.5 mg of NaOAc (0.2 equiv, 0.03 mmol) were added and the reaction was stirred at 60 °C for 5 hours. The reaction was cooled to room temperature and 40 mg of NaBH(OAc)<sub>3</sub> (1.1 equiv., 0.19 mmol) and 1 ml of acetonitrile were added. The

suspension was stirred at room temperature overnight. The reaction mixture was filtered through silica gel, eluting with EtOAc. The filtrate was concentrated and purified by column chromatography, eluting with 100% EtOAc through silica gel. Isolated a yellow oil.

Rf= 0.22 (100% Ethyl Acetate); 31mg (84%), 88% ee, 35:1:<1:<1 dr,  $[\alpha]_D^{21} = -67.33$  (c = 0.0015 g/ml, CHCl<sub>3</sub>) **GC Analysis** CP-Sil 8CB at 130 °C, 1 ml/min. Major: 8.69min. Minor: 5.6 min, 7.33 min, 5.12 min. BDM1 column at 120 °C, 2ml/min. Major: 62.36 min. Minor: 61.63 min. **<sup>1</sup>H NMR:** (300 MHz, CDCl<sub>3</sub>)  $\delta_H$  4.13 (2 H, q, *J* 7.0, A), 3.55 (1 H, d, *J* 6.8, B), 2.60 (1 H, d, *J* 8.7, C), 1.99 (3 H, m, *J* 8.7, D), 1.65 (1 H, d, *J* 7.4, E), 1.54 (1 H, d, *J* 7.3, F), 1.31 (3 H, s, G), 1.22-1.27 (3 H, m, H), 0.94 (3 H, t, *J* 7.4, I). **<sup>13</sup>C NMR:** (100 MHz, CDCl<sub>3</sub>)  $\delta_C$  176.0, 84.4, 80.1, 60.6, 51.2, 44.5, 41.3, 26.5, 22.9, 14.1, 11.8 **IR** (NaCl, neat): 3421, 2964, 2934, 2877, 1729, 1519, 1458, 1376, 1179 cm<sup>-1</sup>. **HRMS:** (ESI+) calcd for C<sub>11</sub>H<sub>21</sub>O<sub>4</sub>, 217.1434. Found 217.1444.

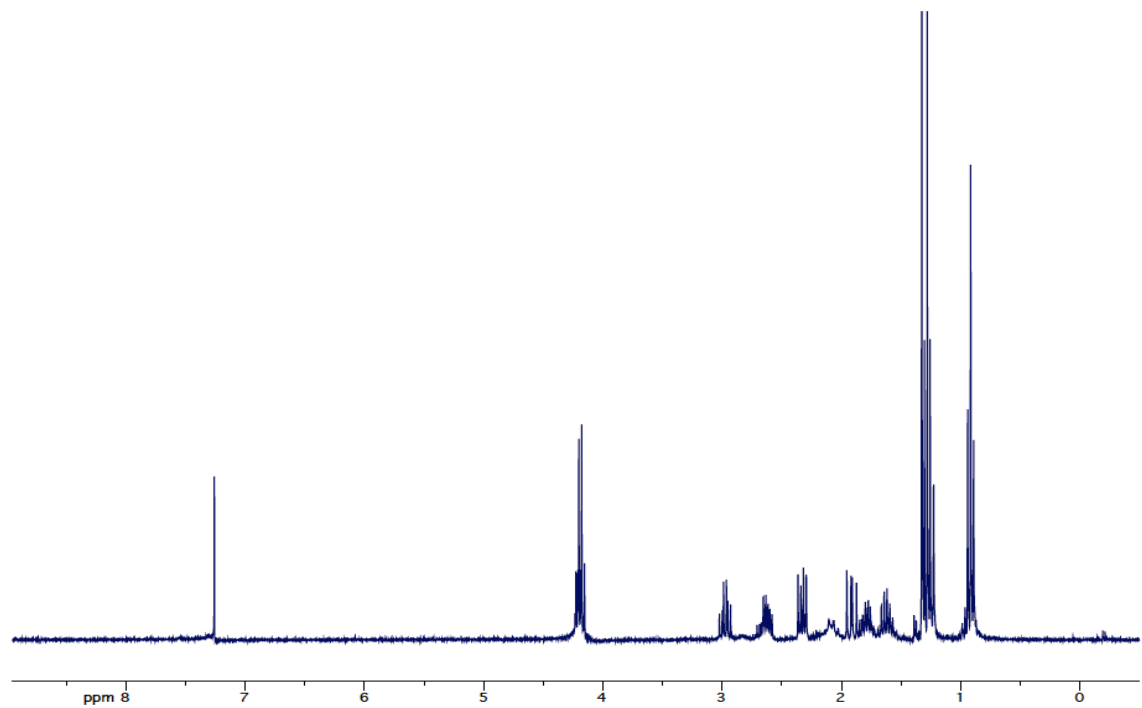
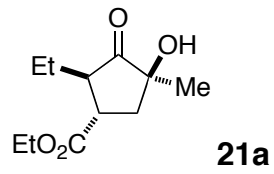


**(2*S*,3*R*)-ethyl 3-formyl-2-(2-oxopropyl)pentanoate (**20**)<sup>8</sup>**

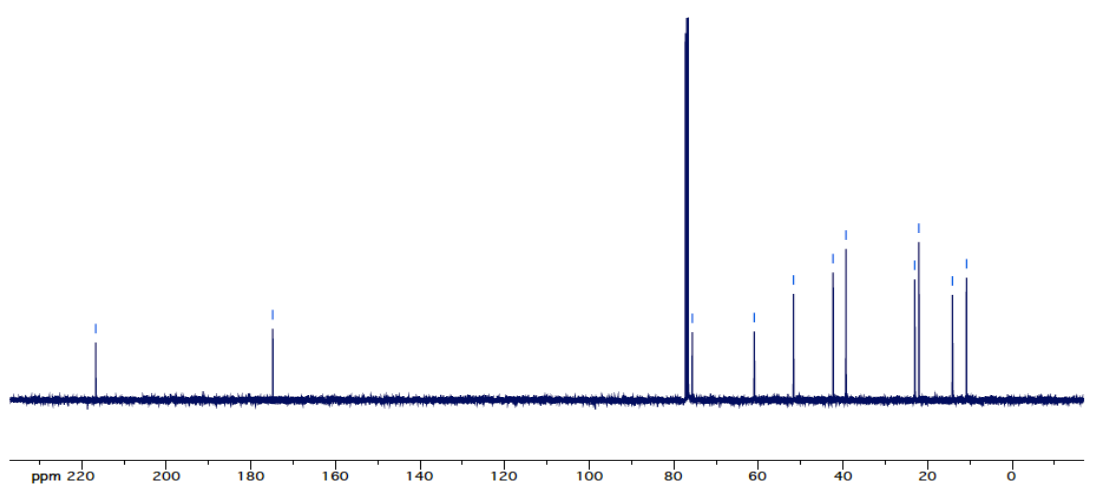
<sup>8</sup> Wang, J.; Ma, A.; Ma, D. *Org Lett.* **2008**, *10*, 5425-5428.

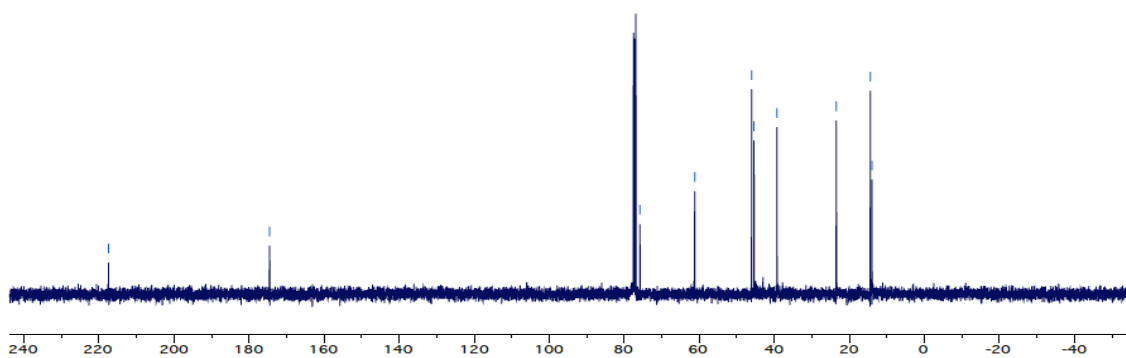
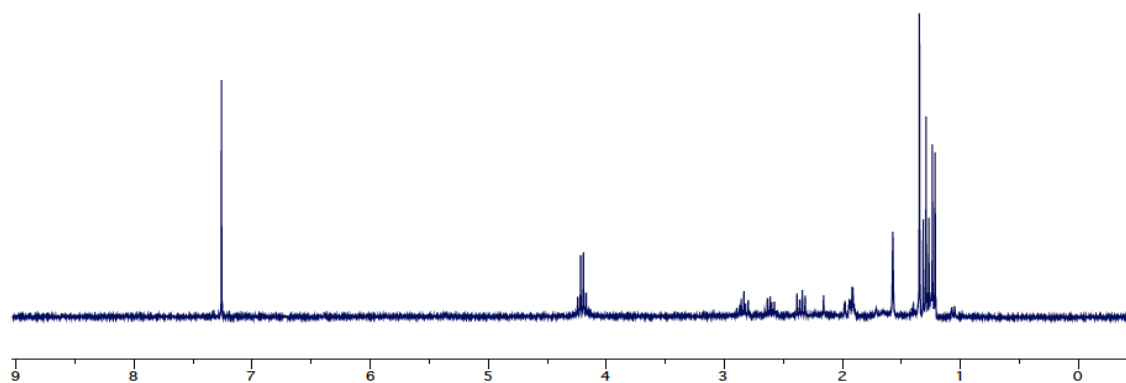
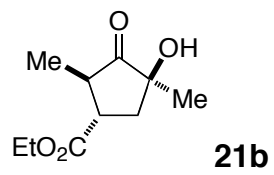
In a 5 ml round bottom flask, combined 200 mg of **2a** (1.41 mmol) with 45 mg of **3** (0.1 equiv, 0.14 mmol). Dissolved in 6 ml of CHCl<sub>3</sub> and 1 ml of MeOH, added 0.15 ml of butyraldehyde (**1a**, 1.2 equiv., 1.69 mmol) and 2 drops of acetic acid. Stirred at 60 °C for 5 hours. Cooled to room temperature and concentrated. Purified by column chromatography, eluting with 10% EtOAc/Hexanes through silica gel. Isolated as a mixture of diastereomers. Product is a yellow oil.

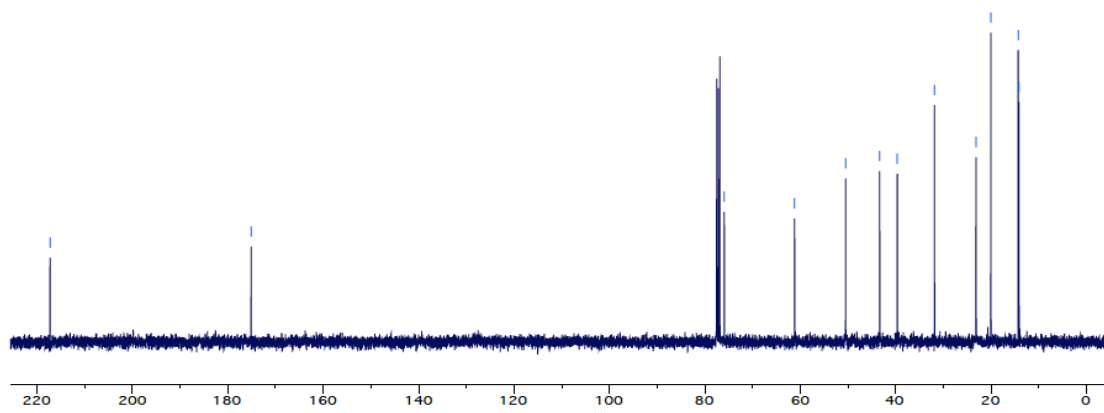
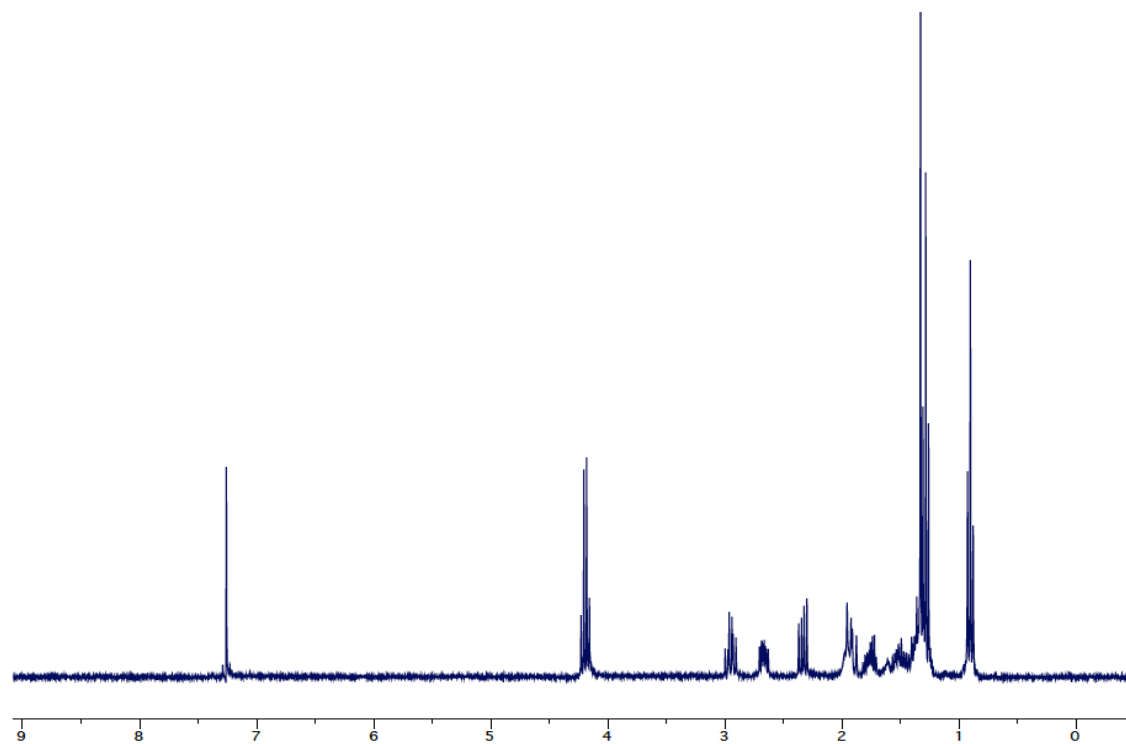
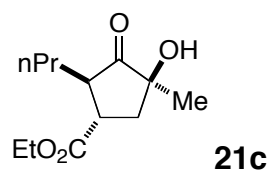
Rf= 0.45 (10% Ethyl Acetate/Dichloromethane); 301mg (99%), 96% ee, 1.1:1 dr,  $[\alpha]_D^{21} = +20.8$  (c = 0.005 g/ml, CHCl<sub>3</sub>) **GC Analysis.** **<sup>1</sup>H NMR:** (300 MHz, CDCl<sub>3</sub>)  $\delta_H$  9.65 (1 H, s), 4.10-4.18 (2 H, m), 3.29-3.39 (1 H, m), 2.97 (1 H, ddd, *J* 25.6, 17.9 and 9.3), 2.53-2.59 (1 H, m), 2.36-2.53 (1 H, m), 2.17-2.22 (3 H, s), 1.70-1.80 (1 H, m), 1.40-1.54 (2 H, m), 1.22-1.32 (3 H, m), 0.94-1.00 (3 H, m). **<sup>13</sup>C NMR:** (100 MHz, CDCl<sub>3</sub>)  $\delta_C$  206.3, 206.1, 202.4, 191.3, 178.7, 18.3, 173.2, 172.9, 61.1, 54.1, 47.8, 47.4, 41.9, 41.5, 41.3, 39.3, 30.0, 29.9, 22.7, 21.9, 19.4, 14.0, 12.0, **IR** (NaCl, neat): 2971, 2881, 1720, 1463, 1369, 1165, 1045 cm<sup>-1</sup>. **HRMS:** (ESI+) calcd for C<sub>11</sub>H<sub>19</sub>O<sub>4</sub>, 215.1278. Found 215.1270.

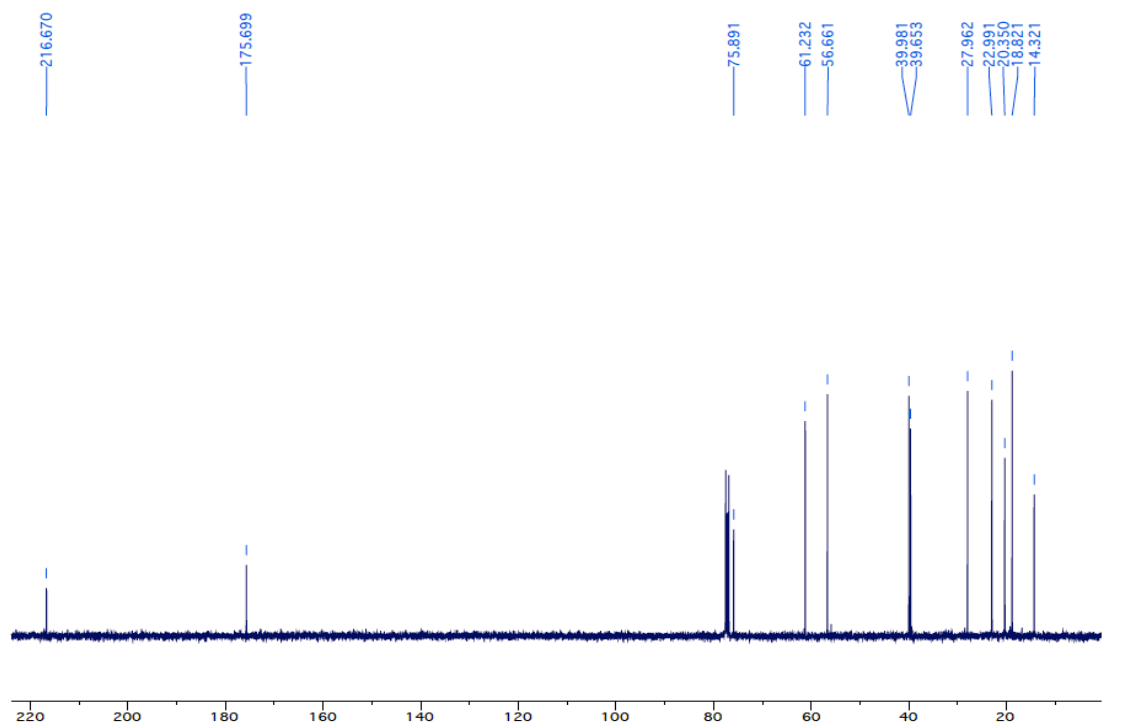
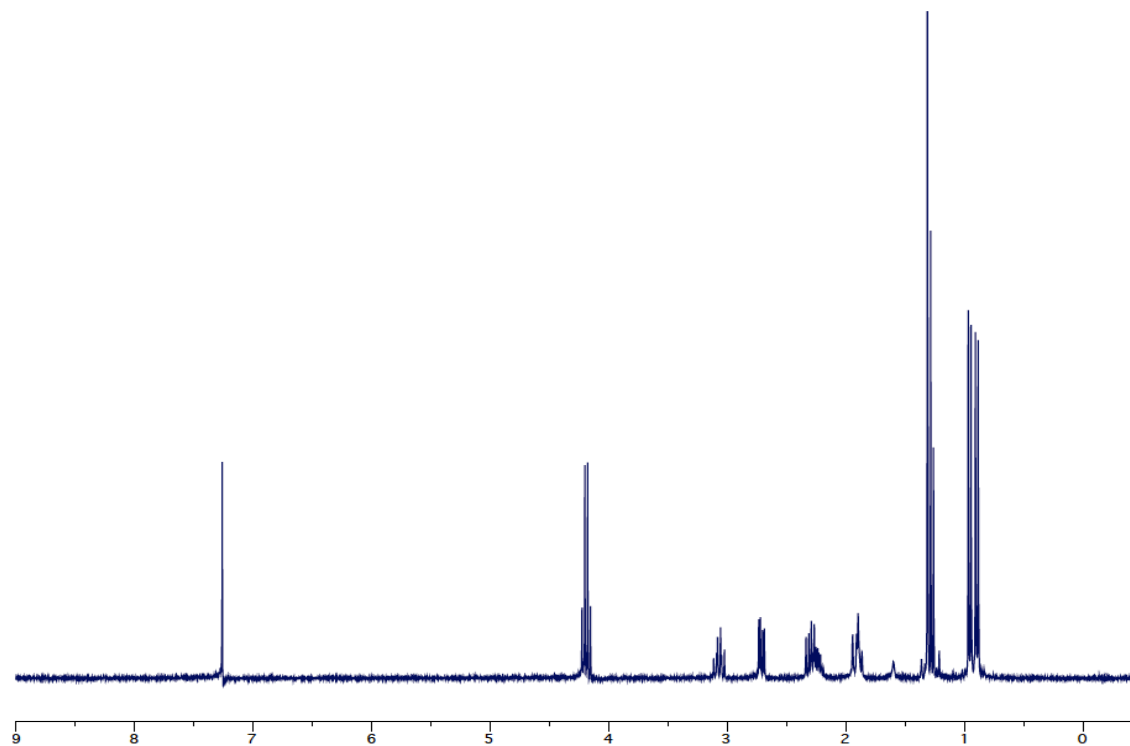
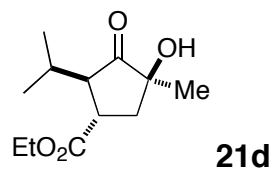


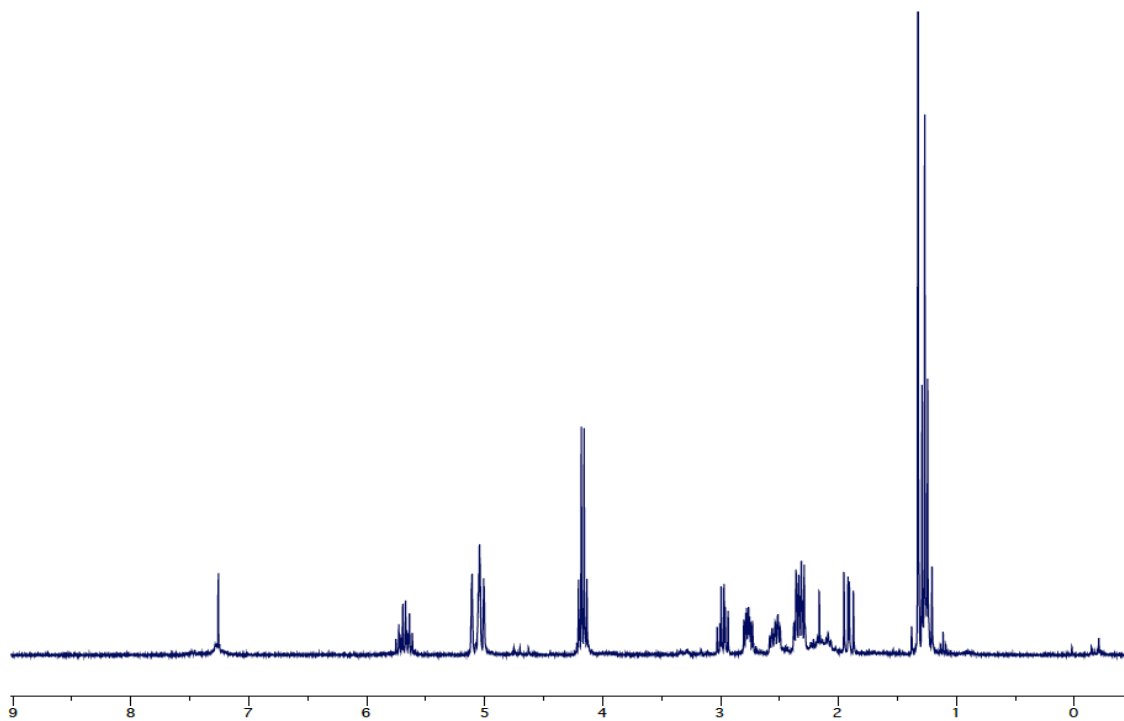
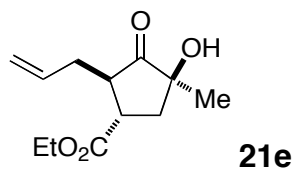
216.688  
174.818  
75.667  
60.984  
51.740  
42.355  
39.318  
23.045  
22.078  
14.147  
10.831



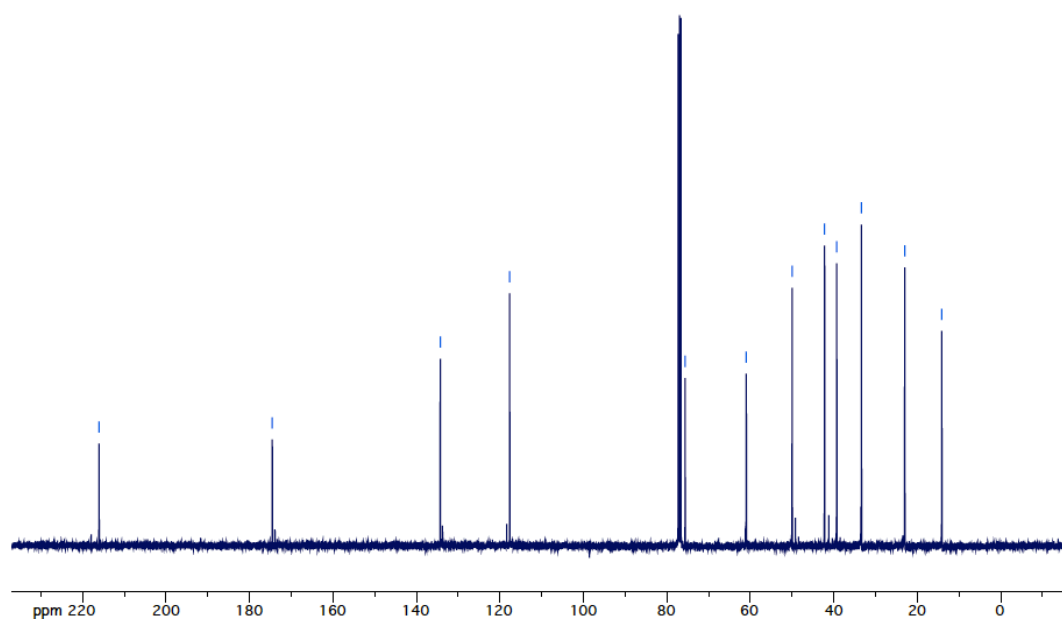


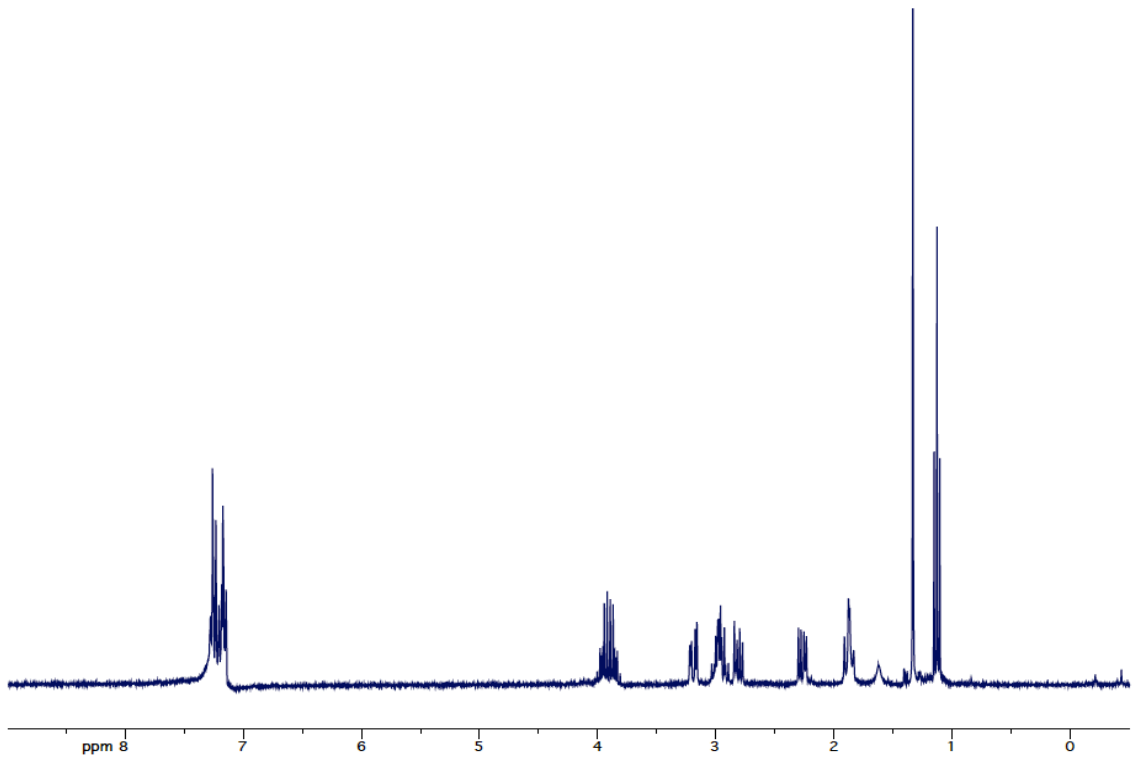
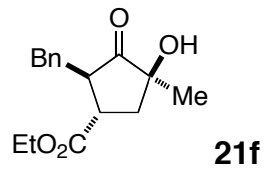




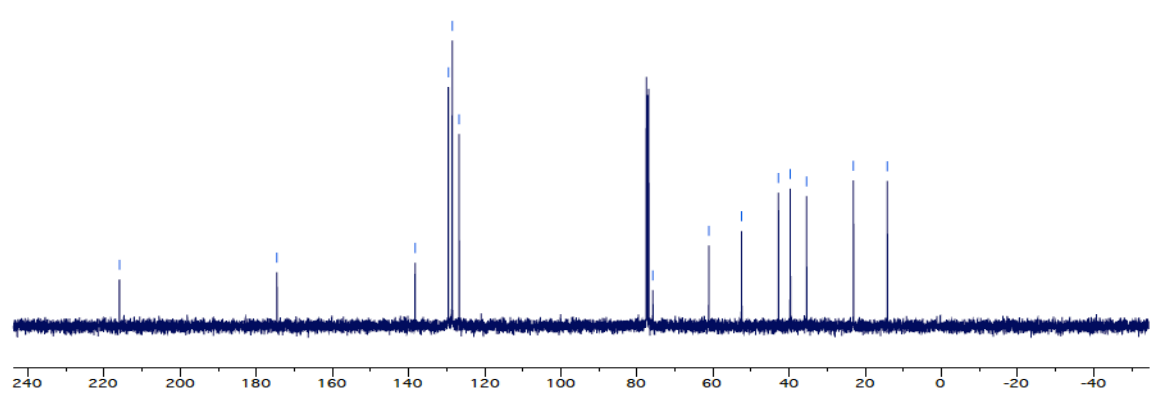


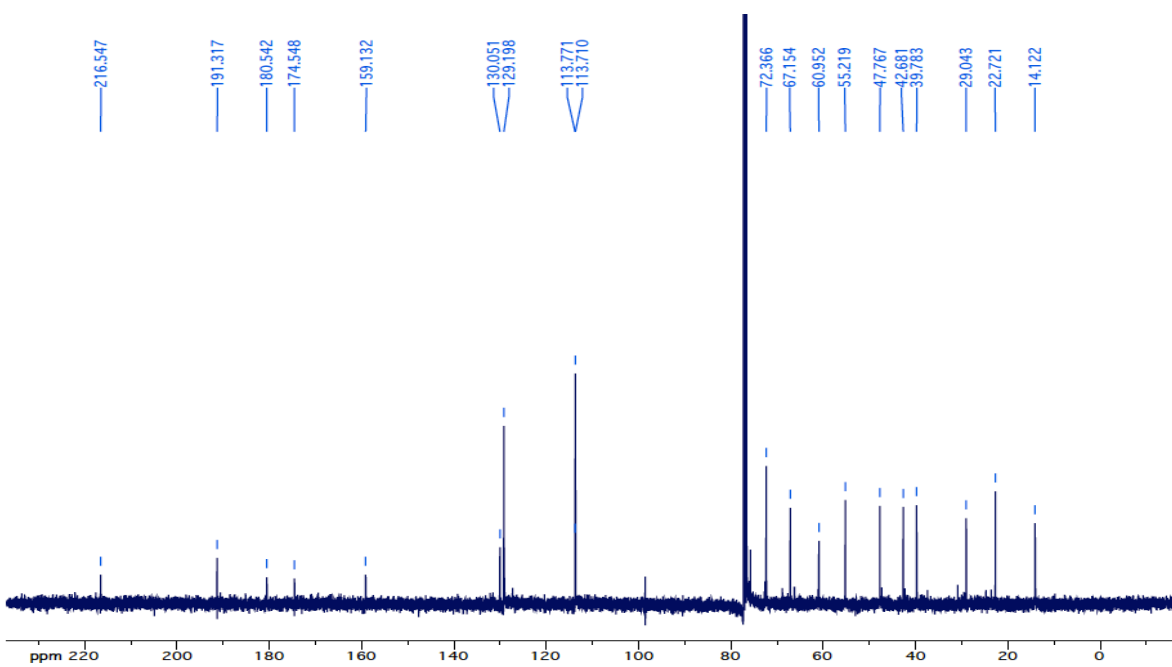
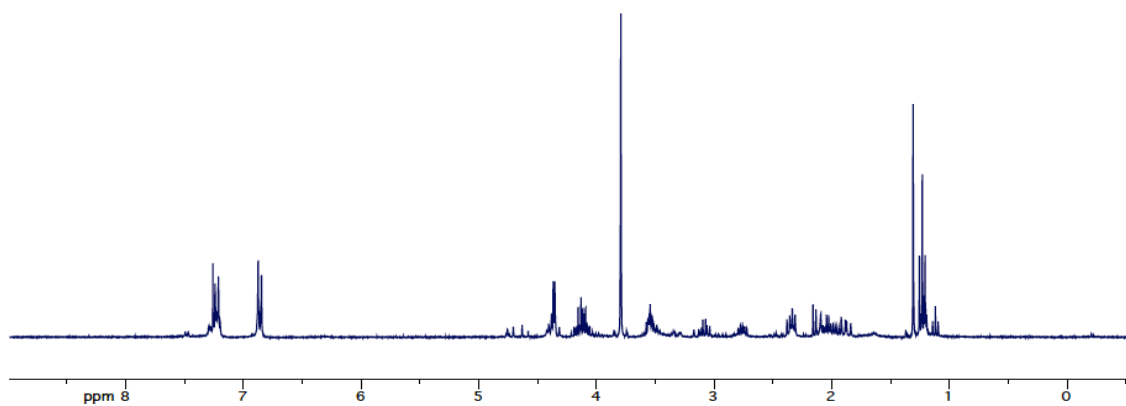
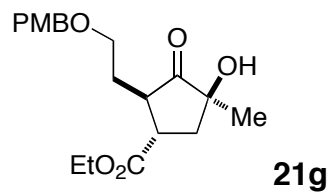
216.087  
174.539  
134.305  
117.675  
75.619  
60.976  
49.976  
42.216  
39.304  
33.386  
23.000  
14.133

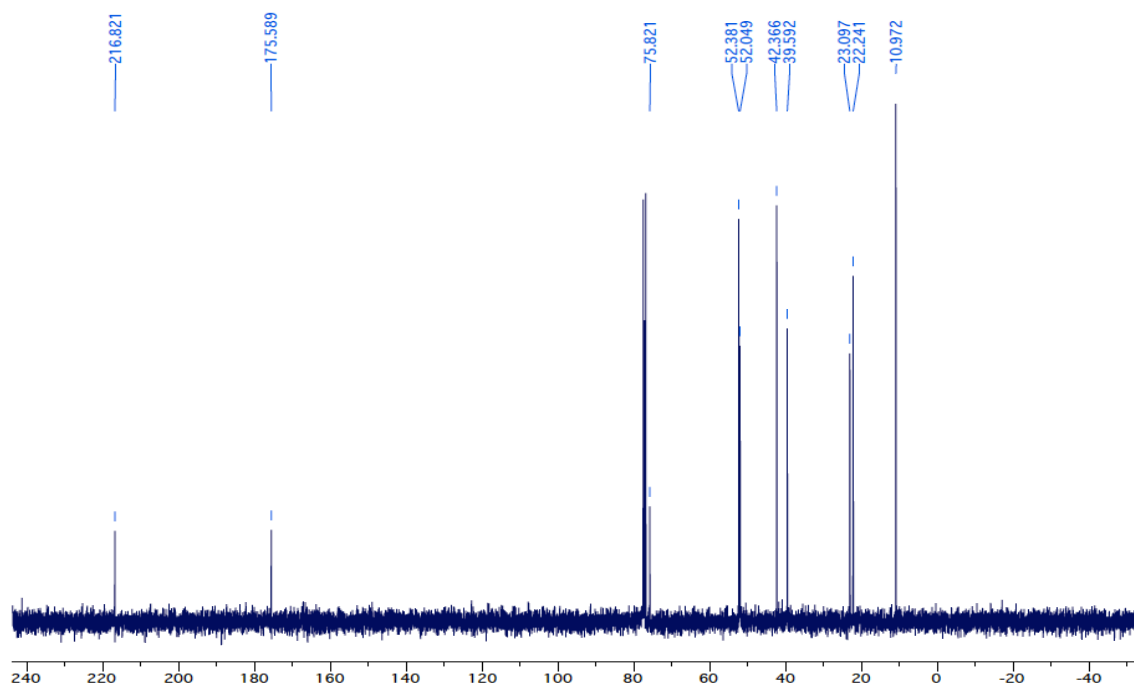
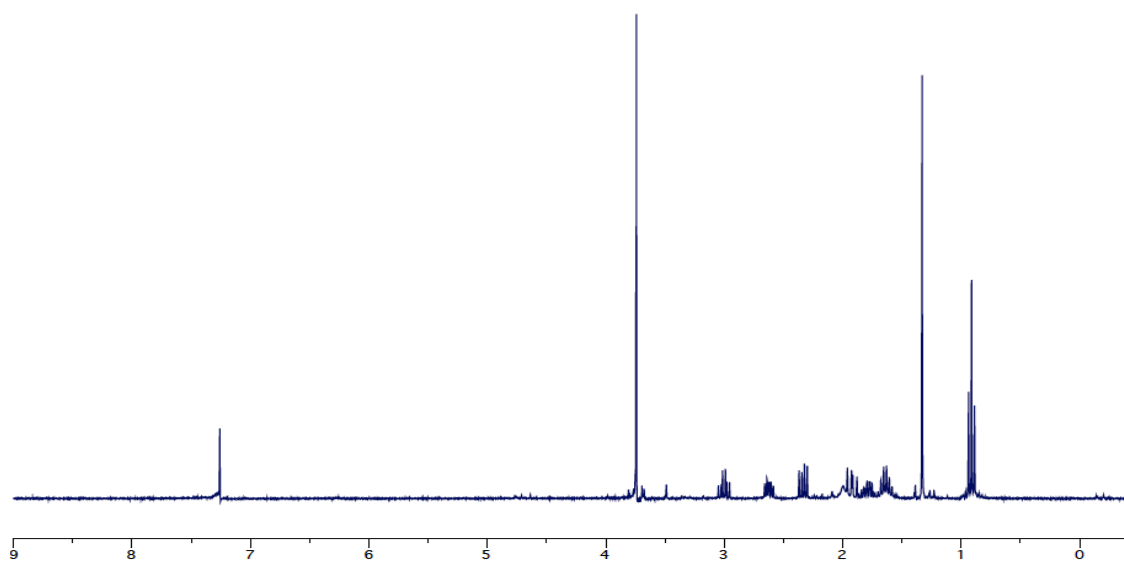
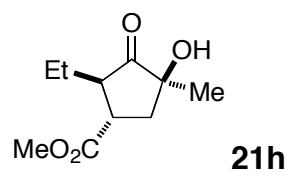


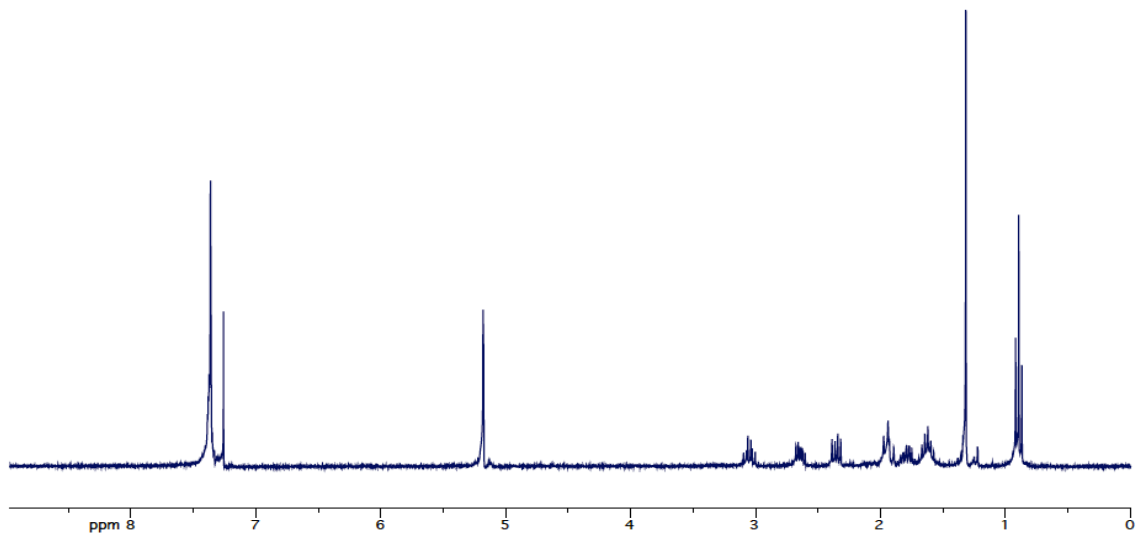
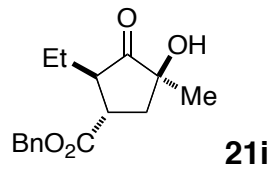


215.978  
174.587  
138.297  
129.553  
128.535  
126.714  
75.808  
61.116  
52.521  
42.806  
39.726  
35.427  
23.120  
14.197

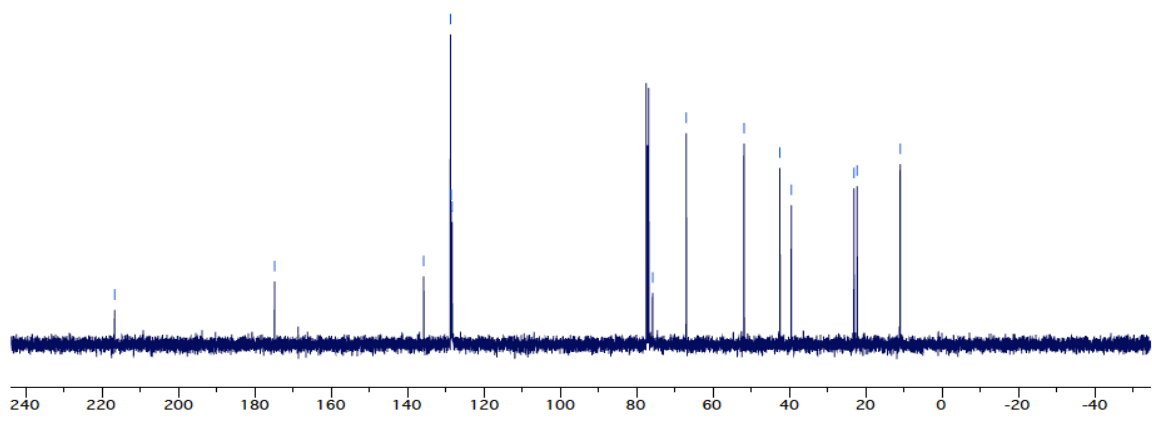


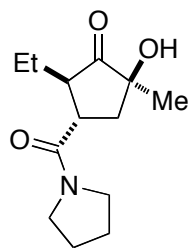




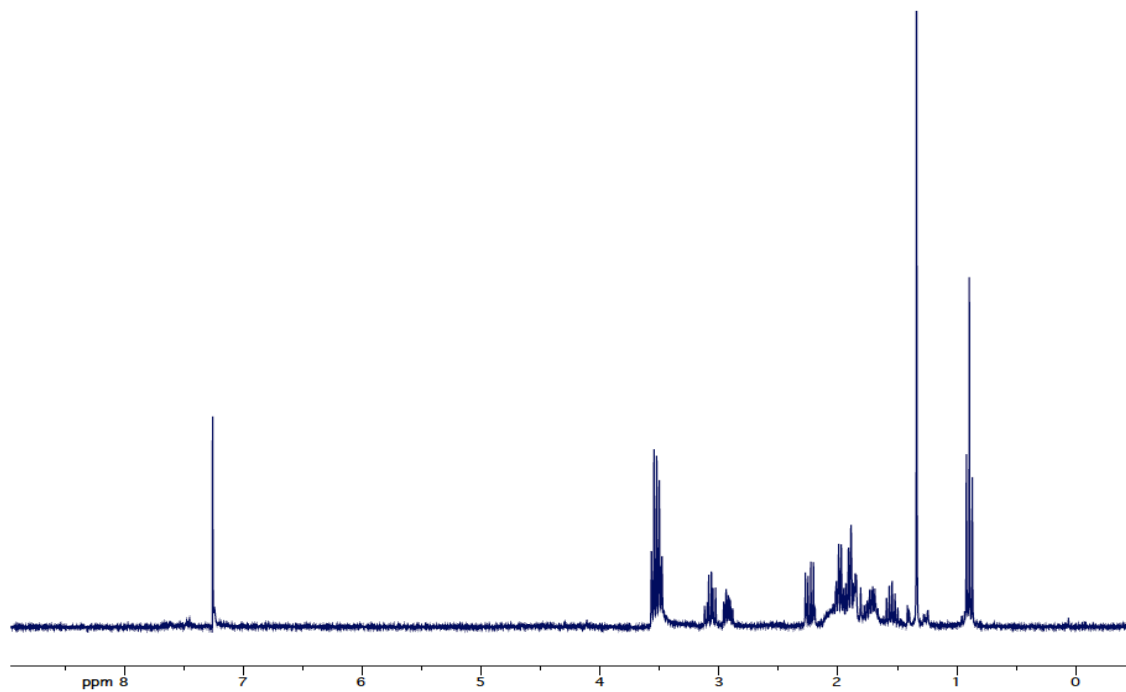


216.745  
 174.861  
 135.800  
 128.808  
 128.589  
 128.364  
 75.873  
 67.040  
 51.944  
 42.548  
 39.541  
 23.139  
 22.318  
 11.045





21j



217.816

172.255

76.034

52.426

46.790

46.754

32.140

39.544

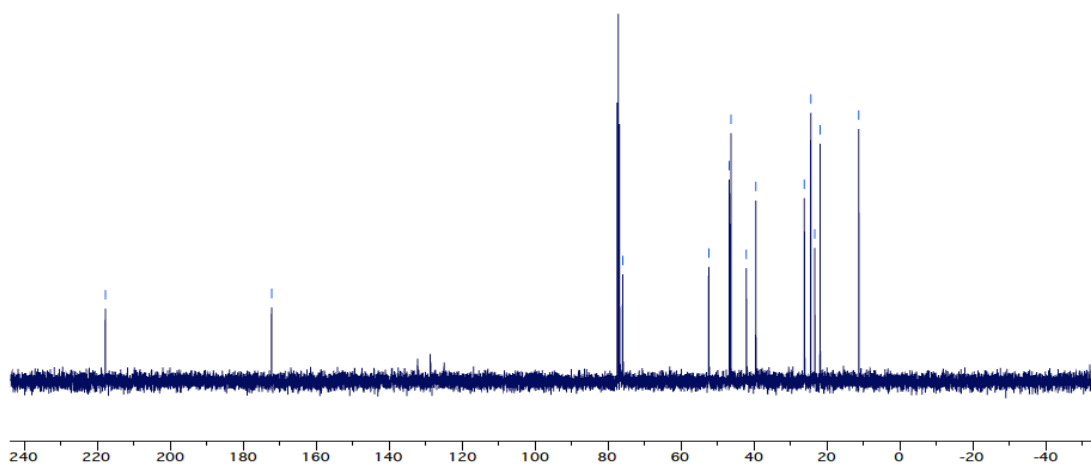
26.233

24.484

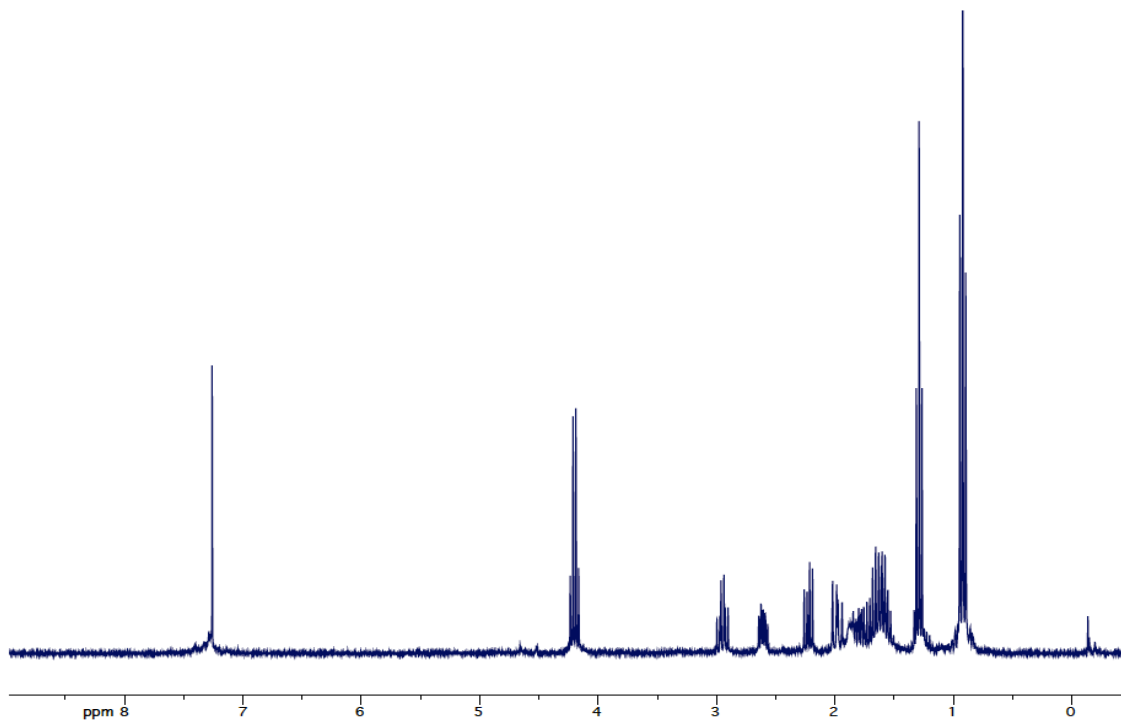
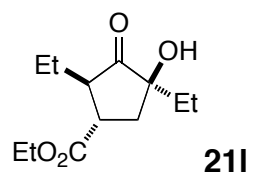
23.361

21.917

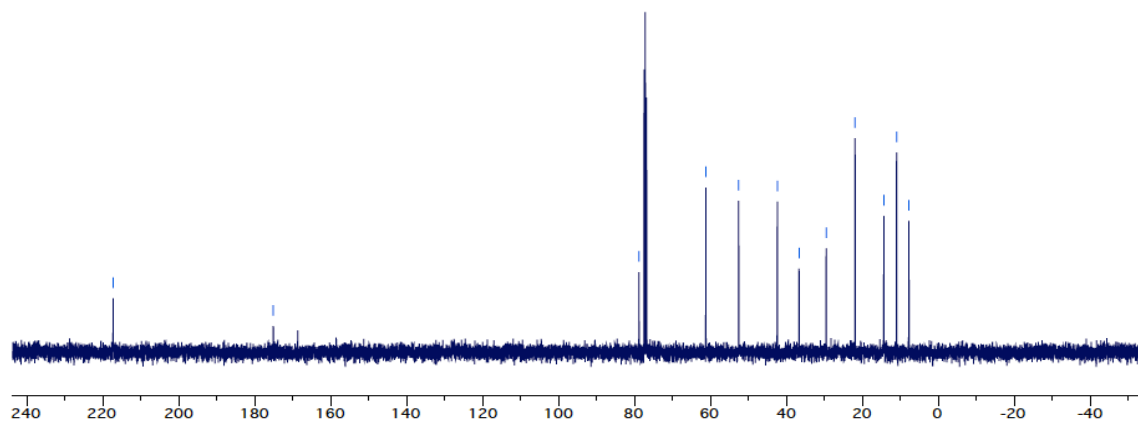
11.318

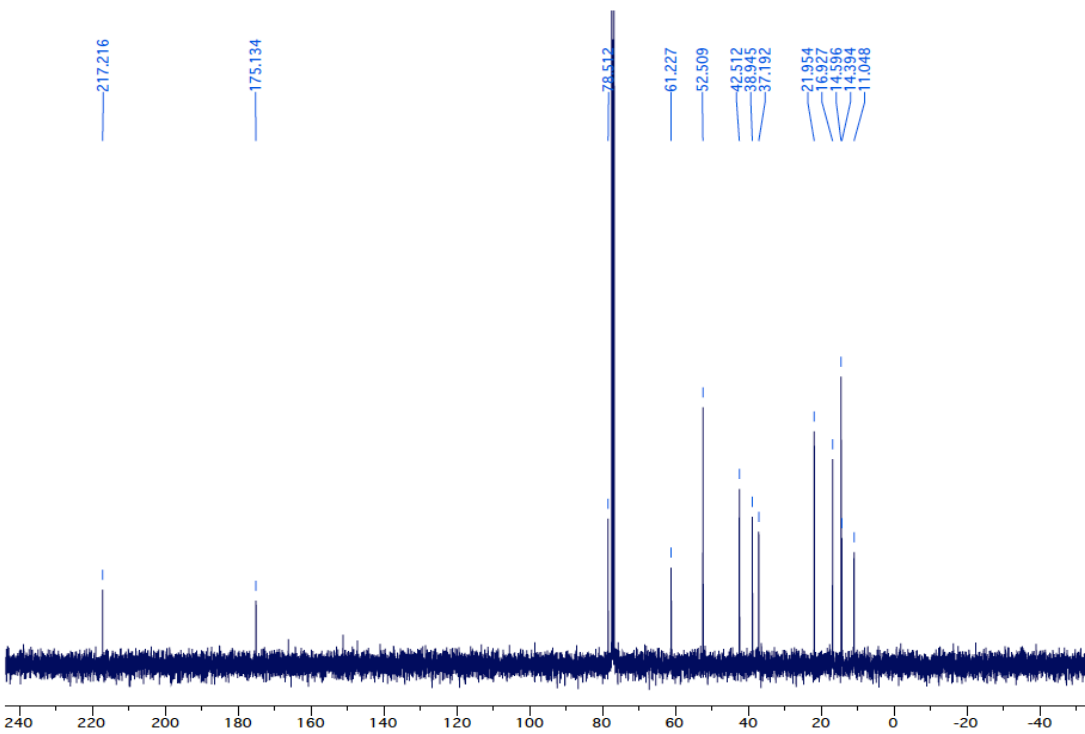
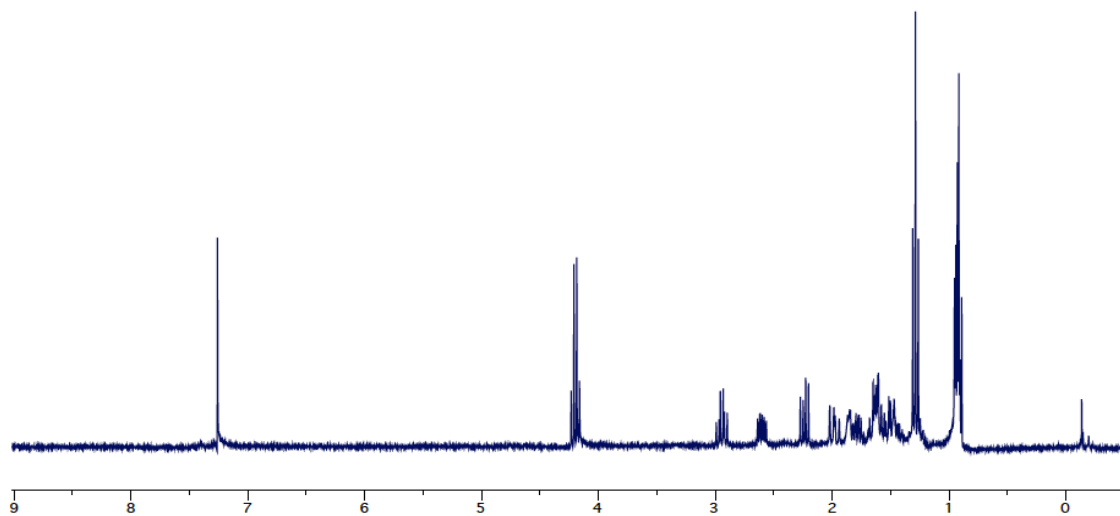
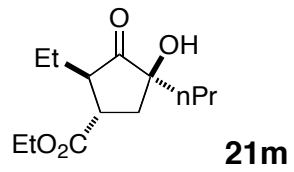




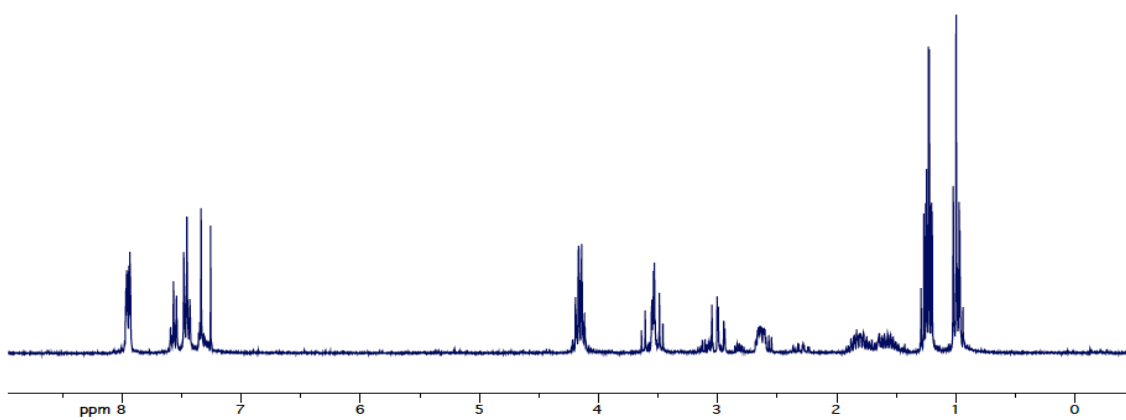
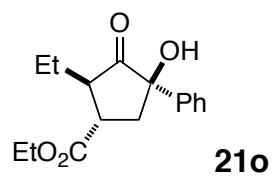


217.308  
 175.140  
 78.858  
 61.231  
 52.618  
 42.421  
 36.695  
 29.560  
 21.953  
 14.379  
 11.046  
 7.786

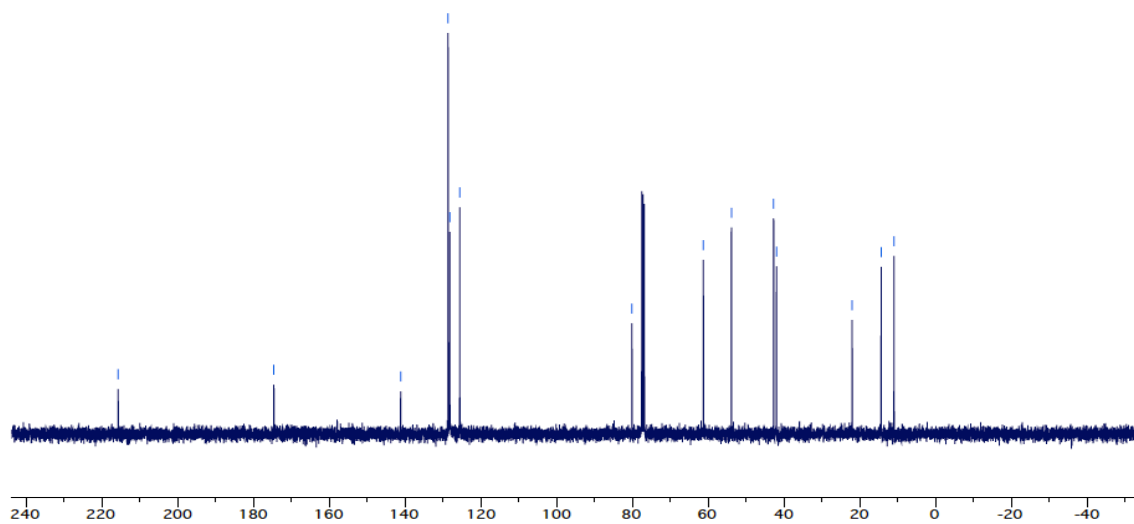


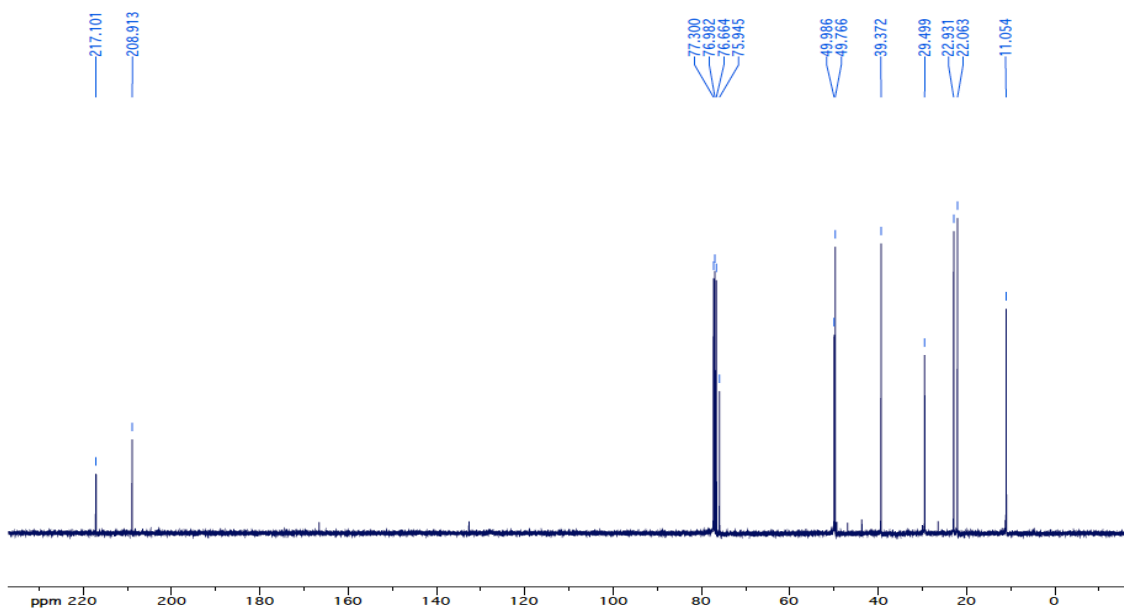
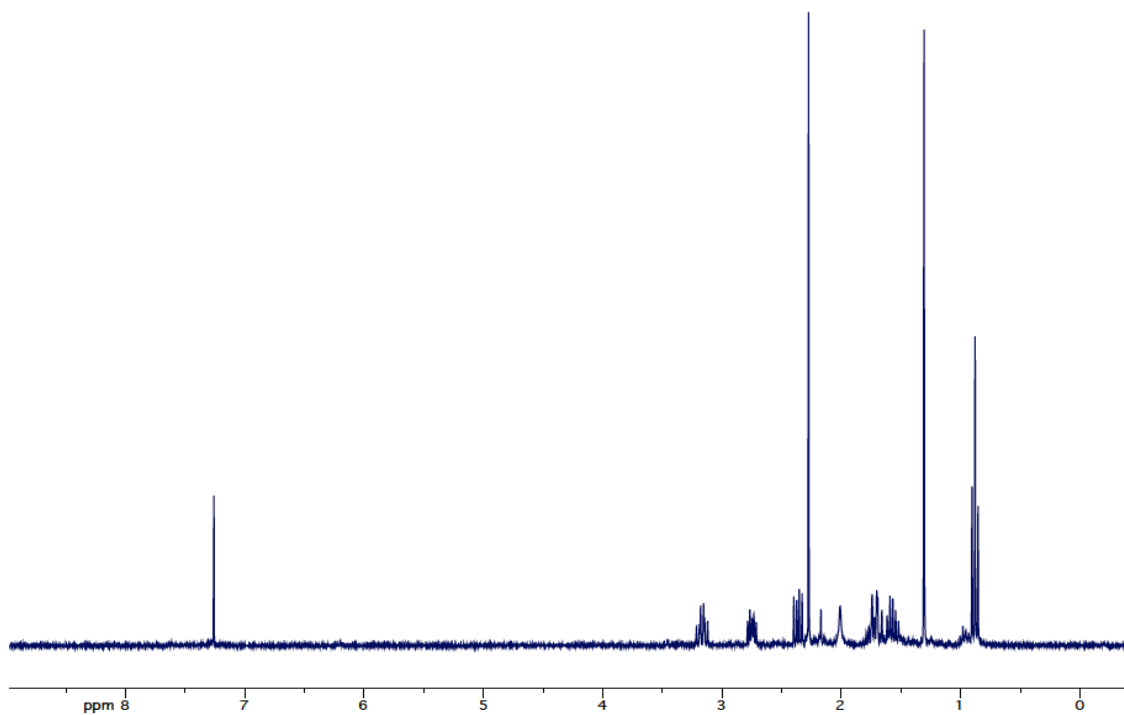
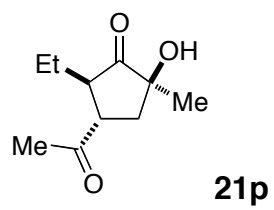


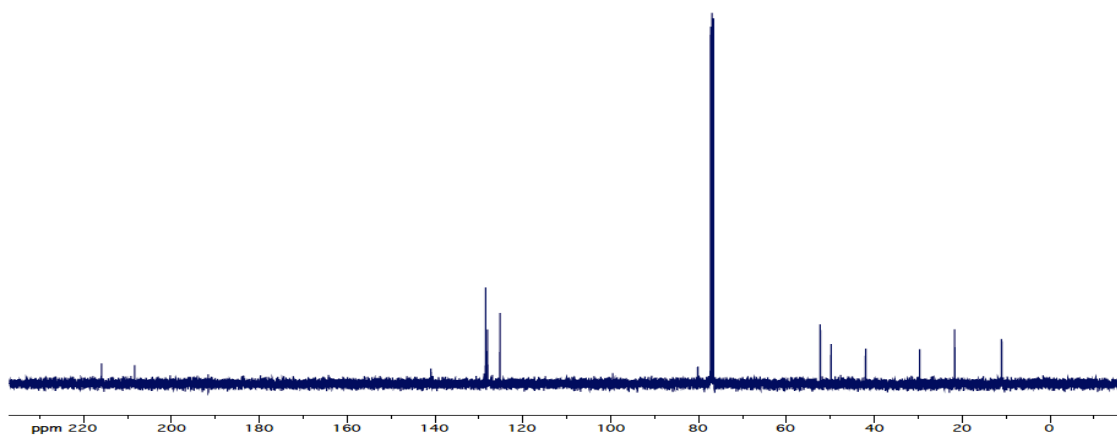
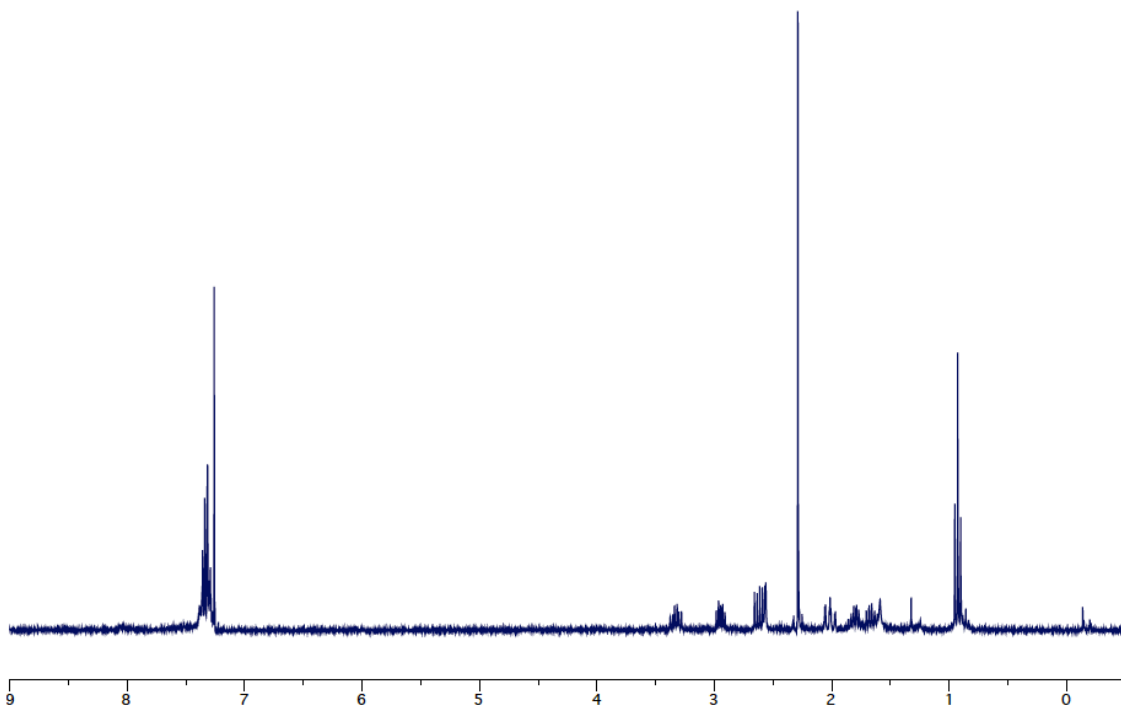
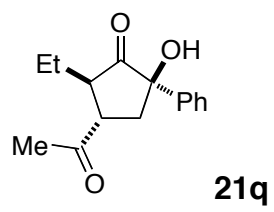


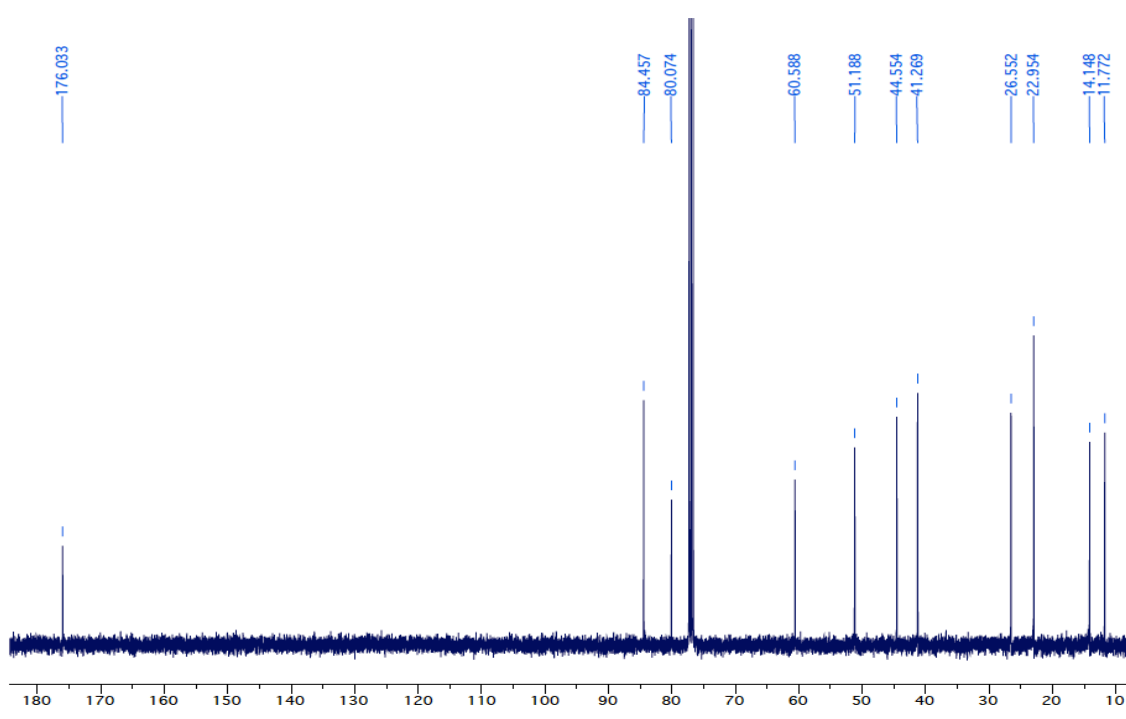
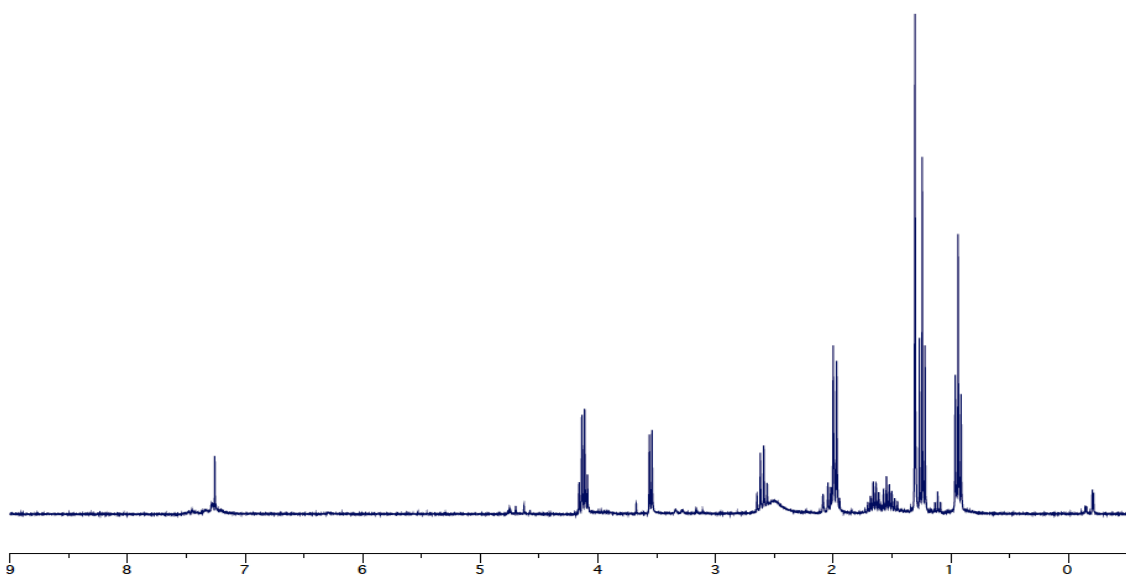
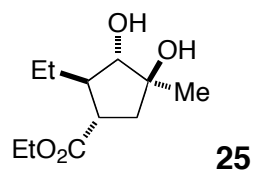


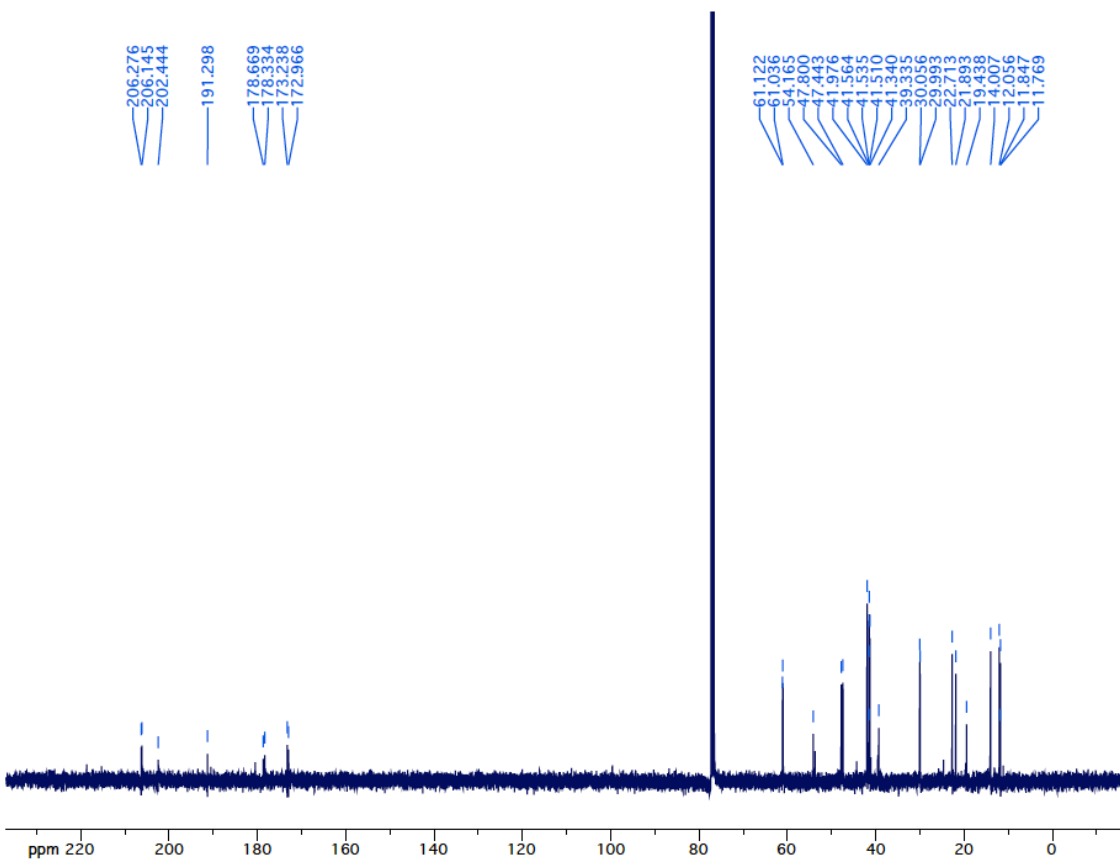
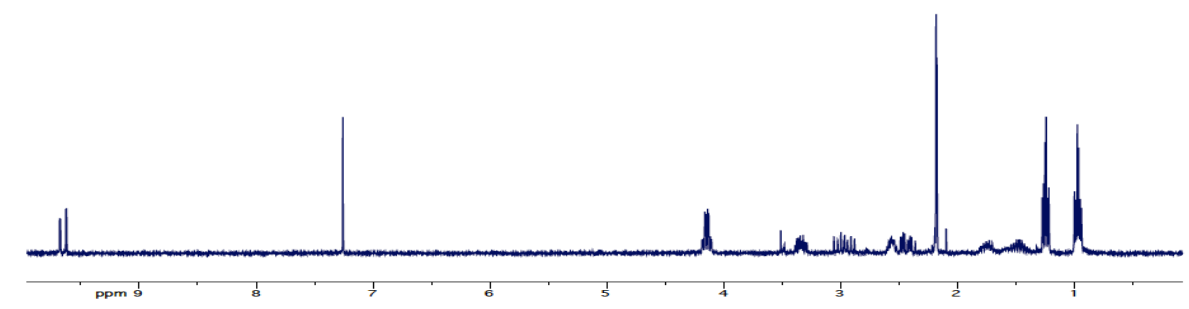
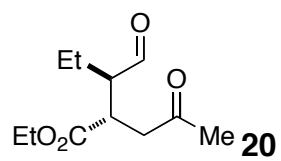
215.722  
 174.643  
 141.189  
 128.661  
 128.207  
 125.569  
 80.152  
 61.305  
 53.911  
 42.767  
 42.020  
 22.037  
 14.378  
 11.028





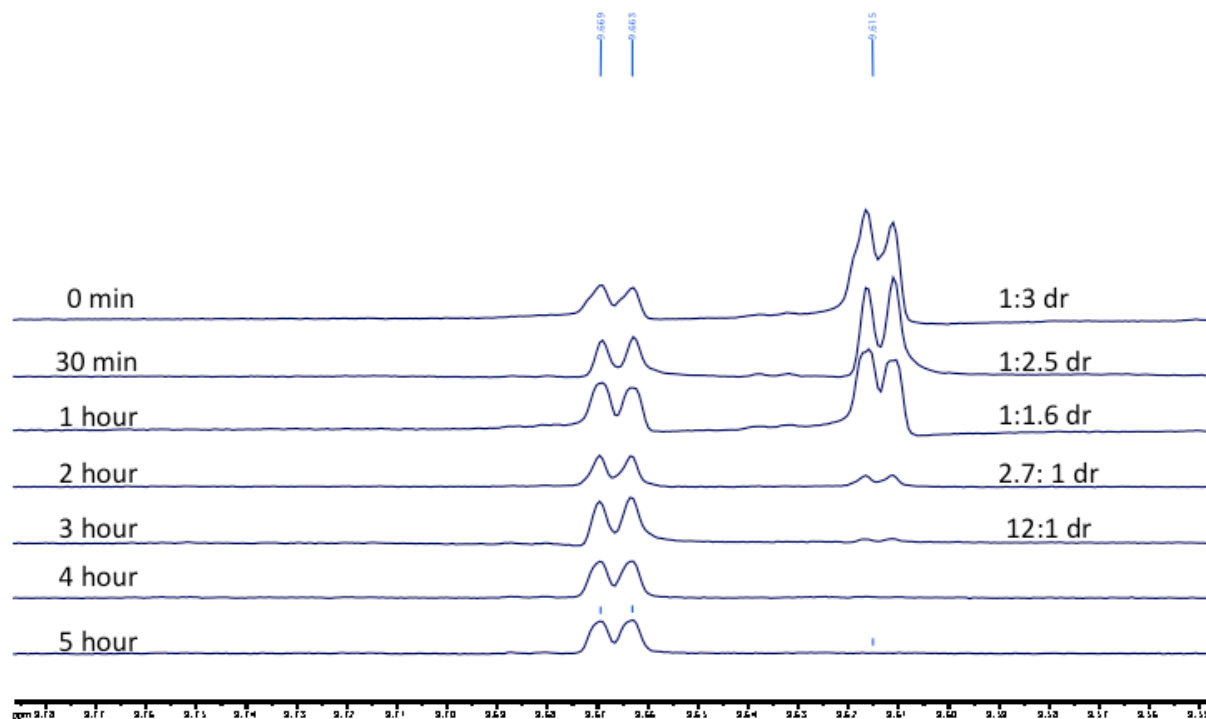
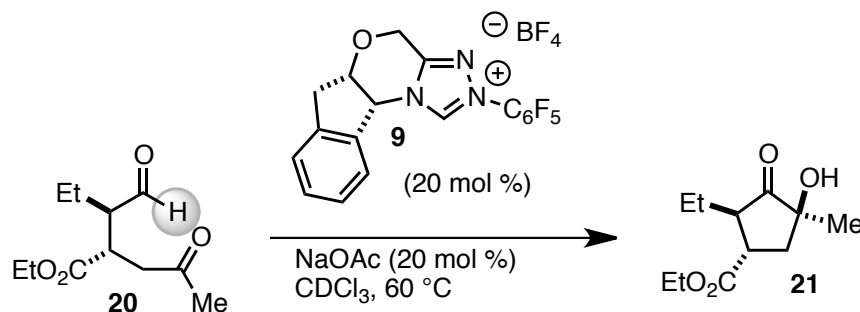




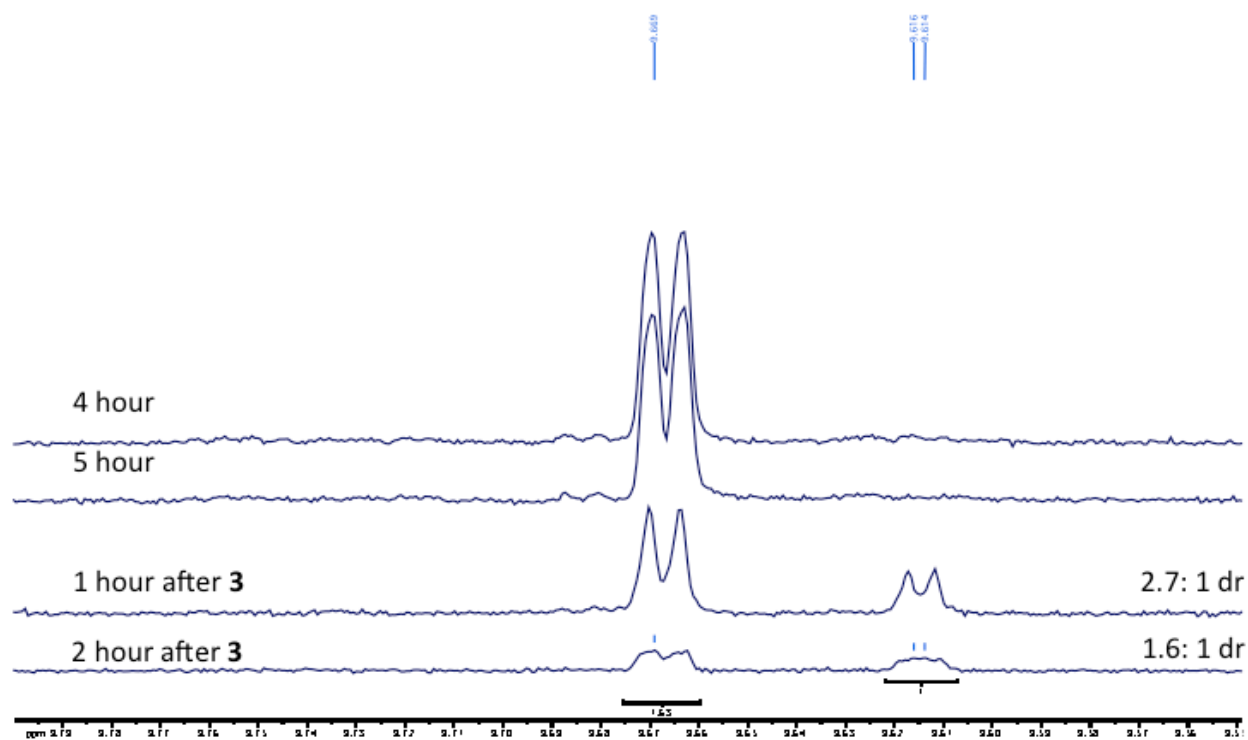


## NMR Studies

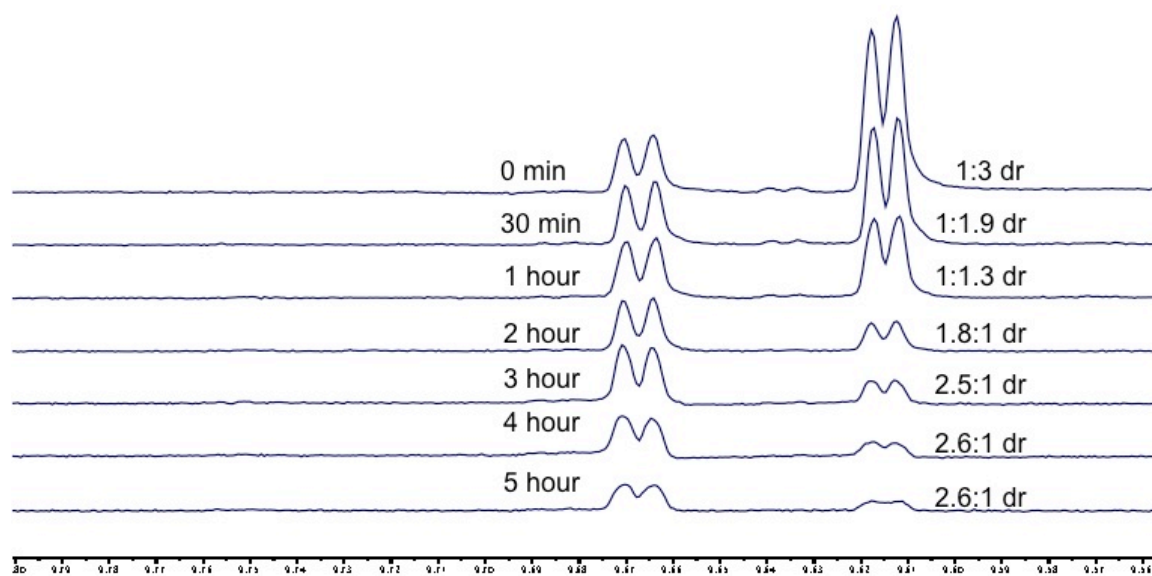
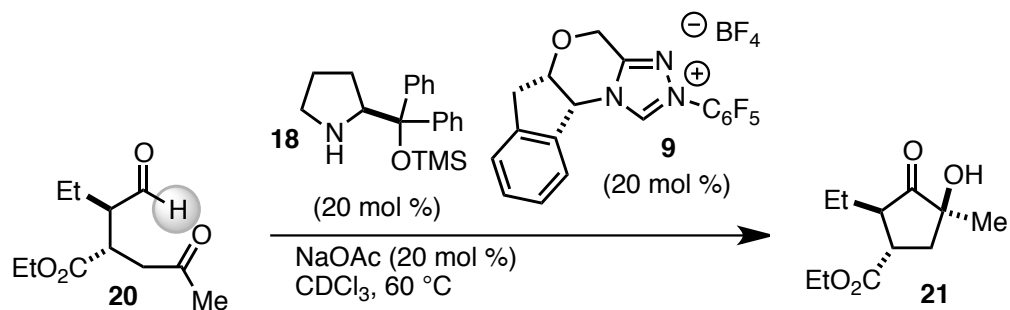
In a 1 dram vial, 25 mg of **20** (0.12 mmol) was combined with 9 mg of **9** (0.2 equiv, 0.02 mmol), 2 mg of NaOAc (0.2 equiv., 0.02 mmol), and 7 mg trimethoxybenzene (internal standard, 0.3 equiv., 0.04 mmol). This mixture was taken up in CDCl<sub>3</sub> and transferred to an NMR tube. The tube was heated in an oil bath at 60 °C. Spectra were taken at intervals throughout the reaction.



After 5 hours, 6.5 mg of **18** (0.2 equiv., 0.02 mmol) was added and continued heating.

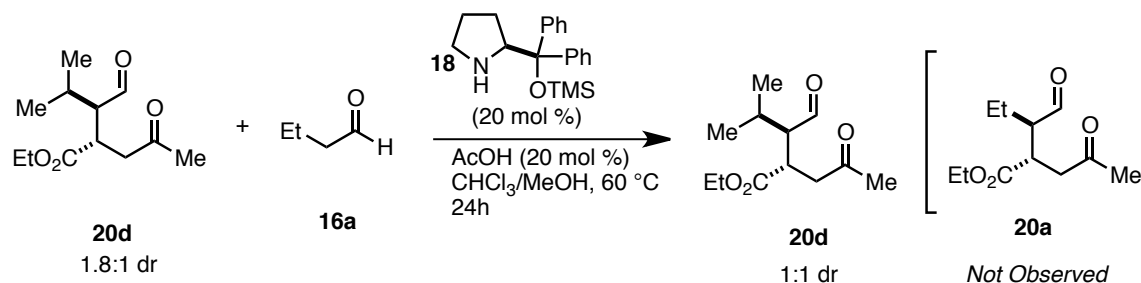


This experiment was repeated, but with amine catalyst **18** present from the beginning.

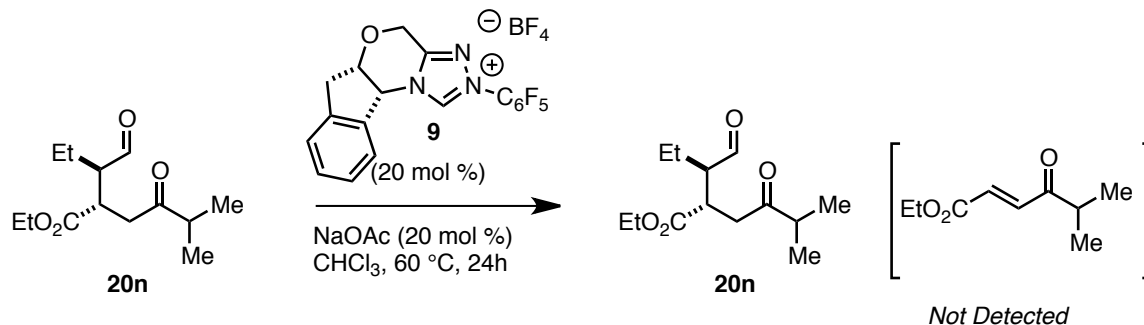


## Crossover Experiments

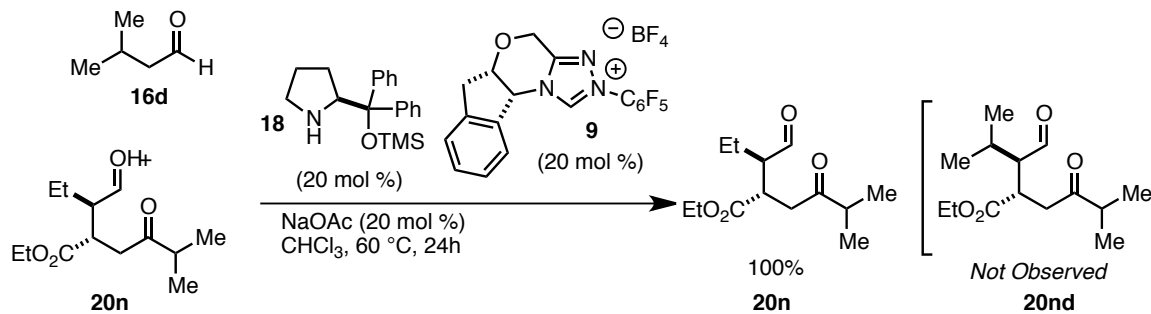
To determine if a retro-Michael was responsible for low diastereoselectivity, a crossover experiment was conducted by heating the intermediate aldehyde **20d** with butyraldehyde in the presence of the amine catalyst. No crossover product was observed, indicating that the amine catalyst is not responsible for this pathway.



To determine if the NHC catalyst played a role in the retro-Michael, compound **20n** was exposed to catalyst **9**, base, and heat for one day. The combination of the bulky isopropyl-ketone and a chiral catalysts prevents the benzoin cyclization. If the retro-Michael occurred, we would expect formation of starting material **17a**. None was observed.



In case the combination of the amine catalyst and the NHC catalyst was responsible, S11 was exposed to both catalysts, isovaleraldehyde, and heat for 1 day. No crossover product was observed.

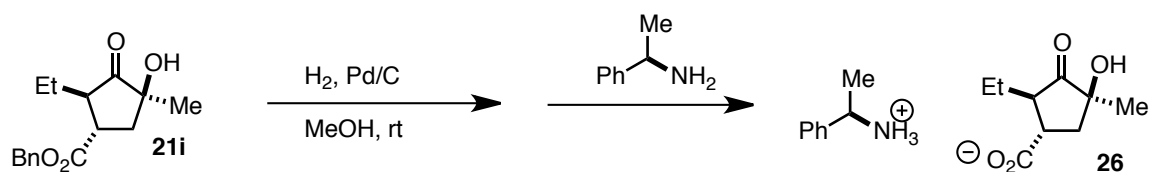


From these results, we are confident that a retro-Michael is not a factor in this new cascade reaction.

## APPENDIX 2

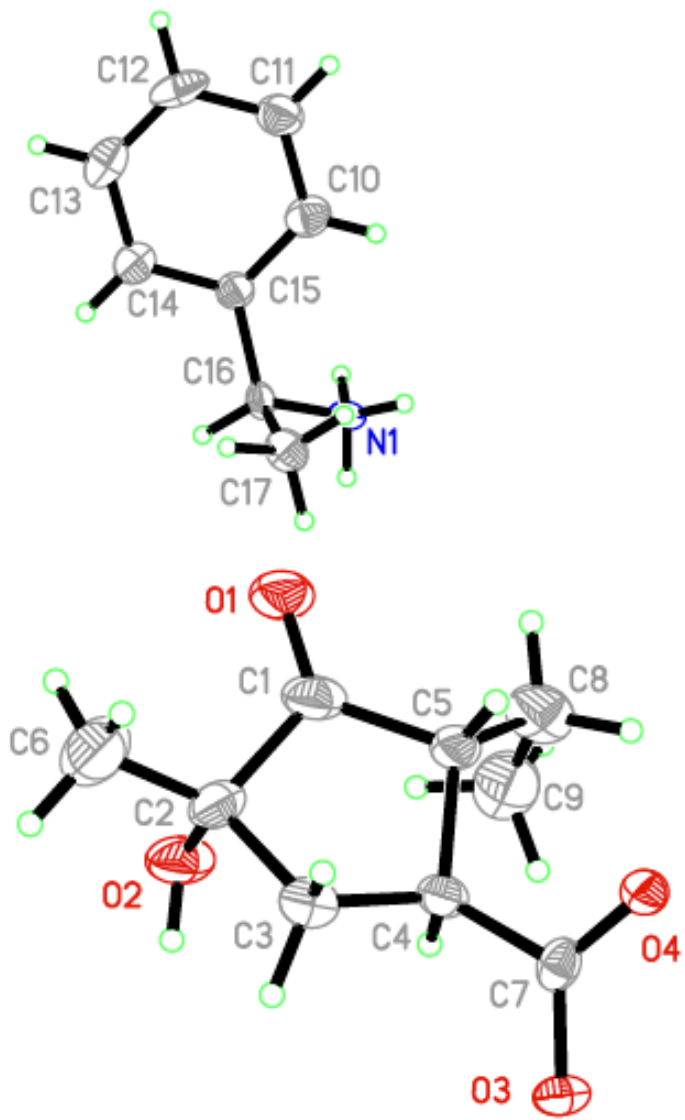
### X-RAY CRYSTAL STRUCTURE DATA FOR CHAPTER 2

#### X-Ray Crystal Structure and Data



#### Procedure:

**21i** was combined with 10% Palladium on Carbon (10 wt%) and suspended in dry methanol. An atmosphere (1 atm) of  $\text{H}_2$  was introduced via balloon and stirred at room temperature overnight. The reaction was filtered through a plug of celite and concentrated to an oil. This crude oil was then dissolved in DCM and the amine (1 equiv.) was added. The reaction was concentrated and the product was recrystallized by slow evaporation from methanol.



\_Table 1. Crystal data and structure refinement for Rovis99\_0m.

Identification code	rovis99_0m	
Empirical formula	C <sub>17</sub> H <sub>25</sub> NO <sub>4</sub>	
Formula weight	307.38	
Temperature	120 K	
Wavelength	0.71073 Å	
Crystal system	Orthorhombic	
Space group	P2 <sub>1</sub> 2 <sub>1</sub> 2 <sub>1</sub>	
Unit cell dimensions	a = 6.1775(5) Å	a = 90°.
	b = 13.7872(10) Å	b = 90°.
	c = 19.8051(14) Å	g = 90°.
Volume	1686.8(2) Å <sup>3</sup>	
Z	4	
Density (calculated)	1.210 Mg/m <sup>3</sup>	
Absorption coefficient	0.086 mm <sup>-1</sup>	
F(000)	664	
Crystal size	0.20 x 0.11 x 0.06 mm <sup>3</sup>	
Theta range for data collection	1.80 to 24.41°.	
Index ranges	-7<=h<=7, -15<=k<=16, -23<=l<=23	
Reflections collected	24929	
Independent reflections	2773 [R(int) = 0.1599]	
Completeness to theta = 24.41°	100.0 %	
Absorption correction	Semi-empirical from equivalents	
Max. and min. transmission	0.9950 and 0.9835	
Refinement method	Full-matrix least-squares on F <sup>2</sup>	
Data / restraints / parameters	2773 / 0 / 204	
Goodness-of-fit on F <sup>2</sup>	1.005	
Final R indices [I>2sigma(I)]	R1 = 0.0559, wR2 = 0.1031	
R indices (all data)	R1 = 0.1341, wR2 = 0.1311	
Absolute structure parameter	-1(2)	
Largest diff. peak and hole	0.191 and -0.253 e.Å <sup>-3</sup>	

Table 2. Atomic coordinates ( $\times 10^4$ ) and equivalent isotropic displacement parameters ( $\text{\AA}^2 \times 10^3$ ) for Rovis99\_0m.  $U(\text{eq})$  is defined as one third of the trace of the orthogonalized  $U^{ij}$  tensor.

	x	y	z	$U(\text{eq})$
C(1)	1189(7)	5403(3)	2272(2)	36(1)
C(2)	2746(7)	5442(3)	1665(2)	32(1)
C(3)	1591(7)	4816(3)	1137(2)	30(1)
C(4)	442(7)	4023(3)	1557(2)	25(1)
C(5)	-428(7)	4592(3)	2162(2)	30(1)
C(6)	3355(10)	6445(3)	1442(2)	56(2)
C(7)	-1185(7)	3485(3)	1119(2)	23(1)
C(8)	-945(8)	4013(4)	2802(2)	44(1)
C(9)	849(9)	3380(3)	3045(2)	53(2)
C(10)	6989(8)	4591(3)	9518(2)	33(1)
C(11)	6401(8)	5494(3)	9768(2)	38(1)
C(12)	7823(9)	6258(3)	9735(2)	43(1)
C(13)	9829(9)	6134(4)	9452(2)	46(1)
C(14)	10428(8)	5231(3)	9207(2)	36(1)
C(15)	9024(7)	4455(3)	9239(2)	25(1)
C(16)	9717(6)	3510(3)	8924(2)	23(1)
C(17)	8800(7)	3376(3)	8215(2)	30(1)
N(1)	9017(5)	2659(2)	9347(1)	22(1)
O(1)	1297(5)	5923(2)	2760(2)	47(1)
O(2)	4568(5)	4940(2)	1949(2)	45(1)
O(3)	-396(4)	2840(2)	731(1)	24(1)
O(4)	-3154(5)	3710(2)	1143(1)	27(1)

Table 3. Bond lengths [ $\text{\AA}$ ] and angles [ $^\circ$ ] for Rovis99\_0m.

---

C(1)-O(1)	1.206(5)
C(1)-C(5)	1.514(6)
C(1)-C(2)	1.540(6)
C(2)-O(2)	1.437(5)
C(2)-C(6)	1.499(6)
C(2)-C(3)	1.532(6)
C(3)-C(4)	1.545(5)
C(4)-C(7)	1.521(6)
C(4)-C(5)	1.530(5)
C(5)-C(8)	1.532(6)
C(7)-O(4)	1.256(5)
C(7)-O(3)	1.272(5)
C(8)-C(9)	1.490(6)
C(10)-C(15)	1.386(6)
C(10)-C(11)	1.388(6)
C(11)-C(12)	1.373(6)
C(12)-C(13)	1.371(7)
C(13)-C(14)	1.387(6)
C(14)-C(15)	1.379(5)
C(15)-C(16)	1.506(5)
C(16)-N(1)	1.505(4)
C(16)-C(17)	1.526(5)
O(1)-C(1)-C(5)	126.2(4)
O(1)-C(1)-C(2)	124.8(4)
C(5)-C(1)-C(2)	109.0(4)
O(2)-C(2)-C(6)	111.3(4)
O(2)-C(2)-C(3)	111.1(3)
C(6)-C(2)-C(3)	115.9(4)
O(2)-C(2)-C(1)	99.6(3)
C(6)-C(2)-C(1)	114.8(4)
C(3)-C(2)-C(1)	102.8(4)
C(2)-C(3)-C(4)	104.2(3)
C(7)-C(4)-C(5)	117.7(4)

C(7)-C(4)-C(3)	110.0(3)
C(5)-C(4)-C(3)	102.7(3)
C(1)-C(5)-C(4)	105.0(4)
C(1)-C(5)-C(8)	113.8(4)
C(4)-C(5)-C(8)	117.0(4)
O(4)-C(7)-O(3)	124.5(4)
O(4)-C(7)-C(4)	119.9(4)
O(3)-C(7)-C(4)	115.6(4)
C(9)-C(8)-C(5)	114.7(4)
C(15)-C(10)-C(11)	120.1(5)
C(12)-C(11)-C(10)	120.3(5)
C(13)-C(12)-C(11)	120.2(4)
C(12)-C(13)-C(14)	119.7(5)
C(15)-C(14)-C(13)	120.9(4)
C(14)-C(15)-C(10)	118.9(4)
C(14)-C(15)-C(16)	118.3(4)
C(10)-C(15)-C(16)	122.7(4)
N(1)-C(16)-C(15)	111.3(3)
N(1)-C(16)-C(17)	108.1(3)
C(15)-C(16)-C(17)	112.3(3)

---

Symmetry transformations used to generate equivalent atoms:

Table 4. Anisotropic displacement parameters ( $\text{\AA}^2 \times 10^3$ ) for Rovis99\_0m. The anisotropic displacement factor exponent takes the form:  $-2p^2 [ h^2 a^2 U^{11} + \dots + 2 h k a^* b^* U^{12} ]$

	U <sup>11</sup>	U <sup>22</sup>	U <sup>33</sup>	U <sup>23</sup>	U <sup>13</sup>	U <sup>12</sup>
C(1)	28(3)	40(3)	40(3)	-14(3)	-1(2)	12(3)
C(2)	30(3)	26(3)	39(3)	-10(2)	-5(2)	2(2)
C(3)	31(3)	33(3)	28(2)	-2(2)	1(2)	5(2)
C(4)	22(3)	29(3)	24(2)	-6(2)	2(2)	3(2)
C(5)	22(3)	36(3)	33(3)	-15(2)	1(2)	-1(2)
C(6)	79(4)	40(3)	50(3)	-7(3)	8(3)	-15(3)
C(7)	28(3)	21(3)	19(2)	3(2)	-2(2)	-7(2)
C(8)	43(3)	64(4)	25(3)	-10(2)	-3(2)	1(3)
C(9)	65(4)	57(4)	37(3)	0(3)	1(3)	-10(3)
C(10)	39(3)	26(3)	33(3)	4(2)	-1(2)	3(3)
C(11)	42(3)	35(3)	38(3)	1(2)	11(3)	4(3)
C(12)	66(4)	20(3)	43(3)	-3(2)	-4(3)	12(3)
C(13)	52(4)	29(3)	58(3)	-1(3)	2(3)	-10(3)
C(14)	40(3)	29(3)	39(3)	-4(2)	4(2)	-4(3)
C(15)	26(3)	22(3)	27(2)	2(2)	0(2)	2(2)
C(16)	19(2)	22(2)	29(2)	3(2)	4(2)	-4(2)
C(17)	35(3)	36(3)	20(2)	5(2)	4(2)	-1(2)
N(1)	23(2)	22(2)	21(2)	-4(2)	3(2)	4(2)
O(1)	34(2)	57(2)	49(2)	-32(2)	2(2)	-2(2)
O(2)	27(2)	54(2)	54(2)	-29(2)	-7(2)	8(2)
O(3)	26(2)	24(2)	23(2)	-8(1)	-2(1)	6(2)
O(4)	19(2)	27(2)	34(2)	-10(1)	1(1)	0(2)

Table 5. Hydrogen coordinates ( $\times 10^4$ ) and isotropic displacement parameters ( $\text{\AA}^2 \times 10^3$ ) for Rovis99\_0m.

	x	y	z	U(eq)
H(3A)	2622	4530	826	36
H(3B)	551	5196	884	36
H(4)	1530	3560	1718	30
H(5)	-1783	4897	2017	36
H(6A)	4503	6407	1117	84
H(6B)	3831	6814	1826	84
H(6C)	2121	6755	1242	84
H(8A)	-1322	4464	3159	53
H(8B)	-2204	3611	2716	53
H(9A)	2190	3732	3026	80
H(9B)	945	2815	2763	80
H(9C)	570	3187	3502	80
H(10)	6017	4077	9539	39
H(11)	5038	5582	9958	46
H(12)	7424	6861	9905	51
H(13)	10785	6654	9424	56
H(14)	11796	5148	9019	43
H(16)	11301	3505	8895	28
H(17A)	7248	3403	8233	46
H(17B)	9245	2759	8040	46
H(17C)	9329	3883	7927	46
H(1A)	7626	2533	9269	33
H(1B)	9201	2798	9782	33
H(1C)	9809	2142	9239	33
H(2)	5129	4598	1659	67

## APPENDIX 3

### EXPERIMENTAL AND SPECTRAL DATA FOR CHAPTER 3

#### **Materials and Methods**

All reactions were carried out under an atmosphere of argon with magnetic stirring.

Column chromatography was performed on SiliCycle®SilicaFlash® P60, 40-63 $\mu$ m 60A. Thin layer chromatography was performed on SiliCycle® 250 $\mu$ m 60A plates. Visualization was accomplished with UV light or KMnO<sub>4</sub> stain followed by heating.

<sup>1</sup>H NMR spectra were obtained on Varian 300 or 400 MHz spectrometers at ambient temperature. Data is reported as follows: chemical shift in parts per million ( $\delta$ , ppm) from CDCl<sub>3</sub> (7.26 ppm) multiplicity (s = singlet, bs = broad singlet, d = doublet, t = triplet, q = quartet, and m = multiplet), coupling constants(Hz).

<sup>13</sup>C NMR was recorded on Varian 300 or 400 MHz spectrometers (at 75 or 100 MHz) at ambient temperature. Chemical shifts are reported in ppm from CDCl<sub>3</sub> (77.2 ppm)

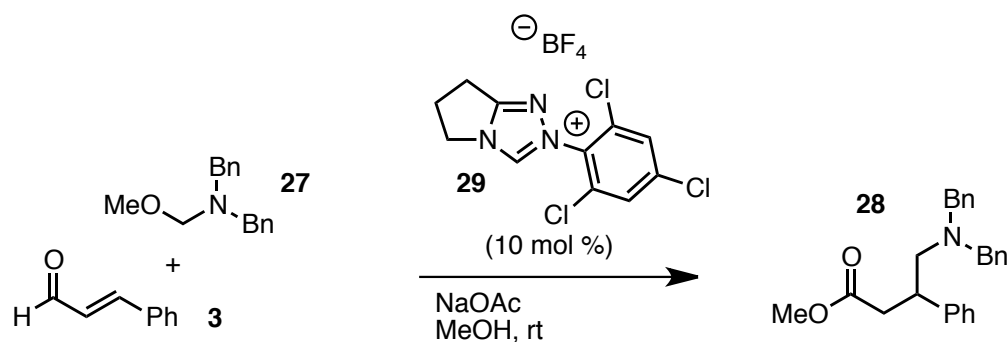
Enantioselectivity was determined by chiral HPLC (Agilent 1100) using Chiralpak IC column (Daicel). Samples were eluted with 98:2 Hexanes/*i*PrOH at 0.5mL/min. Mass spectrometry was accomplished with an Agilent 6130 Quadropole MS with an Agilent 1200 LC system. Infrared Spectrometry was gathered with a Thermo Scientific Nicolet iS50 FT-IR.

Cinnamaldehyde **3** was purchased from Sigma-Aldrich and purified by vacuum distillation and subsequently stored in the refrigerator. Other enals used were obtained from commercial sources (Sigma-Aldrich, Alfa-Aesar). Aminoal **27** was synthesized according to literature methods.<sup>1</sup> Related

---

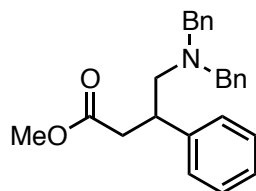
<sup>1</sup> Chi, Y.; Gellman, S. H. *J. Am. Chem. Soc.* **2006**, *128*, 6804-6805.

aminals were constructed analogously with the appropriate amine or solvent. HPLC grade methanol is employed without any further degassing.



**Representative procedure for the aminomethylation of enals:**

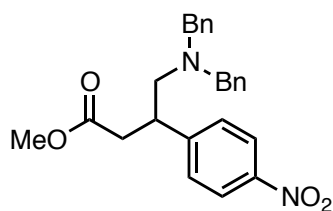
To a dry, 1 dram vial is added 99 mg of aminal **27** (0.44 mmol, 1.2 equiv.), 14 mg of NHC **29** (0.04 mmol, 0.1 equiv.), and 30 mg of NaOAc (0.37 mmol, 1 equiv.). Methanol (2 mL) is added, followed by cinnamaldehyde (50 mg, 0.37 mmol, 1 equiv.) and a magnetic stir bar. The vial is sealed by screw cap and stirred at room temperature for 8h. Upon reaction completion (judged by TLC) trimethoxybenzene (6 mg, 0.037 mmol, 0.1 equiv) is then added to the reaction and stirred for 30 min. The reaction mixture is filtered through a plug of silica gel, washing with DCM, then EtOAc. The organic phase is concentrated in vacuo. NMR is used to judge reaction completion (84% yield). The crude reaction mixture can be purified by column chromatography, eluting with 20-50% EtOAc/Hexane through silica gel. Isolated 91 mg of a yellow oil (65% isolated yield).



**Methyl 4-(dibenzylamino)-3-phenylbutanoate (28a)**

84% (NMR) *r<sub>f</sub>* = 0.6 (20% EtOAc/Hexane)

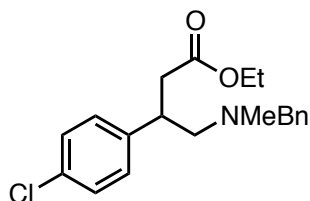
**<sup>1</sup>H-NMR** (300 MHz; CDCl<sub>3</sub>): δ 7.38 (s, 3H), 7.24 (t, *J* = 6.0 Hz, 11H), 7.04 (d, *J* = 6.8 Hz, 2H), 3.68 (d, *J* = 9.1 Hz, 2H), 3.62 (s, 1H), 3.54 (s, 3H), 3.48 (d, *J* = 13.7 Hz, 2H), 3.40 (s, 1H), 2.87 (dd, *J* = 15.7, 5.8 Hz, 1H), 2.56 (d, *J* = 7.7 Hz, 2H), 2.37 (dd, *J* = 15.7, 8.9 Hz, 1H). **<sup>13</sup>C-NMR** (101 MHz; CDCl<sub>3</sub>): δ 173.1, 142.7, 139.3, 128.9, 128.31, 128.15, 127.7, 126.9, 126.6, 59.4, 58.6, 51.4, 40.3, 38.8. **MS**: calcd for C<sub>25</sub>H<sub>27</sub>NO<sub>2</sub> Expect: 373.49 Found: 374.2 (M+H). **IR** (neat): 3060, 3026, 2947, 2786, 2360, 1733, 1674, 1602, 1494, 1451, 1365, 1255, 1167, 1122, 974, 745 cm<sup>-1</sup>



**Methyl 4-(dibenzylamino)-3-(4-nitrophenyl)butanoate (28b)**

78% (NMR) *r<sub>f</sub>* = 0.4 (20% EtOAc/Hexane)

**<sup>1</sup>H-NMR** (400 MHz; CDCl<sub>3</sub>): δ 8.08 (d, *J* = 8.6 Hz, 2H), 7.30-7.25 (m, 13H), 7.16-7.12 (m, 4H), 3.84 (s, 1H), 3.62 (t, *J* = 6.7 Hz, 3H), 3.56 (s, 2H), 3.50 (d, *J* = 13.5 Hz, 2H), 2.80 (dd, *J* = 16.1, 5.8 Hz, 1H), 2.60 (dt, *J* = 12.1, 6.3 Hz, 2H), 2.38 (dd, *J* = 16.0, 9.0 Hz, 1H). **<sup>13</sup>C-NMR** (101 MHz; CDCl<sub>3</sub>): δ 172.2, 150.6, 146.7, 139.7, 138.8, 128.95, 128.85, 128.6, 128.22, 128.11, 127.1, 126.7, 123.5, 72.3, 58.82, 58.72, 56.1, 51.7, 40.3, 38.4. **MS**: calcd for C<sub>25</sub>H<sub>26</sub>N<sub>2</sub>O<sub>4</sub> Expect: 418.48 Found 419.2 (M+H). **IR** (neat): 3061, 3026, 2947, 2796, 2360, 1734, 1599, 1518, 1493, 1451, 1345, 1253, 1169, 1122, 1072, 973, 855, 745, 697 cm<sup>-1</sup>



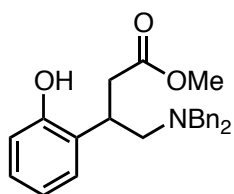
**Ethyl 3-(4-chlorophenyl)-4-(dibenzylamino)butanoate (36c<sup>2</sup>)**

88% (NMR) *r<sub>f</sub>* = 0.6 (20% EtOAc/Hexane)

---

<sup>2</sup> Ethyl ester was prepared for improved purification

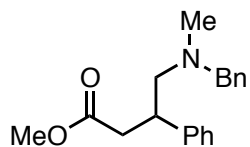
**<sup>1</sup>H-NMR** (400 MHz; CDCl<sub>3</sub>): δ 7.27 (dd, *J* = 15.4, 7.9 Hz, 12H), 7.09 (d, *J* = 8.3 Hz, 2H), 4.02 (tt, *J* = 7.1, 3.5 Hz, 2H), 3.57-3.51 (m, 2H), 3.47-3.36 (m, 2H), 2.87 (dd, *J* = 15.7, 5.9 Hz, 1H), 2.49-2.44 (m, 3H), 2.25 (s, 3H), 1.15 (t, *J* = 7.1 Hz, 3H). **<sup>13</sup>C-NMR** (101 MHz; CDCl<sub>3</sub>): δ 173.2, 157.2, 155.7, 138.6, 136.7, 129.7, 128.8, 128.4, 128.2, 127.5, 125.7, 120.6, 120.1, 118.0, 110.8, 60.3, 59.1, 55.3, 51.8. **MS**: calcd for C<sub>20</sub>H<sub>24</sub>ClNO<sub>2</sub> Expect: 345.86 Found: 346.2 (M+H). **IR** (neat) 3026, 2979, 2842, 2790, 1735, 1683, 1492, 14533, 1371, 1252, 1164, 1091, 1014, 823, 742 cm<sup>-1</sup>.



**Methyl 4-(benzyl(methyl)amino)-3-(2-hydroxyphenyl)butanoate (28d)**

66% (NMR) rf = 0.5 (20% EtOAc/Hexane)

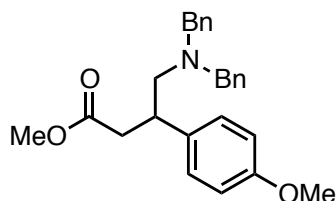
**<sup>1</sup>H-NMR** (400 MHz; CDCl<sub>3</sub>): δ 7.30-7.25 (m, 0H), 7.08 (t, *J* = 7.6 Hz, 2H), 6.91 (d, *J* = 8.0 Hz, 1H), 6.82 (d, *J* = 7.5 Hz, 1H), 6.76 (t, *J* = 7.4 Hz, 1H), 3.97 (d, *J* = 13.3 Hz, 2H), 3.77-3.69 (m, 2H), 3.66 (s, 3H), 3.63 (s, 1H), 3.41 (d, *J* = 13.3 Hz, 2H), 2.77-2.65 (m, 4H). **<sup>13</sup>C-NMR** (101 MHz; CDCl<sub>3</sub>): δ 173.2, 155.7, 139.7, 136.7, 130.4, 129.7, 129.0, 128.4, 128.1, 127.9, 127.5, 125.6, 120.1, 118.1, 60.4, 59.1, 51.8, 36.8, 34.2. **MS**: calcd for C<sub>19</sub>H<sub>23</sub>NO<sub>3</sub> Expect: 389.49 Found: 390.2 (M+H). **IR** (neat): 3060, 3026, 2947, 2799, 2360, 1770, 1734, 1602, 1493, 1452, 1364, 1252, 1164, 1120, 1027, 736 cm<sup>-1</sup>



**Methyl 4-(benzyl(methyl)amino)-3-phenylbutanoate (36)**

78% (NMR) rf = 0.5 (20% EtOAc/Hexane)

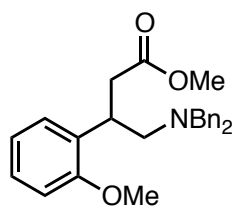
**<sup>1</sup>H-NMR** (400 MHz; CDCl<sub>3</sub>): δ 7.29-7.16 (m, 10H), 3.58 (s, 3H), 3.52 (d, *J* = 21.3 Hz, 2H), 3.46 (s, 2H), 2.94 (dd, *J* = 15.6, 6.1 Hz, 1H), 2.58 (d, *J* = 9.6 Hz, 1H), 2.52 (dd, *J* = 15.5, 8.6 Hz, 2H), 2.24 (s, 3H). **<sup>13</sup>C-NMR** (101 MHz; CDCl<sub>3</sub>): δ 173.1, 142.8, 138.99, 138.97, 129.0, 128.4, 128.1, 127.5, 126.9, 126.6, 63.3, 62.8, 51.4, 42.3, 40.3, 39.0. **MS**: calcd C<sub>19</sub>H<sub>23</sub>NO<sub>2</sub> Expect: 297.39 Found: 298.2 (M+H). **IR** (neat): 3027, 2948, 2841, 2788, 1702, 1602, 1494, 1452, 1435, 1356, 1255, 1195, 1163, 1022, 739, 697 cm<sup>-1</sup>



**Methyl 4-(dibenzylamino)-3-(4-methoxyphenyl)butanoate (28f)**

70% (NMR) rf = 0.6 (20% EtOAc/Hexane)

**<sup>1</sup>H-NMR** (400 MHz; CDCl<sub>3</sub>): δ 7.48 (d, *J* = 8.2 Hz, 1H), 7.30-7.23 (m, 9H), 6.97 (d, *J* = 8.6 Hz, 2H), 6.80 (d, *J* = 8.6 Hz, 2H), 3.79 (s, 3H), 3.67 (s, 1H), 3.63 (d, *J* = 5.9 Hz, 3H), 3.55 (s, 3H), 3.50 (s, 2H), 2.87 (dd, *J* = 15.6, 5.8 Hz, 1H), 2.54 (dd, *J* = 7.7, 3.3 Hz, 2H), 2.33 (dd, *J* = 15.6, 9.1 Hz, 1H). **<sup>13</sup>C-NMR** (101 MHz; CDCl<sub>3</sub>): δ 173.1, 158.2, 139.7, 139.3, 134.8, 128.96, 128.89, 128.6, 128.1, 126.8, 113.7, 59.5, 58.6, 56.1, 55.2, 51.4, 39.4, 39.0. **MS**: calcd for C<sub>26</sub>H<sub>29</sub>NO<sub>3</sub> Expect: 403.51 Found: 404.2 (M+H). **IR** (neat): 3060, 3026, 2948, 2833, 2796, 2359, 1734, 1603, 1494, 1452, 1247, 1167, 1028, 828, 745, 698 cm<sup>-1</sup>

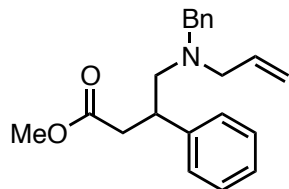


**Methyl 4-(dibenzylamino)-3-(2-methoxyphenyl)butanoate (28g)**

84% (NMR) rf = 0.5 (20%EtOAc/Hexanes)

**<sup>1</sup>H-NMR** (300 MHz; CDCl<sub>3</sub>): δ 7.29-7.18 (m, 11H), 7.06 (d, *J* = 1.4 Hz, 1H), 6.88-6.82 (m, 2H), 3.91-3.83 (m, 1H), 3.82-3.79 (m, 1H), 3.77 (s, 3H), 3.57 (s, 3H), 3.53-3.47 (m, 1H), 2.88 (dd, *J* = 15.5, 6.7 Hz, 1H), 2.61 (dd, *J* = 15.4, 7.8 Hz, 2H). **<sup>13</sup>C-NMR** (101 MHz; CDCl<sub>3</sub>): δ 173.2, 157.2, 155.7, 136.7, 129.7, 128.8,

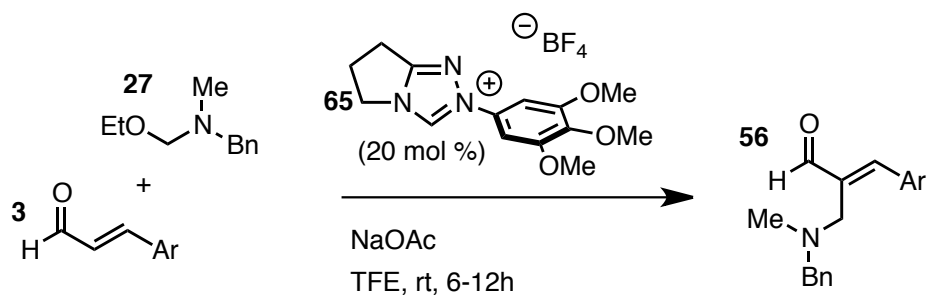
128.4, 128.2, 127.8, 127.5, 125.7, 120.6, 120.1, 118.0, 110.8, 60.3, 59.20, 59.06, 55.3, 51.8, 51.4, 37.6, 36.9, 34.2. **MS**: calcd for C<sub>20</sub>H<sub>25</sub>NO<sub>3</sub> Expect: 327.42 Found: 328.2 (M+H). **IR** (neat): 3061, 3027, 2947, 2836, 2794, 1724, 1697, 1599, 1492, 1452, 1243, 1163, 1026, 749, 698 cm<sup>-1</sup>.



### Methyl 4-(allyl(benzyl)amino)-3-phenylbutanoate (36h)

74% (NMR) rf = 0.6 (20% EtOAc/Hexane)

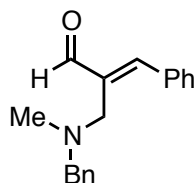
**<sup>1</sup>H-NMR** (300 MHz; CDCl<sub>3</sub>): δ 7.39-7.19 (m, 9H), 7.13-7.10 (m, 1H), 5.86-5.76 (m, 1H), 5.17-5.11 (m, 2H), 3.74-3.69 (m, 1H), 3.56 (s, 3H), 3.43 (d, *J* = 13.7 Hz, 2H), 3.18 (dd, *J* = 14.1, 5.7 Hz, 1H), 3.00-2.92 (m, 1H), 2.95-2.87 (m, 1H), 2.58-2.53 (m, 2H), 2.45 (dd, *J* = 15.6, 8.6 Hz, 1H). **<sup>13</sup>C-NMR** (101 MHz; CDCl<sub>3</sub>): δ 195.3, 173.2, 144.8, 142.9, 139.3, 135.7, 128.91, 128.87, 128.3, 128.10, 128.05, 127.6, 126.8, 126.5, 117.5, 56.9, 51.4, 40.3, 38.8. **MS**: calcd for C<sub>21</sub>H<sub>25</sub>NO<sub>2</sub> Expect: 323.43 Found: 324.2 (M+H). **IR** (neat): 3062, 3027, 2948, 2801, 2359, 1744, 1494, 1452, 1255, 1168, 919, 741, 698 cm<sup>-1</sup>



### General Procedure for the Aza-Stetter Coupling of Enals and Iminiums

To a 1.5 dram vial was added enal (50 mg, 0.378 mmol, 1.0 equiv) and aminal followed by sodium acetate (0.378 mmol, 1.0 equiv), NHC **65** (0.076 mmol, 0.2 equiv), and TFE (0.2 M, 2 mL). A magnetic stir bar was added and the reaction mixture was allowed to stir for 24-48 h. TLC was taken to confirm completion. The mixture was then filtered through a silica gel plug and washed with dichloromethane, then EtOAc. The filtrate was collected and concentrated. The crude mixture was then purified by column chromatography (100% DCM → 50% EtOAc/Hexane) to provide the product.

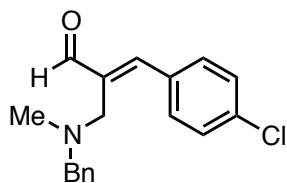
### Representative Spectral Data



#### (*E*)-2-((benzyl(methyl)amino)methyl)-3-phenylacrylaldehyde (**56**)

Prepared according to the general procedure: 94% yield; yellow oil; R<sub>f</sub>=0.35 (8:2 hex/EtOAc);

<sup>1</sup>H-NMR (300 MHz, CDCl<sub>3</sub>): δ 9.65 (d, *J* = 3.84, 1H), 7.89 (m, *J* = 3.88, 1.64, 2H), 7.67 (m, *J* = 3.86, 1.96, 1H), 7.49-7.41 (m, 5H), 7.31-7.24 (m, 6H), 3.54 (s, 2H), 3.42 (s, 2H), 2.16 (d, *J* = 4.99, 3H); <sup>13</sup>C-NMR (101 MHz; CDCl<sub>3</sub>): δ 195.2, 194.1, 155.7, 154.4, 139.1, 138.9, 134.6, 131.3, 130.9, 130.35, 130.27, 129.14, 129.09, 128.96, 128.65, 128.47, 128.2, 127.0, 62.2, 50.2, 41.8. LRMS (ESI+) calcd for C<sub>18</sub>H<sub>19</sub>NO, 265.35. Found 266.1 (M+H).

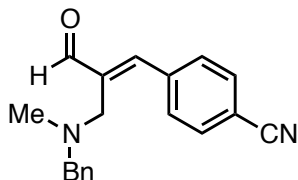


#### (*E*)-2-((benzyl(methyl)amino)methyl)-3-(4-chlorophenyl)acrylaldehyde (**56a**)

99% yield; yellow oil; R<sub>f</sub>=0.48 (8:2 hex/EtOAc);

<sup>1</sup>H-NMR (300 MHz, CDCl<sub>3</sub>): δ 9.613 (d, *J* = 7.54, 1 H), 7.835 (d, *J* = 8.27, 2H), 7.610 (d, *J* = 8.46, 1H),

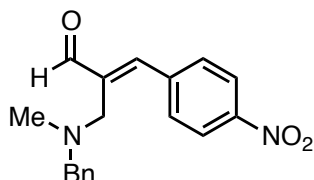
7.45-7.22 (m, 9H), 3.507 (s, 2H), 3.362 (s, 2H), 2.144 (d,  $J = 7.79$ , 3H);  $^{13}\text{C-NMR}$  (101 MHz;  $\text{CDCl}_3$ ):  $\delta$  194.9, 152.9, 139.1, 138.8, 133.0, 132.6, 129.1, 128.9, 128.2, 127.1, 62.2, 50.8, 50.0, 41.8. **LRMS** (ESI+) calcd for  $\text{C}_{18}\text{H}_{18}\text{ClNO}$ , 299.11. Found 300.2 (M+H).



**(E)-4-(3-(benzyl(methyl)amino)-2-formylprop-1-en-1-yl)benzonitrile (56b)**

53% yield; yellow oil;  $R_f=0.33$  (8:2 hex/EtOAc);

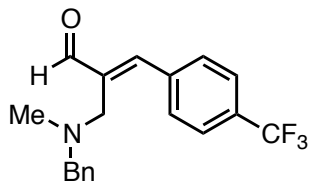
$^1\text{H-NMR}$  (300 MHz,  $\text{CDCl}_3$ ):  $\delta$  9.67 (m, 1H), 7.97 (d,  $J = 8.31$ , 2H), 7.66 (s, 1H), 7.671 (d,  $J = 8.38$ , 2H), 7.29 (m, 6H), 3.521 (s, 2H), 3.362 (s, 2H), 2.163 (s, 3H);  $^{13}\text{C-NMR}$  (101 MHz;  $\text{CDCl}_3$ ):  $\delta$  194.5, 151.0, 141.3, 138.65, 138.52, 132.5, 132.2, 131.5, 130.5, 129.2, 128.3, 127.3, 62.4, 49.8, 42.0. **LRMS** (ESI+) calcd for  $\text{C}_{19}\text{H}_{18}\text{N}_2\text{O}$ , 290.36. Found 291.2 (M+H).



**(E)-2-((benzyl(methyl)amino)methyl)-3-(4-nitrophenyl)acrylaldehyde (56c)**

72% yield; yellow oil;  $R_f=0.33$  (8:2 hex/EtOAc);

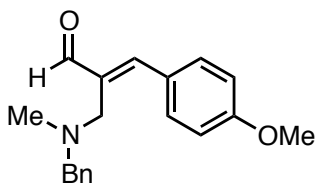
$^1\text{H-NMR}$  (300 MHz,  $\text{CDCl}_3$ ):  $\delta$  9.69 (d,  $J = 7.30$ , 1H), 8.34-8.20 (m, 3H), 8.07-8.02 (m, 2H), 7.85-7.82 (m, 1H), 7.49-7.42 (m, 1H), 7.39-7.24 (m, 6H), 3.533 (s, 2H), 3.371 (s, 2H), 2.175 (s, 3H);  $^{13}\text{C-NMR}$  (101 MHz;  $\text{CDCl}_3$ ):  $\delta$  194.4, 150.4, 141.7, 140.5, 138.4, 131.8, 130.8, 129.2, 128.3, 127.3, 124.0, 123.6, 62.4, 50.8, 49.8, 42.0. **LRMS** (ESI+) calcd for  $\text{C}_{18}\text{H}_{18}\text{N}_2\text{O}_3$ , 310.35. Found 311.2 (M+H).



**(E)-2-((benzyl(methyl)amino)methyl)-3-(4-(trifluoromethyl)phenyl)acrylaldehyde (56d)**

63% yield; yellow oil; Rf=0.48 (8:2 hex/EtOAc);

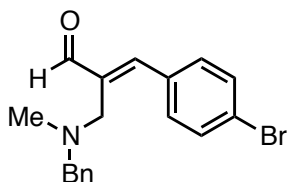
<sup>1</sup>H-NMR (300 MHz, CDCl<sub>3</sub>): δ 9.67 (d, J = 6.50, 1H), 8.00 (d, J = 8.16, 1H), 7.70 (m, 3H), 7.45 (s, 1H), 7.274 (m, 4H), 3.53 (s, 2H), 3.38 (s, 2H), 2.17 (m, 3H); <sup>13</sup>C-NMR (101 MHz; CDCl<sub>3</sub>): δ 194.7, 193.5, 153.1, 151.8, 140.7, 138.7, 131.3, 130.3, 129.1, 128.3, 127.2, 125.85, 125.81, 125.48, 125.44, 63.0, 62.2, 50.0, 41.9. LRMS (ESI+) calcd for C<sub>19</sub>H<sub>18</sub>F<sub>3</sub>NO, 333.35. Found 334.1 (M+H).



**(E)-2-((benzyl(methyl)amino)methyl)-3-(4-methoxyphenyl)acrylaldehyde (56e)**

40% yield; yellow oil; Rf=0.38 (8:2 hex/EtOAc);

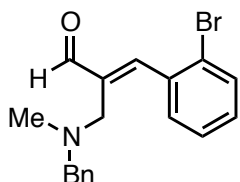
<sup>1</sup>H-NMR (300 MHz, CDCl<sub>3</sub>): δ 9.58 (m, 1H), 7.89-7.86 (m, 2H), 7.36-7.23 (m, 8H), 6.95-6.92 (m, 3H), 3.53 (m, 2H), 3.40 (d, J = 4.44, 2H), 2.16 (s, 3H); <sup>13</sup>C-NMR (101 MHz; CDCl<sub>3</sub>): δ 195.3, 154.8, 139.2, 136.6, 133.6, 129.2, 128.2, 127.0, 114.1, 62.1, 55.4, 50.8, 50.2, 41.8, 29.7. LRMS (ESI+) calcd for C<sub>19</sub>H<sub>21</sub>NO<sub>2</sub>, 295.38. Found 296.3 (M+H).



**(E)-2-((benzyl(methyl)amino)methyl)-3-(4-bromophenyl)acrylaldehyde (56g)**

61% yield; yellow oil; Rf=0.46 (8:2 hex/EtOAc);

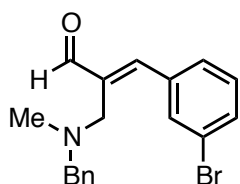
**<sup>1</sup>H-NMR** (300 MHz, CDCl<sub>3</sub>): δ 9.63 (d, *J* = 5.97, 1H), 7.78 (d, *J* = 8.49, 2H), 7.55 (m, 3H), 7.29 (s, 5H), 3.517 (s, 2H), 3.35 (m, 2H), 2.145 (s, 3H); **<sup>13</sup>C-NMR** (101 MHz; CDCl<sub>3</sub>): δ 194.9, 152.9, 139.3, 132.8, 131.9, 129.1, 128.2, 127.1, 125.0, 62.2, 50.0, 41.8 **LRMS** (ESI+) calcd for C<sub>18</sub>H<sub>18</sub>BrNO, 344.25. Found 346.1 (M+H).



**(E)-2-((benzyl(methyl)amino)methyl)-3-(2-bromophenyl)acrylaldehyde (56h)**

88% yield; yellow oil; R<sub>f</sub>=0.39 (8:2 hex/EtOAc);

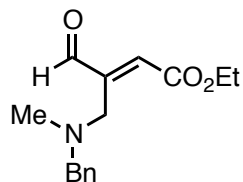
**<sup>1</sup>H-NMR** (300 MHz, CDCl<sub>3</sub>): δ 9.72 (s, 1H), 8.25-8.22 (m, 1H), 7.75-7.68 (m, 1H), 7.65 (m, *J* = 8.00, 1H), 7.38-7.22 (m, 8H), 3.48 (s, 2H), 3.32 (s, 2H), 2.10 (s, 3H); **<sup>13</sup>C-NMR** (101 MHz; CDCl<sub>3</sub>): δ 194.7, 152.4, 140.0, 138.8, 136.6, 134.0, 133.0, 130.1, 129.7, 129.1, 128.2, 127.0, 122.9, 62.0, 50.3, 41.3. **LRMS** (ESI+) calcd for C<sub>18</sub>H<sub>18</sub>BrNO, 344.25. Found 346.1 (M+H).



**(E)-2-((benzyl(methyl)amino)methyl)-3-(3-bromophenyl)acrylaldehyde (56i)**

43% yield; yellow oil; R<sub>f</sub>=0.26 (8:2 hex/EtOAc);

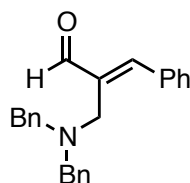
**<sup>1</sup>H-NMR** (300 MHz, CDCl<sub>3</sub>): δ 9.62 (s, 1H), 7.77 (t, *J* = 9.11, 2H), 7.62-7.54 (m, 2H), 7.38-7.25 (m, 8H), 3.54 (s, 2H), 3.39 (d, *J* = 3.58, 2H), 2.13 (s, 3H); **<sup>13</sup>C-NMR** (101 MHz; CDCl<sub>3</sub>): δ 194.7, 152.4, 140.0, 138.8, 136.6, 134.0, 133.0, 130.1, 129.7, 129.1, 128.2, 127.0, 122.9, 62.0, 50.3, 41.3. **LRMS** (ESI+) calcd for C<sub>18</sub>H<sub>18</sub>BrNO, 344.35. Found 346.1(M+H).



**(E)-ethyl 4-(benzyl(methyl)amino)-3-formylbut-2-enoate (56j)**

53% yield; yellow oil; Rf=0.05 (8:2 hex/EtOAc);

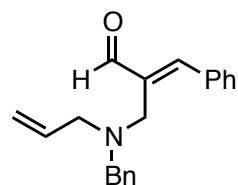
<sup>1</sup>H-NMR (300 MHz, CDCl<sub>3</sub>): δ 9.00 (s, 1H), 7.38 (m, 4H), 7.23 (m, *J* = 8.39, 6.96, 3H), 6.95 (s, 1H), 4.504 (m, 2H), 4.113 (q, *J* = 7.13, 3H), 3.463 (s, 2H), 3.091 (s, 3H); <sup>13</sup>C-NMR (101 MHz; CDCl<sub>3</sub>): δ 207.0, 129.1, 128.2, 126.9, 50.8, 30.9, 29.7 **LRMS** (ESI+) calcd for C<sup>15</sup>H<sup>19</sup>NO<sup>3</sup>, 261.32. Found 281.1 (M+H).



**(E)-2-((dibenzylamino)methyl)-3-phenylacrylaldehyde (56l)**

96% yield; yellow oil; Rf=0.58 (8:2 hex/EtOAc);

<sup>1</sup>H-NMR(300 MHz, CDCl<sub>3</sub>): δ 9.56 (s, 1H), 7.73 (m, 2H), 7.56-7.20 (m, 15H), 5.29 (m, 3H), 3.52 (m, *J* = 2.46, 6H); <sup>13</sup>C-NMR (101 MHz; CDCl<sub>3</sub>): δ 195.4, 153.7, 139.1, 138.5, 131.4, 130.2, 129.4, 128.5, 128.2, 127.1, 59.0, 47.7. **LRMS** (ESI+) calcd for C<sub>24</sub>H<sub>23</sub>NO, 341.45. Found 342.3 (M+H).

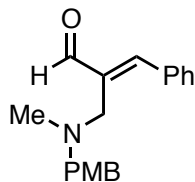


**(E)-2-((allyl(benzyl)amino)methyl)-3-phenylacrylaldehyde (56m)**

72% yield; yellow oil; Rf=0.56 (8:2 hex/EtOAc);

<sup>1</sup>H-NMR (300 MHz, CDCl<sub>3</sub>): δ 9.59 (s, 1H), 7.91-7.84 (m, 2H), 7.68 (m, 1H), 7.57-7.35 (m, 5H), 7.35-7.21 (m, 2H), 5.921 (m, 1H), 3.50 (m, 4H), 3.06 (d, *J* = 6.37, 2H); <sup>13</sup>C-NMR (101 MHz; CDCl<sub>3</sub>): δ 195.3, 153.8,

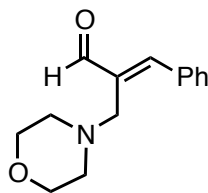
138.8, 135.5, 131.3, 130.36, 130.21, 129.2, 129.0, 128.5, 128.1, 126.9, 118.0, 58.4, 57.1, 47.4. **LRMS**  
(ESI+) calcd for C<sub>20</sub>H<sub>21</sub>NO, 291.39. Found 292.2 (M+H).



**(E)-2-(((4-methoxybenzyl)(methyl)amino)methyl)-3-phenylacrylaldehyde (56n)**

50% yield; yellow oil; Rf=0.41 (8:2 hex/EtOAc);

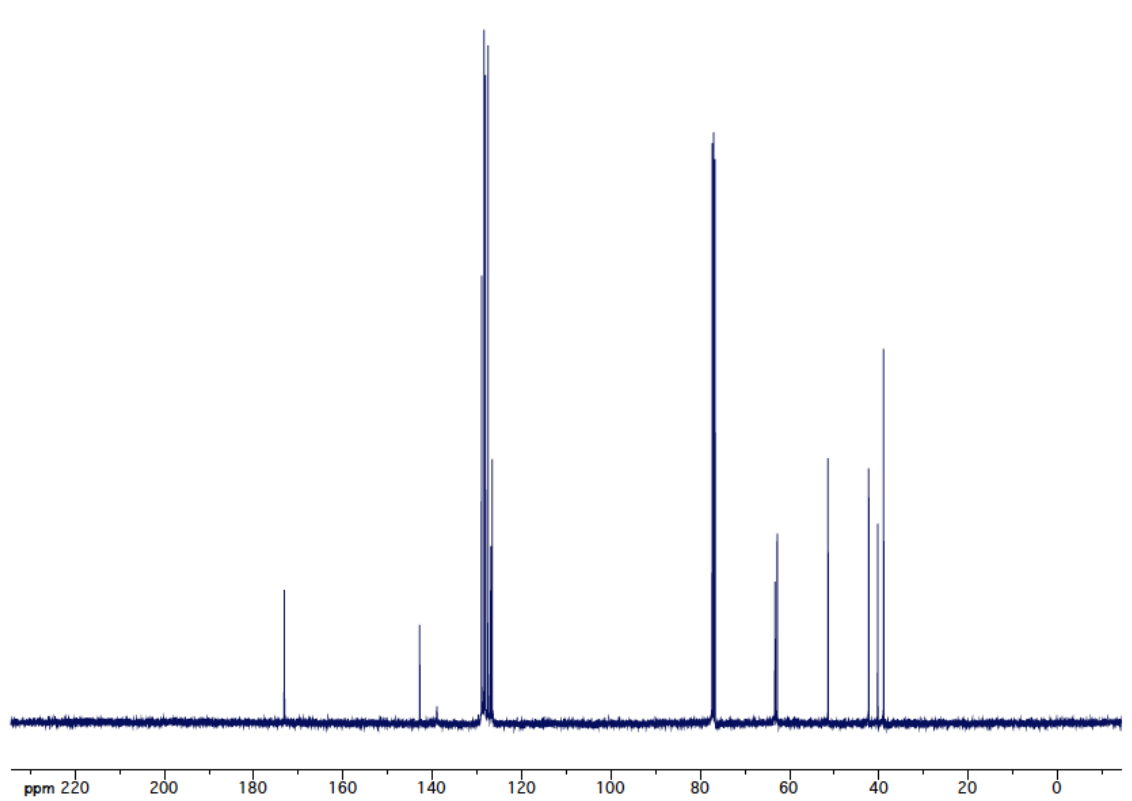
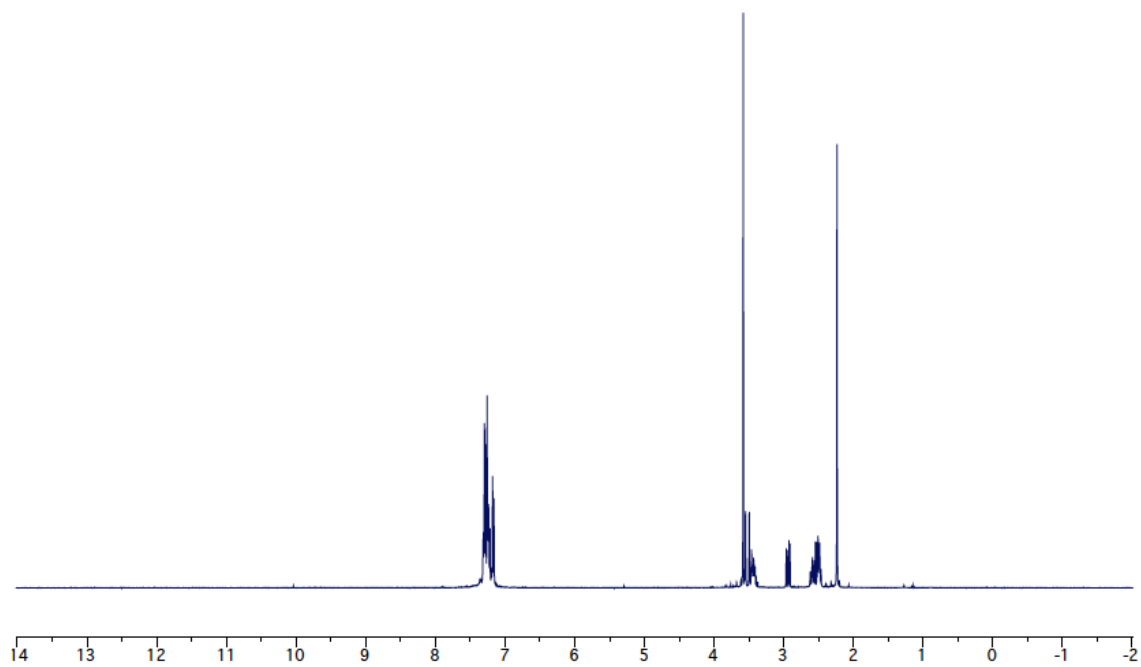
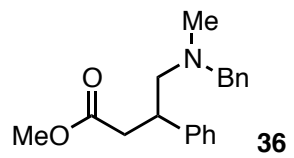
**<sup>1</sup>H-NMR** (300 MHz, CDCl<sub>3</sub>): δ 9.63 (s, 1H), 7.89 (s, 2H), 7.43 (s, 4H), 7.24 (t, *J* = 7.16, 2H), 6.84 (d, *J* = 8.45, 2H), 3.79 (s, 3H), 3.44 (d, 4H), 2.14 (s, 3H); **<sup>13</sup>C-NMR** (101 MHz; CDCl<sub>3</sub>): δ 195.3, 158.7, 154.3, 138.9, 134.6, 131.3, 131.1, 130.28, 130.26, 128.6, 61.6, 55.2, 50.0, 41.7 **LRMS** (ESI+) calcd for C<sub>19</sub>H<sub>21</sub>NO<sub>2</sub>, 295.38. Found 296.2 (M+H).

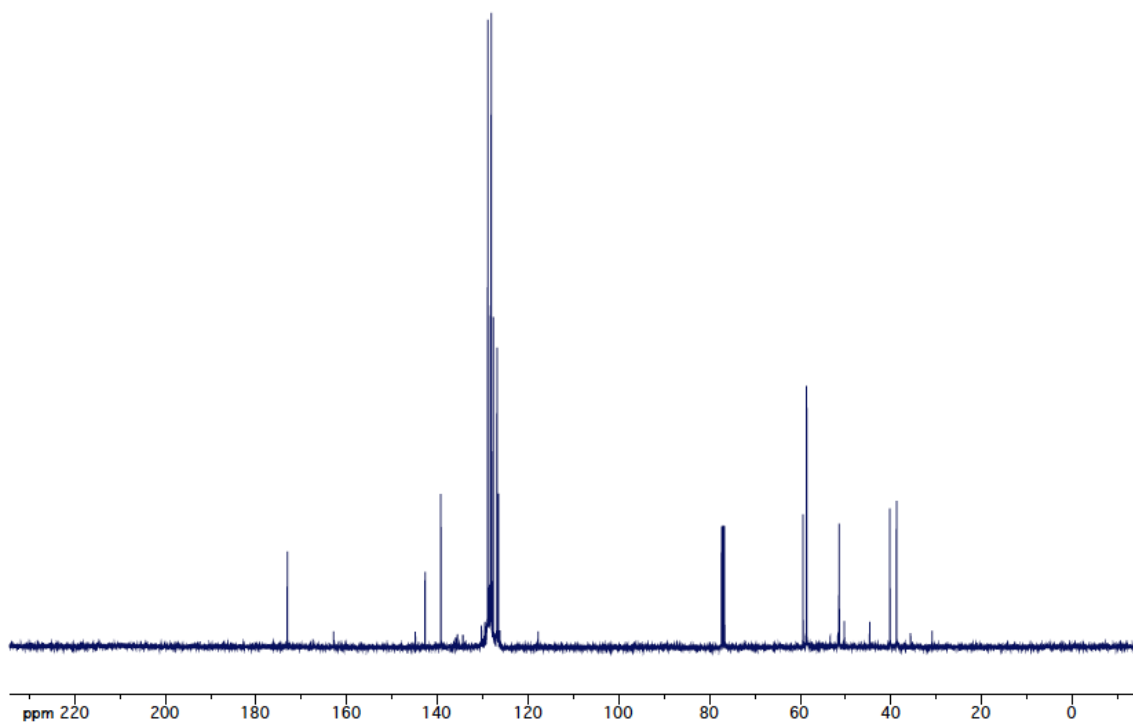
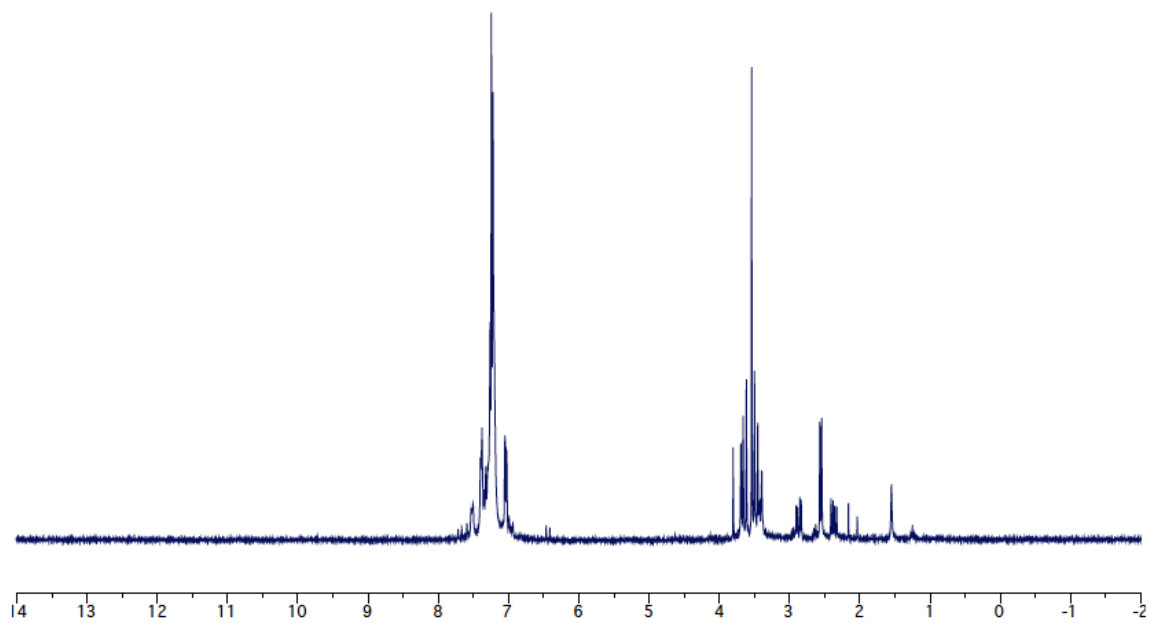
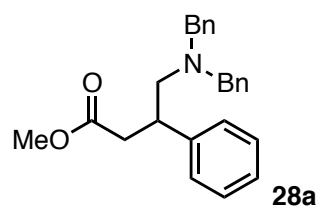


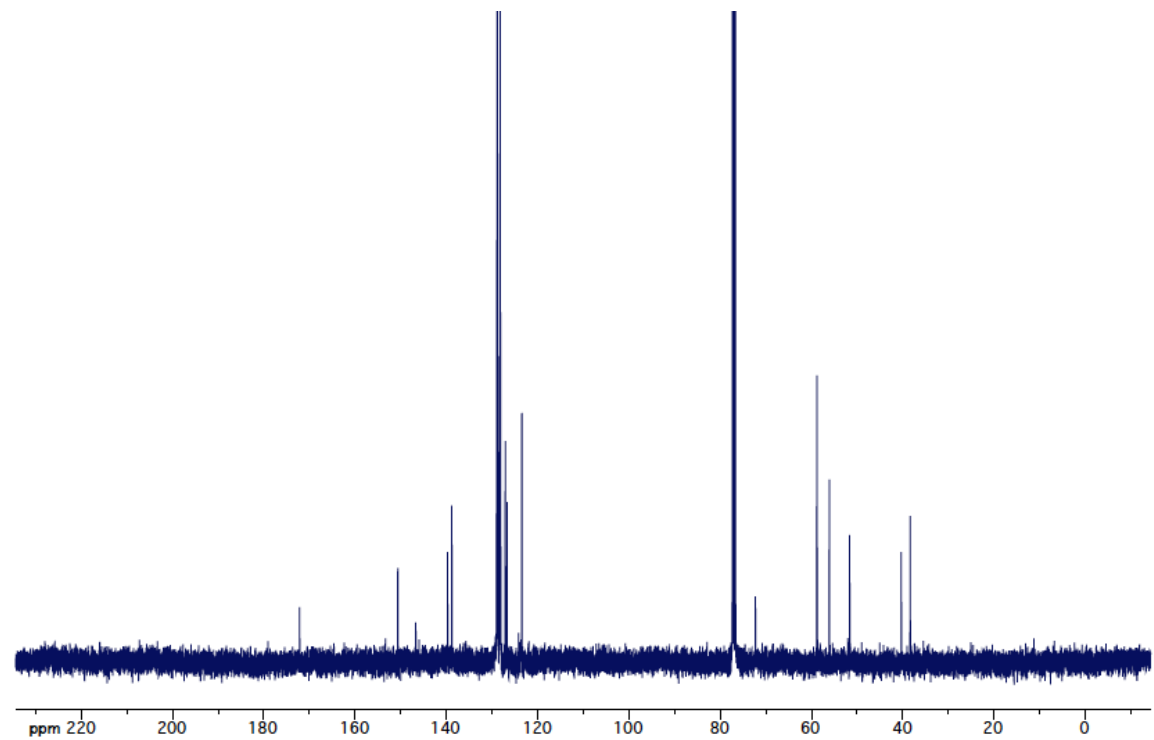
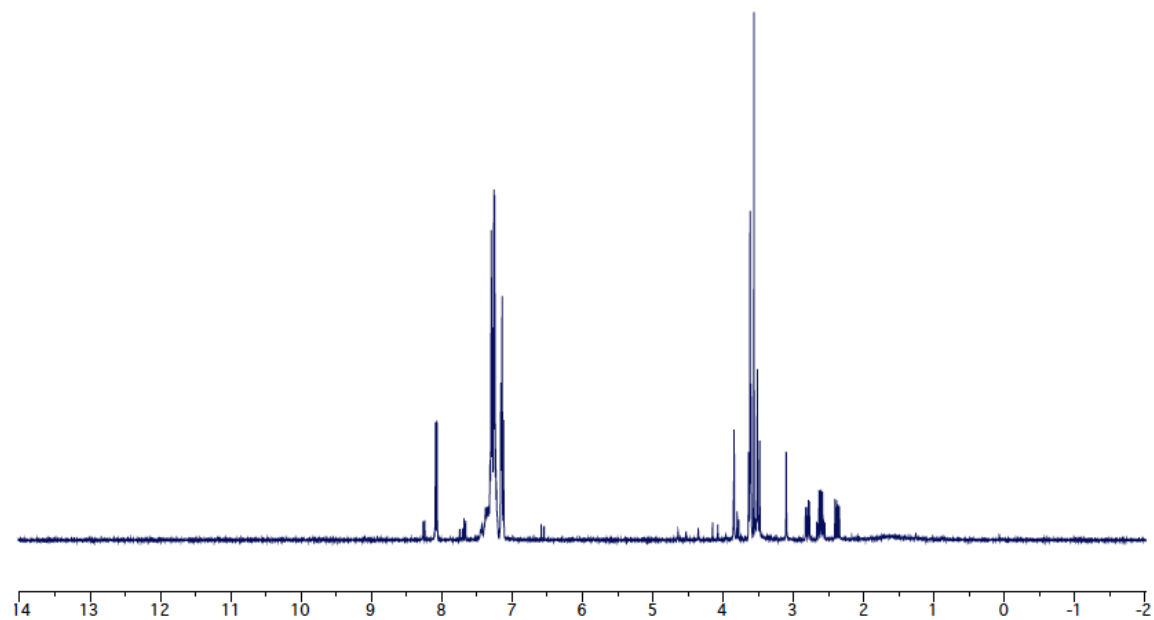
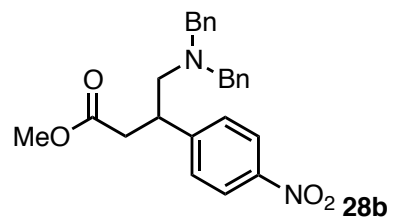
**(E)-2-(morpholinomethyl)-3-phenylacrylaldehyde (56o)**

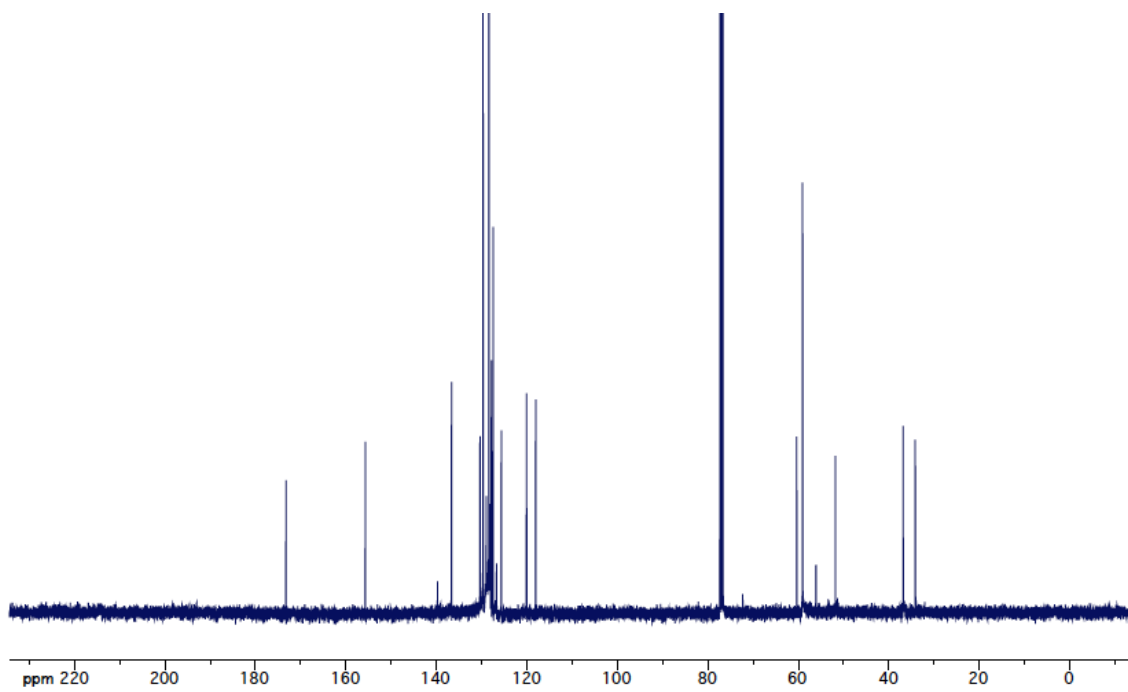
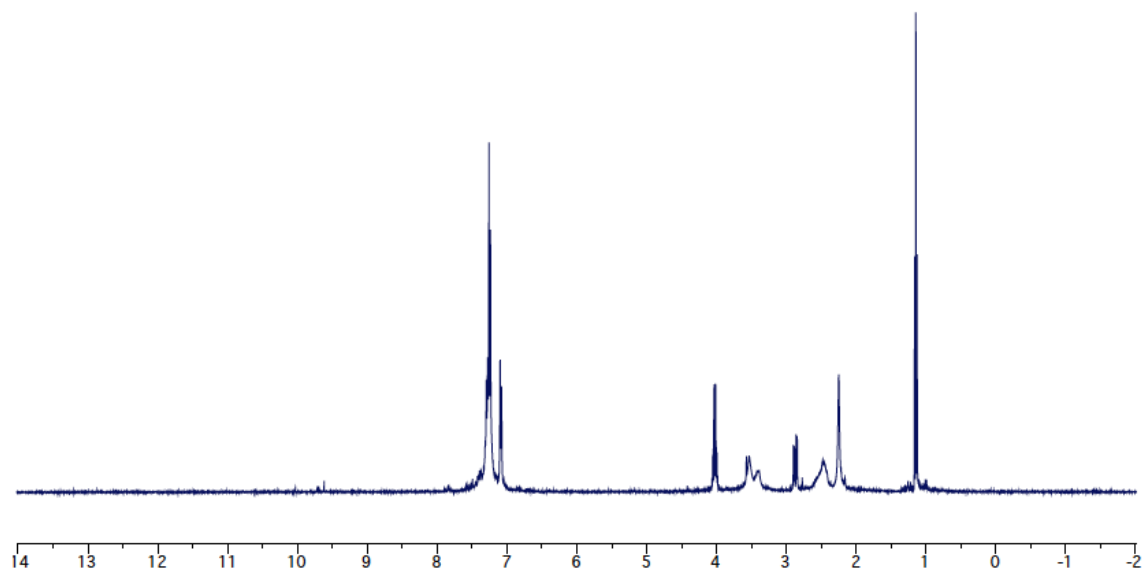
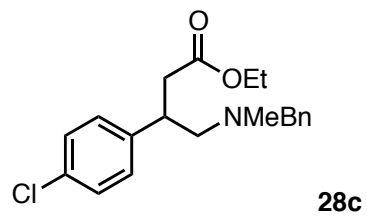
75% yield; light yellow oil; Rf=0.15 (8:2 hex/EtOAc);

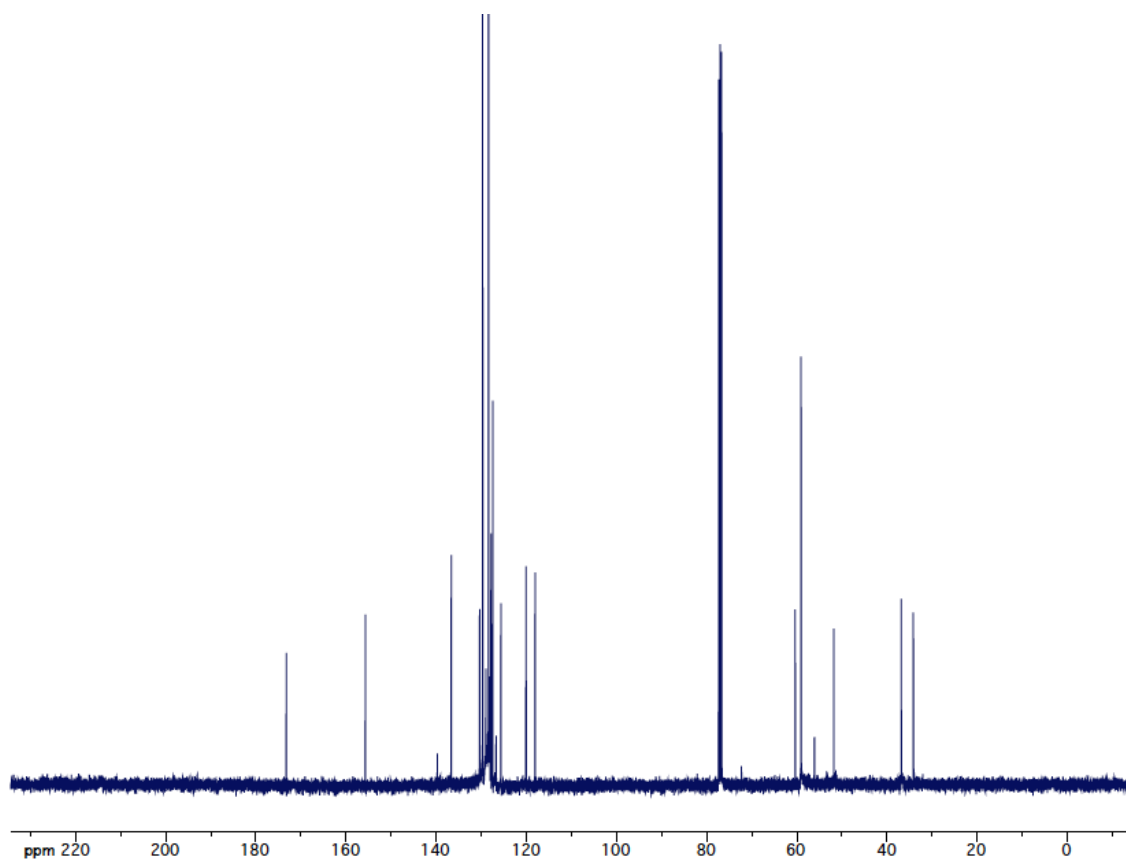
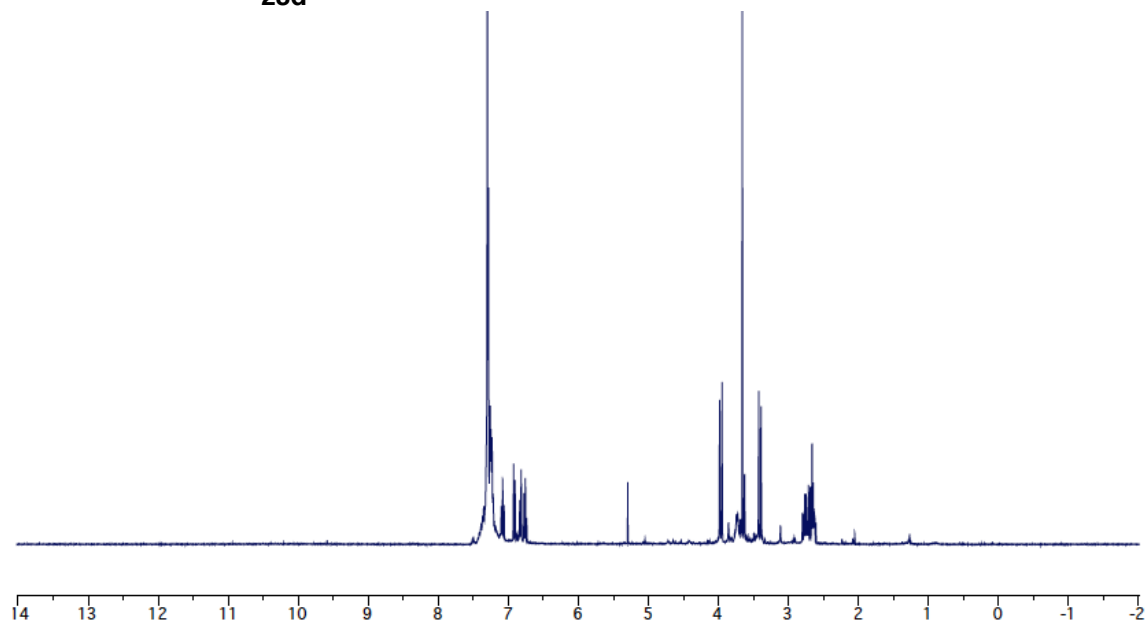
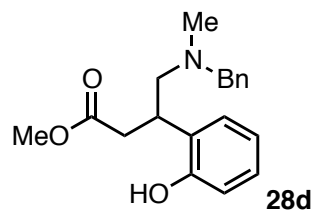
**<sup>1</sup>H-NMR** (300 MHz, CDCl<sub>3</sub>): δ 9.64 (s, 1H), 7.86 (m, *J* = 5.83, 2H), 7.48-7.44 (m, 4H), 3.69 (t, *J* = 4.65, 4H), 3.32 (s, 2H) 2.49 (t, *J* = 4.65, 4H); **<sup>13</sup>C-NMR** (101 MHz; CDCl<sub>3</sub>): δ 194.9, 154.7, 138.1, 134.6, 131.1, 130.3, 128.7, 67.0, 53.2, 50.8. **LRMS** (ESI+) calcd for C<sub>14</sub>H<sub>17</sub>NO<sub>2</sub>, 231.29. Found 232.2 (M+H).

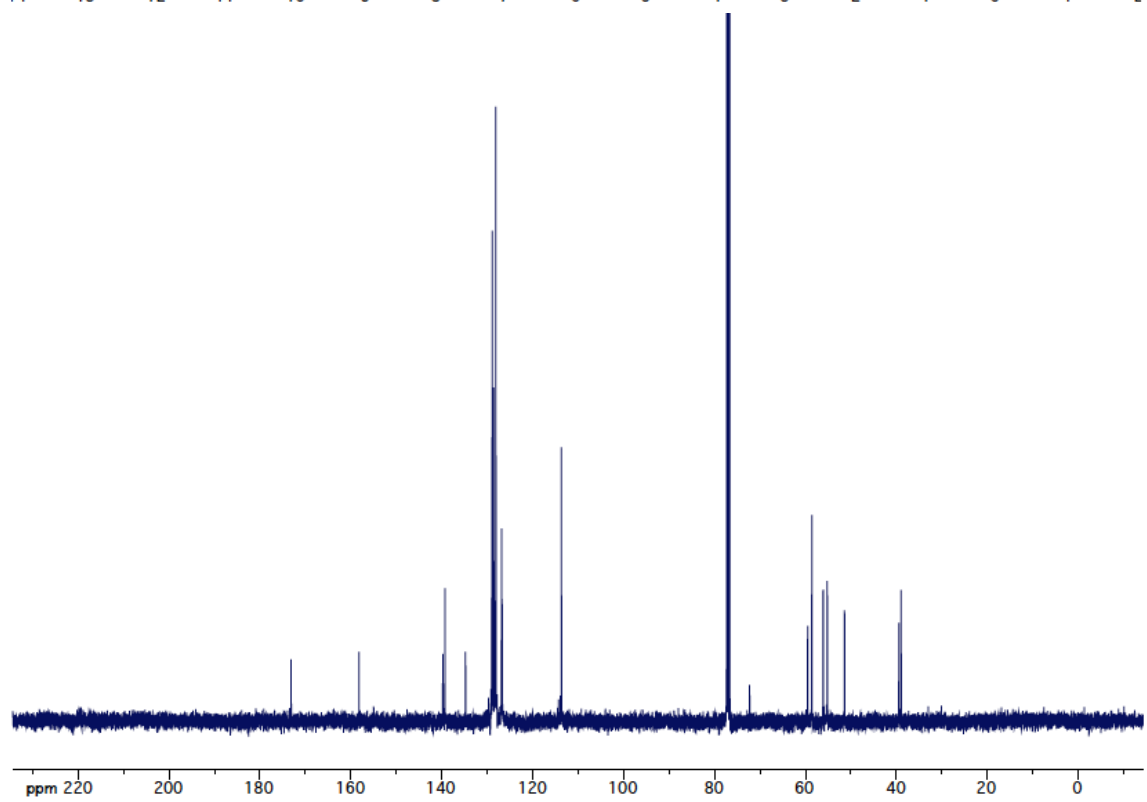
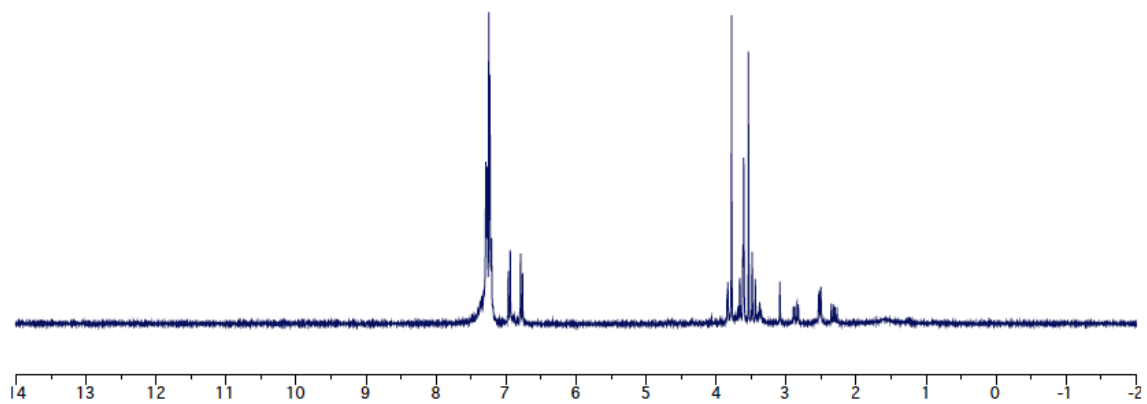
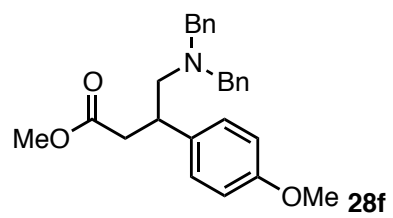


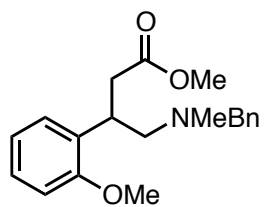




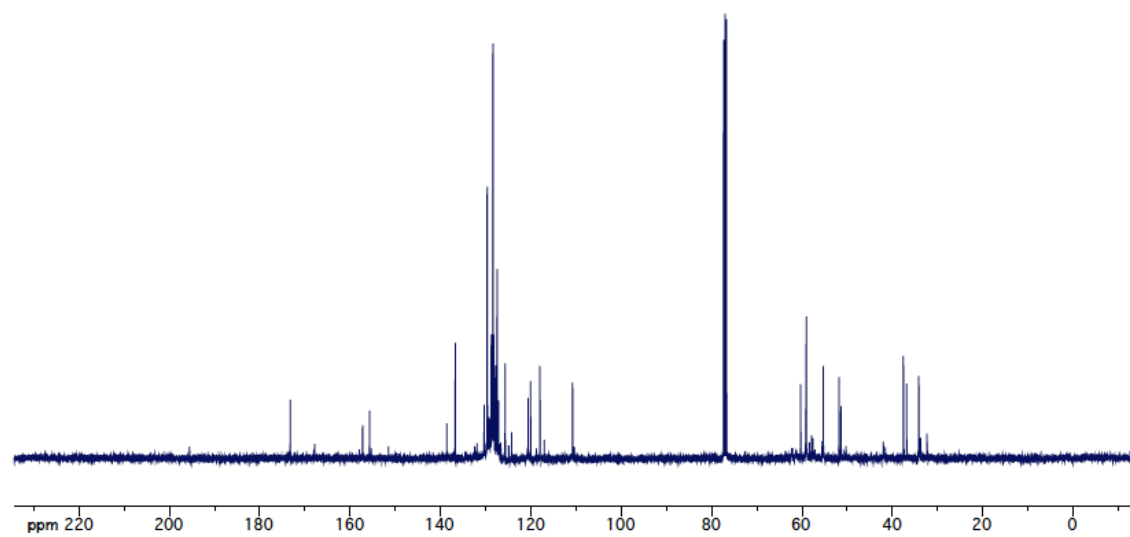
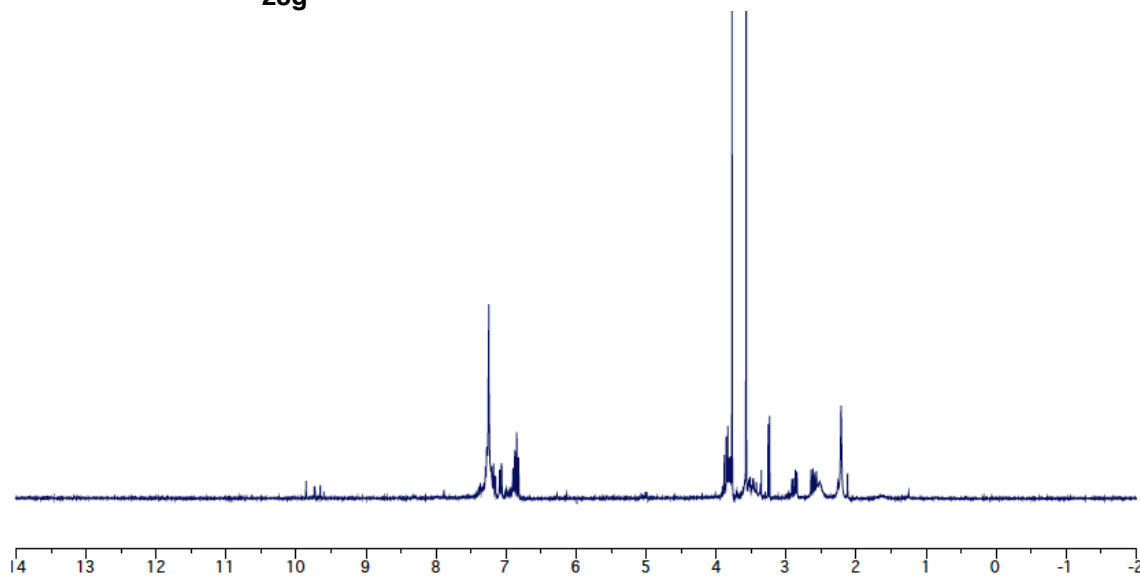


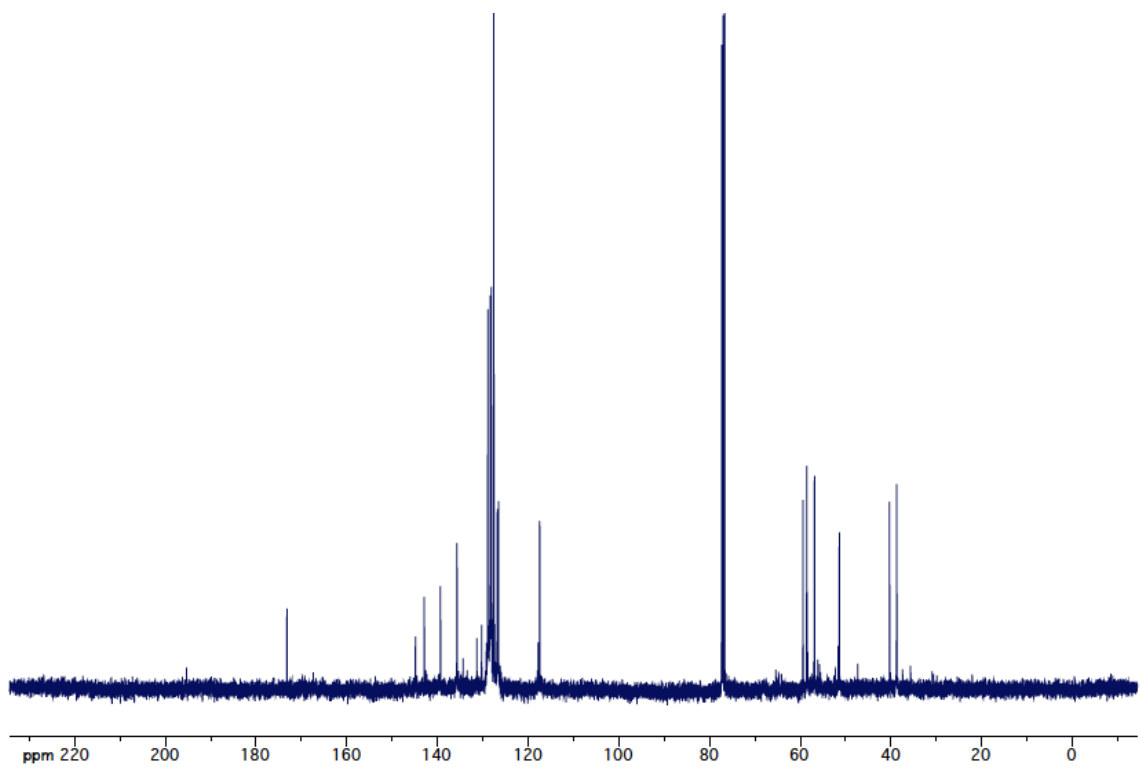
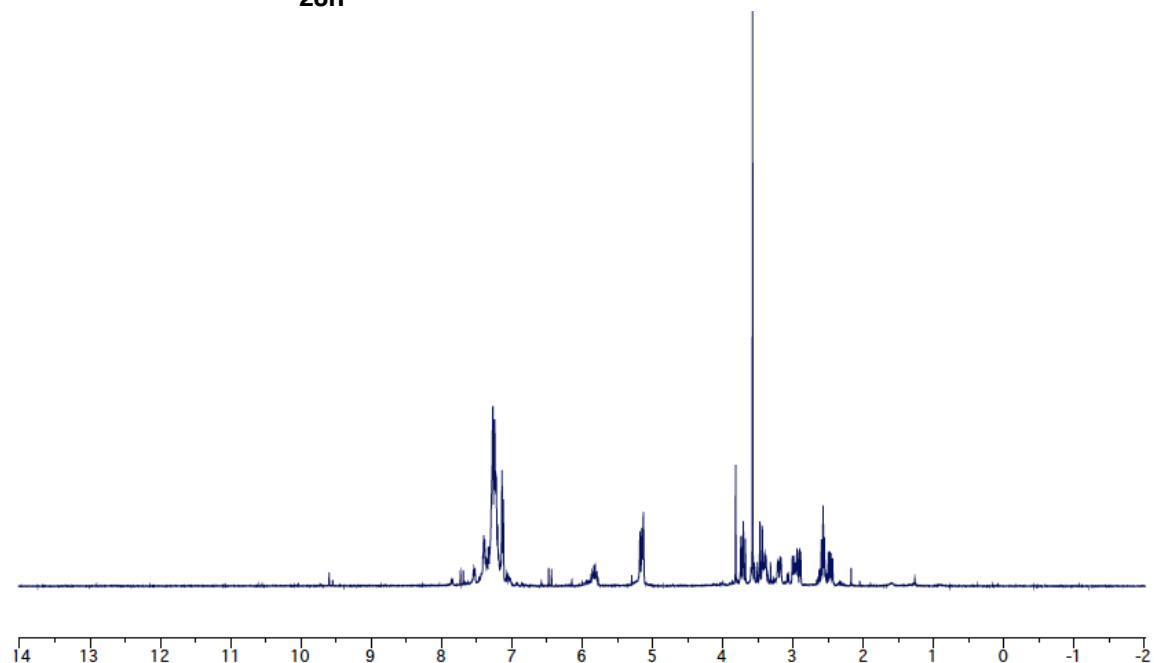
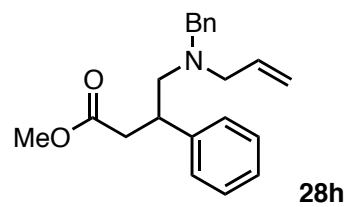


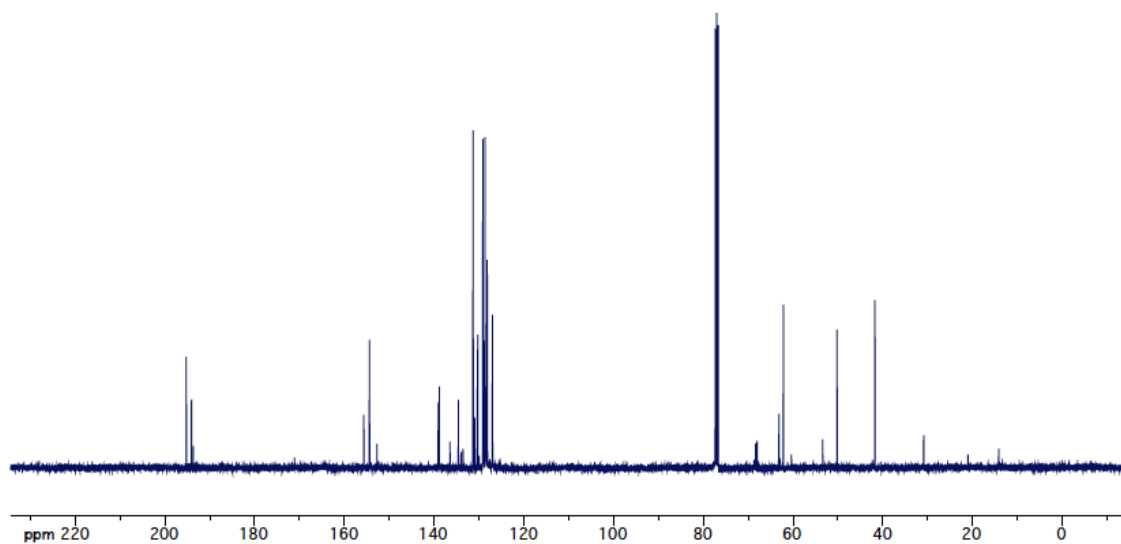
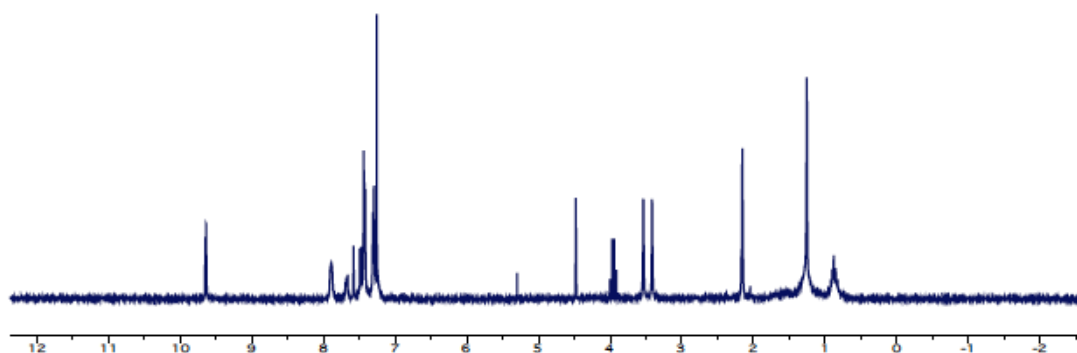
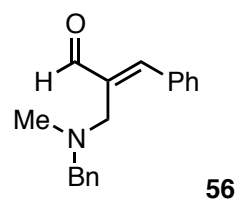


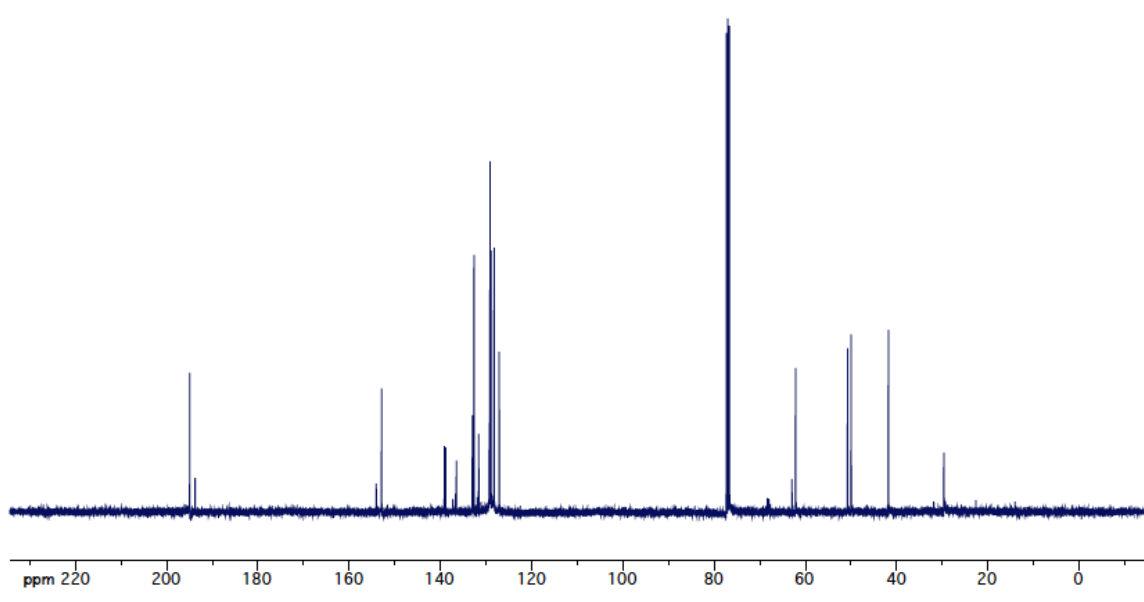
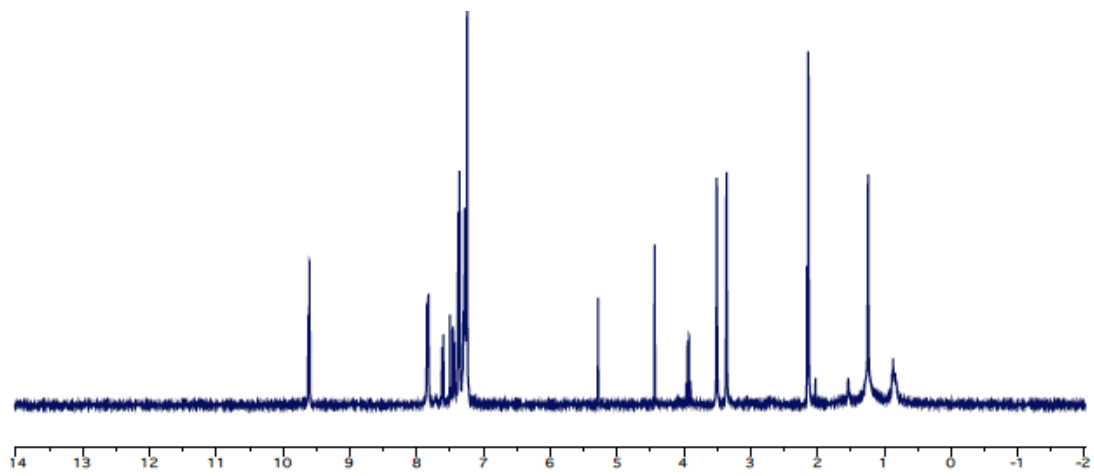
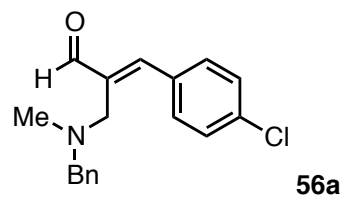


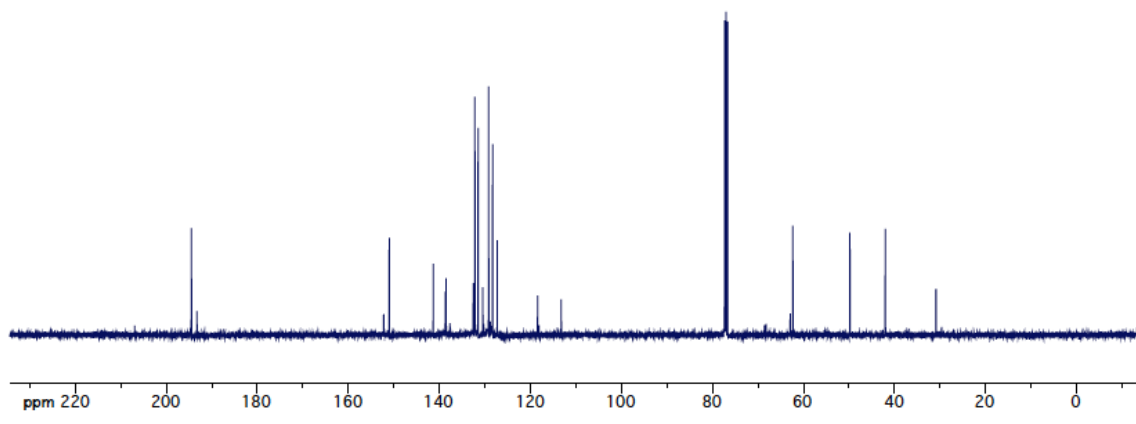
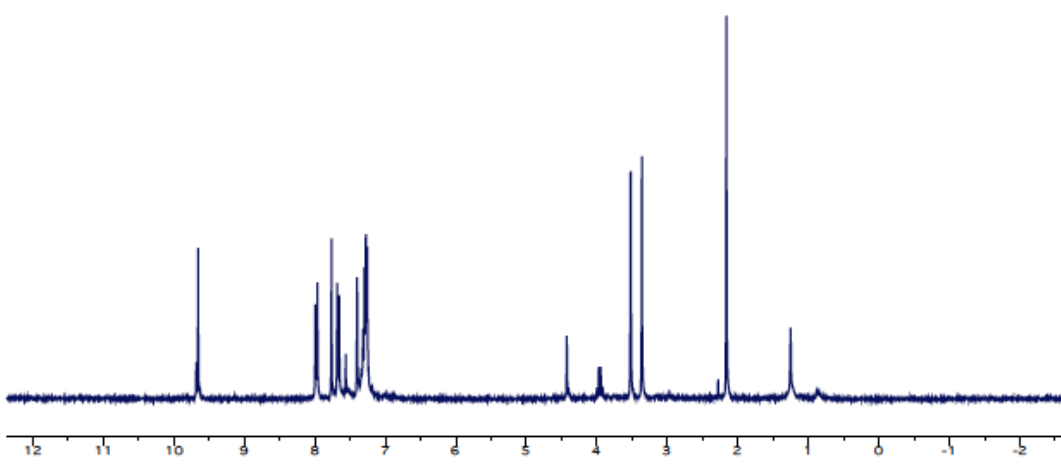
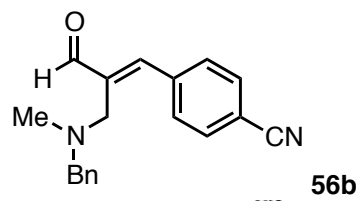
28g

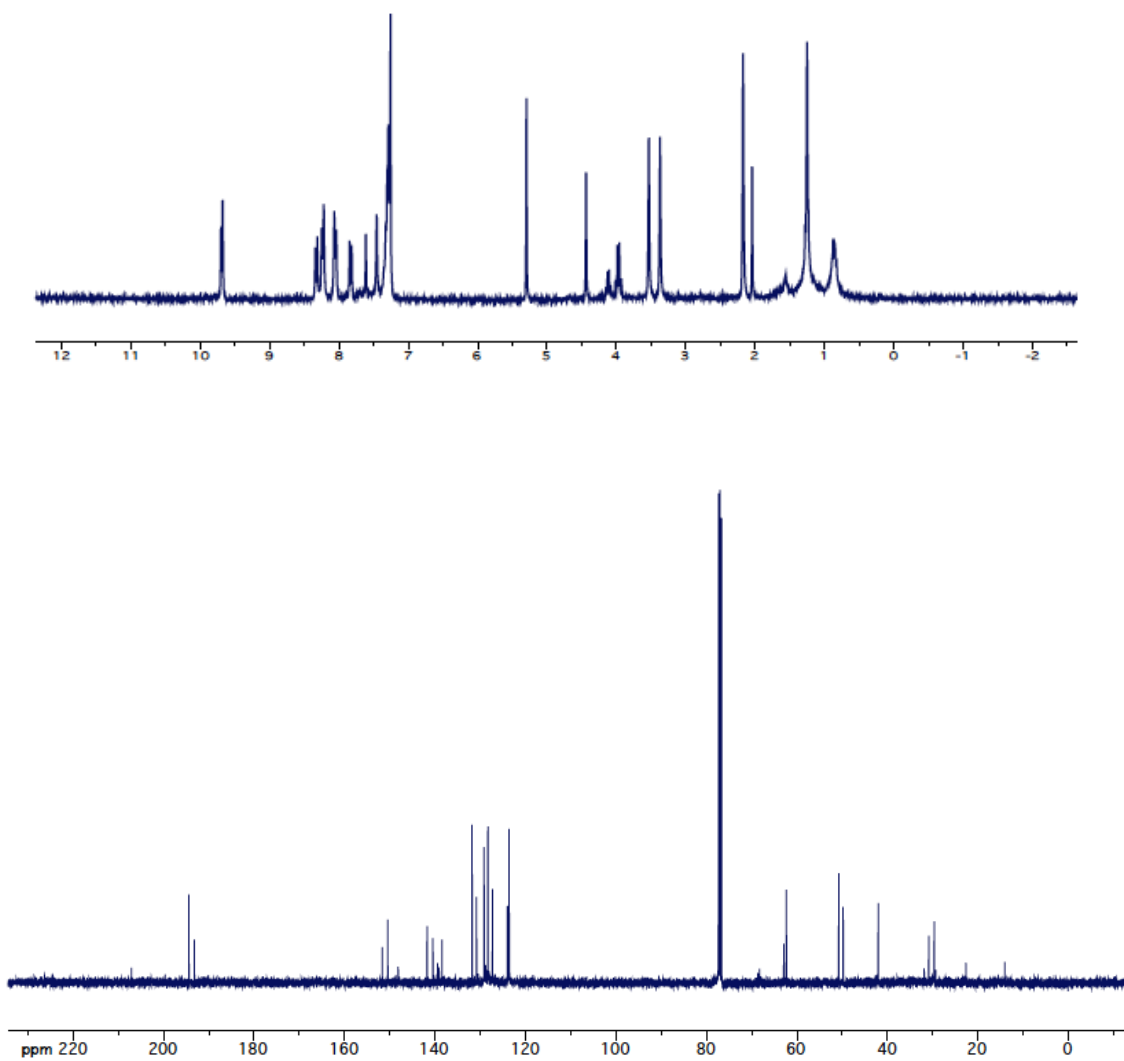
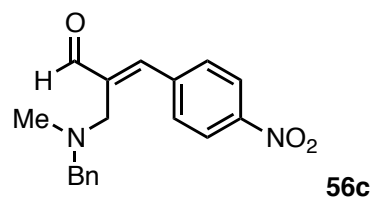


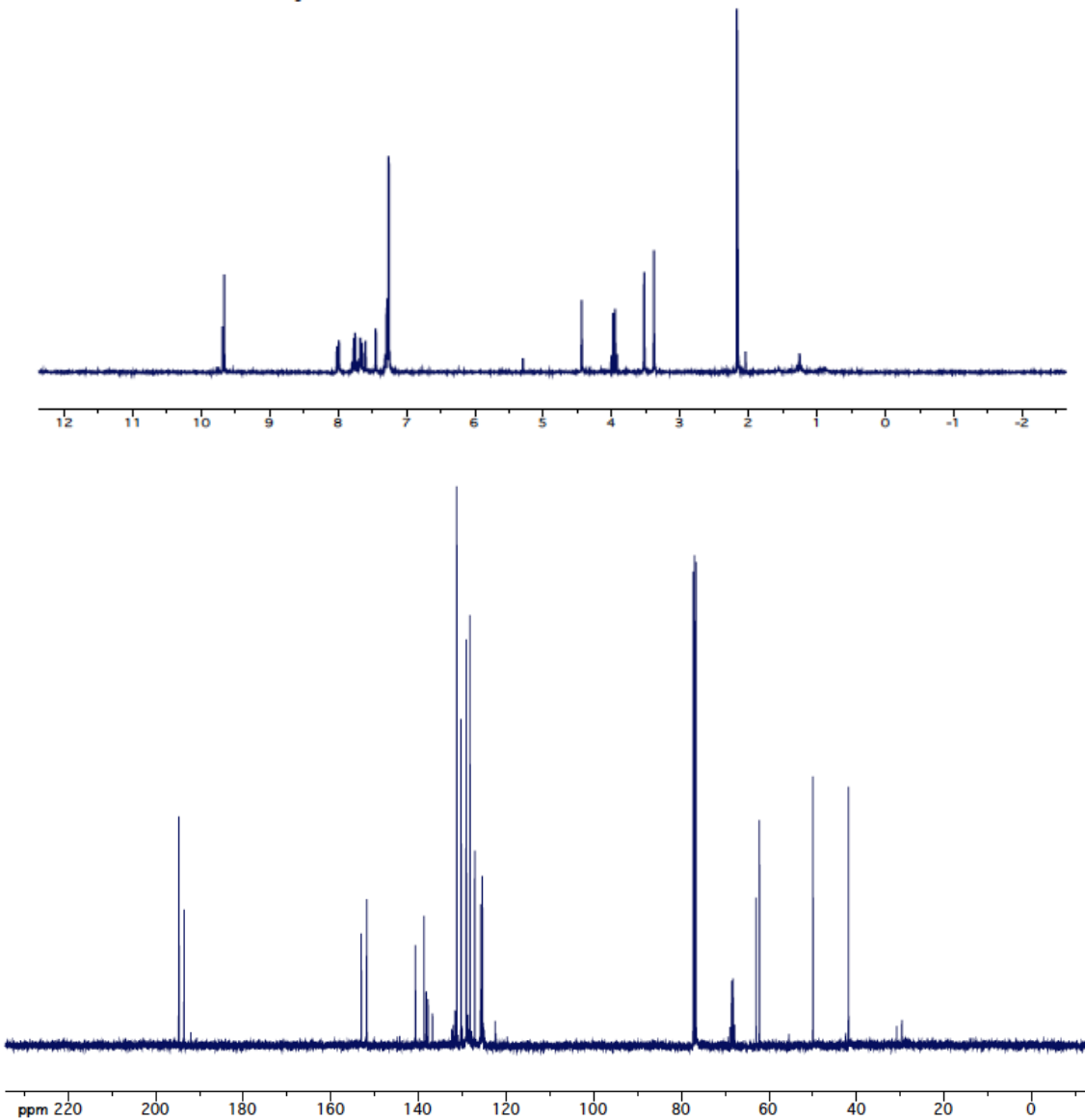
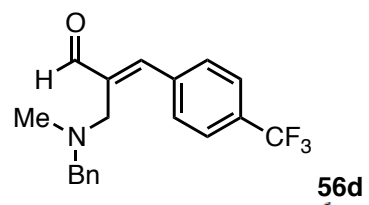


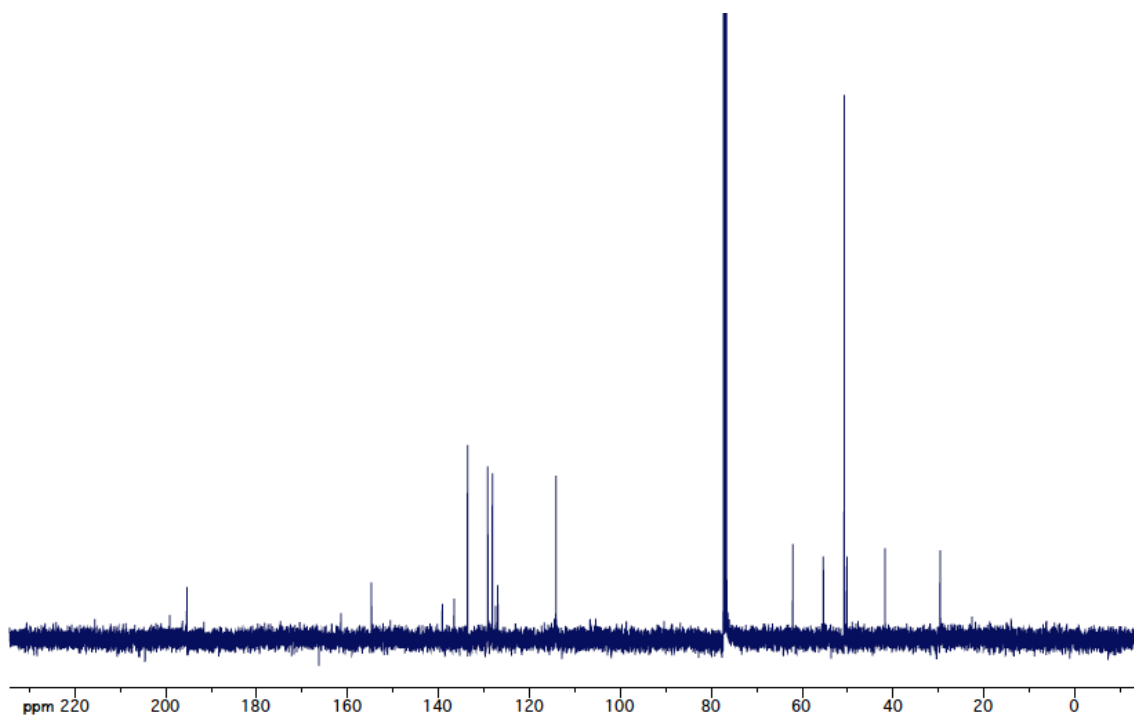
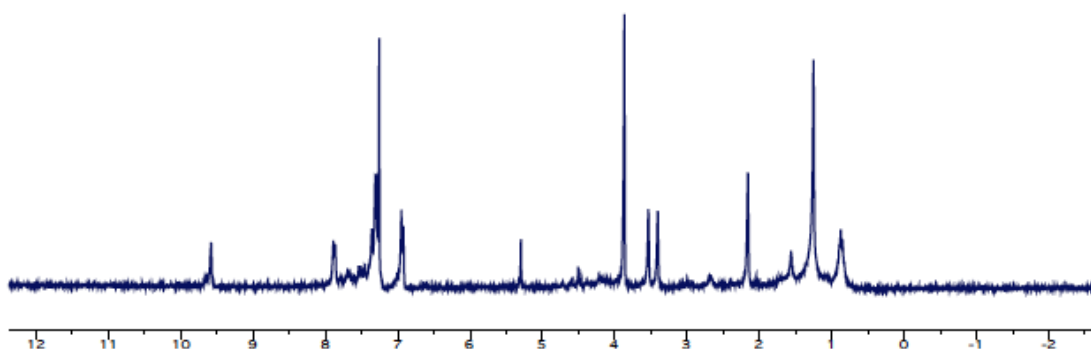
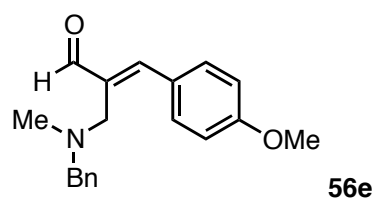


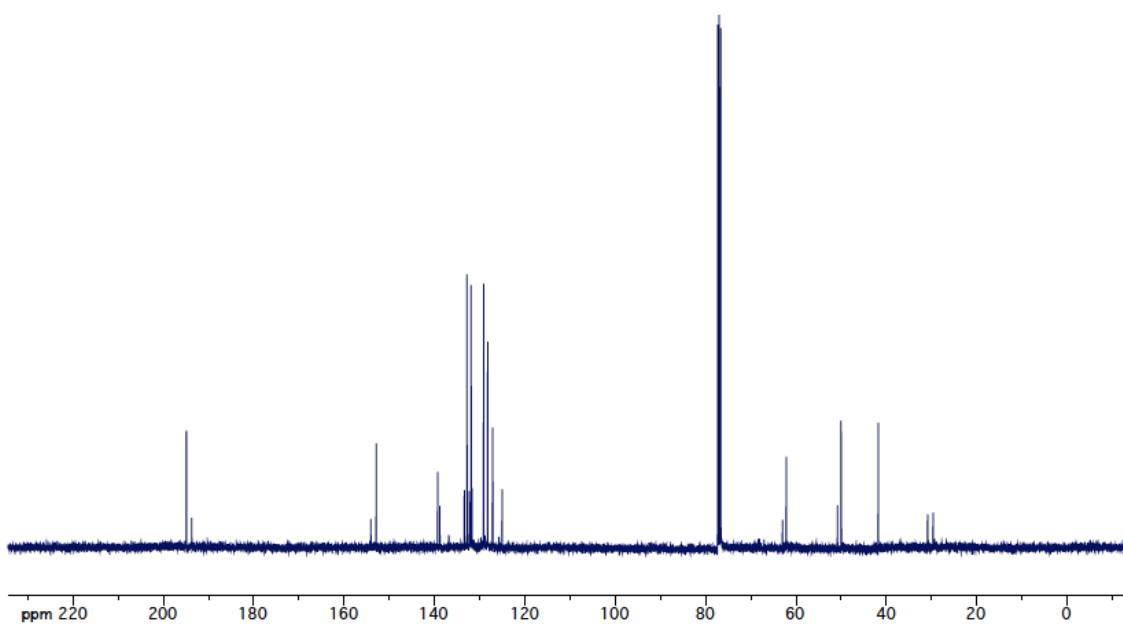
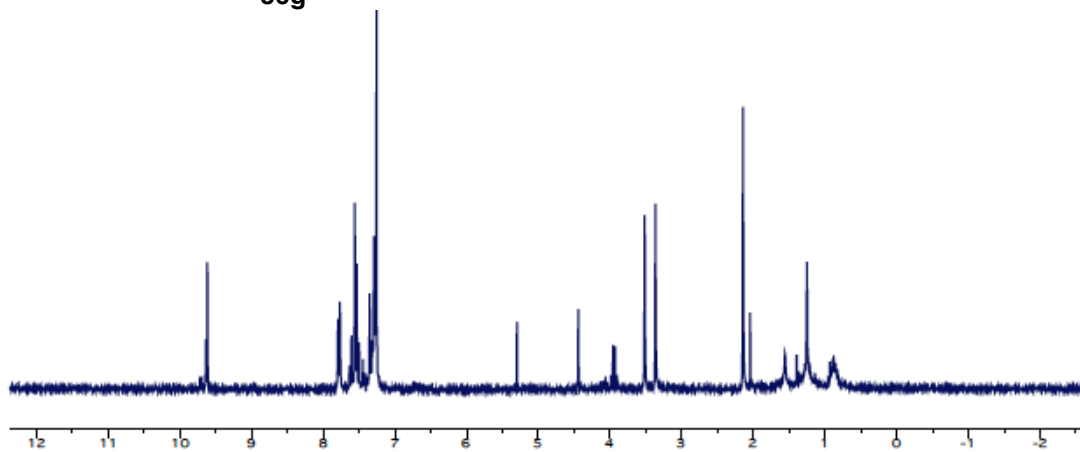
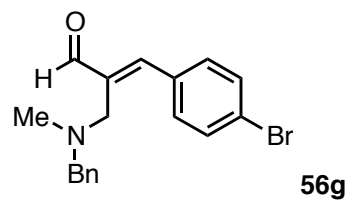


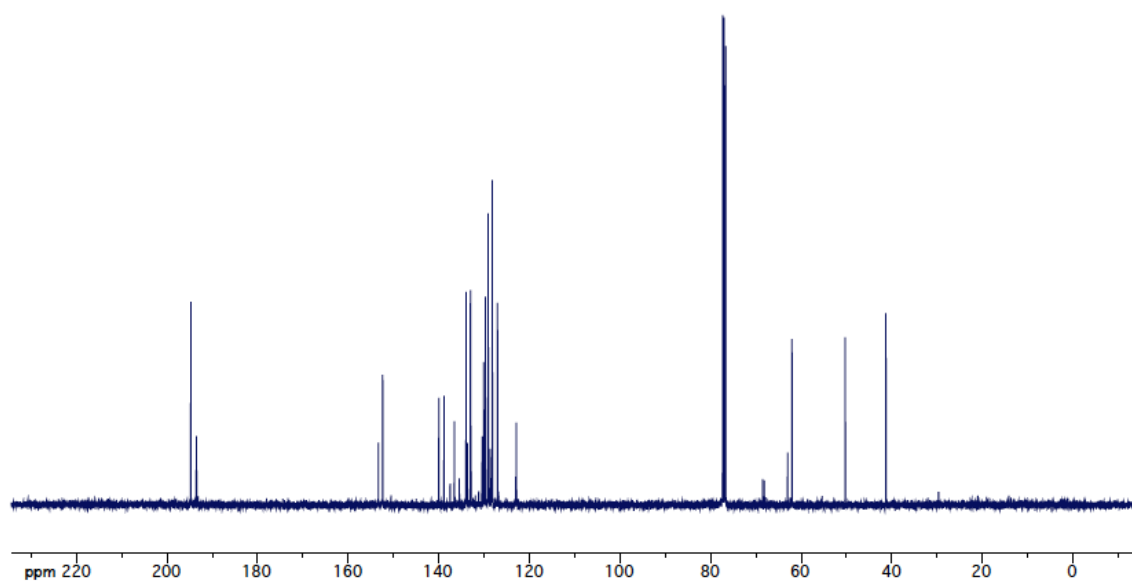
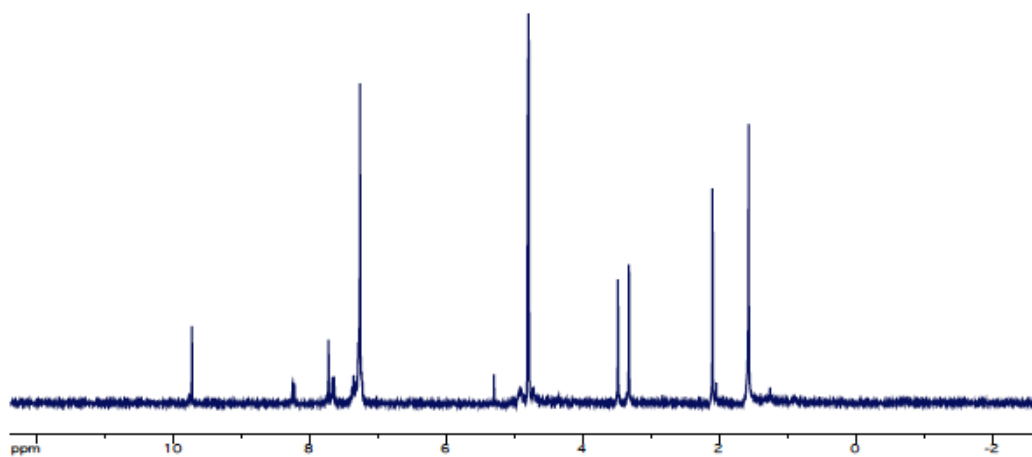
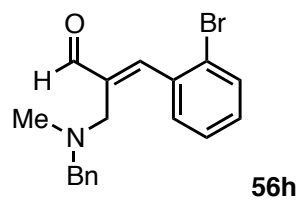


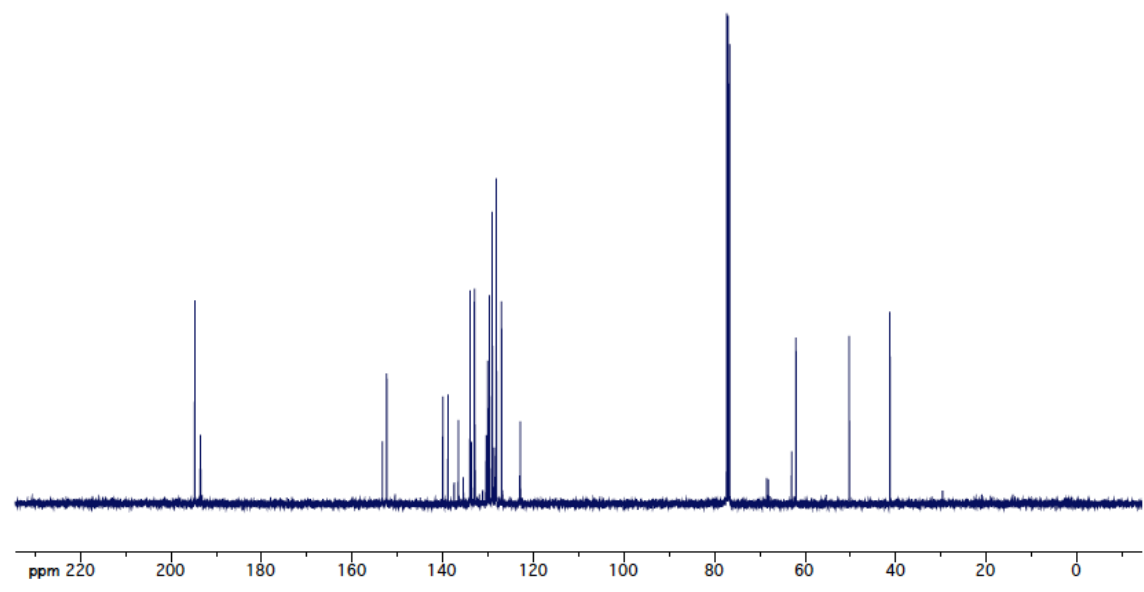
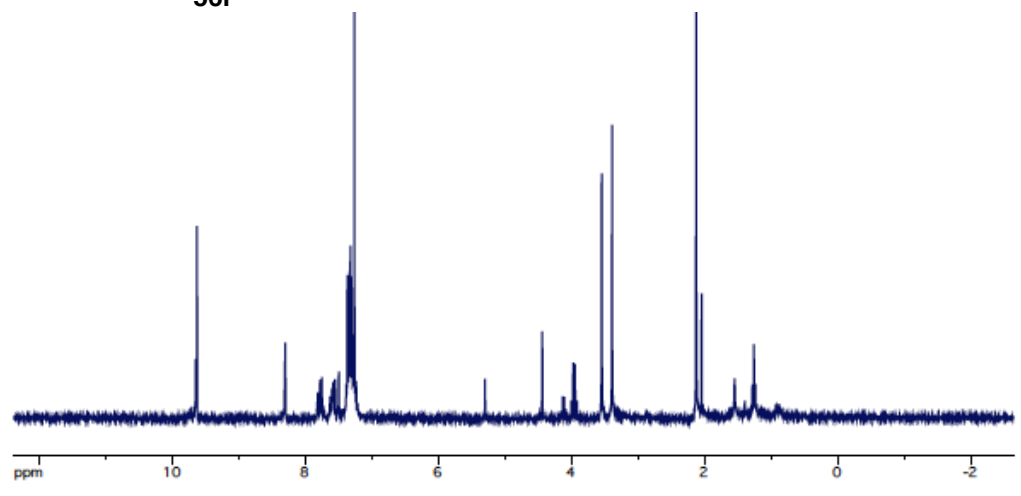
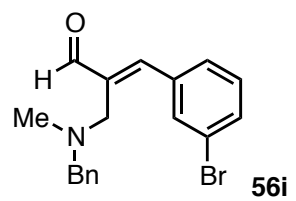


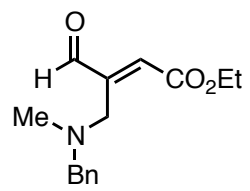




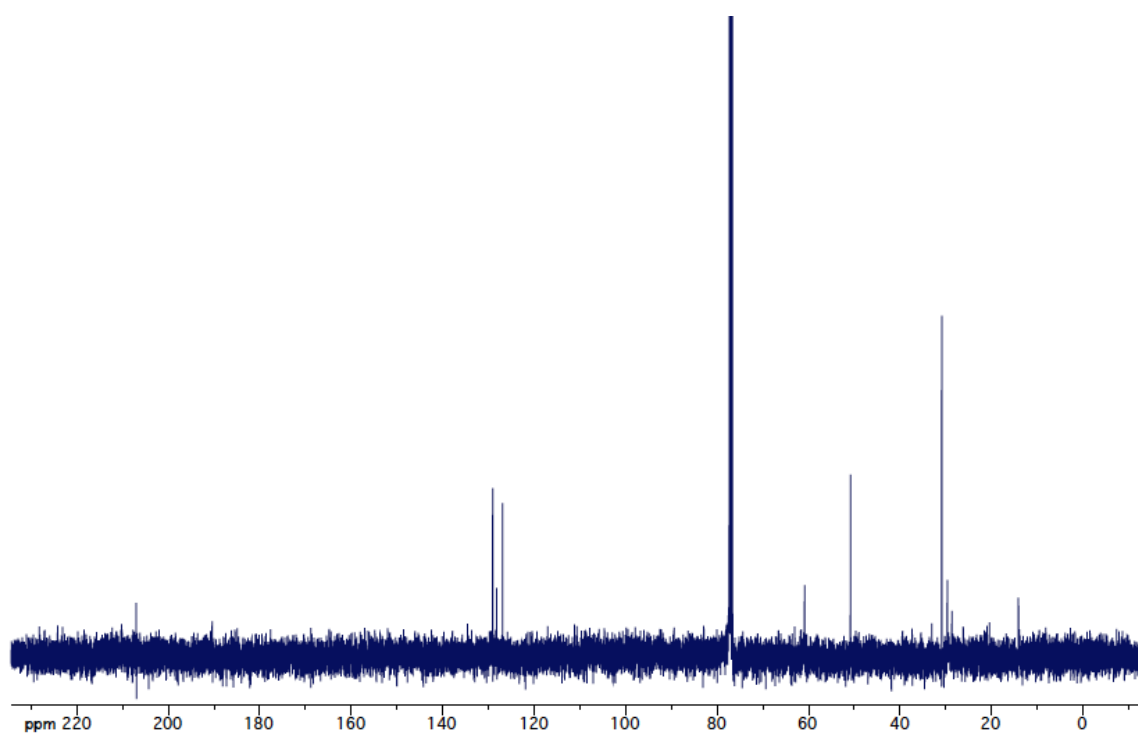
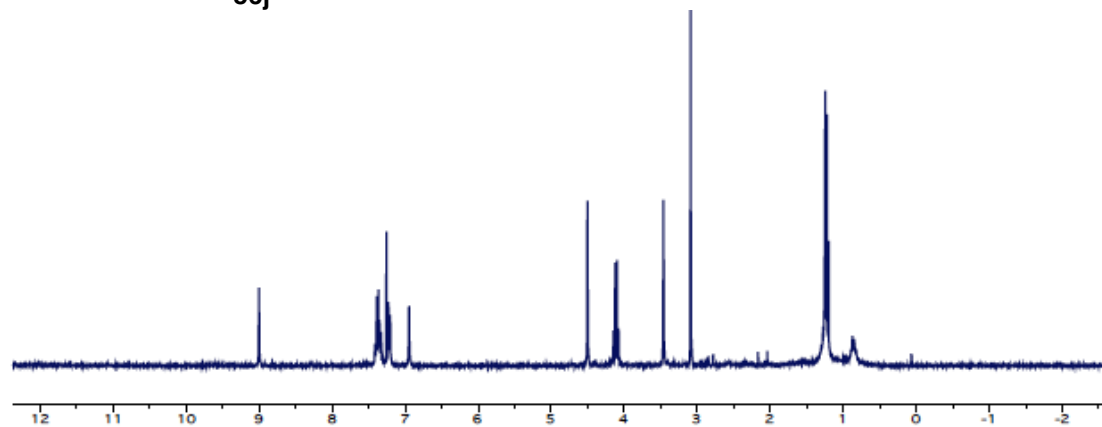


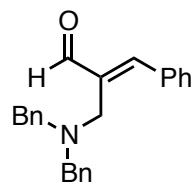




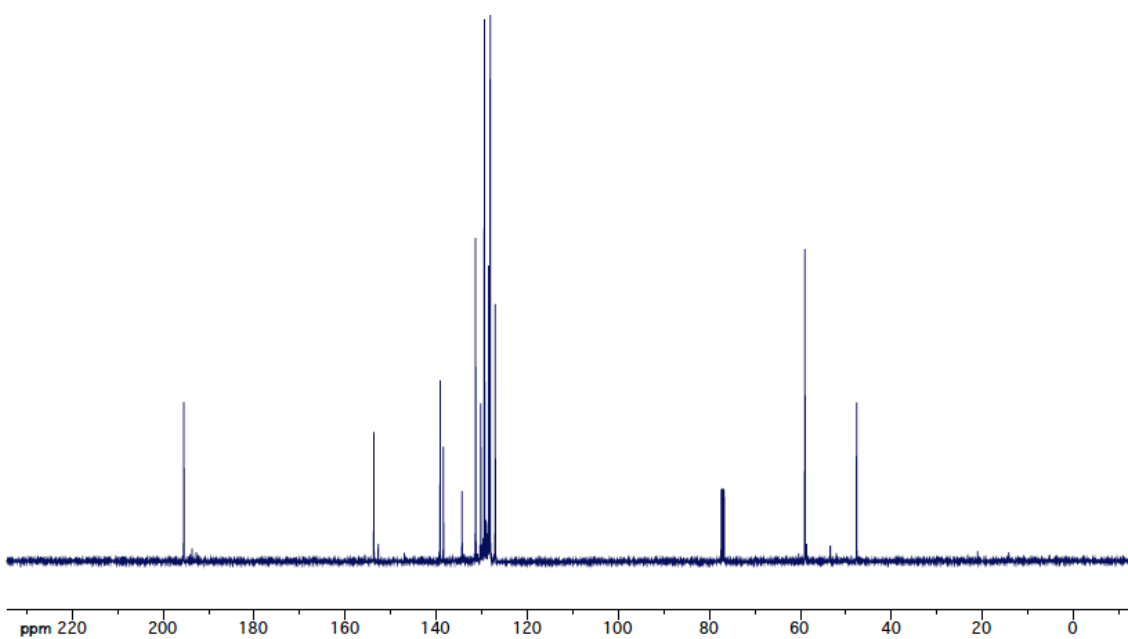
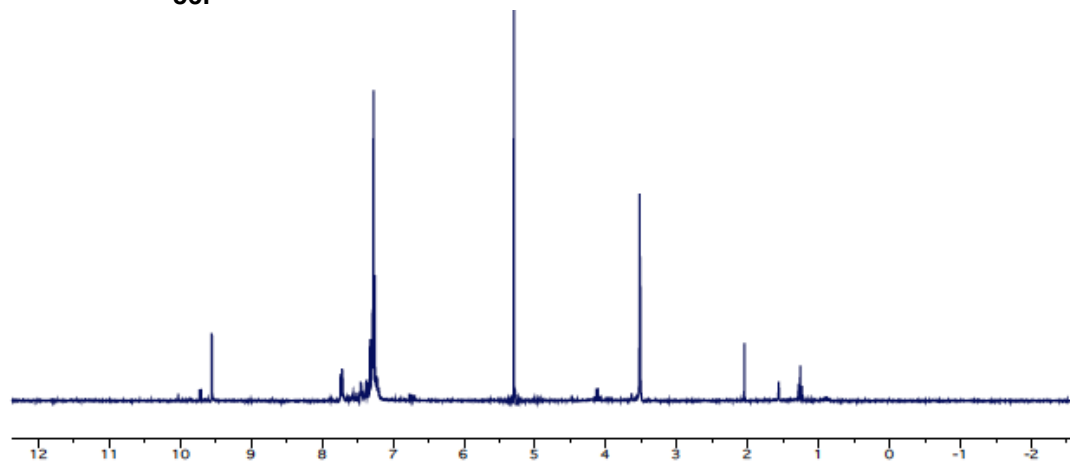


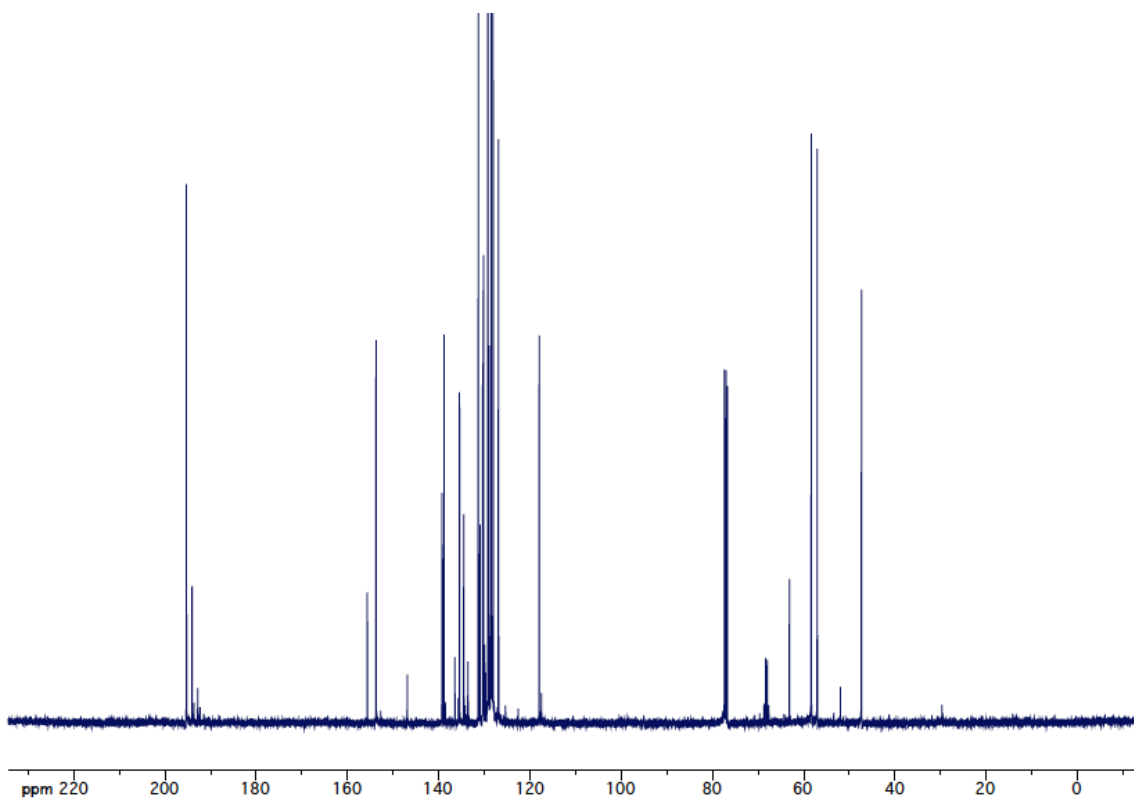
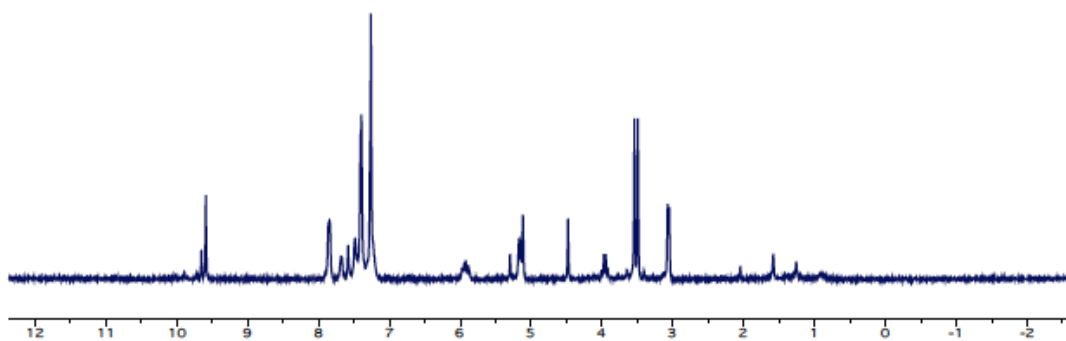
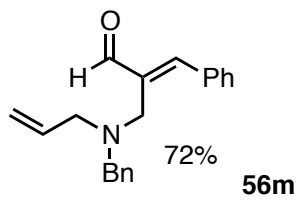
56j

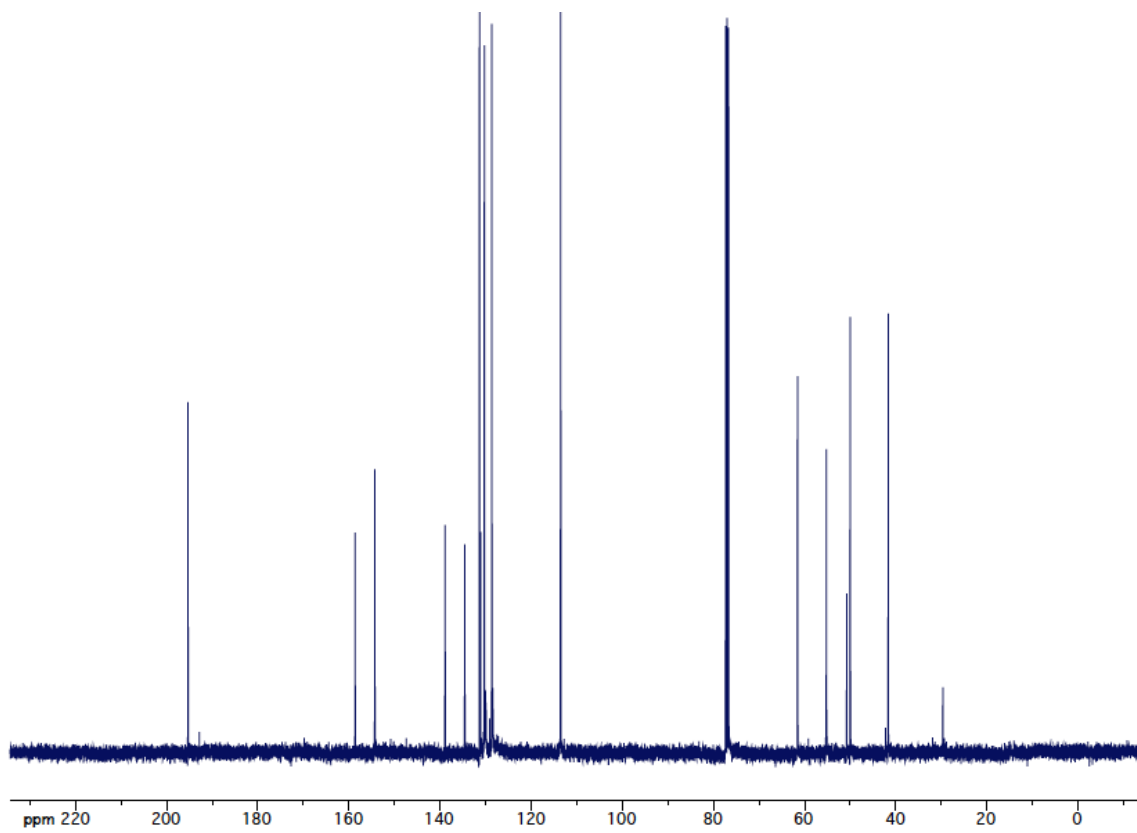
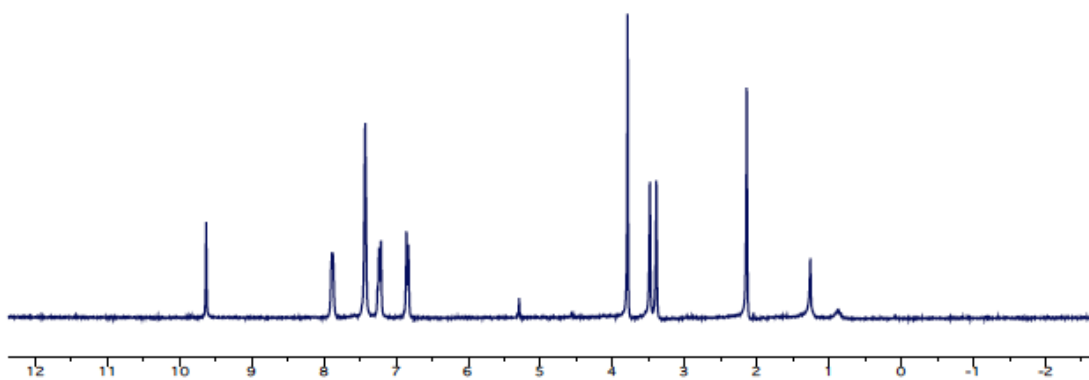
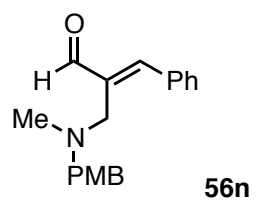


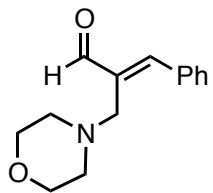


56I

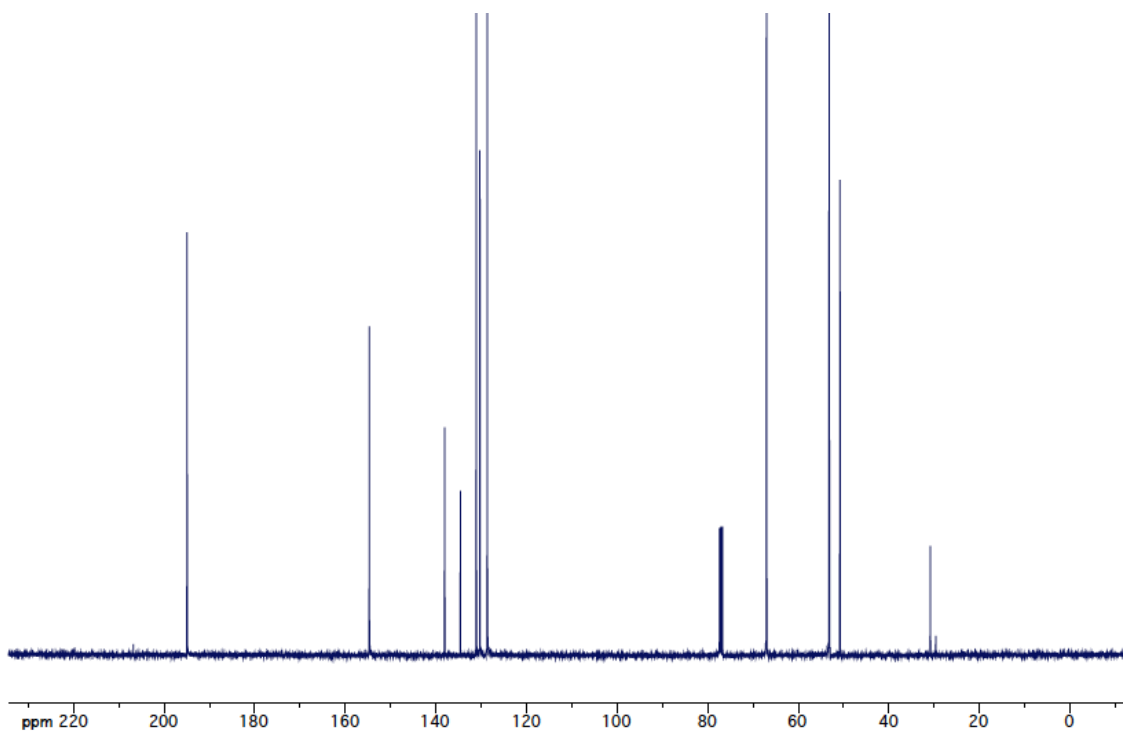
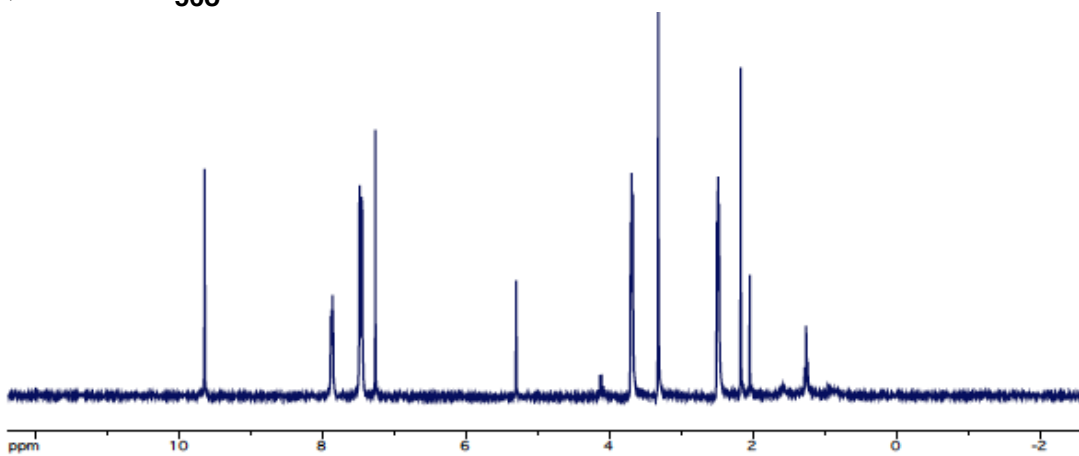








56o



## APPENDIX 4

### EXPERIMENTAL AND SPECTRAL DATA FOR CHAPTER 4

#### **Materials and Methods:**

##### Instrumentation:

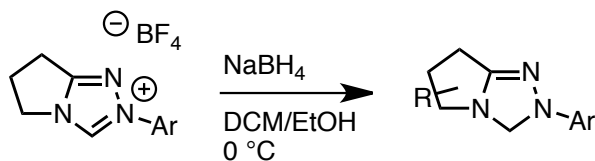
Thin Layer chromatography was performed with SiliCycle 250  $\mu\text{m}$  60A plates. Visualization by UV light (254 nm) or treatment with  $\text{I}_2$  or  $\text{KMnO}_4$  was effective. Flash column chromatography was conducted with aluminum oxide (Sigma-Aldrich, activated, basic, Brockmann I).

NMR studies were conducted on a Varian 400 MHz spectrometer or Varian 300 MHz spectrometer at ambient temperature.  $^1\text{H}$ -NMR is recorded as follows: Chemical shifts ( $\delta$ , ppm), multiplicity, coupling constant, and integration.  $^{13}\text{C}$ -NMR is recorded as chemical shifts ( $\delta$ , ppm). Mass Spectrometry was achieved with an Agilent Technologies 6130 Quadrupole LC/MS. Infrared Spectrometry was achieved with a Thermo Scientific Nicolet iS50 FT-IR.

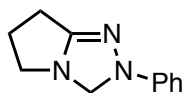
##### Materials:

Boronic acids were purchased from Sigma-Aldrich or AKSci. Trityl salts were purchased from Sigma-Aldrich or Oakwood Chemicals. Palladium catalyst was purchased from Sigma-Aldrich. NHC catalysts were prepared according to literature procedures. Solvents were obtained from VWR and purified through aluminum oxide column. HPLC grade water was used as well. No solvent was degassed.  $\text{CDCl}_3$  and Acetone- $\text{D}_6$  was obtained from Cambridge Isotope Laboratories, with Acetone- $\text{D}_6$  containing 0.05% tetramethylsilane (TMS).

### General Procedure for Reduction of Triazolium salt to Triazoline



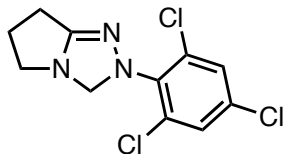
In a 50 mL round-bottomed flask with a magnetic stir bar, the triazolium salt (1.83 mmol, 1 equiv.) is dissolved in DCM (10 mL) and cooled to 0 °C by ice-water bath. After 10 minutes, sodium borohydride (69 mg, 1.83 mmol, 1 equiv) is carefully added. This is followed by 1 ml of Ethanol, where upon the reaction bubbles vigorously. The reaction is continued to stir at 0 °C for 3-4 hours. The reaction is diluted with DCM (20 mL) and washed with water (2 X 15 mL). The aqueous fractions are combined and extracted with DCM (20 mL). The DCM fractions are dried over MgSO<sub>4</sub>, filtered, and concentrated. Crude product is typically pure enough to continue, but can easily be purified by flash column chromatography (0 to 50% EtOAc/Hexanes through basic Al<sub>2</sub>O<sub>3</sub>).



#### **2-phenyl-3,5,6,7-tetrahydro-2H-pyrrolo[2,1-c] [1,2,4]triazole (28a)**

282 mg of light brown solid (82% yield from 500 mg SM). *r<sub>f</sub>* = 0.5 (50% EtOAc/Hexane)

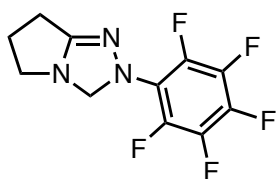
**<sup>1</sup>H-NMR** (300 MHz; acetone-D<sub>6</sub>): δ 7.22-7.17 (m, 2H), 6.89-6.85 (m, 2H), 6.75 (d, *J* = 7.4 Hz, 1H), 4.62 (s, 2H), 3.07 (t, *J* = 6.4 Hz, 2H), 2.45-2.35 (m, 4H). **<sup>13</sup>C-NMR** (101 MHz; acetone-D<sub>6</sub>): δ 162.1, 148.3, 128.7, 118.3, 112.8, 71.1, 46.9, 25.1, 19.7. **MS** calcd for C<sub>11</sub>H<sub>13</sub>N<sub>3</sub>: 187.24, found: 188.10 (M+H).



**2-(2,4,6-trichlorophenyl)-3,5,6,7-tetrahydro-2H-pyrrolo[2,1-c][1,2,4]triazole (28e)**

151 mg of light brown oil (98% yield from 200 mg SM).  $r_f = 0.55$  (50% EtOAc/Hexane)

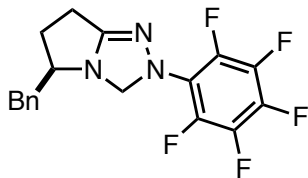
$^1\text{H-NMR}$  (300 MHz;  $\text{CDCl}_3$ ):  $\delta$  7.32 (s, 2H), 4.70 (s, 2H), 3.10 (t,  $J = 6.5$  Hz, 2H), 2.51 (dd,  $J = 6.7, 1.3$  Hz, 2H), 2.44-2.39 (m, 2H).  $^{13}\text{C-NMR}$  (101 MHz;  $\text{CDCl}_3$ ):  $\delta$  162.9, 139.6, 137.6, 135.8, 132.4, 129.5, 129.22, 129.19, 72.6, 70.0, 46.7, 45.9, 25.7, 25.4, 22.4, 20.3 **MS**: calcd for  $\text{C}_{11}\text{H}_{10}\text{Cl}_3\text{N}_3$  Expect 290.58 Found 292.0 (M+2H).



**2-(perfluorophenyl)-3,5,6,7-tetrahydro-2H-pyrrolo[2,1-c][1,2,4]triazole (28g)**

74 mg (99% yield from 200mg SM).  $r_f = 0.6$  (50% EtOAc/Hexane)

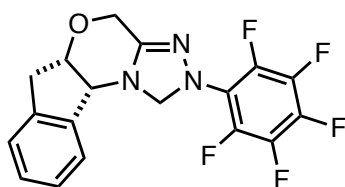
$^1\text{H-NMR}$  (300 MHz;  $\text{CDCl}_3$ ):  $\delta$  4.74 (s, 2H), 3.09 (t,  $J = 6.5$  Hz, 2H), 2.54 (m, 2H), 2.43 (m, 2H).  $^{13}\text{C-NMR}$  (101 MHz; acetone):  $\delta$  164.2, 139.31, 139.27, 137.5, 135.1, 73.3, 46.8, 25.3, 19.0 **MS**: calcd for  $\text{C}_{11}\text{H}_8\text{F}_5\text{N}_3$  Expect 277.15 Found 278.1.



**(R)-5-benzyl-2-(perfluorophenyl)-3,5,6,7-tetrahydro-2H-pyrrolo[2,1-c][1,2,4]triazole (30a)**

136 mg of light brown solid (84% yield from 200mg of SM).  $r_f = 0.65$  (50% EtOAc/Hexane)

$^1\text{H-NMR}$  (300 MHz; acetone- $d_6$ ):  $\delta$  10.50 (d,  $J = 0.3$  Hz, 1H), 4.82 (t,  $J = 7.4$  Hz, 2H), 3.46 (t,  $J = 7.7$  Hz, 2H), 3.04 (t,  $J = 7.5$  Hz, 2H).  $^{13}\text{C-NMR}$  (101 MHz; acetone):  $\delta$  163.51, 163.50, 138.4, 129.21, 129.12, 128.56, 128.39, 126.5, 72.9, 61.8, 41.2, 32.0, 19.8. MS. calcd for  $\text{C}_{18}\text{H}_{14}\text{F}_5\text{N}_3$  Expect: 367.32 Found: 368.1 (M+H). IR: (neat) 3028, 2939, 2848, 1649, 1500, 1455, 1366, 1294, 1193, 1041, 992, 825  $\text{cm}^{-1}$ .  $[\alpha]_D^{23} = +20.00$  (c = 5, acetone)

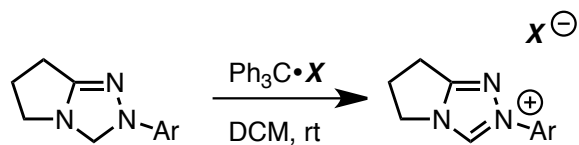


**(5a*S*,10b*R*)-2-(perfluorophenyl)-1,2,4,5a,6,10b-hexahydroindeno[2,1-*b*][1,2,4]triazolo[4,3-*d*][1,4]oxazine (31a)**

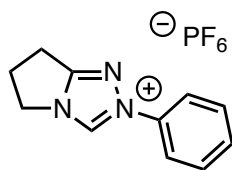
139 mg of white solid (85% yield from 200mg of SM).  $r_f = 0.6$  (50% EtOAc/Hexane)

$^1\text{H-NMR}$  (400 MHz; acetone- $d_6$ ):  $\delta$  7.44 (d,  $J = 7.1$  Hz, 1H), 7.33-7.25 (m, 3H), 5.56 (d,  $J = 1.4$  Hz, 1H), 5.00 (s, 1H), 4.72 (q,  $J = 5.0$  Hz, 1H), 4.58 (d,  $J = 15.6$  Hz, 1H), 4.49 (d,  $J = 5.4$  Hz, 1H), 4.44 (d,  $J = 15.6$  Hz, 1H), 3.23 (dd,  $J = 7.3, 5.2$  Hz, 2H).  $^{13}\text{C-NMR}$  (101 MHz; acetone):  $\delta$  149.0, 140.8, 140.4, 128.3, 126.9, 125.2, 124.7, 76.9, 73.52, 73.48, 73.43, 62.2, 59.2, 35.2. MS: calcd for  $\text{C}_{18}\text{H}_{12}\text{F}_5\text{N}_3\text{O}$  Expect 381.30 Found 382.10 (M+H). IR: (neat) 2913, 1627, 1502, 1459, 1429, 1337, 1311, 1297, 1280, 1147, 1098, 1064, 1053, 973  $\text{cm}^{-1}$ .  $[\alpha]_D^{23} = +103.48$  (c = 2.3, acetone)

### General Procedure for Oxidation by Trityl Salts.



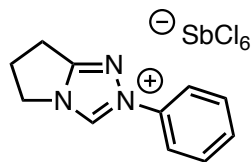
A dry, 5 mL round-bottomed flask is equipped with a magnetic stir bar. The triazoline (1 equiv.) is added to this flask, dissolved in DCM (0.2 M), and an Ar atmosphere is introduced. The desired Trityl salt (1 equiv.) is added in one portion. The reaction is stirred at room temperature for overnight, and completion is judged by TLC. Typically, addition of  $\text{Et}_2\text{O}$  causes precipitation of the desired triazolium salt, which is recovered by filtration.



### **2-phenyl-6,7-dihydro-5H-pyrrolo[2,1-c][1,2,4]triazol-2-ium hexafluorophosphate(V) (29b)**

128 mg of white solid (73% yield from 100 mg SM) rf: 0.1 (50% EtOAc/Hexane)

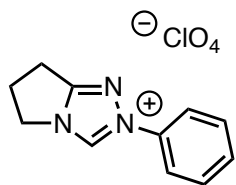
**$^1\text{H-NMR}$**  (400 MHz; acetone- $\text{D}_6$ ):  $\delta$  10.36 (s, 1H), 7.92 (d,  $J = 8.2$  Hz, 2H), 7.70-7.67 (m, 3H), 4.68 (t,  $J = 7.4$  Hz, 2H), 3.37 (t,  $J = 7.7$  Hz, 2H), 2.98 (t,  $J = 7.5$  Hz, 2H).  **$^{13}\text{C NMR}$**  (101 MHz; acetone):  $\delta$  163.8, 137.8, 130.7, 121.1, 47.6, 26.8, 21.4. **MS** calcd for  $\text{PF}_6^-$ : (-)144.96 Found: (-)145.1. **IR**: (neat) 3153, 2359, 2341, 1595, 831  $\text{cm}^{-1}$



### **2-phenyl-6,7-dihydro-5H-pyrrolo[2,1-c][1,2,4]triazol-2-ium hexachlorostibate(V) (29c)**

179 mg of pale, purple solid (65% yield from 100 mg SM). rf = 0.12 (50% EtOAc/Hexane)

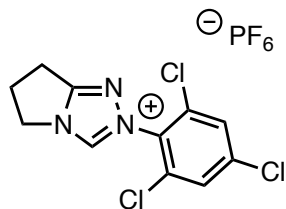
**<sup>1</sup>H-NMR** (400 MHz; CD<sub>3</sub>OD): δ 10.39 (s, 1H), 7.87 (d, *J* = 8.1 Hz, 2H), 7.65-7.62 (m, 3H), 4.50 (t, *J* = 7.4 Hz, 2H), 3.25 (d, *J* = 7.7 Hz, 2H), 2.87 (t, *J* = 7.5 Hz, 2H). **<sup>13</sup>C NMR** (101 MHz; CD<sub>3</sub>OD): δ 163.4, 137.6, 135.9, 130.4, 129.9, 120.6, 26.4, 21.1. **MS** calcd for SbCl<sub>6</sub>: (-)334.48 Found: (-)334.8 **IR**: (neat) 2360, 2341, 1590, 1388, 762 cm<sup>-1</sup>



**2-phenyl-6,7-dihydro-5H-pyrrolo[2,1-c][1,2,4]triazol-2-ium perchlorate (29d)**

70mg of brown solid (46% yield from 100 mg SM). rf = 0.1 (50% EtOAc/Hexane)

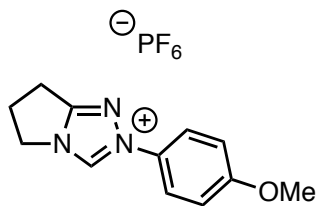
**<sup>1</sup>H-NMR** (400 MHz; acetone-d<sub>6</sub>): δ 10.38 (s, 1H), 7.94-7.91 (m, 2H), 7.69-7.66 (m, 3H), 4.68 (t, *J* = 7.4 Hz, 2H), 3.37 (t, *J* = 7.7 Hz, 2H), 2.98 (t, *J* = 7.4 Hz, 2H). **<sup>13</sup>C NMR** (101 MHz; acetone-d<sub>6</sub>): δ 164.2, 163.7, 138.0, 130.6, 130.2, 121.1, 47.6, 26.8, 21.5. **MS** calcd for C<sub>11</sub>H<sub>12</sub>N<sub>3</sub><sup>+</sup> Expect 186.23 Found 186.1 (M<sup>+</sup>). **IR**: (neat) 2360, 2341, 1593, 1524, 1091, 764 cm<sup>-1</sup>



**2-(2,4,6-trichlorophenyl)-6,7-dihydro-5H-pyrrolo[2,1-c][1,2,4]triazol-2-ium hexafluorophosphate(V) (29e)**

120 mg of pale beige solid (53% yield from 151 mg SM). rf = 0.09 (50% EtOAc/ Hexane).

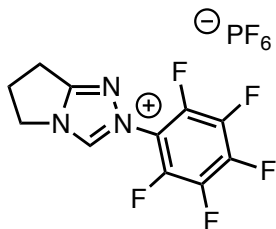
**<sup>1</sup>H-NMR** (400 MHz; acetone-d<sub>6</sub>): δ 10.38 (s, 1H), 7.94 (s, 2H), 4.83 (t, *J* = 7.4 Hz, 2H), 3.45 (t, *J* = 7.8 Hz, 2H), 3.03 (t, *J* = 7.5 Hz, 2H). **<sup>13</sup>C NMR** (101 MHz; acetone): δ 164.7, 143.1, 138.8, 134.2, 129.4, 48.6, 26.7, 21.7. **MS** calcd for C<sub>11</sub>H<sub>19</sub>Cl<sub>3</sub>N<sub>3</sub><sup>+</sup> Expect: 289.57 Found 290.0 (M<sup>+</sup>) calcd for PF<sub>6</sub><sup>-</sup> Expect:-144.96 Found: -145.0. **IR** (neat): 3144, 1598, 1573, 1523, 1416, 1154, 954 cm<sup>-1</sup>.



**2-(4-methoxyphenyl)-6,7-dihydro-5H-pyrrolo[2,1-c][1,2,4]triazol-2-ium hexafluorophosphate(V) (29f)<sup>1</sup>**

105 mg of white solid (71% yield from 89 mg SM). rf= 0.1 (50% EtOAc/Hexane)

**<sup>1</sup>H-NMR** (300 MHz; acetone-d<sub>6</sub>): δ 10.34 (s, 1H), 7.84 (d, *J* = 9.1 Hz, 2H), 7.21 (d, *J* = 9.1 Hz, 2H), 4.68 (t, *J* = 7.4 Hz, 2H), 3.92 (s, 2H), 3.37 (t, *J* = 7.7 Hz, 2H), 2.99 (t, *J* = 7.4 Hz, 2H). **<sup>13</sup>C-NMR** (101 MHz; acetone): δ 163.5, 161.3, 137.3, 129.26, 129.09, 128.2, 122.9, 115.1, 55.3, 47.5, 26.7, 21.4 **MS**: calcd for C<sub>12</sub>H<sub>14</sub>N<sub>3</sub>O: (+) 216.26, Found (+)216.26; calcd for PF<sub>6</sub>: (-) 144.6, Found (-) 145.0. **IR**: (neat) 3651, 3152, 2975, 2348, 1590, 1530, 1465, 1393, 1306, 1258, 1176, 1044, 977, 950 cm<sup>-1</sup>.

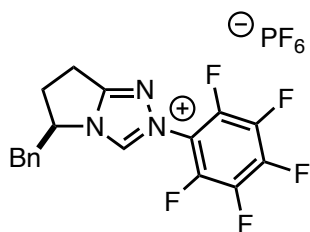


**2-(perfluorophenyl)-6,7-dihydro-5H-pyrrolo[2,1-c][1,2,4]triazol-2-ium hexafluorophosphate(V) (29g)**

<sup>1</sup> **28f** is unstable, and is oxidized immediately after reduction.

61 mg of beige solid (53% yield from 74 mg SM). *r<sub>f</sub>* = 0.1 (50% EtOAc/Hexane)

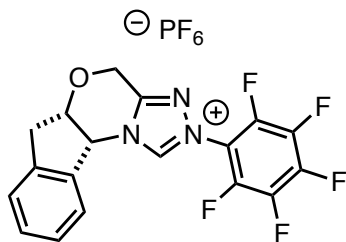
**<sup>1</sup>H-NMR** (300 MHz; acetone-*d*<sub>6</sub>): δ 10.50 (d, *J* = 0.3 Hz, 1H), 4.82 (t, *J* = 7.4 Hz, 2H), 3.46 (t, *J* = 7.7 Hz, 2H), 3.04 (t, *J* = 7.5 Hz, 2H). **<sup>13</sup>C-NMR** (101 MHz; acetone): δ 165.0, 144.5, 143.61, 143.60, 143.55, 142.8, 138.1, 48.7, 26.8, 21.7. **MS**: calcd for C<sub>11</sub>H<sub>7</sub>F<sub>5</sub>N<sub>3</sub><sup>+</sup> Expect: 276.18 Found 276.0 (M<sup>+</sup>) calcd for PF<sub>6</sub><sup>-</sup> Expect: -144.96 Found: -145.0. **IR**: (neat) 3156, 1710, 1604, 1525, 1295, 1075, 997, 869, 831 cm<sup>-1</sup>.



**(R)-5-benzyl-2-(perfluorophenyl)-6,7-dihydro-5H-pyrrolo[2,1-c][1,2,4]triazol-2-ium hexafluorophosphate(V) (30)**

149 mg of light brown solid (79% yield from 136mg of SM). *r<sub>f</sub>* = 0.1 (50% EtOAc/Hexane)

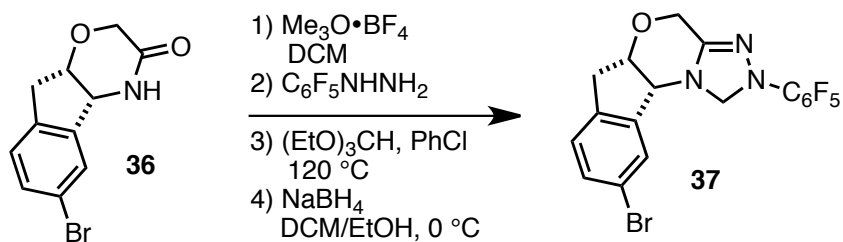
**<sup>1</sup>H-NMR** (300 MHz; acetone-*d*<sub>6</sub>): δ 10.02 (s, 1H), 7.41-7.39 (m, 5H), 5.51-5.46 (m, 1H), 3.58 (dd, *J* = 13.8, 7.3 Hz, 1H), 3.44 (m, 3H), 3.19-3.12 (m, 1H), 2.92-2.85 (m, 1H). **<sup>13</sup>C-NMR**: (101 MHz; acetone): δ 164.4, 142.82, 142.80, 135.5, 129.3, 129.10, 128.98, 127.6, 63.4, 39.2, 32.8, 21.4. **MS**: calcd for C<sub>18</sub>H<sub>14</sub>F<sub>5</sub>N<sub>3</sub><sup>+</sup> Expect: 366.31 Found: 366.10 (M<sup>+</sup>) calcd for PF<sub>6</sub><sup>-</sup> Expect: -144.96 Found: -145.0. **IR**: (neat) 3139, 1600, 1544, 1513, 1490, 1457, 1377, 1217, 1072, 1004, 838 cm<sup>-1</sup>. [*α*]<sub>D</sub><sup>23</sup> = -7.10 (c = 3.1, acetone)



**(5a*S*,10b*R*)-2-(perfluorophenyl)-4,5a,6,10b-tetrahydroindeno[2,1-*b*][1,2,4]triazolo[4,3-*d*][1,4]oxazin-2-ium hexafluorophosphate(V) (31)**

111 mg of white solid (59% yield from 139 mg of SM). rf = 0.1 (50% EtOAc/Hexane)

**<sup>1</sup>H-NMR** (300 MHz; acetone-d<sub>6</sub>): δ 11.33 (s, 1H), 7.63 (d, *J* = 7.5 Hz, 1H), 7.45 (dd, *J* = 6.7, 0.5 Hz, 2H), 7.37-7.35 (m, 1H), 6.38 (d, *J* = 3.9 Hz, 1H), 5.44 (d, *J* = 16.5 Hz, 1H), 5.27 (d, *J* = 16.5 Hz, 1H), 5.21 (d, *J* = 4.7 Hz, 1H), 3.56 (dd, *J* = 17.3, 5.3 Hz, 1H), 3.31 (d, *J* = 17.1 Hz, 1H). **<sup>13</sup>C-NMR**(101 MHz; acetone): δ 151.8, 146.19, 146.18, 140.9, 135.1, 129.7, 127.2, 125.6, 125.0, 124.2, 77.3, 62.6, 59.9, 37.0. **MS**: calcd for C<sub>18</sub>H<sub>11</sub>F<sub>5</sub>N<sub>3</sub>O<sup>+</sup> Expect 380.29 Found 380.30 (M<sup>+</sup>) calcd for PF<sub>6</sub><sup>-</sup> Expect: -144.96 Found -145.0. **IR**: (neat) 2913, 1627, 1502, 1459, 1429, 1337, 1311, 1297, 1280, 1147, 1098, 1064, 1053, 973 cm<sup>-1</sup>. **[α]<sub>D</sub><sup>23</sup>** = -141.11 (c = 3.6, acetone)



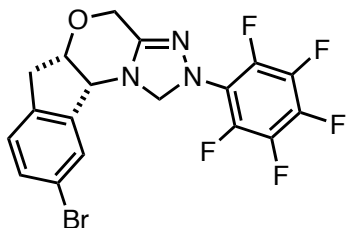
Synthesis of 37.

Bromolactam **36** (2.09 g, 7.81 mmol, 1 equiv.), prepared according to Bode,<sup>2</sup> is dissolved in CH<sub>2</sub>Cl<sub>2</sub> (40 mL) in a dry flask 100mL round-bottom flask. Trimethyloxonium tetrafluoroborate (1.15g, 7.81 mmol, 1 equiv.) is added, the flask is flushed with Ar, and the reaction is stirred at room temperature overnight. After aliquot NMR indicates complete consumption of starting material, pentafluorophenylhydrazine (1.55 g, 7.81 mmol, 1 equiv.) is added and the reaction is stirred overnight. The reaction is monitored by aliquot NMR, and after completion CH<sub>2</sub>Cl<sub>2</sub> is removed by rotary evaporator. The crude hydrazide is then taken up in chlorobenzene (30 mL) and triethylorthoformate (5 mL) and the reaction is stirred at 120 °C for 2 days. After the reaction is determined to be complete by NMR, solvent and triethylorthoformate is removed in vacuo. The crude product is then dissolved in a 10:1 DCM/EtOH solution (30 mL) and cooled to 0 °C by ice-water bath. Sodium borohydride is added (295 mg, 7.81 mmol, 1 equiv.) and the reaction is stirred at 0°C for 5 hours. Water is added carefully, and after gas evolution has ceased, the reaction is extracted with DCM (2 X 30 mL). The organic layer is dried over MgSO<sub>4</sub>, filtered, and concentrated. The crude product is purified by flash column chromatography, eluting with 0 to 50% EtOAc/Hexane through basic alumina. Isolated 2.02g of a light brown solid (56% yield).<sup>3</sup>

---

<sup>2</sup> Hsieh, S.-Y.; Binanzer, M.; Kreituss, I.; Bode, J. W. *Chem. Commun.* **2012**, *48*, 8892-8894.

<sup>3</sup> Based upon: Vora, H. U.; Lathrop, S. P.; Reynolds, N. T.; Kerr, M. S.; Read de Alaniz, J.; Rovis, T. *Org. Synth.* **2010**, *87*, 350.

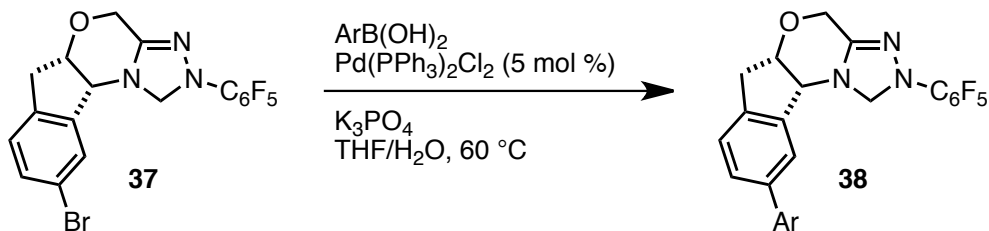


**(5a*S*,10b*R*)-9-bromo-2-(perfluorophenyl)-1,2,4,5a,6,10b-hexahydroindeno[2,1-*b*][1,2,4]triazolo[4,3-*d*][1,4]oxazine (37)**

2.02 g (56% yield) of light brown solid.  $r_f = 0.5$  (50% EtOAc/Hexane)

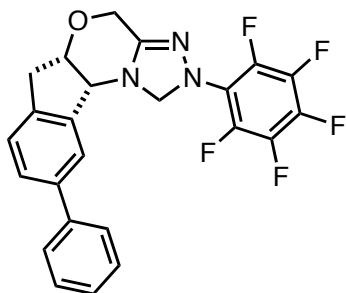
**$^1\text{H-NMR}$**  (400 MHz; acetone- $d_6$ ):  $\delta$  7.63 (dd,  $J = 0.8, 0.4$  Hz, 1H), 7.46 (dd,  $J = 8.1, 1.9$  Hz, 1H), 7.29 (d,  $J = 8.1$  Hz, 1H), 5.65 (t,  $J = 1.0$  Hz, 1H), 5.00 (t,  $J = 1.0$  Hz, 1H), 4.72 (d,  $J = 4.9$  Hz, 1H), 4.59 (d,  $J = 15.7$  Hz, 1H), 4.55 (d,  $J = 5.2$  Hz, 1H), 4.46 (d,  $J = 15.7$  Hz, 1H), 3.20 (d,  $J = 4.7$  Hz, 2H).  **$^{13}\text{C-NMR}$**  (101 MHz; acetone):  $\delta$  148.9, 143.7, 139.9, 131.2, 127.8, 127.1, 120.0, 77.1, 73.6, 62.2, 59.6, 35.1. **MS**: calcd for  $\text{C}_{18}\text{H}_{11}\text{BrF}_5\text{N}_3\text{O}$  Expect: 460.20 Found 462.0 (M+2H). **IR** (neat): 3273, 2916, 1698, 1653, 1521, 1471, 1402, 1324, 1247, 1215, 1075, 1026, 993  $\text{cm}^{-1}$ .  **$[\alpha]_D^{23}$**  = -81.8 ( $c = 1$ , acetone)

**General Procedure for Suzuki-Miyaura reaction with Triazolines.**



In a glove box, a dry 2-dram glass vial is loaded with  $\text{PdCl}_2(\text{PPh}_3)_2$  (7 mg, 0.01 mmol, 0.05 equiv.). The vial is sealed and removed from the glove box. To this vial is added triazoline (100 mg, 0.22 mmol, 1 equiv.), arylboronic acid (0.32 mmol, 1.5 equiv.) and potassium phosphate tribasic (93 mg, 0.44 mmol, 2 equiv.). Dry THF (1.5 mL) is added followed by water (0.5 mL), as well as a magnetic stir bar. The vial is sealed, secured with Teflon tape, and heated by oil bath at 60 °C for 6-12 h. Reaction is deemed complete by TLC. The reaction is cooled to rt and 1 mL of brine and 1 mL of EtOAc is added to the

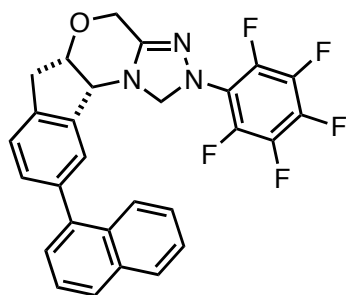
reaction. The aqueous fraction is removed, and the organic layer is dried over MgSO<sub>4</sub>. The crude reaction product is filtered and concentrated. The crude product is purified by flash column chromatography, eluting with 0 to 50% EtOAc/Hexanes through basic alumina.



**(5a*S*,10b*R*)-2-(perfluorophenyl)-9-phenyl-1,2,4,5a,6,10b-hexahydroindeno[2,1-*b*][1,2,4]triazolo[4,3-*d*][1,4]oxazine (38a)**

60 mg of dark brown solid (60% yield). *r<sub>f</sub>* = 0.5 (50% EtOAc/Hexane)

**<sup>1</sup>H-NMR** (300 MHz; acetone-*d*<sub>6</sub>): δ 7.70-7.60 (m, 4H), 7.47-7.35 (m, 4H), 5.68-5.67 (m, 1H), 5.04 (t, *J* = 1.1 Hz, 1H), 4.78 (dd, *J* = 5.6, 1.1 Hz, 1H), 4.64-4.55 (m, 2H), 4.47 (d, *J* = 15.6 Hz, 1H), 3.30-3.28 (m, 2H). **<sup>13</sup>C-NMR** (101 MHz; acetone-*d*<sub>6</sub>): δ 149.0, 141.6, 140.9, 140.3, 139.6, 129.82, 129.73, 128.49, 128.44, 128.38, 127.8, 127.25, 127.18, 127.16, 126.8, 125.6, 123.8, 123.2, 77.1, 73.6, 62.3, 59.2, 34.8. **MS** calcd for C<sub>24</sub>H<sub>16</sub>F<sub>5</sub>N<sub>3</sub>O: 457.4, found 458.1 (M+H). **IR**: (neat) 2914, 1626, 1504, 1479, 1429, 1340, 1307, 1055, 1039, 977 cm<sup>-1</sup>. **[α]<sub>D</sub><sup>23</sup>** = -39.17 (c = 2.4, acetone)



**(5a*S*,10b*R*)-9-(naphthalen-1-yl)-2-(perfluorophenyl)-1,2,4,5a,6,10b-hexahydroindeno[2,1-*b*][1,2,4]**

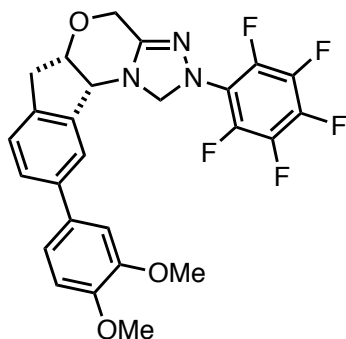
**triazolo[4,3-*d*][1,4]oxazine (38b)**

72 mg of light brown solid (64% yield). *r<sub>f</sub>* = 0.7 (50% EtOAc/Hexane)

**<sup>1</sup>H-NMR** (400 MHz; acetone-*D*<sub>6</sub>): δ 7.99-7.92 (m, 2H), 7.85 (d, *J* = 8.4 Hz, 1H), 7.58-7.42 (m, 7H), 5.60-5.60 (m, 1H), 5.00 (t, *J* = 1.1 Hz, 1H), 4.85-4.82 (m, 1H), 4.65 (d, *J* = 15.5 Hz, 2H),

4.49 (d, *J* = 15.6 Hz, 1H), 3.36 (s, 2H). **<sup>13</sup>C NMR** (101 MHz; acetone-*D*<sub>6</sub>): δ 149.1, 140.0, 139.7, 134.0, 131.6, 130.1, 128.3, 127.6, 126.9, 126.16, 126.06, 125.8, 125.55, 125.39, 125.2, 77.1, 62.3, 59.3, 35.2.

**MS** calcd for C<sub>28</sub>H<sub>18</sub>F<sub>5</sub>N<sub>3</sub>O: 507.45, Found: 508.20 (M+H) **IR:** (neat) 2913, 1700, 1503, 1428, 1338, 1312, 1247, 1105, 1039, 993, 800 cm<sup>-1</sup>. [**α**]<sub>D</sub><sup>23</sup> = -91.02 (c = 3.6, acetone)

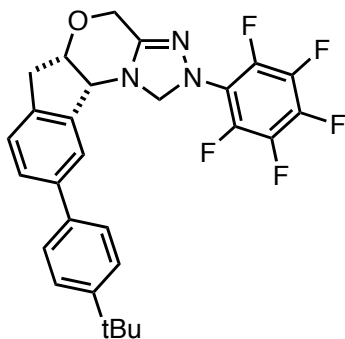


**(5a*S*,10b*R*)-9-(3,4-dimethoxyphenyl)-2-(perfluorophenyl)-1,2,4,5a,6,10b-hexahydroindeno[2,1-*b*][1,2,4]triazolo[4,3-*d*][1,4] oxazine (38c)**

74 mg of light brown solid (66% yield). *r<sub>f</sub>* = 0.5 (50% EtOAc/Hexane)

**<sup>1</sup>H-NMR** (400 MHz; acetone-*D*<sub>6</sub>): δ 7.66 (t, *J* = 0.8 Hz, 1H), 7.55 (dd, *J* = 7.9, 1.7 Hz, 1H), 7.37 (d, *J* = 7.9 Hz, 1H), 7.22 (d, *J* = 2.2 Hz, 1H), 7.18 (d, *J* = 2.2 Hz, 1H), 7.16 (d, *J* = 2.2 Hz, ), 7.01 (d, *J* = 8.3 Hz, 1H), 5.66 (m, 1H), 5.03 (t, *J* = 1.1 Hz, 1H), 4.77 (td, *J* = 5.8, 4.0 Hz, 1H), 4.61 (d, *J* = 15.5 Hz, 1H), 4.54 (d, *J* = 5.3 Hz, 1H), 4.46 (d, *J* = 15.6 Hz, 1H), 3.87 (s, 4H), 3.84 (s, 4H), 3.26 (dd, *J* = 11.9, 5.2 Hz, 2H). **<sup>13</sup>C-NMR** (101 MHz; acetone-*D*<sub>6</sub>): δ 180.4, 177.5, 149.2, 141.5, 140.3, 138.9, 133.8, 127.0, 125.5, 122.9, 119.2, 112.3, 111.1, 77.1, 73.5, 62.3, 59.2, 55.3, 34.8. **MS** calcd for

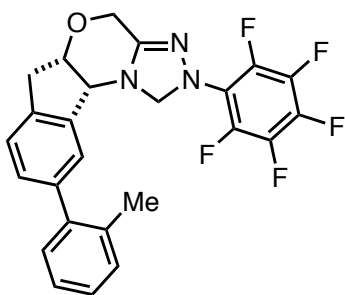
C<sub>26</sub>H<sub>20</sub>F<sub>5</sub>N<sub>3</sub>O<sub>3</sub> Expect: 517.45 Found 518.10 (M+H) IR: (neat) 2999, 2837, 1700, 1521, 1488, 1250, 1174, 1141, 1025, 993 cm<sup>-1</sup>. [α]<sub>D</sub><sup>23</sup> = -124.70 (c = 1.7g/mL, acetone)



**(5a*S*,10b*R*)-9-(4-(*tert*-butyl)phenyl)-2-(perfluorophenyl)-1,2,4,5a,6,10b-hexahydroindeno[2,1-*b*][1,2,4]triazolo[4,3-*d*][1,4]oxazine (38d)**

64 mg of brown solid (57% yield). rf = 0.5 (50% EtOAc/Hexane)

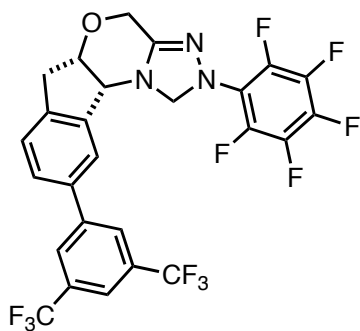
<sup>1</sup>H-NMR (400 MHz; acetone-d<sub>6</sub>): δ 7.67 (d, *J* = 0.8 Hz, 1H), 7.58-7.55 (m, 4H), 7.49 (td, *J* = 5.5, 2.0 Hz, 3H), 7.40 (s, 1H), 5.67 (d, *J* = 1.3 Hz, 1H), 5.04 (d, *J* = 1.1 Hz, 1H), 4.77 (s, 2H), 4.60 (d, *J* = 15.5 Hz, 1H), 4.54 (d, *J* = 5.3 Hz, 1H), 4.47-4.43 (m, 1H), 3.36 (d, *J* = 3.3 Hz, 1H), 3.26 (dd, *J* = 11.0, 5.2 Hz, 2H), 1.35 (s, 9H). <sup>13</sup>C-NMR (101 MHz; acetone): δ 150.0, 149.1, 141.6, 140.2, 139.3, 138.0, 127.1, 126.61, 126.43, 125.62, 125.58, 123.1, 77.1, 73.6, 62.3, 59.2, 34.9, 30.7. MS: calcd for C<sub>28</sub>H<sub>24</sub>F<sub>5</sub>N<sub>3</sub>O Expect: 513.40 Found 514.20 (M+H). IR: (neat) 2963, 2905, 1698, 1517, 1364, 1269, 1112, 1076, 993 cm<sup>-1</sup> [α]<sub>D</sub><sup>23</sup> = -99.50 (c =4, acetone)



**(5a*S*,10b*R*)-2-(perfluorophenyl)-9-(*o*-tolyl)-1,2,4,5a,6,10b-hexahydroindeno[2,1-*b*][1,2,4]triazolo[4,3-*d*][1,4]oxazine (38e)**

35 mg of red solid (67% yield).<sup>4</sup> *r*<sub>f</sub> = 0.5 (50% EtOAc/Hexanes)

**<sup>1</sup>H-NMR** (300 MHz; acetone-*d*<sub>6</sub>): δ 7.39-7.38 (m, 2H), 7.27-7.25 (m, 5H), 5.61 (d, *J* = 2.2 Hz, 1H), 5.00 (t, *J* = 1.1 Hz, 1H), 4.78 (q, *J* = 5.0 Hz, 1H), 4.62 (d, *J* = 15.6 Hz, 1H), 4.56 (d, *J* = 5.3 Hz, 1H), 4.46 (d, *J* = 15.6 Hz, 1H), 3.29 (t, *J* = 4.6 Hz, 2H), 2.24 (s, 3H). **<sup>13</sup>C-NMR** (101 MHz; acetone): δ 149.1, 141.7, 140.97, 140.89, 139.0, 135.0, 130.2, 129.6, 129.3, 127.2, 125.8, 125.3, 125.0, 77.0, 73.5, 62.2, 59.3, 35.0, 19.7  
**MS**: calcd for C<sub>25</sub>H<sub>18</sub>F<sub>5</sub>N<sub>3</sub>O Expect: 471.42 Found 472.10. **IR**: (neat) 2918, 1701, 1627, 1503, 1428, 1339, 1312, 1246, 1106, 1037, 974, 761. **[α]<sub>D</sub><sup>23</sup>** = -41.02 (*c* = 11.8, acetone)



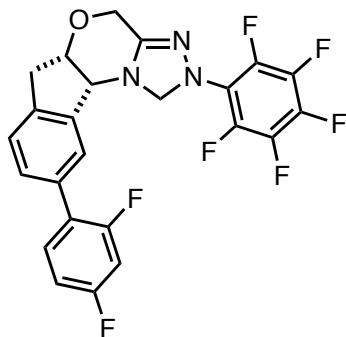
**(5a*S*,10b*R*)-9-(3,5-bis(trifluoromethyl)phenyl)-2-(perfluorophenyl)-1,2,4,5a,6,10b-hexahydroindeno[2,1-*b*][1,2,4]triazolo[4,3-*d*][1,4]oxazine (38f)**

41 mg of off-white solid (63% yield).<sup>3</sup> *r*<sub>f</sub> = 0.45 (50% EtOAc/Hexane)

**<sup>1</sup>H-NMR** (400 MHz; acetone-*D*<sub>6</sub>): δ 8.28 (s, 2H), 8.02-7.96 (m, 2H), 7.77 (dd, *J* = 7.9, 1.8 Hz, 1H), 7.52 (d, *J* = 7.8 Hz, 1H), 5.69 (dd, *J* = 2.3, 1.3 Hz, 1H), 5.00 (dt, *J* = 2.2, 1.1 Hz, 1H), 4.80 (td, *J* = 5.6, 4.2 Hz, 1H), 4.65-4.46 (m, 4H), 3.33 (dd, *J* = 7.3, 5.0 Hz, 2H). **<sup>13</sup>C NMR** (101 MHz; acetone-*D*<sub>6</sub>): δ 149.0, 143.5, 142.2, 141.6, 137.1, 131.8, 127.9, 127.56, 127.53, 126.1, 123.9, 120.67, 120.63, 120.61, 77.1, 73.7, 62.4,

<sup>4</sup> Reaction performed with 50mg of triazolone starting material.

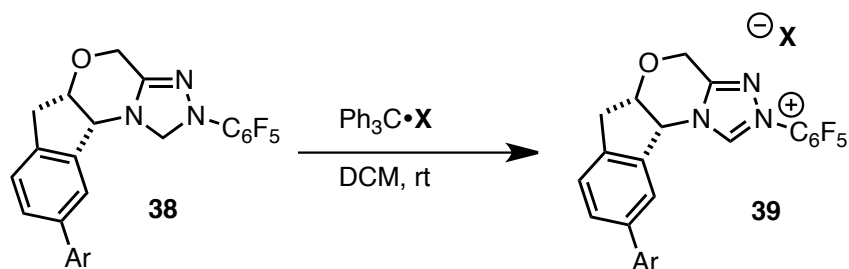
59.3, 35.0 **MS**: calcd for C<sub>26</sub>H<sub>14</sub>F<sub>11</sub>N<sub>3</sub>O Expect: 593.39 Found: 594.10 (M+H). **IR**: (neat) 2971, 2348, 1625, 1523, 1505, 1379, 1280, 1183, 1126, 1039 cm<sup>-1</sup>. [ $\alpha$ ]<sub>D</sub><sup>23</sup> = -66.06 (c = 2.3, acetone)



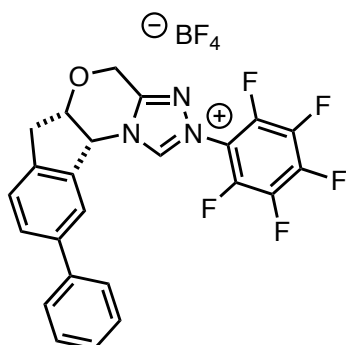
**(5a*S*,10b*R*)-9-(2,4-difluorophenyl)-2-(perfluorophenyl)-1,2,4,5a,6,10b-hexahydroindeno[2,1-b][1,2,4]triazolo[4,3-*d*][1,4]oxazine (38g)**

26 mg of light orange solid (48% yield).<sup>3</sup> rf = 0.5 (50% EtOAc/Hexane)

**<sup>1</sup>H-NMR** (300 MHz; acetone-d<sub>6</sub>):  $\delta$  7.60 (s, 2H), 7.45 (d, *J* = 3.6 Hz, 2H), 7.16-7.10 (m, 2H), 5.62 (d, *J* = 2.0 Hz, 1H), 5.02 (t, *J* = 1.0 Hz, 1H), 4.79 (q, *J* = 5.0 Hz, 1H), 4.65-4.57 (m, 2H), 4.47 (d, *J* = 15.6 Hz, 1H), 3.31-3.28 (m, 2H). **<sup>13</sup>C-NMR** (101 MHz; acetone-d<sub>6</sub>):  $\delta$  149.7, 149.2, 141.5, 140.3, 138.9, 133.8, 127.0, 125.5, 122.9, 119.2, 112.28, 112.25, 111.1, 110.8, 77.1, 73.6, 62.3, 59.2, 55.30, 55.28, 55.26, 34.8 **MS** calcd for C<sub>24</sub>H<sub>14</sub>F<sub>7</sub>N<sub>3</sub>O Expect: 493.38 Found 494.10 (M+H) **IR** (neat) 2937, 2837, 1700, 1504, 1465, 1335, 1249, 1174, 1141, 1026, 992 cm<sup>-1</sup>. [ $\alpha$ ]<sub>D</sub><sup>23</sup> = -82 (c = 2.0, acetone)



Elaborated Triazolines were oxidized according to the general method described earlier.

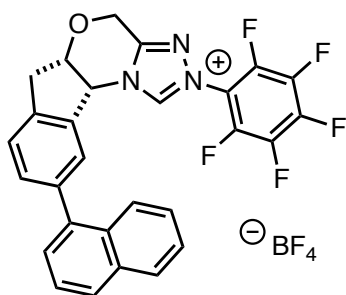


**(5a*S*,10b*R*)-2-(perfluorophenyl)-9-phenyl-4,5a,6,10b-tetrahydroindeno[2,1-*b*][1,2,4]triazolo[4,3-*d*][1,4]oxazin-2-ium tetrafluoroborate (39a)**

46 mg of off-white solid (65% yield). *r<sub>f</sub>* = 0.1 (50% EtOAc/Hexane)

**<sup>1</sup>H-NMR** (400 MHz; acetone-*d*<sub>6</sub>): δ 11.32 (s, 1H), 7.88 (s, 1H), 7.72 (d, *J* = 7.9 Hz, 1H), 7.64 (d, *J* = 7.4 Hz, 2H), 7.54 (d, *J* = 7.9 Hz, 1H), 7.43 (d, *J* = 7.9 Hz, 2H), 7.36 (d, *J* = 7.3 Hz, 1H), 6.42 (d, *J* = 4.2 Hz, 1H), 5.43 (d, *J* = 16.4 Hz, 1H), 5.31-5.24 (m, 2H), 3.60 (dd, *J* = 17.2, 5.1 Hz, 1H), 3.35 (d, *J* = 17.2 Hz, 1H). **<sup>13</sup>C-NMR** (101 MHz; acetone): δ 151.7, 144.1, 140.5, 140.0, 136.0, 129.3, 128.9, 128.4, 127.5, 126.9, 126.0, 122.9, 77.6, 62.6, 60.0, 36.7 **MS** calcd for C<sub>24</sub>H<sub>15</sub>F<sub>5</sub>N<sub>3</sub>O<sup>+</sup> Expect: 456.39 Found: 456.1(M<sup>+</sup>).

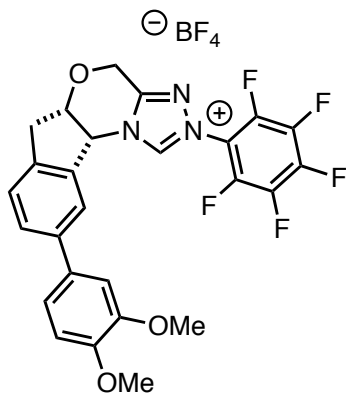
**IR:** (neat) 3061, 1699, 1595, 1550, 1529, 1518, 1481, 1250, 1075, 1004 cm<sup>-1</sup> [**α**]<sub>D</sub><sup>23</sup> = -73 (c = 2.0, acetone)



**(5a*S*,10b*R*)-9-(naphthalen-1-yl)-2-(perfluorophenyl)-4,5a,6,10b-tetrahydroindeno[2,1-*b*][1,2,4]triazolo[4,3-*d*][1,4]oxazin-2-ium tetrafluoroborate (39b)**

44 mg of off-white solid (37% yield). *r<sub>f</sub>* = 0.1 (50% EtOAc/Hexane)

**<sup>1</sup>H-NMR** (400 MHz; acetone-*d*<sub>6</sub>): δ 11.27 (s, 1H), 8.00-7.94 (m, 2H), 7.82-7.80 (m, 1H), 7.74 (s, 1H), 7.63 (d, *J* = 7.7 Hz, 1H), 7.54 (td, *J* = 7.9, 1.4 Hz, 3H), 7.47-7.39 (m, 3H), 6.49 (d, *J* = 4.1 Hz, 1H), 5.46 (d, *J* = 16.4 Hz, 1H), 5.33-5.29 (m, 2H), 3.68 (m, 1H), 3.44-3.41 (m, 1H). **<sup>13</sup>C-NMR** (101 MHz; acetone): δ 151.8, 140.06, 139.94, 139.3, 135.6, 134.0, 131.43, 131.37, 129.3, 128.53, 128.35, 127.9, 127.0, 126.3, 125.9, 125.66, 125.60, 125.41, 122.4, 77.6, 62.7, 60.1, 36.9. **MS** calcd for C<sub>28</sub>H<sub>17</sub>F<sub>5</sub>N<sub>3</sub>O<sup>+</sup> Expect: 506.45; Found: 506.1 (M<sup>+</sup>). **IR** (neat) 3058, 1698, 1594, 1550, 1529, 1482, 1394, 1250, 1075, 1003, 861, 800, 780 cm<sup>-1</sup>. **[α]<sub>D</sub><sup>23</sup>** = -67.86 (*c* = 2.8, acetone)

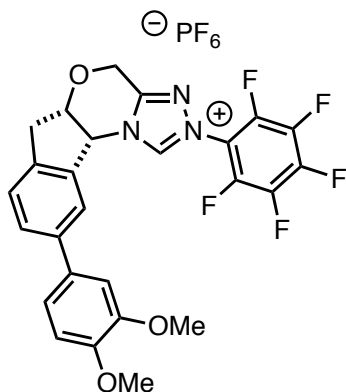


**(5a*S*,10b*R*)-9-(3,4-dimethoxyphenyl)-2-(perfluorophenyl)-4,5a,6,10b-tetrahydroindeno[2,1-*b*][1,2,4]triazolo[4,3-*d*][1,4]oxazin-2-ium tetrafluoroborate (39c)**

91 mg of light brown solid (99% yield). *r<sub>f</sub>* = 0.1 (50% EtOAc/Hexane)

**<sup>1</sup>H-NMR** (300 MHz; acetone-*d*<sub>6</sub>): δ 7.83 (s, 1H), 7.71-7.68 (m, 1H), 7.51-7.48 (m, 1H), 7.31-7.16 (m, 5H), 7.01 (d, *J* = 8.3 Hz, 1H), 6.40-6.39 (m, 1H), 5.43 (d, *J* = 16.4 Hz, 1H), 5.31-5.23 (m, 2H), 3.58 (dd, *J* = 17.1, 4.5 Hz, 1H), 3.33 (d, *J* = 17.2 Hz, 1H). **<sup>13</sup>C-NMR** (101 MHz; acetone): δ 151.6, 149.8, 149.4, 140.5, 139.2, 135.8, 133.0, 129.3, 128.22, 128.05, 126.2, 125.8, 122.4, 119.2, 112.2, 110.9, 77.6, 62.6, 59.9,

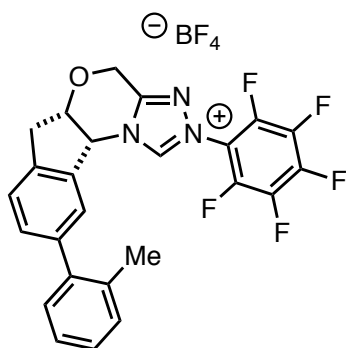
55.3, 36.7 **MS**: calcd for  $C_{26}H_{19}F_5N_3O_3^+$  Expect 516.41 Found: 516.10 (M+) **IR** (neat) 3060, 2944, 1669, 1595, 1518, 1489, 1320, 1250, 1174, 1142, 1075, 1023, 864  $cm^{-1}$ .  $[\alpha]_D^{23} = -84.70$  (c = 1.7, acetone)



**(5a*S*,10b*R*)-9-(3,4-dimethoxyphenyl)-2-(perfluorophenyl)-4,5a,6,10b-tetrahydroindeno[2,1-*b*][1,2,4]triazolo[4,3-*d*][1,4]oxazin-2-ium hexafluorophosphate (39d)**

46 mg of light brown solid (58% yield). *r<sub>f</sub>* = 0.1 (50% EtOAc/Hexane)

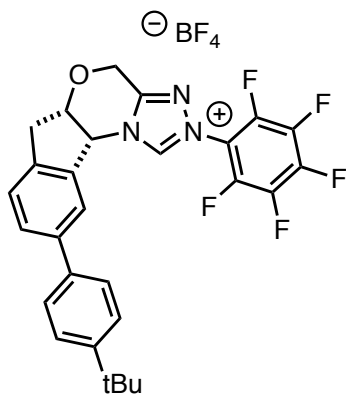
**<sup>1</sup>H-NMR** (300 MHz; acetone-*d*<sub>6</sub>): δ 11.63 (bs, 1H), 7.84 (s, 1H), 7.71-7.68 (m, 1H), 7.52-7.49 (m, 1H), 7.21-7.14 (m, 2H), 7.02 (d, *J* = 8.3 Hz, 1H), 6.42-6.41 (m, 1H), 5.44 (d, *J* = 16.4 Hz, 1H), 5.32-5.24 (m, 2H), 3.86 (s, 3H), 3.84 (s, 3H), 3.58 (dd, *J* = 16.7, 4.6 Hz, 1H), 3.33 (dd, *J* = 16.9, 0.6 Hz, 1H). **<sup>13</sup>C-NMR** (101 MHz; acetone): δ 166.8, 144.5, 140.5, 139.2, 135.7, 134.6, 133.0, 130.2, 128.9, 128.18, 128.07, 125.9, 122.5, 119.2, 118.3, 112.2, 111.1, 77.6, 62.6, 59.9, 55.34, 55.30, 36.7 **MS**: calcd for  $C_{26}H_{19}F_5N_3O_3^+$  Expect 516.41 Found: 516.10 (M+) calcd for  $PF_6^-$  Expect: -144.96 Found -145.00 (M-).



**(5a*S*,10b*R*)-2-(perfluorophenyl)-9-(*o*-tolyl)-4,5a,6,10b-tetrahydroindeno[2,1-*b*][1,2,4]triazolo[4,3-*d*][1,4]oxazin-2-ium tetrafluoroborate (39e)**

62 mg of light rusty-brown solid (99% yield). rf = 0.1 (50% EtOAc/Hexane)

<sup>1</sup>H-NMR (300 MHz; aceton-d<sub>6</sub>): δ 7.58-7.52 (m, 2H), 7.41-7.38 (m, 1H), 7.28-7.26 (m, 3H), 7.16 (dd, *J* = 2.5, 0.6 Hz, 1H), 6.45-6.43 (m, 1H), 5.45 (d, *J* = 16.4 Hz, 1H), 5.32-5.25 (m, 2H), 3.62 (dd, *J* = 17.0, 5.0 Hz, 1H), 3.37 (d, *J* = 17.2 Hz, 1H), 2.20 (s, 3H). <sup>13</sup>C-NMR (101 MHz; acetone): δ 151.7, 141.3, 139.4, 135.4, 135.1, 130.54, 130.35, 129.6, 129.3, 128.2, 127.5, 125.9, 125.4, 124.8, 77.6, 62.6, 60.0, 36.8, 19.6  
MS calcd for C<sub>25</sub>H<sub>17</sub>F<sub>5</sub>N<sub>3</sub>O<sup>+</sup> Expect: 470.41 Found 470.1 IR: (neat) 3059, 1698, 1594, 1550, 1528, 1517, 1479, 1249, 1074, 1002, 858 cm<sup>-1</sup>. [α]<sub>D</sub><sup>23</sup> = -75.79 (c = 1.9, acetone)

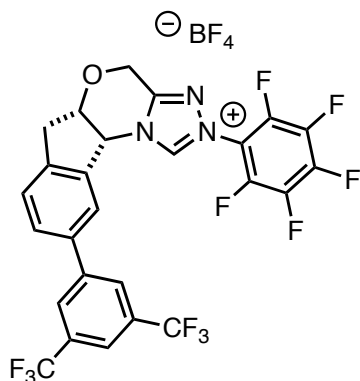


**(5a*S*,10b*R*)-9-(4-(*tert*-butyl)phenyl)-2-(perfluorophenyl)-4,5a,6,10b-tetrahydroindeno[2,1-*b*][1,2,4]triazolo[4,3-*d*][1,4]oxazin-2-ium tetrafluoroborate (39f)**

58 mg of light brown solid (80% yield). rf = 0.15 (50% EtOAc/Hexane)

<sup>1</sup>H-NMR (300 MHz; aceton-d<sub>6</sub>): δ 7.86 (s, 1H), 7.70 (dd, *J* = 7.8, 0.9 Hz, 1H), 7.58-7.47 (m, 4H), 7.28-7.14 (m, 1H), 6.42 (s, 1H), 5.44 (d, *J* = 16.4 Hz, 1H), 5.32-5.25 (m, 2H), 3.59 (dd, *J* = 17.3, 5.2 Hz, 1H), 3.37-3.31 (m, 2H), 1.33 (s, 9H). <sup>13</sup>C-NMR (101 MHz; acetone): δ 151.7, 140.5, 139.6, 137.4, 135.9, 134.2, 133.9, 133.7, 132.0, 131.6, 130.5, 129.3, 128.24, 128.21, 126.9, 126.6, 125.9, 125.7, 122.8, 77.6, 62.6,

59.9, 36.7, 30.7 **MS**: calcd for C<sub>28</sub>H<sub>23</sub>F<sub>5</sub>N<sub>3</sub>O Expect: 512.49 Found: 512.2 **IR**: (neat) 2963, 1595, 1550, 1529, 1483, 1075, 1004, 804 cm<sup>-1</sup>. [ $\alpha$ ]<sub>D</sub><sup>23</sup> = -66.67 (c = 1.2, acetone)

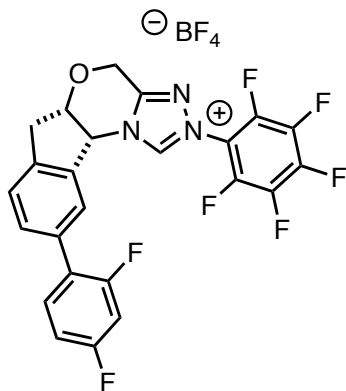


**(5a*S*,10b*R*)-9-(3,5-bis(trifluoromethyl)phenyl)-2-(perfluorophenyl)-4,5a,6,10b-tetrahydroindeno[2,1-*b*][1,2,4]triazolo[4,3-*d*][1,4]oxazin-2-ium tetrafluoroborate (39g)**

60 mg of light brown solid (80% yield).<sup>5</sup> rf = 0.1 (50% EtOAc/Hexane)

**<sup>1</sup>H-NMR** (400 MHz; acetone-D<sub>6</sub>):  $\delta$  11.29 (br s, 1H), 8.24 (s, 2H), 8.07 (s, 1H), 8.04 (d,  $J$  = 0.7 Hz, 1H), 7.92-7.90 (m, 1H), 7.65 (d,  $J$  = 7.9 Hz, 1H), 7.31-7.29 (m, 1H), 7.24-7.14 (m, 1H), 6.46 (d,  $J$  = 4.2 Hz, 1H), 5.43 (d,  $J$  = 16.4 Hz, 1H), 5.32-5.28 (m, 2H), 3.69-3.63 (m, 1H), 3.39 (d,  $J$  = 17.4 Hz, 1H). **<sup>13</sup>C-NMR** (101 MHz; acetone-D<sub>6</sub>):  $\delta$  151.5, 142.9, 141.9, 137.2, 136.5, 132.0, 131.7, 129.26, 129.06, 128.2, 128.0, 127.52, 127.50, 127.47, 126.4, 126.2, 123.6, 122.2, 121.01, 120.97, 77.6, 62.5, 60.0, 36.9. **MS** calcd for C<sub>26</sub>H<sub>13</sub>F<sub>11</sub>N<sub>3</sub>O<sup>+</sup>: 592.38, found: 592.1 (M<sup>+</sup>). **IR**: (neat) 3098, 1700, 1596, 1529, 1518, 1378, 1320, 1180, 1134, 1076, 1004 cm<sup>-1</sup>. [ $\alpha$ ]<sub>D</sub><sup>23</sup> = -138.52 (c = 2.7, acetone)

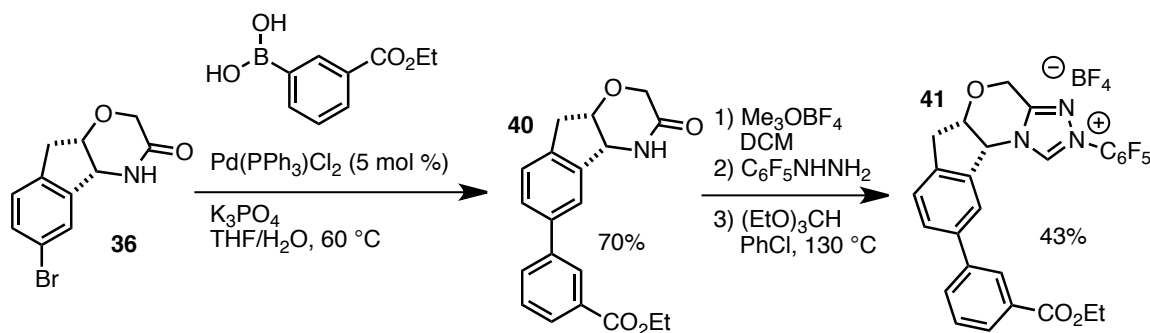
<sup>5</sup> Alternative purification was used: Solvent is removed by rotary evaporator. The crude product is dissolved in minimal amount of Et<sub>2</sub>O and the triazolium salt is precipitated by addition of hexanes. Filtration through filter paper yields the desired compound.



**(5aS,10bR)-9-(2,4-difluorophenyl)-2-(perfluorophenyl)-4,5a,6,10b-tetrahydroindeno[2,1-b][1,2,4]triazolo[4,3-d][1,4]oxazin-2-ium tetrafluoroborate (39h)**

53 mg of light purple solid (65% yield). rf = 0.1 (50% EtOAc/Hexane)

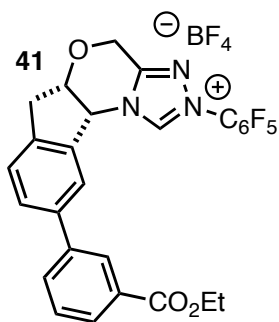
**<sup>1</sup>H-NMR** (400 MHz; acetone-D<sub>6</sub>): δ 11.23 (br s, 1H), 7.77 (t, *J* = 0.4 Hz, 1H), 7.61-7.55 (m, 3H), 7.15-7.10 (m, 2H), 6.42 (d, *J* = 4.2 Hz, 1H), 5.43 (d, *J* = 16.4 Hz, 1H), 5.29 (dd, *J* = 16.3, 0.3 Hz, 1H), 5.26 (d, *J* = 4.3 Hz, 1H), 3.64-3.59 (m, 1H), 3.38-3.34 (m, 1H). **<sup>13</sup>C-NMR** (101 MHz; acetone-D<sub>6</sub>): δ 163.7, 151.7, 146.3, 140.6, 135.9, 134.2, 132.23, 132.19, 132.14, 132.09, 130.47, 130.43, 129.3, 128.2, 126.2, 125.7, 124.78, 124.76, 111.97, 111.93, 111.76, 111.72, 104.1, 103.8, 77.5, 62.5, 60.0, 36.8. **MS** calcd for C<sub>24</sub>H<sub>13</sub>F<sub>7</sub>N<sub>3</sub>O<sup>+</sup>: 492.37, found: 492.1 (M<sup>+</sup>). **IR**: (neat) 3648, 3095, 2361, 2341, 1596, 1529, 1516, 1484, 1268, 1076, 1004, 856 cm<sup>-1</sup> [α]<sub>D</sub><sup>23</sup> = -78.71 (c = 1.7, acetone)



Synthesis of **41** via **40**

To a dry, 2 dram glass vial is added lactam **36** (166mg, 0.62 mmol, 1 equiv.), boronic acid (180 mg, 0.93 mmol, 1.5 equiv.), Pd(PPh<sub>3</sub>)<sub>2</sub>Cl<sub>2</sub> (21 mg, 0.03mmol, 0.05 equiv.), and potassium phosphate (263 mg, 1.24 mmol, 2 equiv.). An argon atmosphere is introduced, and 3 ml of tetrahydrofuran/water solution (3:1 v/v) is added. The vial is sealed, the cap is wrapped with Teflon tape, and heated at 60 °C for 5 hours. The reaction is cooled to room temperature and diluted with ethyl acetate (2 mL). The reaction mixture is washed with brine (2 x 1 mL) and the organic phase is dried over MgSO<sub>4</sub>. The drying agent is filtered off, washed with ethyl acetate, and concentrated by rotary evaporator. The crude product is purified by column chromatography, eluting with 50% ethyl acetate/hexane through silica gel. Isolated 146 mg (70%) of a light brown solid.

In a dry, 10 mL round bottom flask, 146 mg of **40** (0.43 mmol, 1 equiv) is dissolved in 3 mL of DCM. Trimethyloxonium tetrafluoroborate (63 mg, 0.43 mmol, 1 equiv) is added and the reaction is stirred at room temperature for 6 h. Upon visual disappearance of solids in the reaction mixture, pentafluorophenylhydrazine (85 mg, 0.43 mmol, 1 equiv.) is added and the reaction is stirred overnight at room temperature. Product formation is determined by aliquot NMR. Solvent is removed in vacuo and 1 ml of triethylorthoformate and 2 ml of chlorobenzene is added. A reflux condenser is attached and the reaction is stirred at 130 °C for 2 days. The solvent is removed by rotary evaporator and the crude product is purified by column chromatography, eluting with 10%MeOH/DCM through silica gel. Isolated 114 mg of a red solid (43% yield).

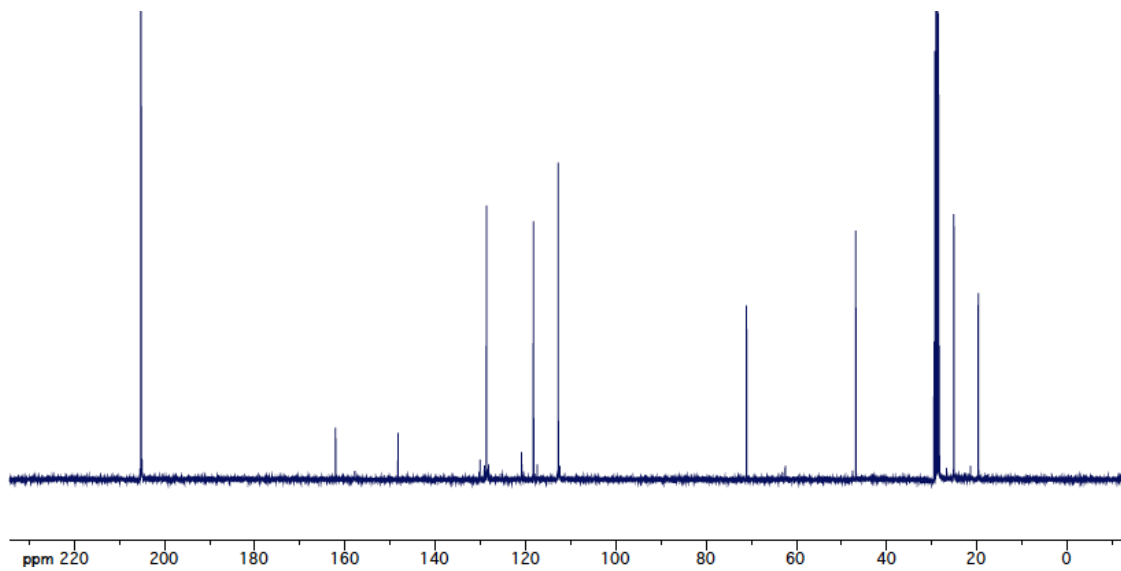
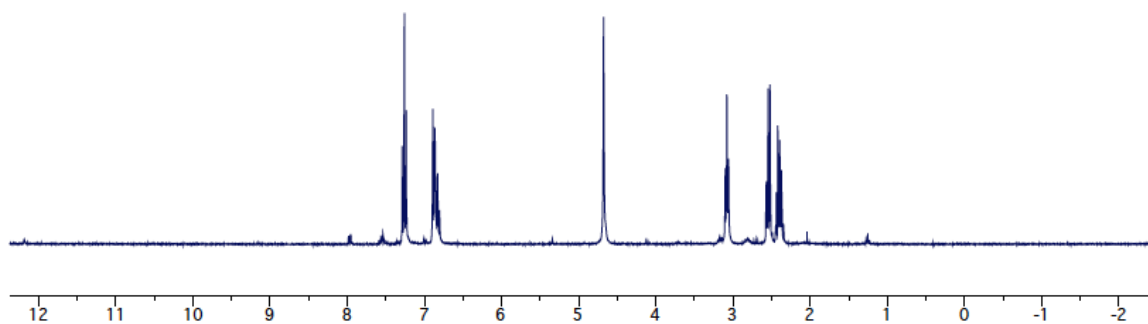
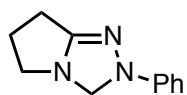


**(5a*S*,10b*R*)-9-(3-(ethoxycarbonyl)phenyl)-2-(perfluorophenyl)-4,5a,6,10b-tetrahydroindeno[2,1-*b*][1,2,4]triazolo[4,3-*d*][1,4]oxazin-2-ium tetrafluoroborate (41)**

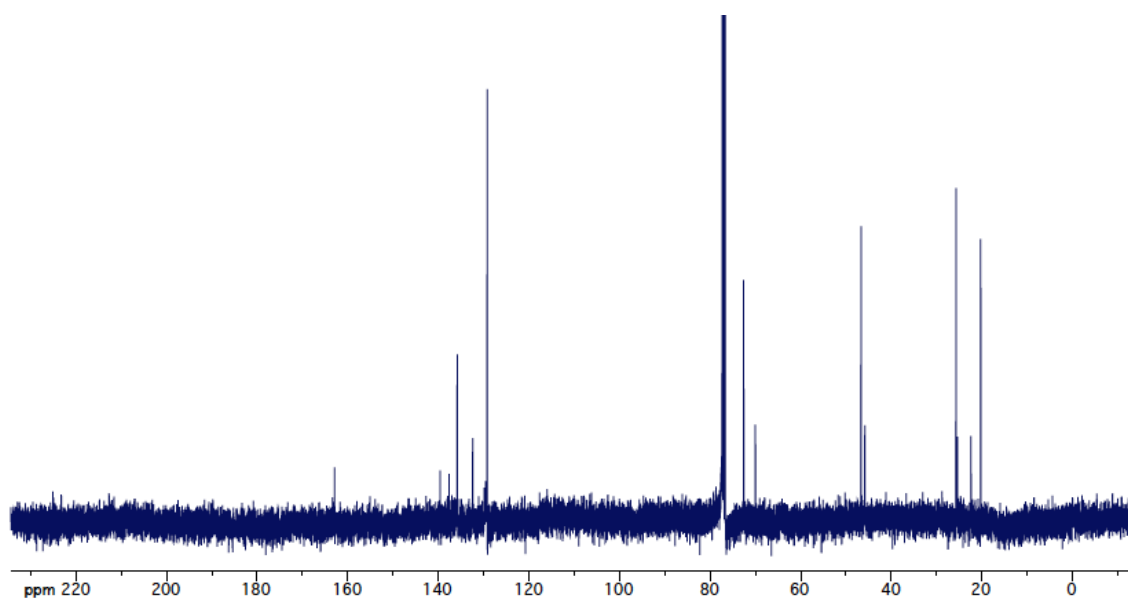
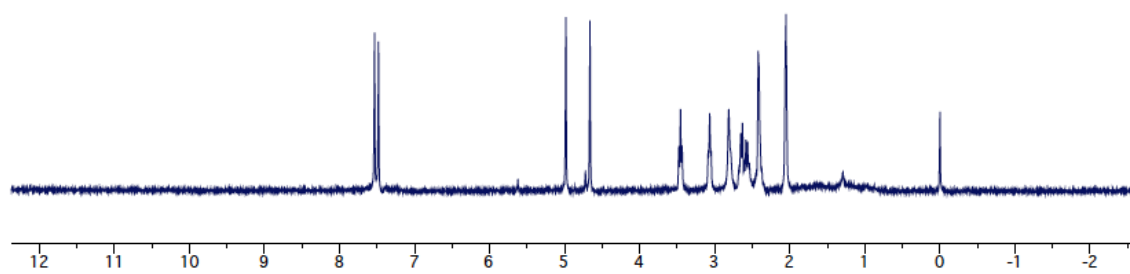
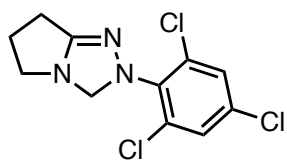
114 mg of red solid (43% yield).  $r_f = 0.2$  (50% EtOAc/Hexane)

**<sup>1</sup>H-NMR** (400 MHz; acetone-*d*<sub>6</sub>):  $\delta$  11.33 (s, 1H), 8.22 (t,  $J = 1.7$  Hz, 1H), 8.01-7.99 (m, 2H), 7.94-7.91 (m, 2H), 7.76 (d,  $J = 7.9$  Hz, 1H), 7.59 (t,  $J = 7.6$  Hz, 2H), 6.44 (d,  $J = 4.0$  Hz, 1H), 5.73 (s, 1H), 5.41 (s, 1H), 5.30 (d,  $J = 16.6$  Hz, 2H), 4.38 (t,  $J = 7.1$  Hz, 2H), 3.65-3.59 (m, 1H), 3.36 (d,  $J = 17.3$  Hz, 1H), 1.37 (t,  $J = 7.0$  Hz, 3H). **<sup>13</sup>C NMR** (101 MHz; acetone):  $\delta$  165.7, 151.6, 146.4, 140.65, 140.59, 139.4, 136.2, 131.6, 131.3, 129.3, 128.6, 128.3, 127.54, 127.49, 126.2, 123.1, 77.6, 62.6, 60.7, 60.0, 36.8, 13.67, 13.64. **MS** calcd for C<sub>27</sub>H<sub>19</sub>F<sub>5</sub>N<sub>3</sub>O<sub>3</sub><sup>+</sup> Expect: 528.45 Found: 528.20 (M<sup>+</sup>).

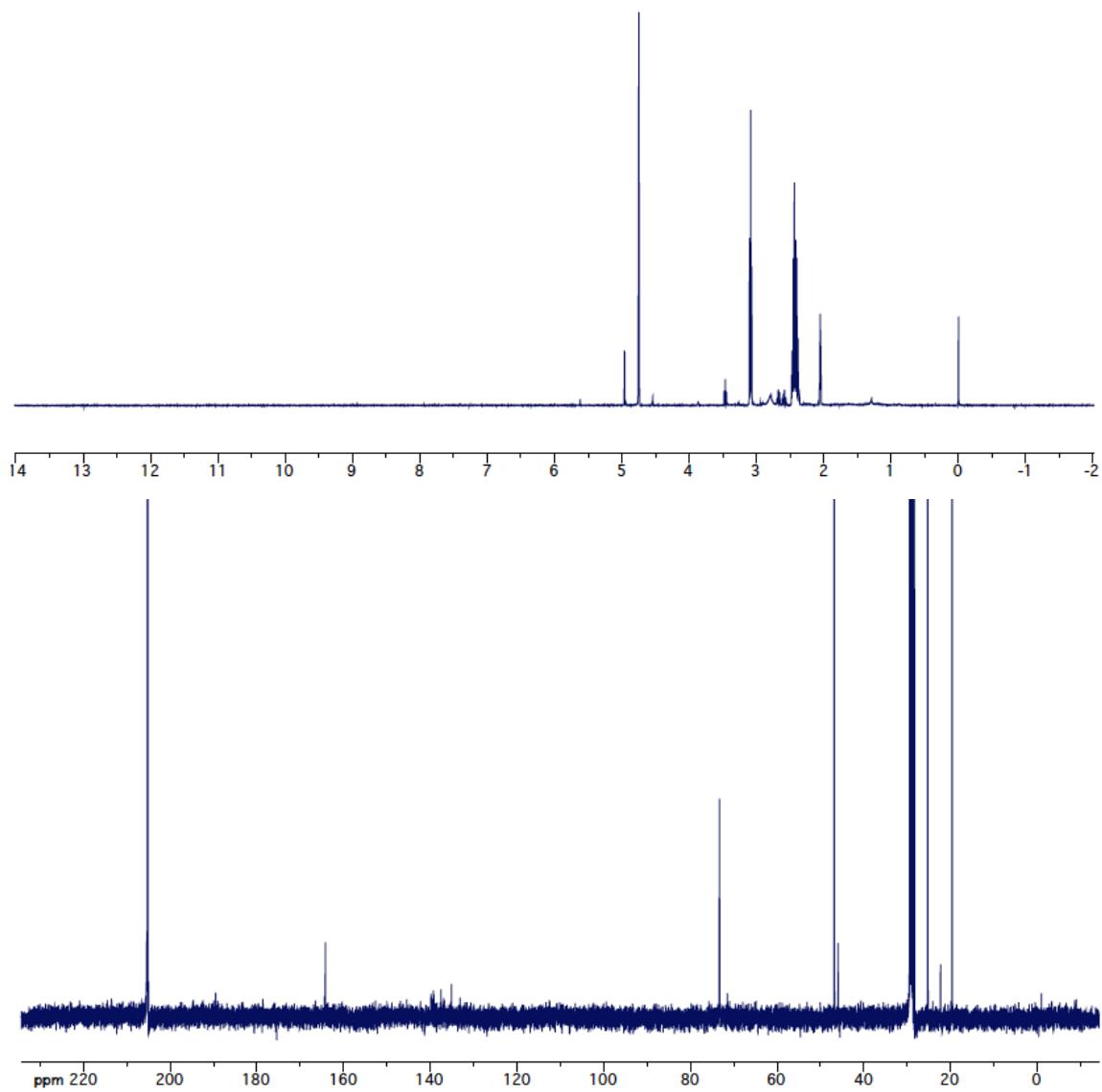
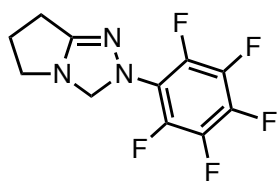
28a



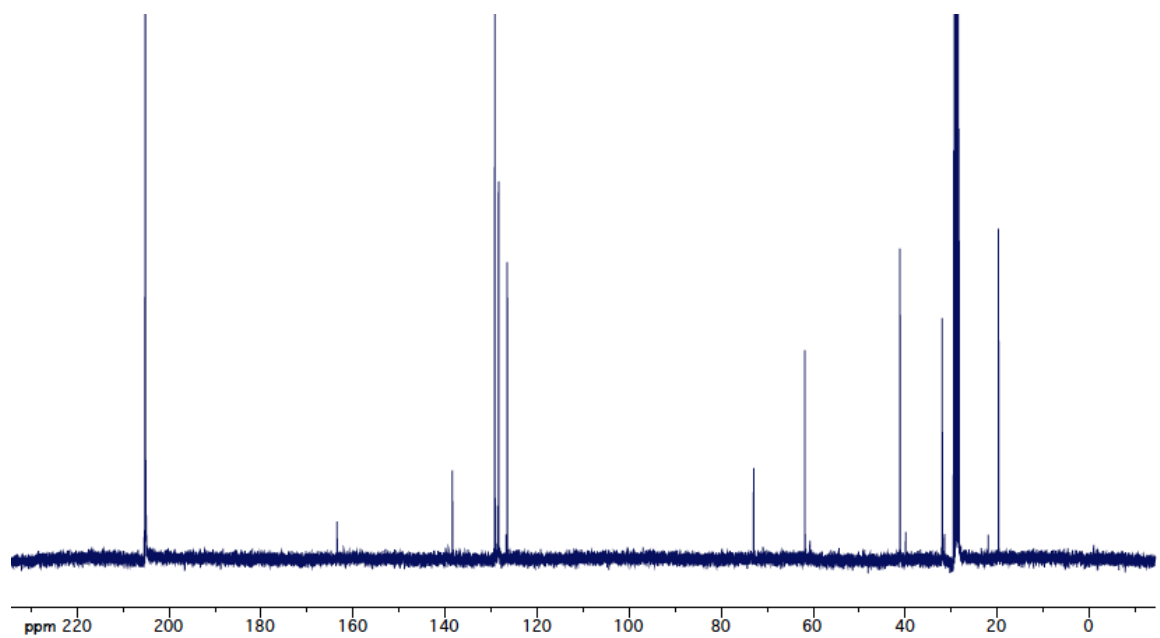
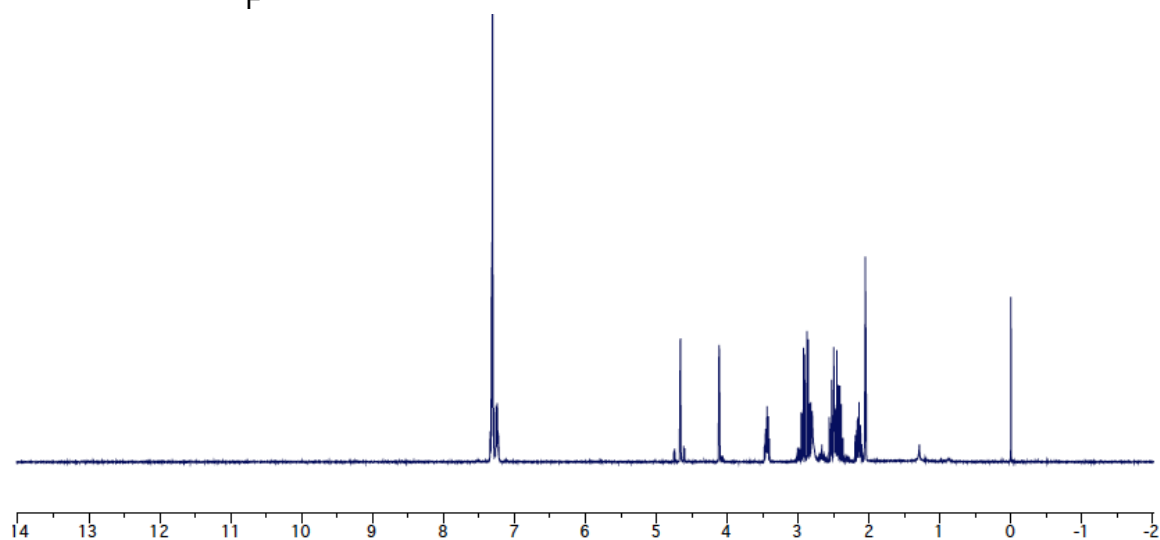
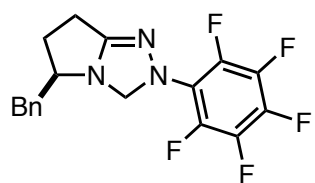
28e



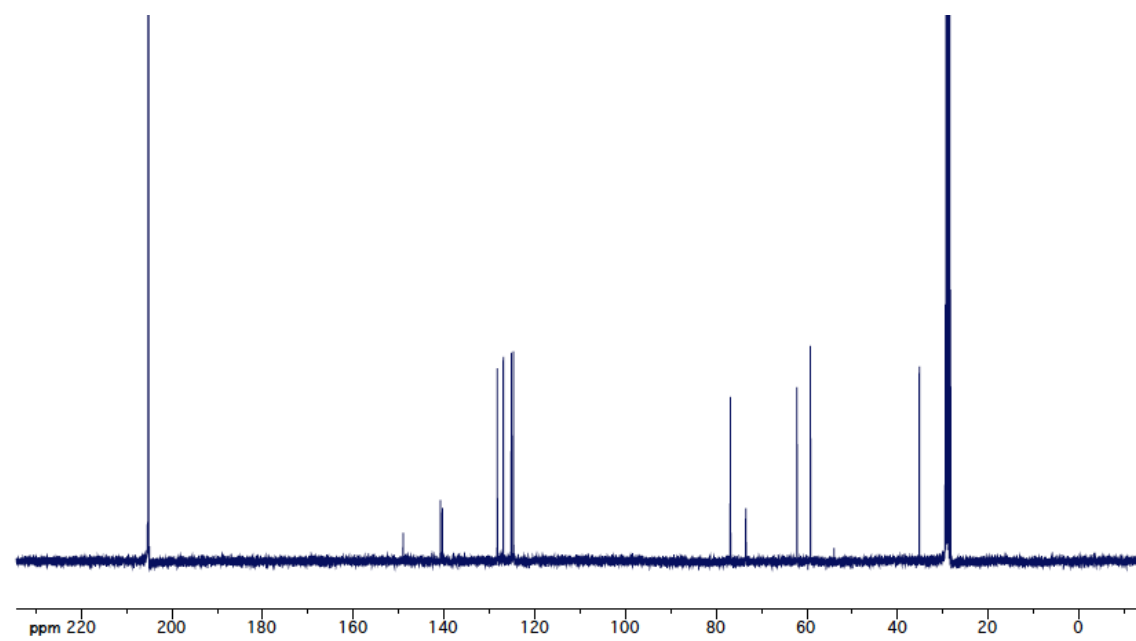
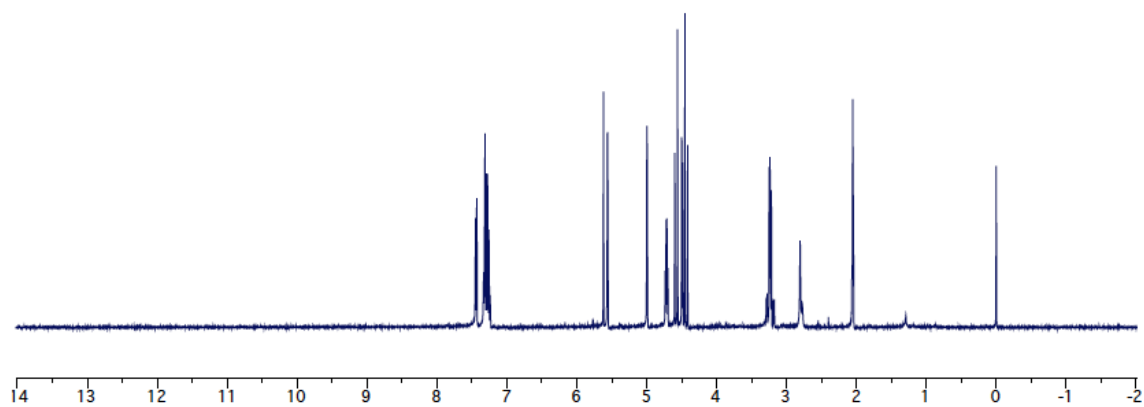
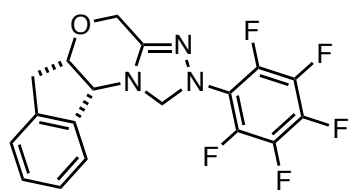
12a



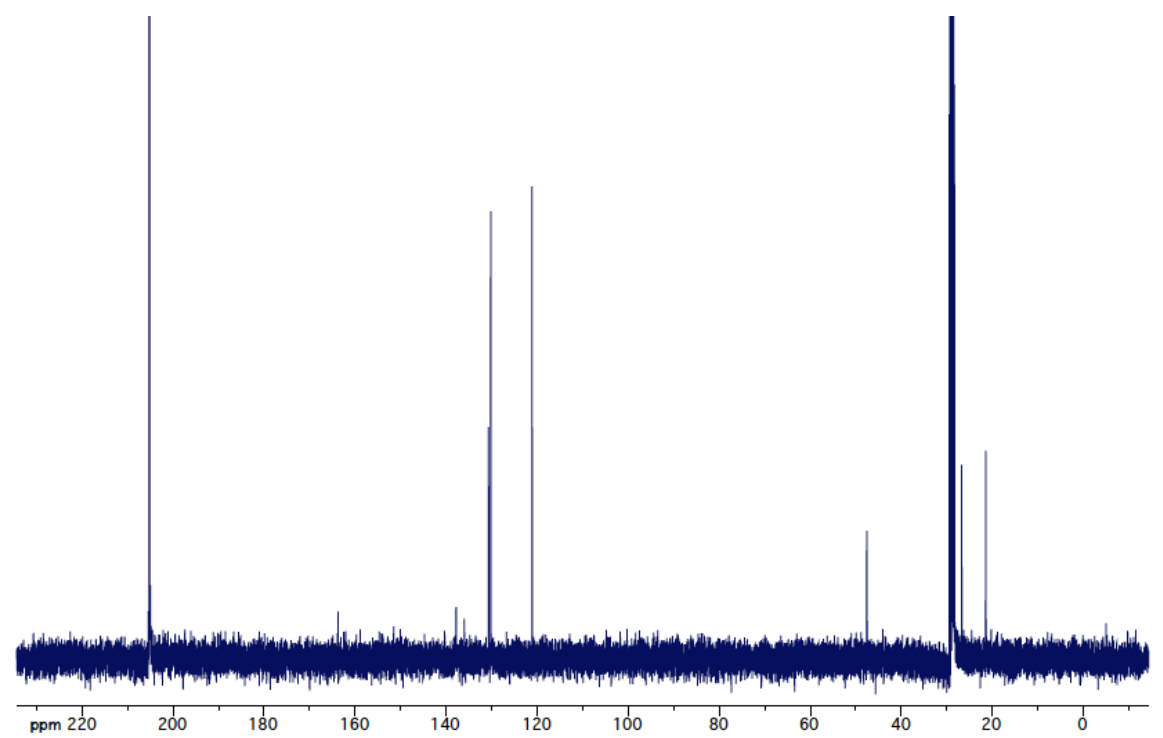
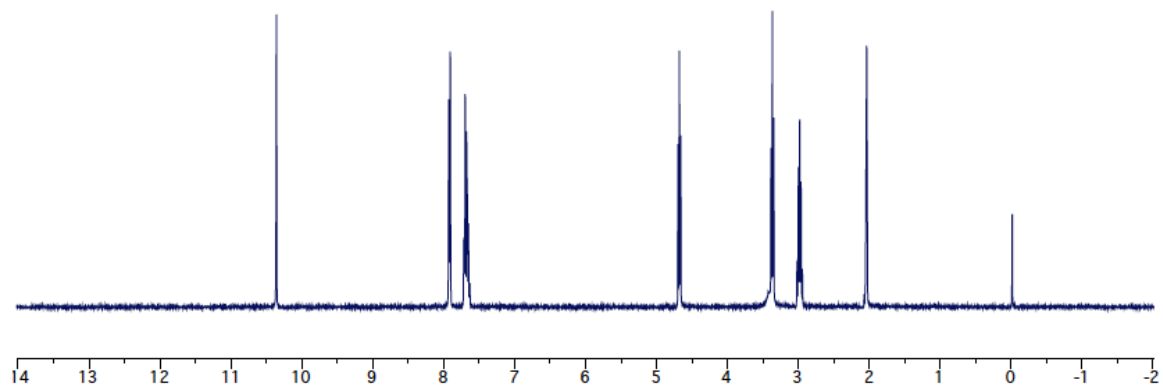
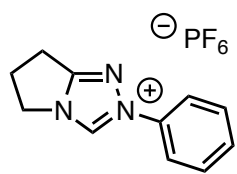
30a



31a

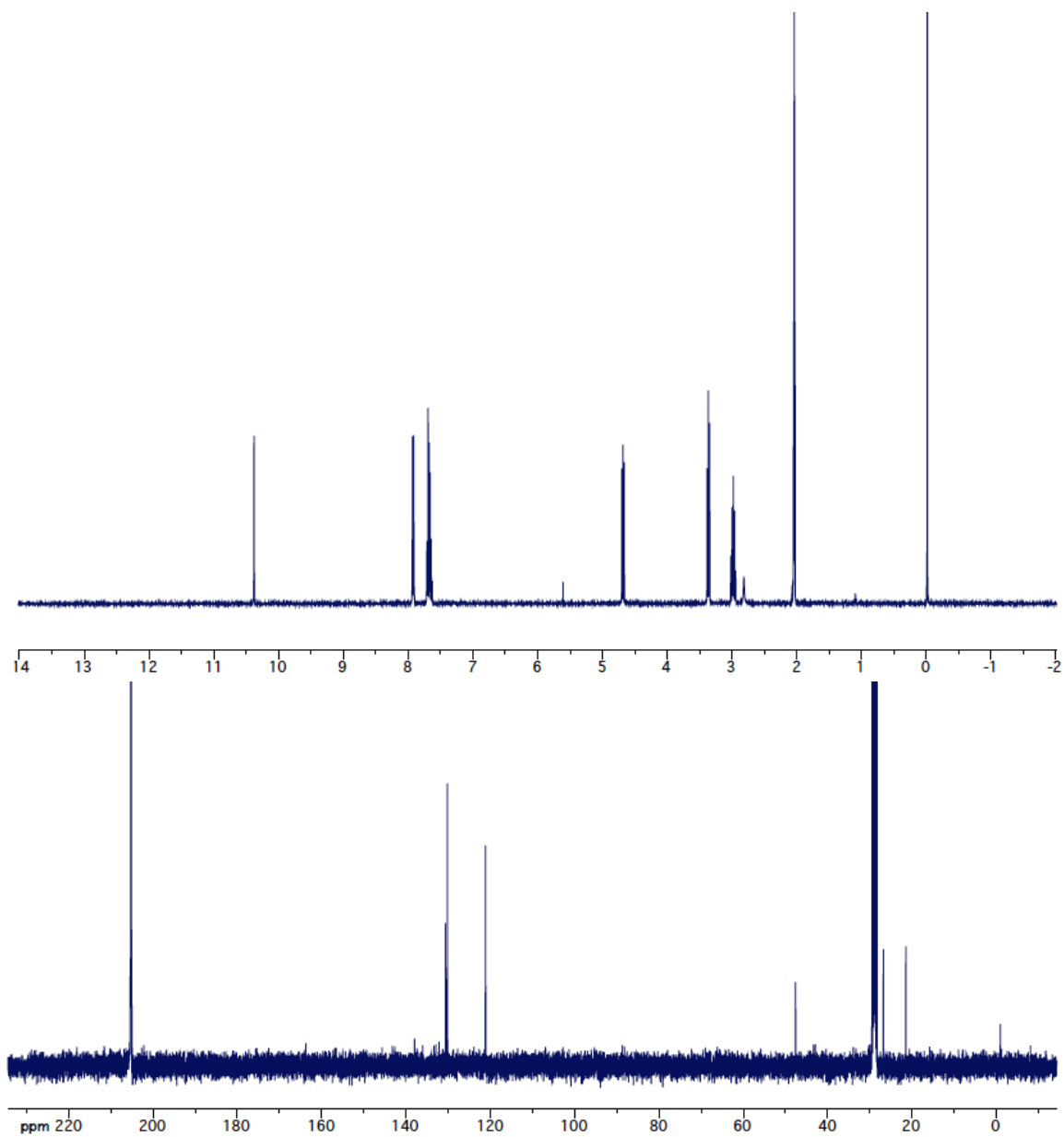
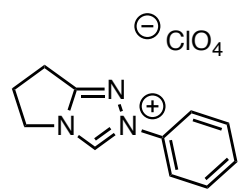


29b

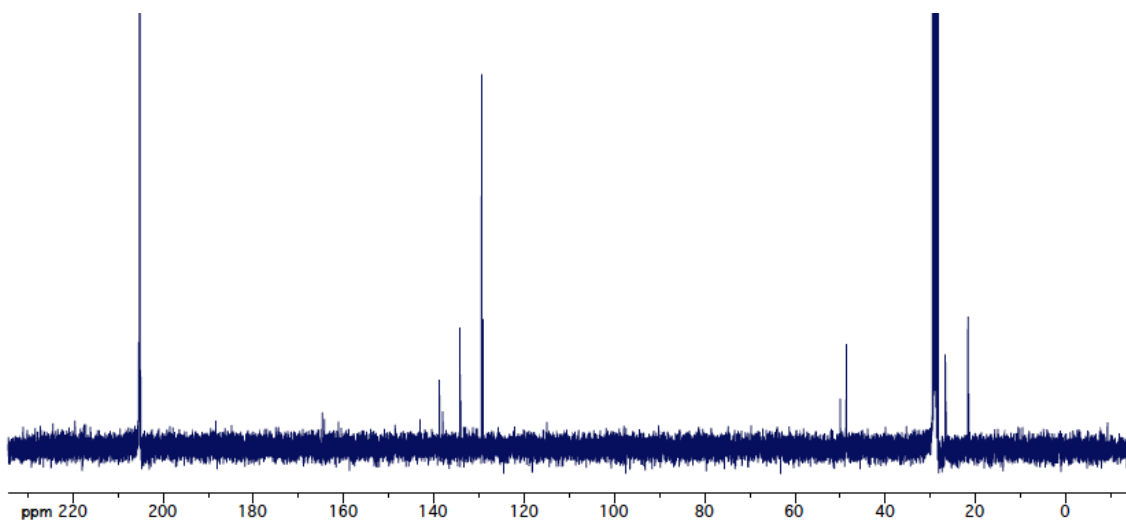
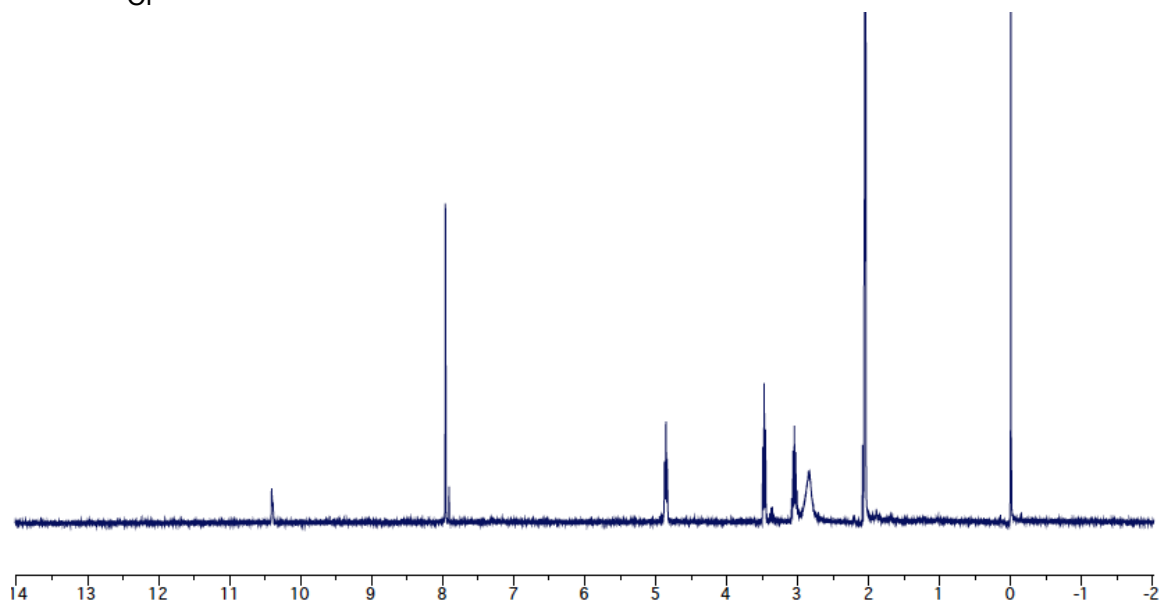
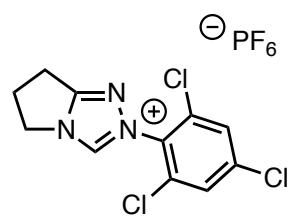




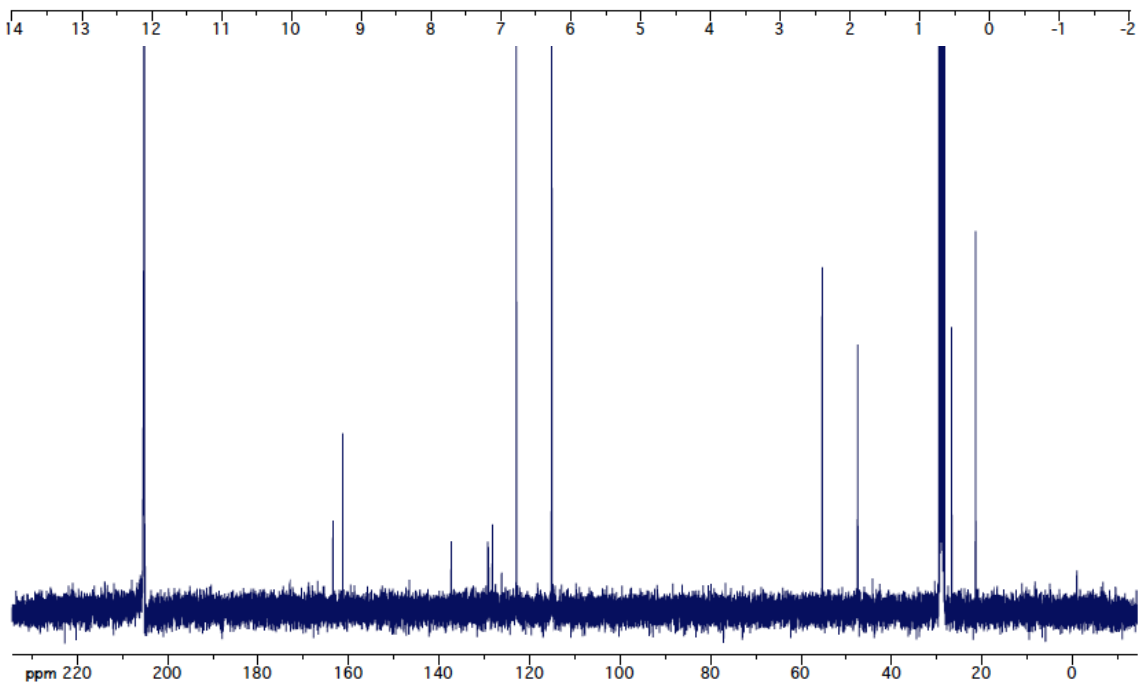
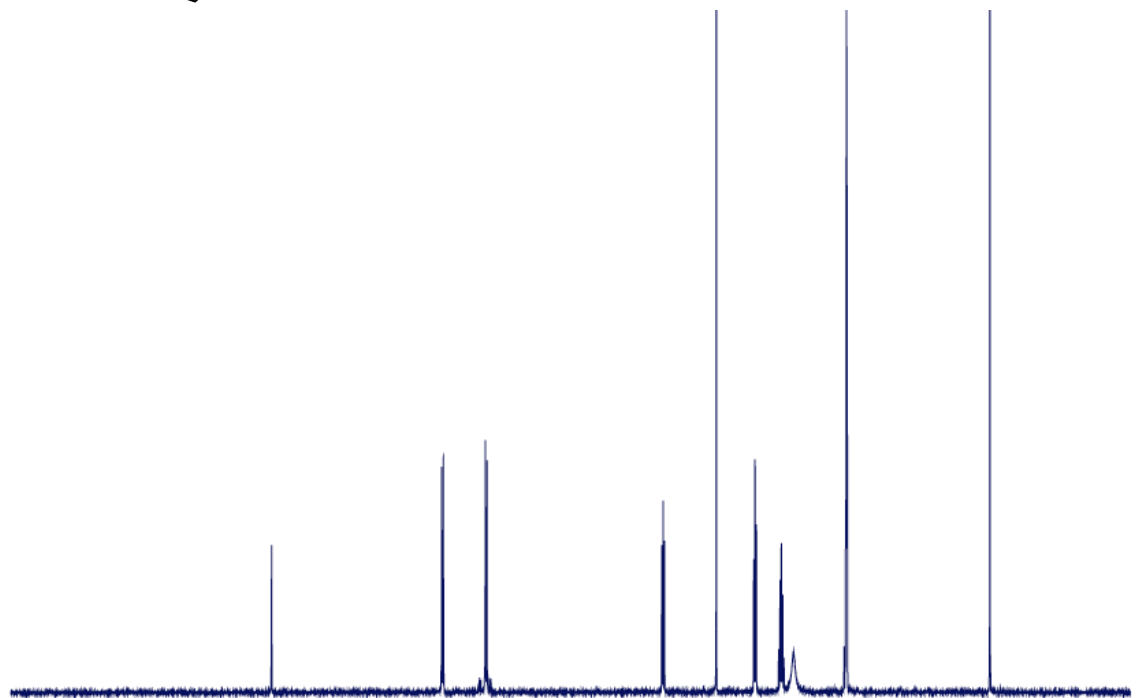
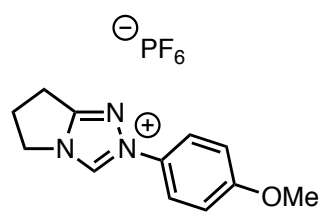
29d



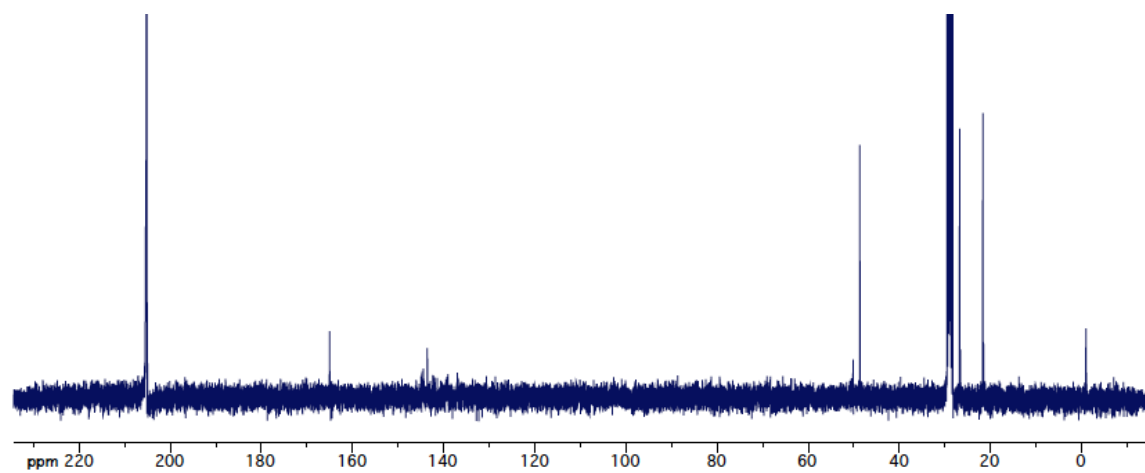
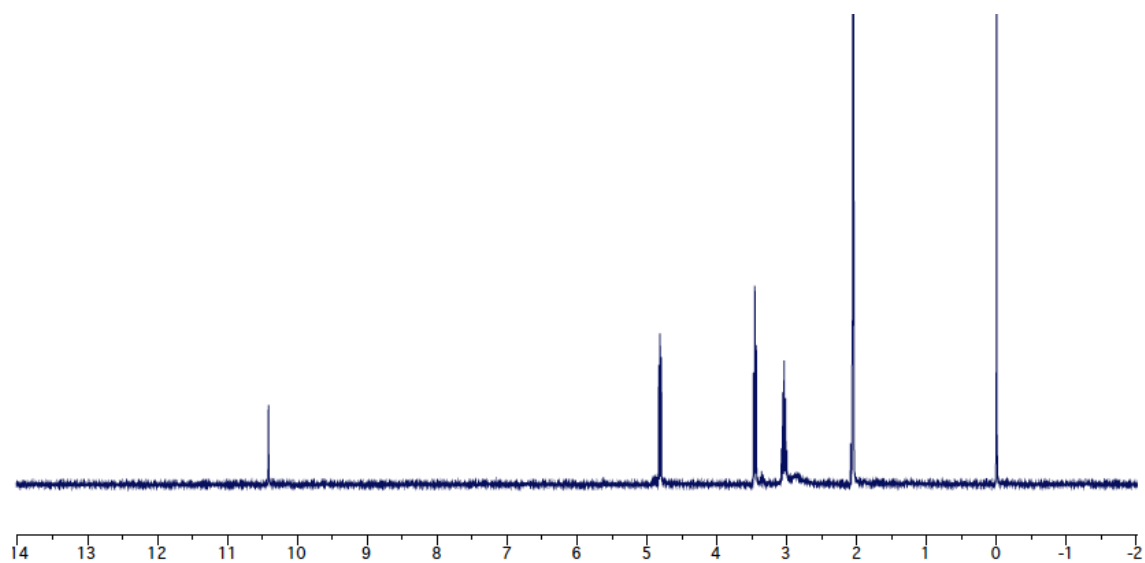
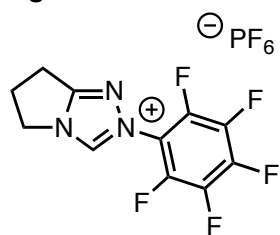
29e



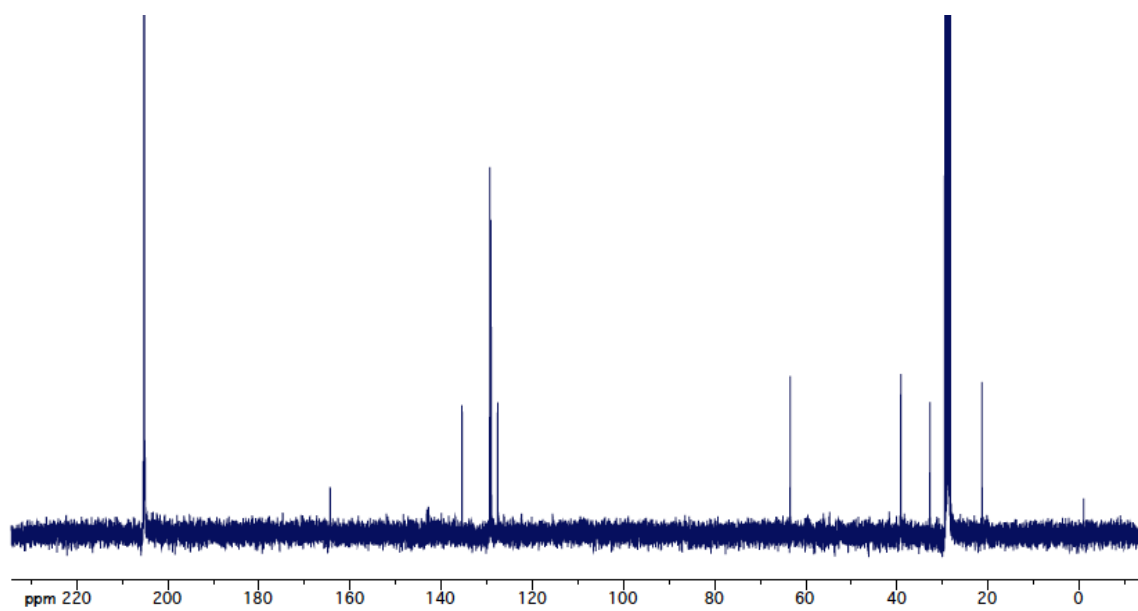
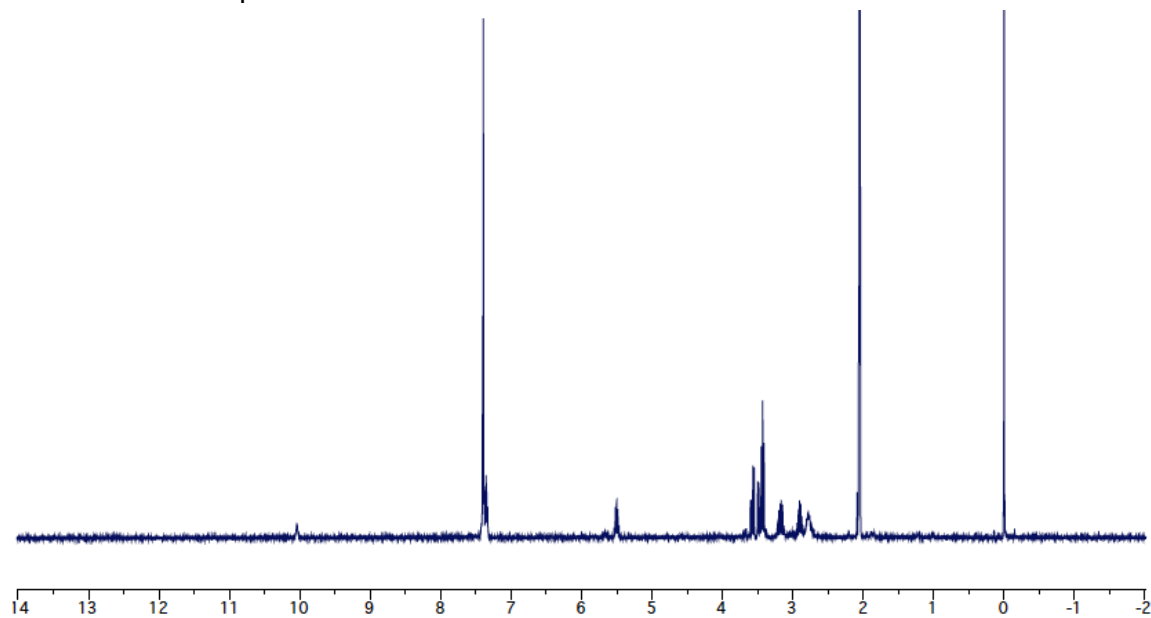
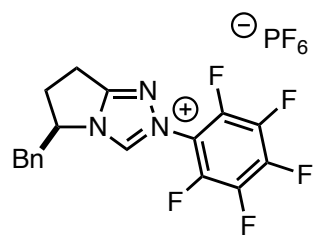
29f



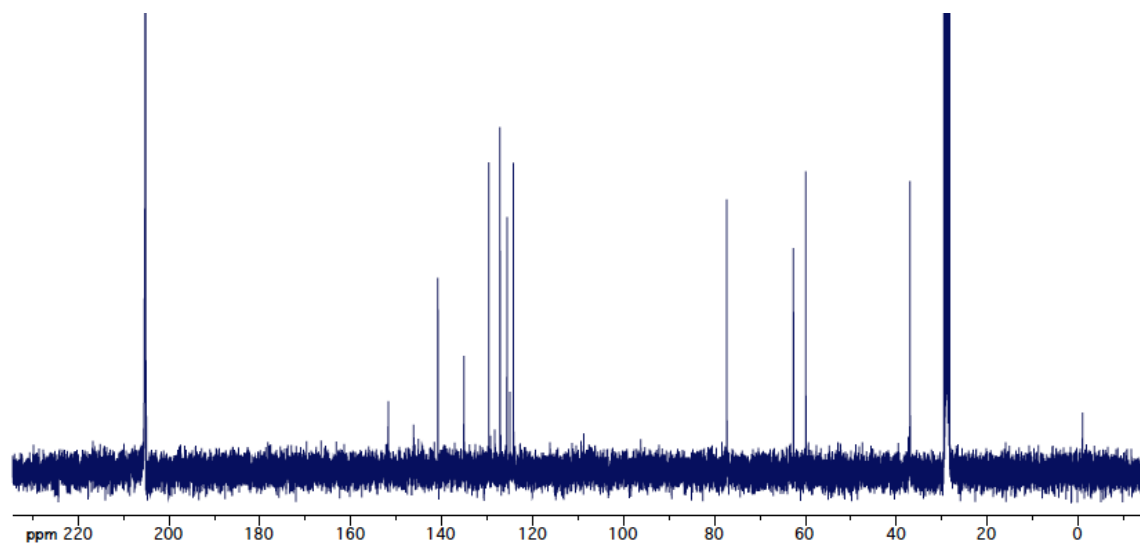
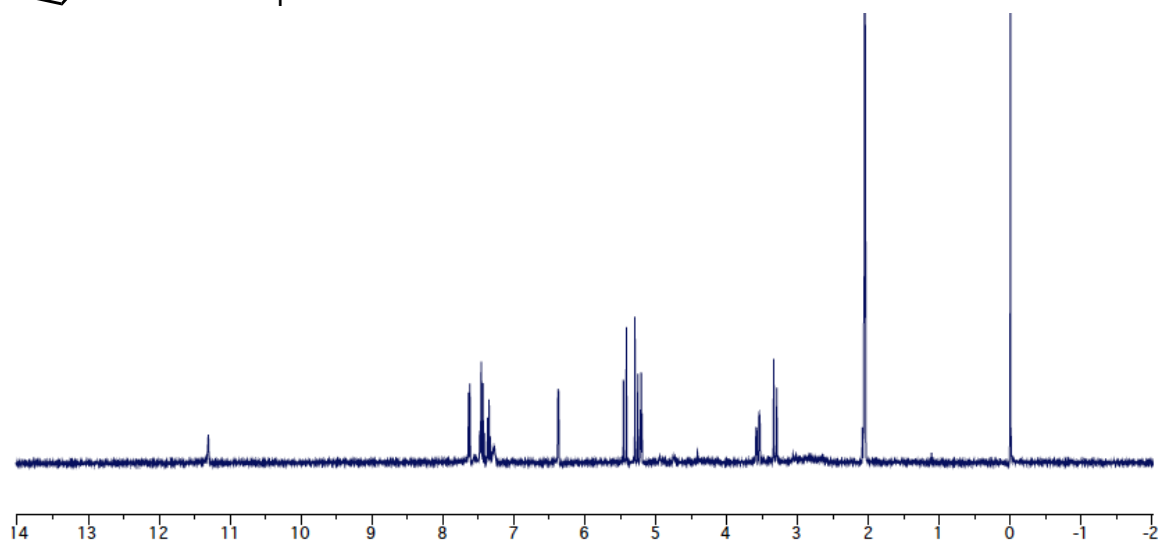
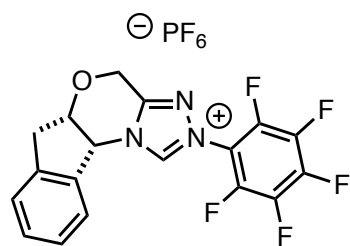
29g



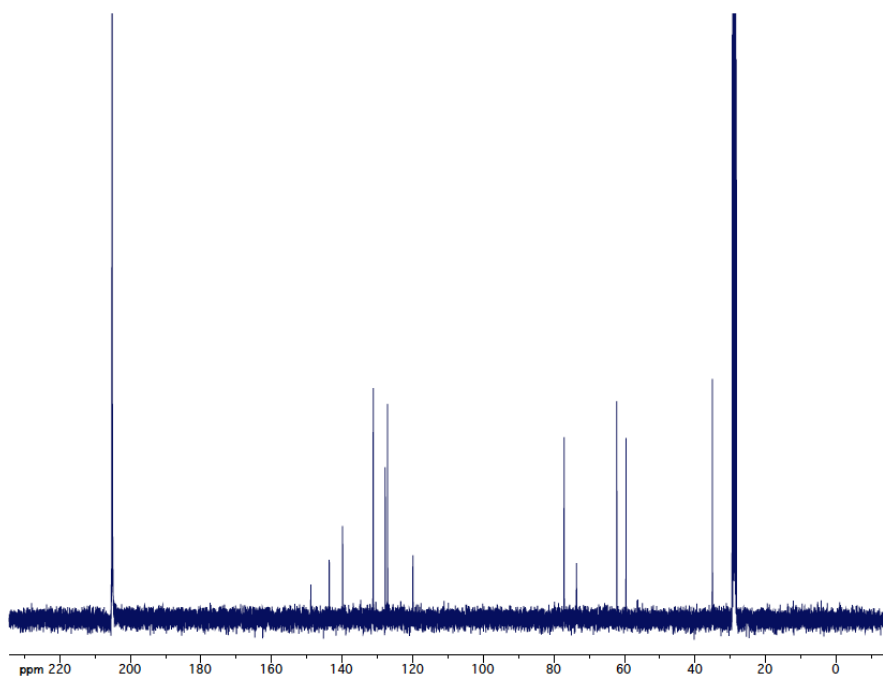
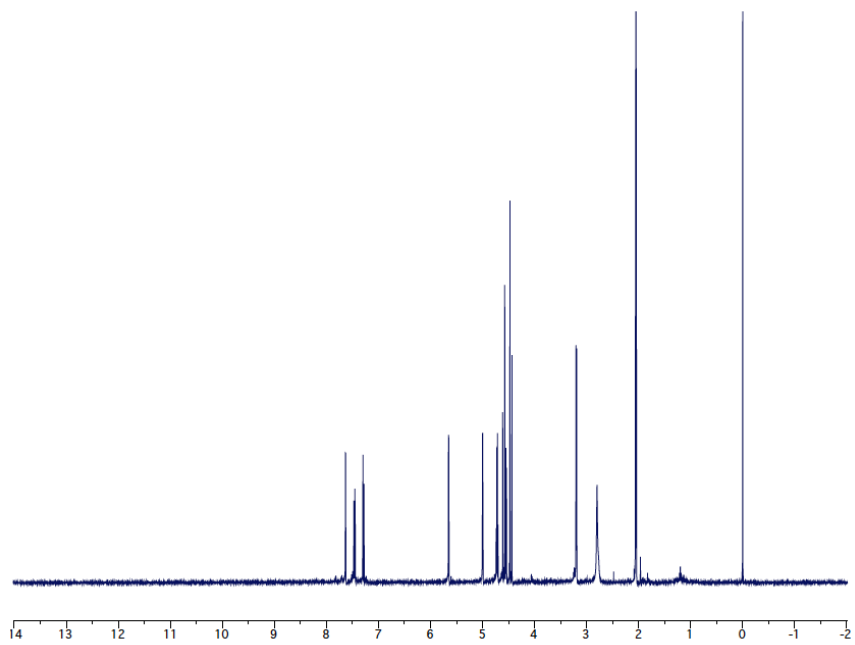
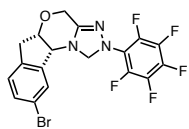
30



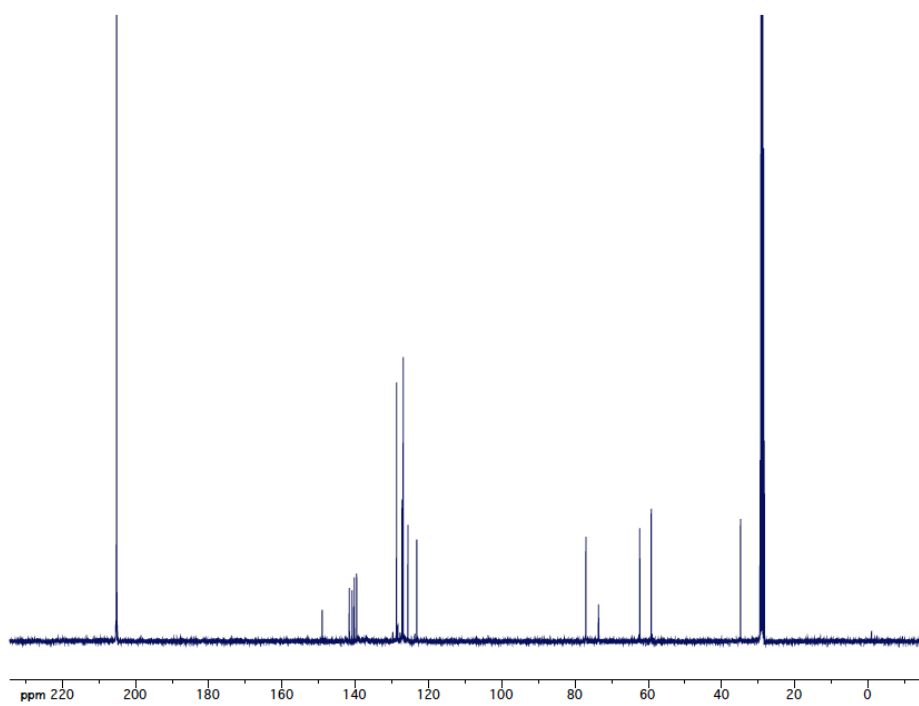
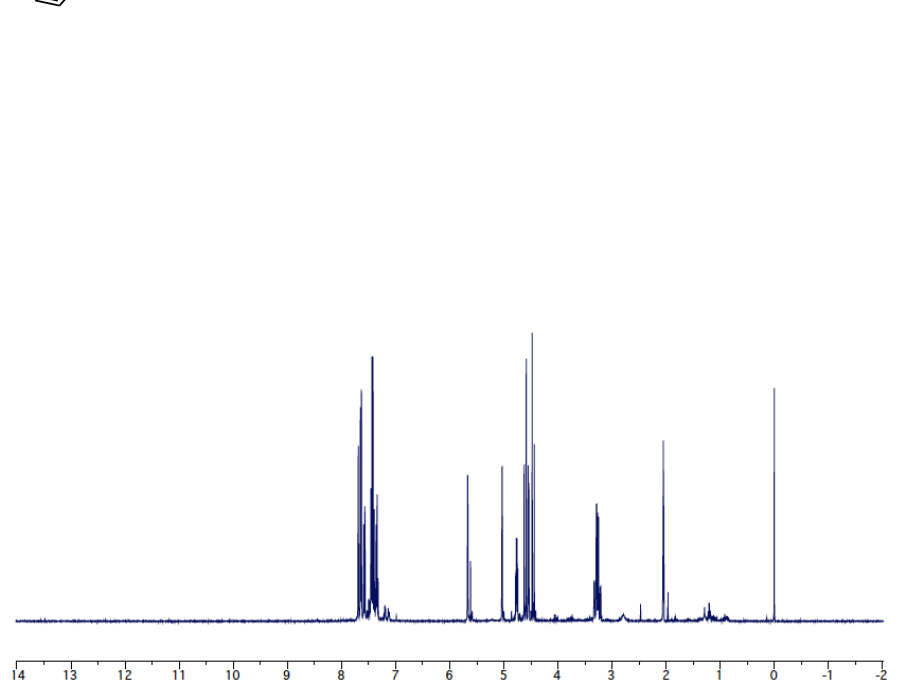
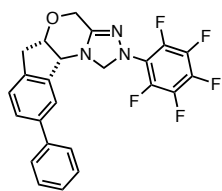
31



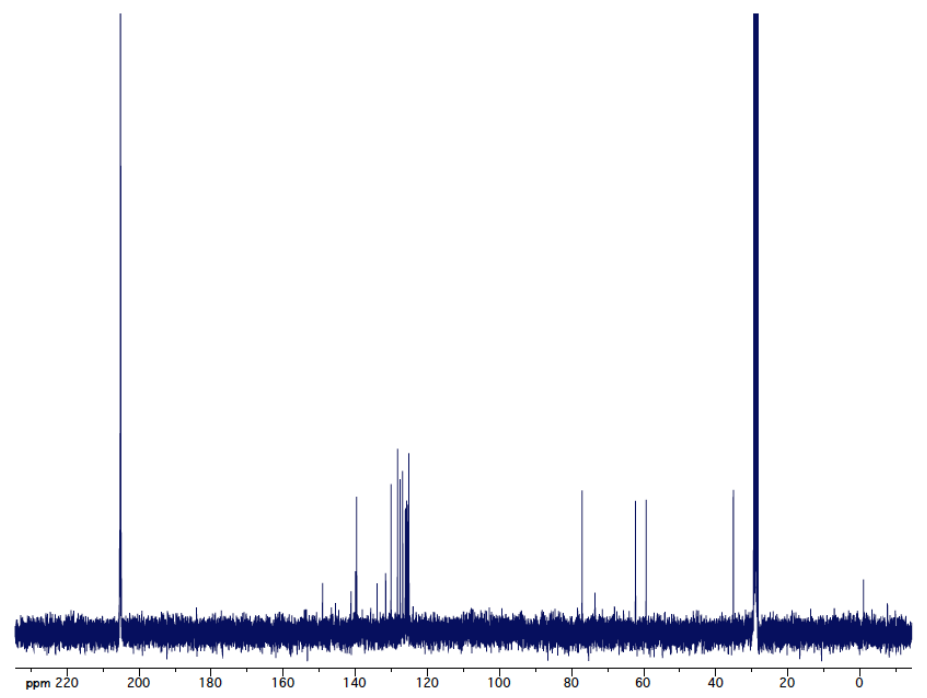
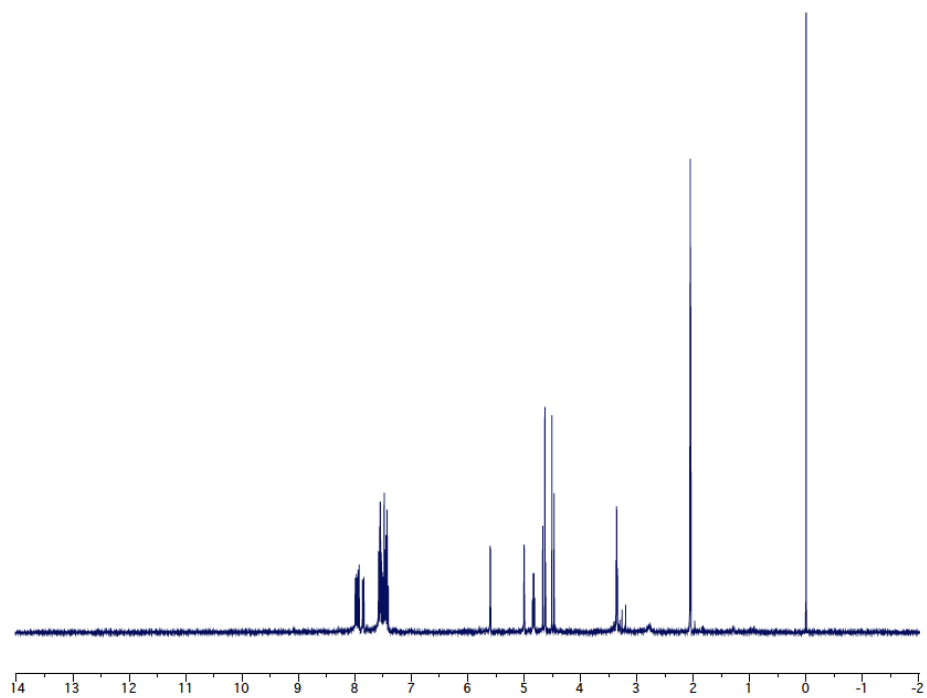
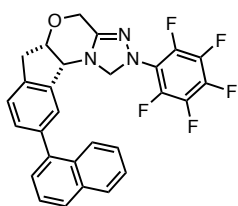
37



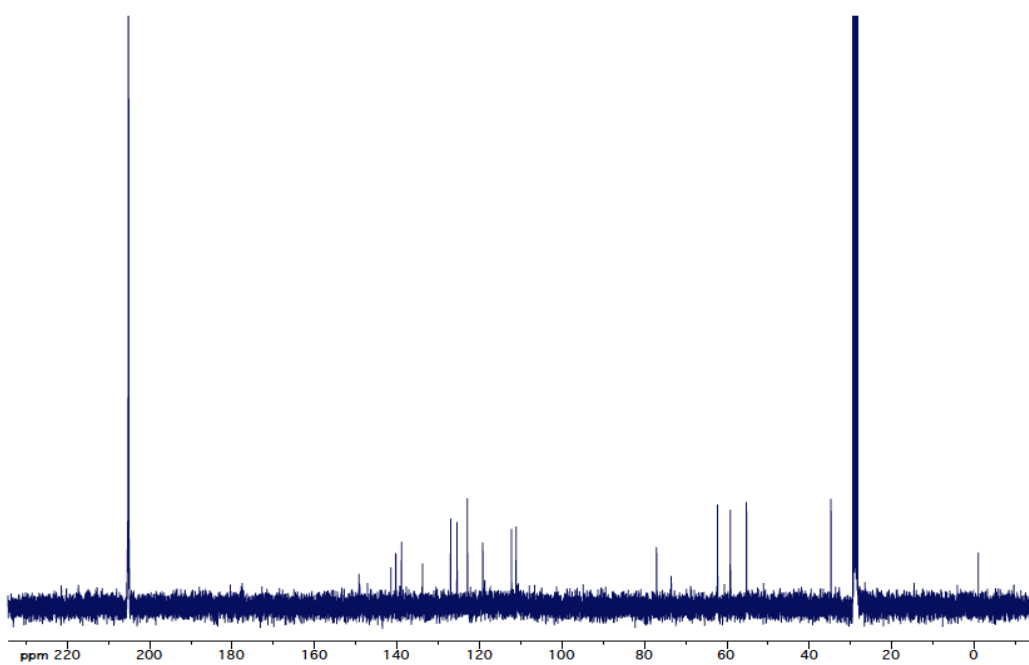
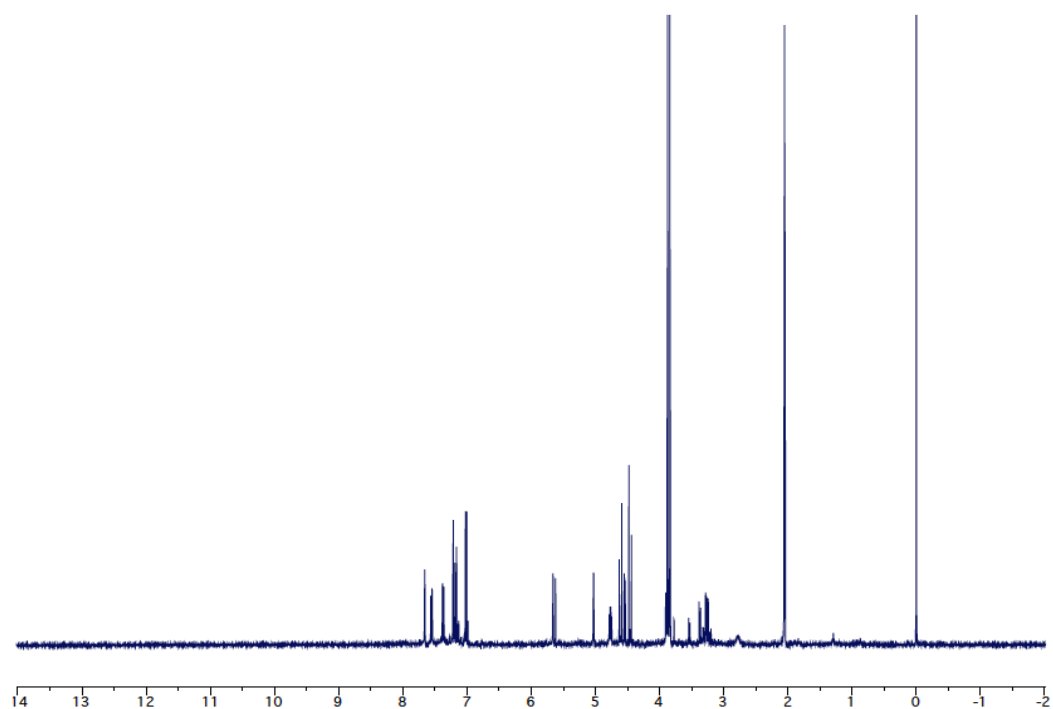
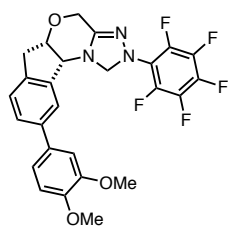
**38a**



38b

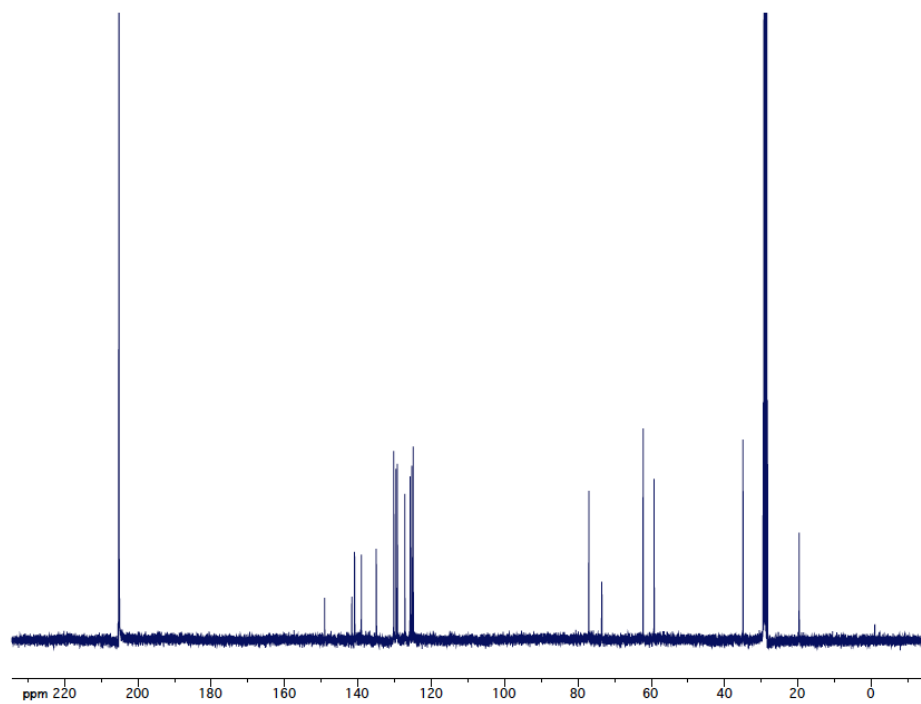
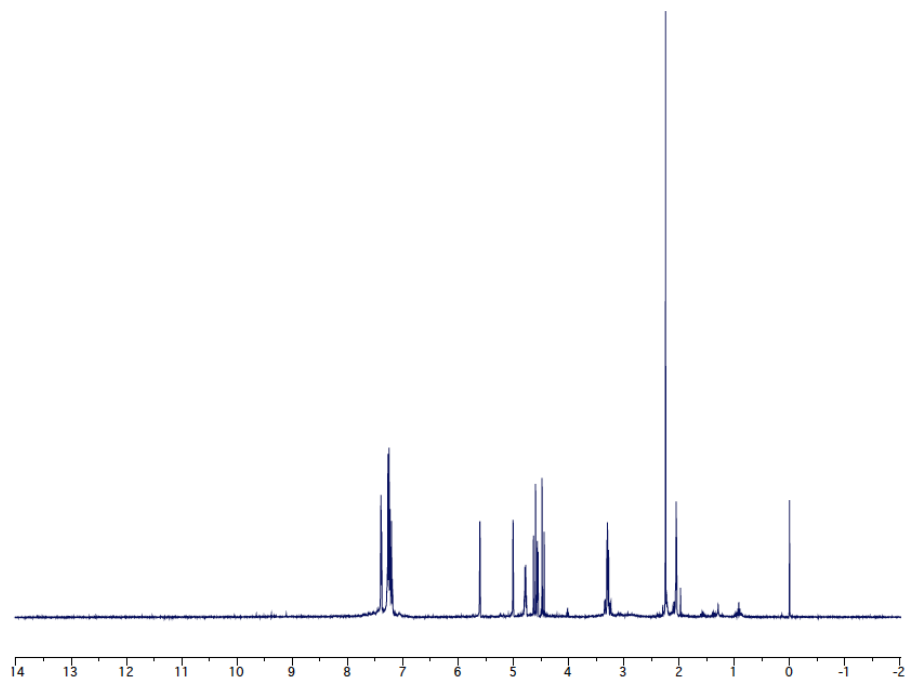
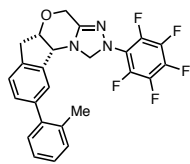


38c

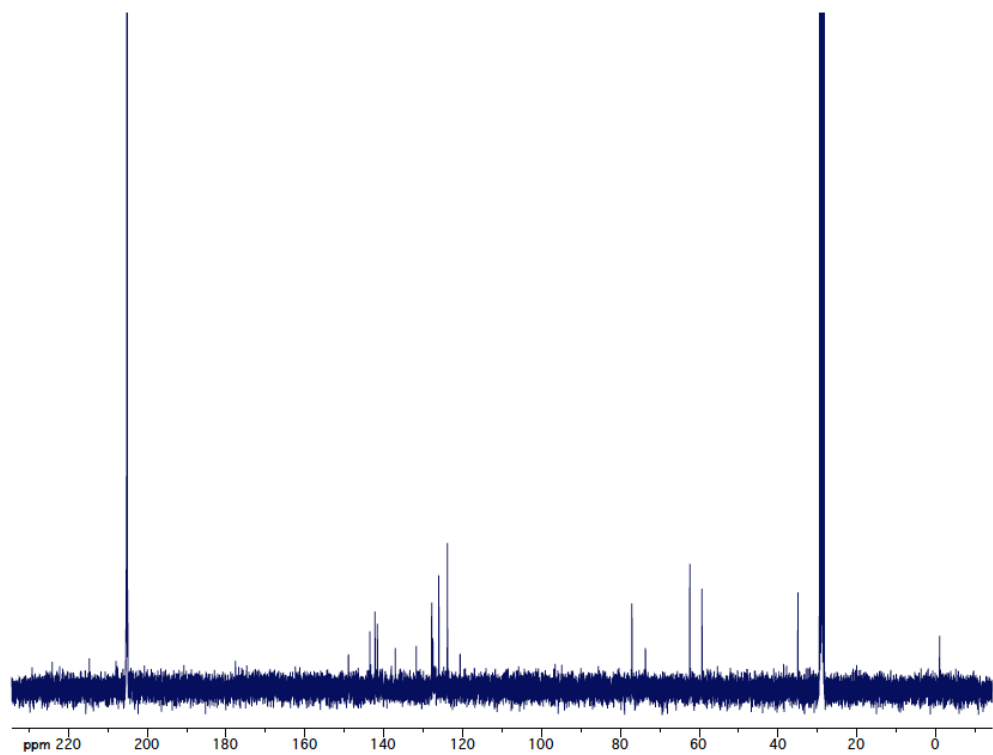
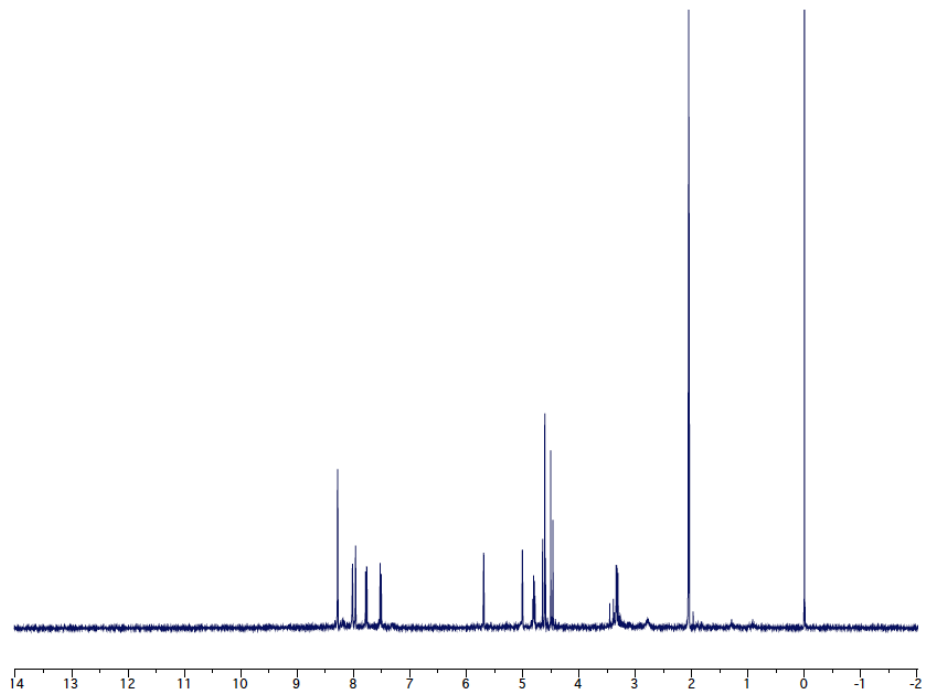
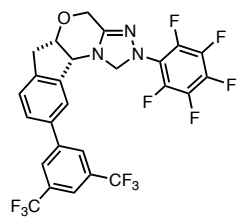




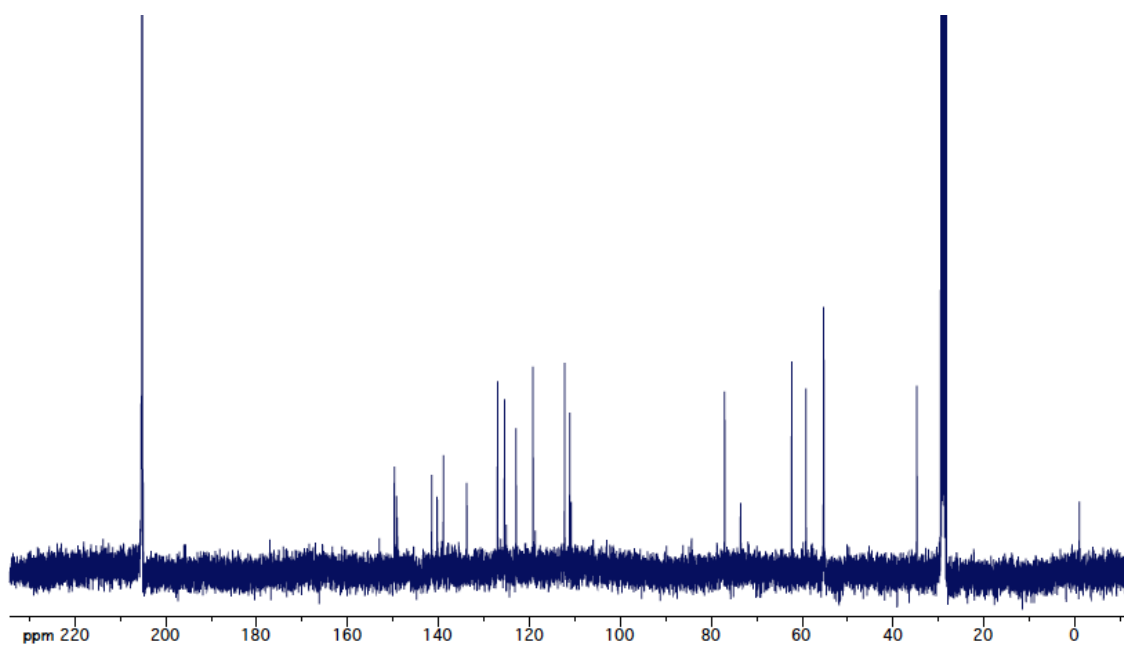
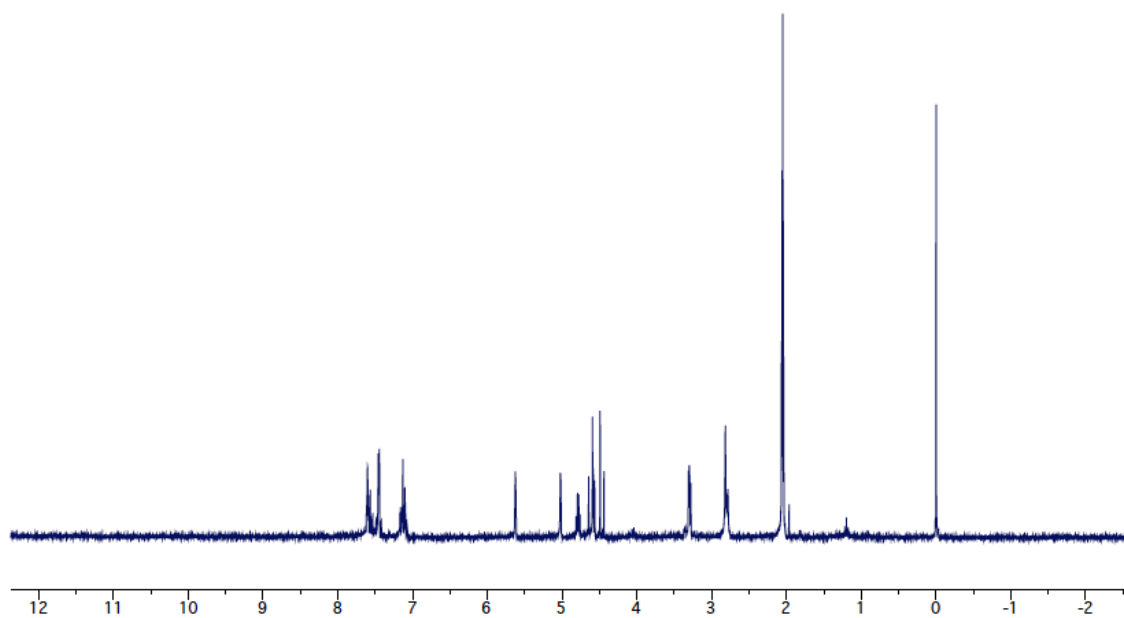
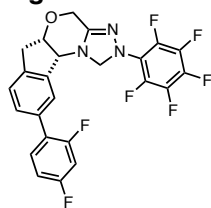
**38e**



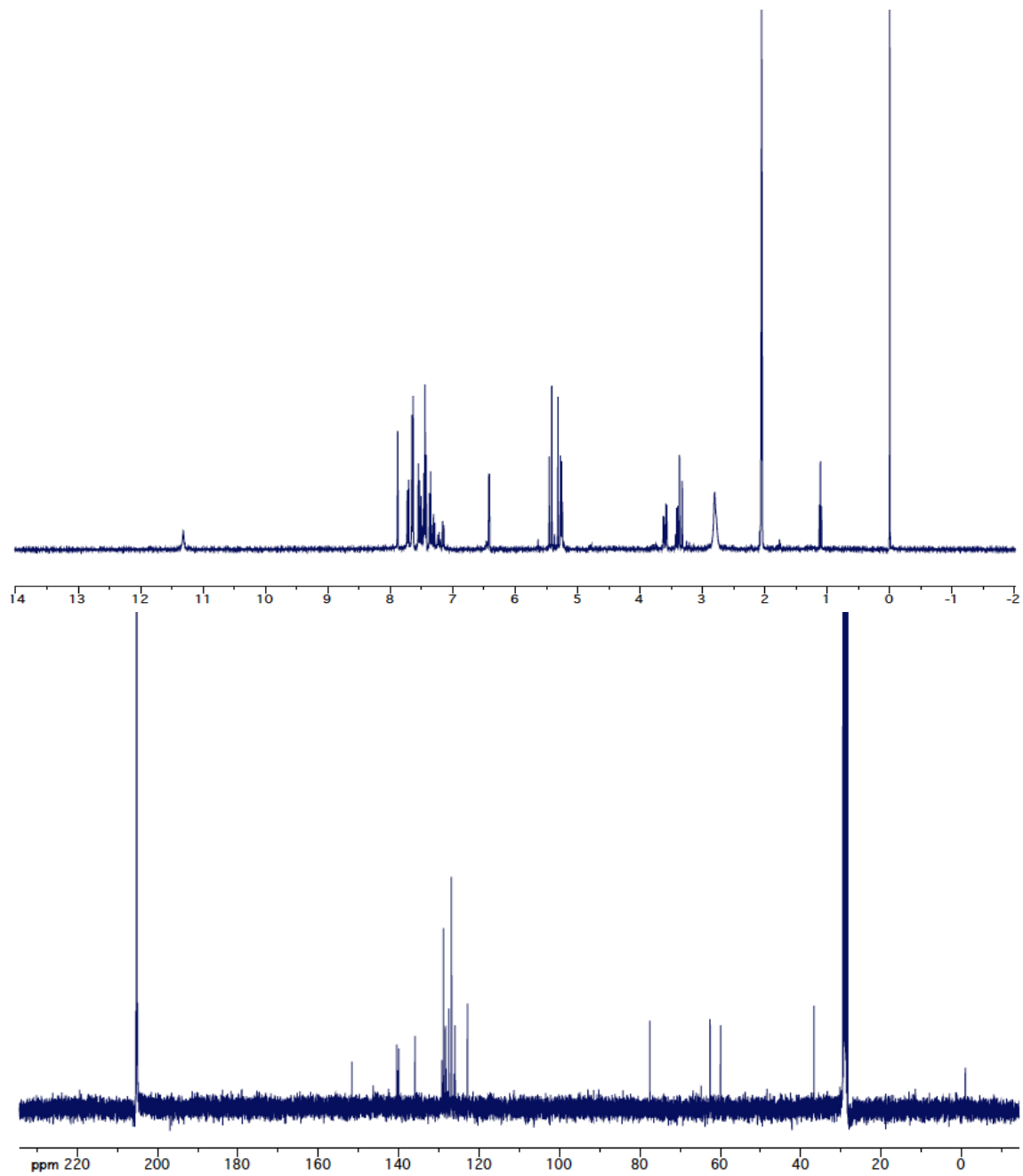
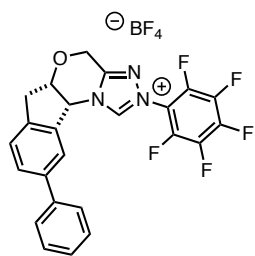
38f



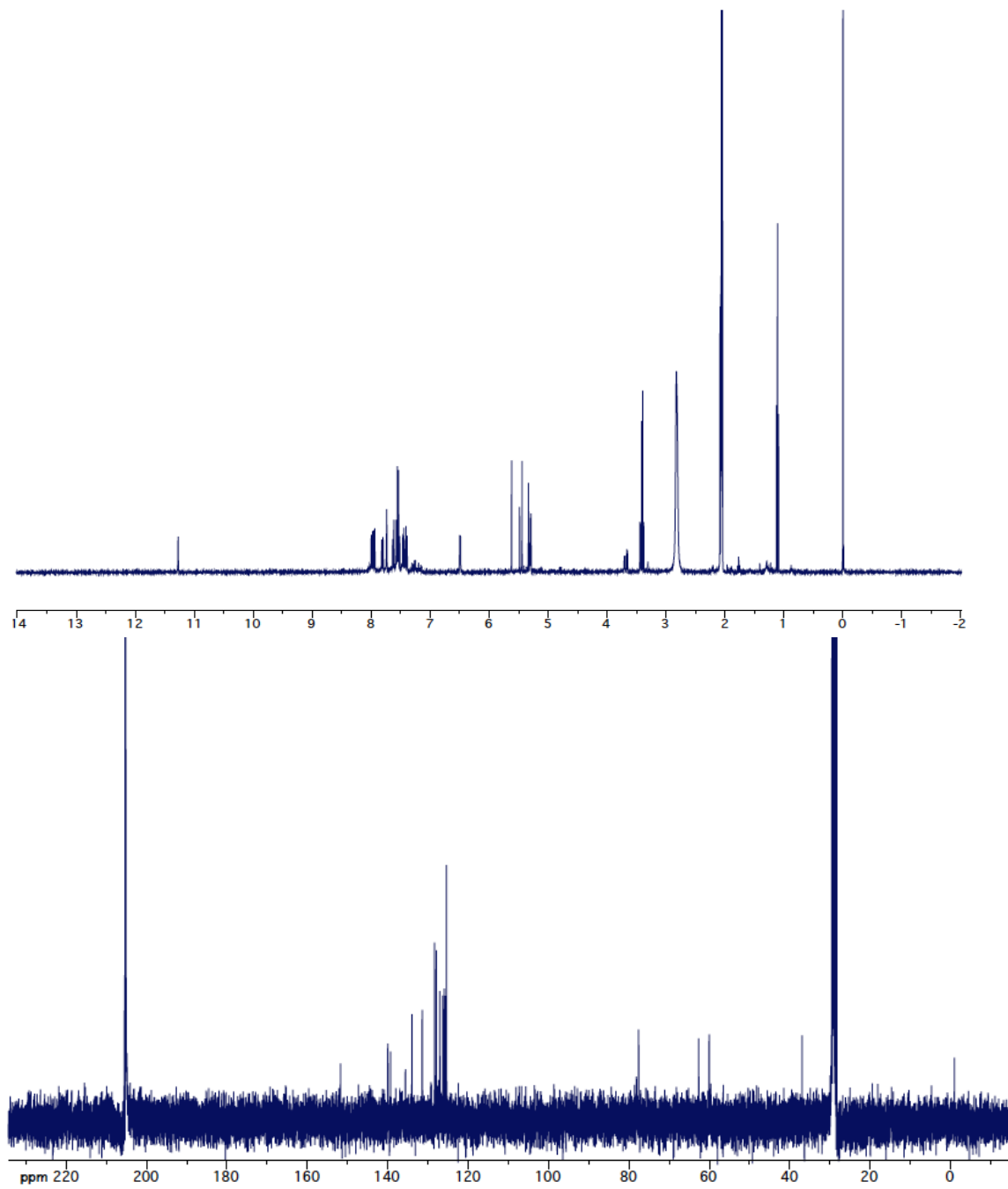
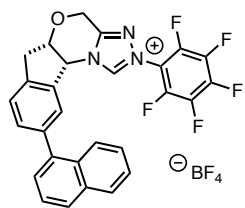
**38g**



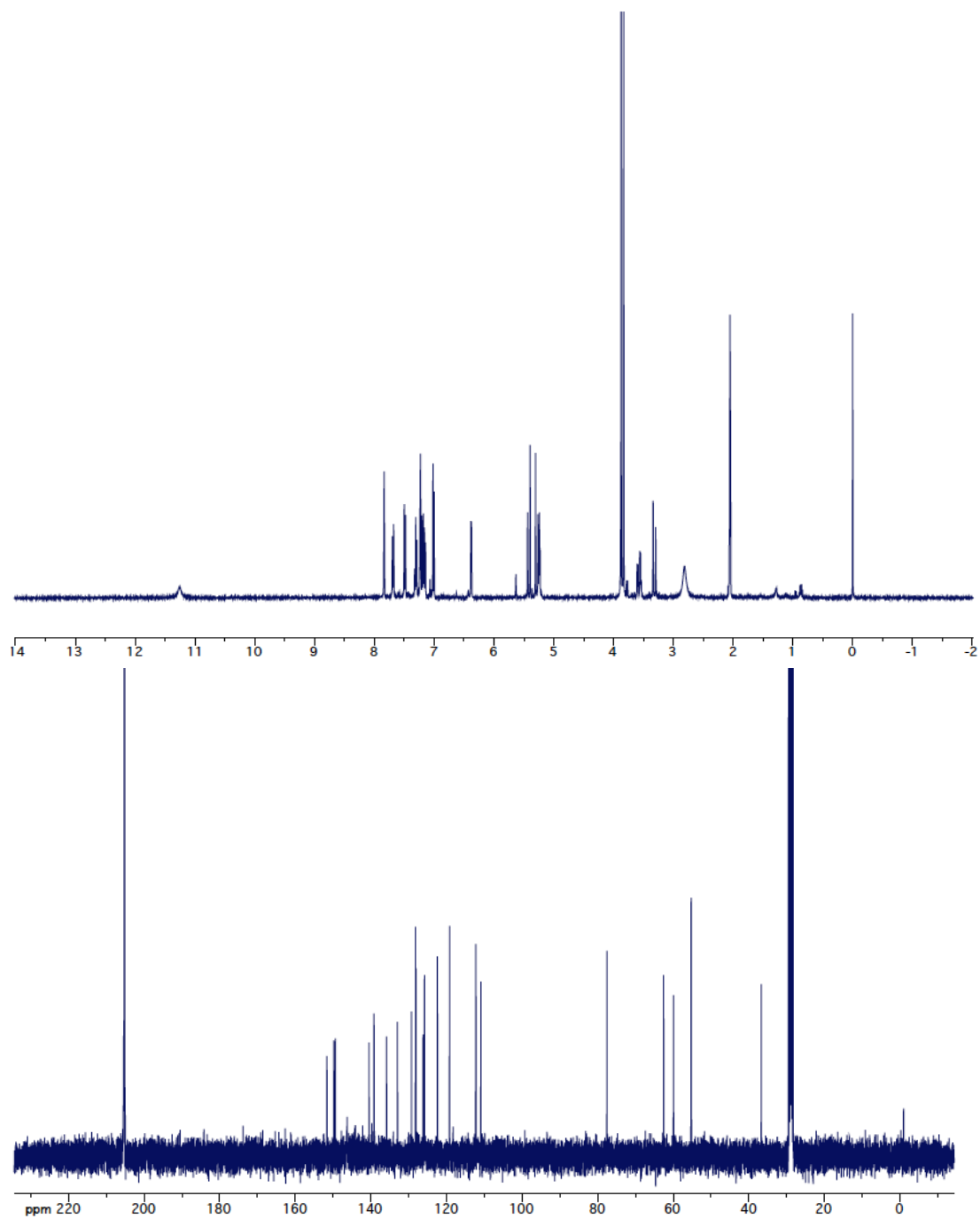
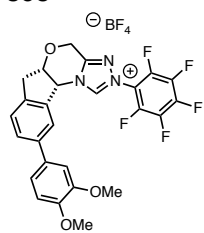
39a



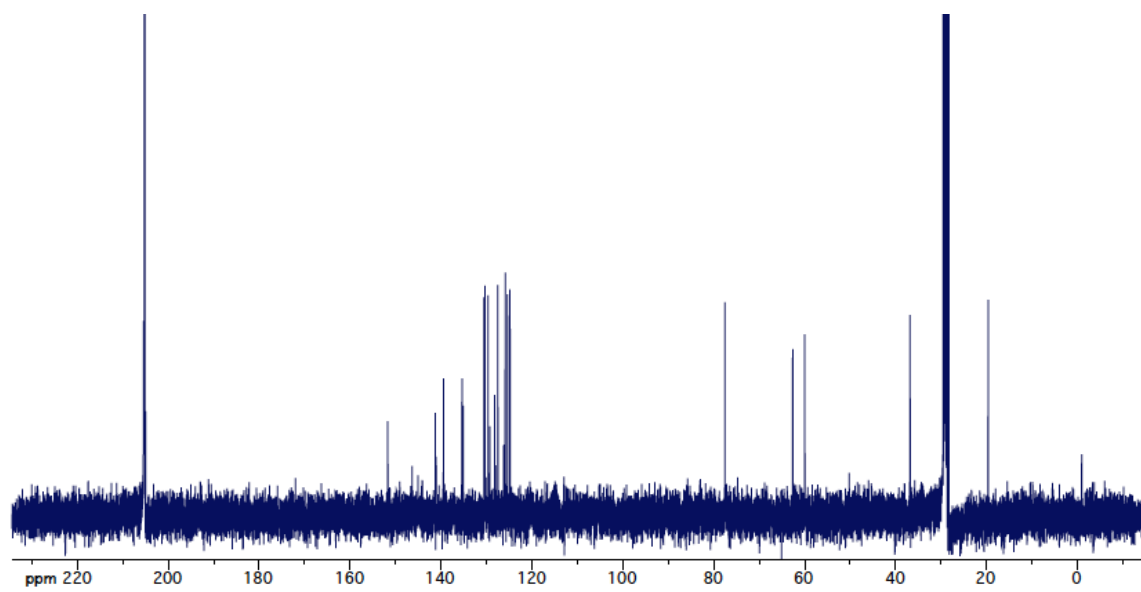
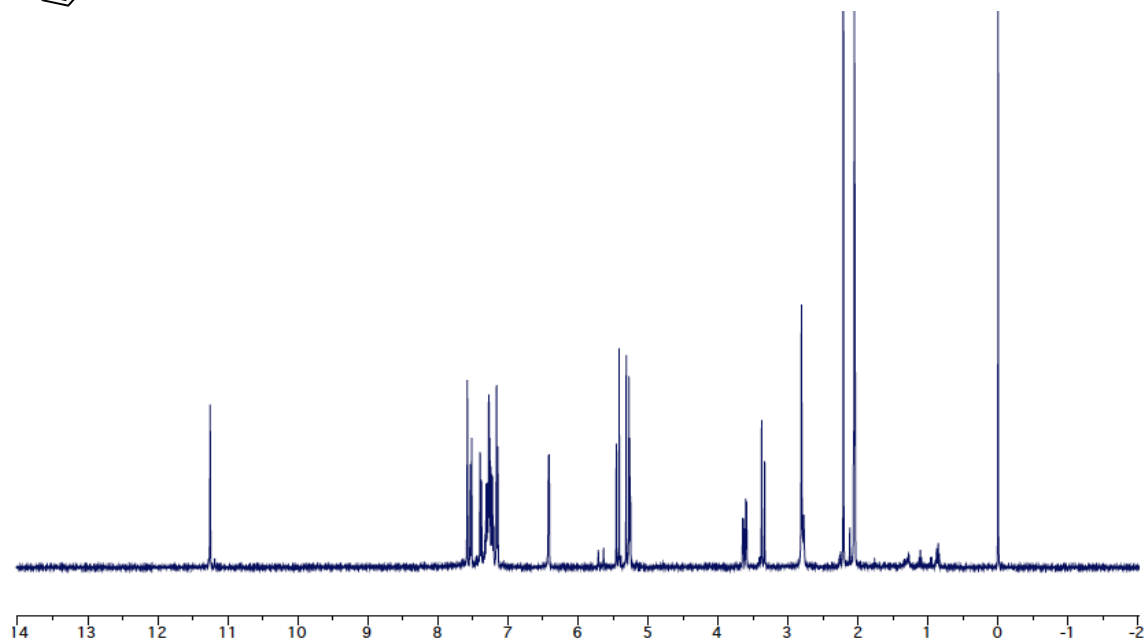
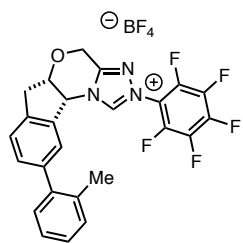
39b



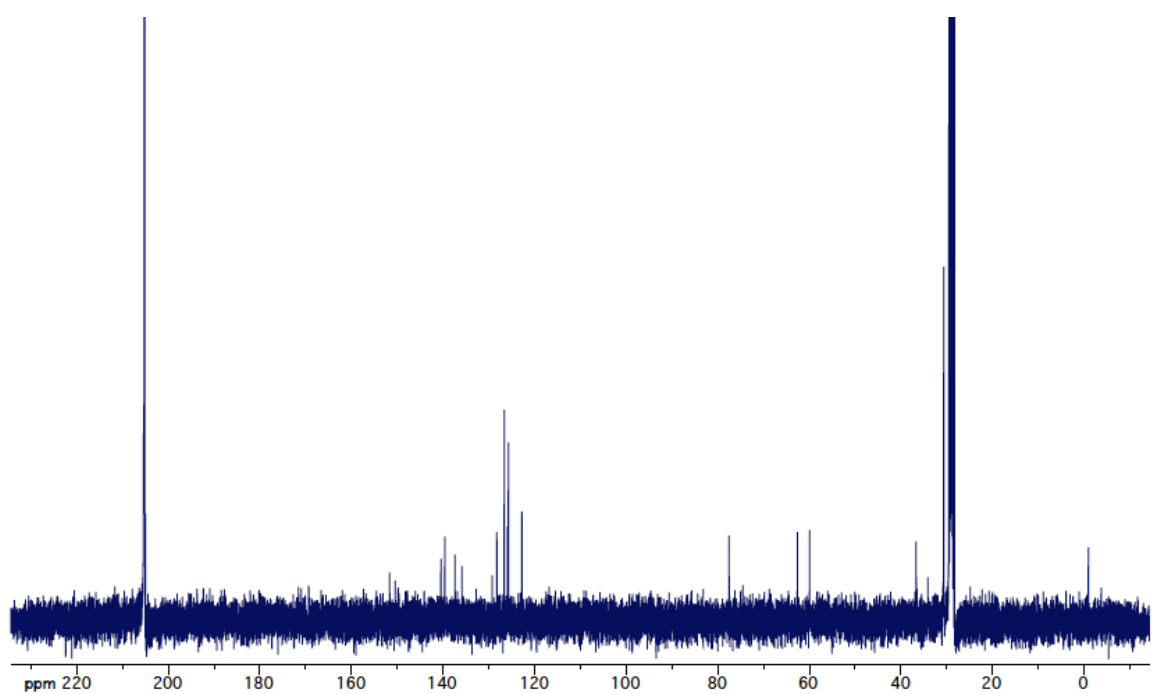
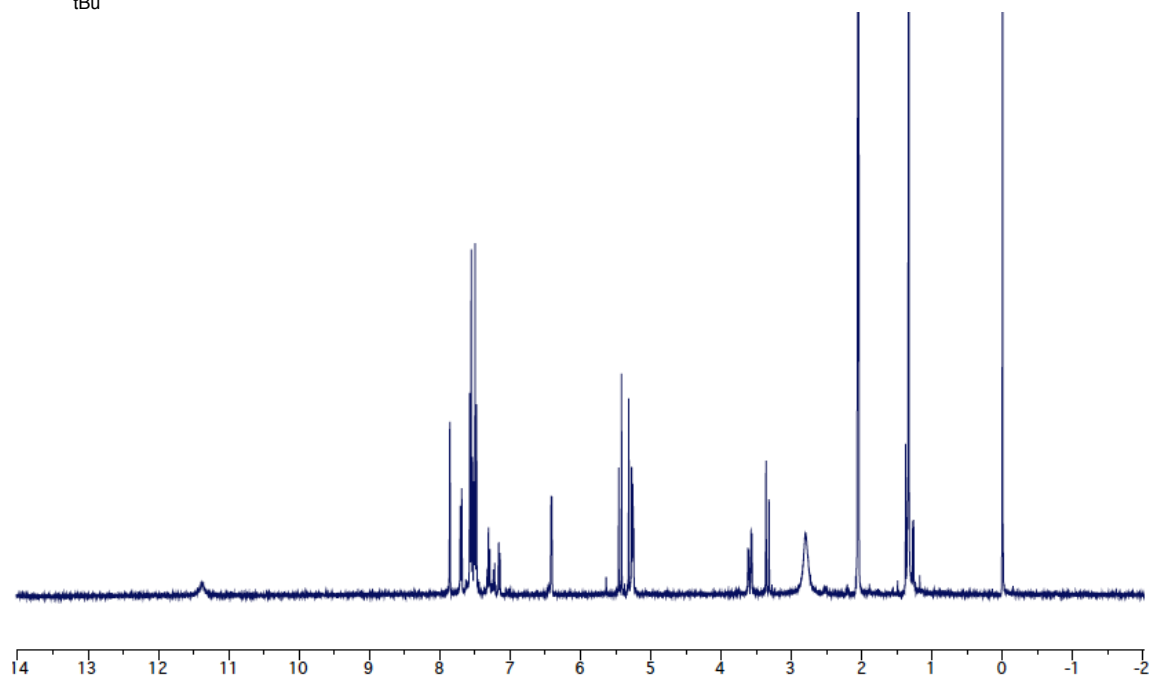
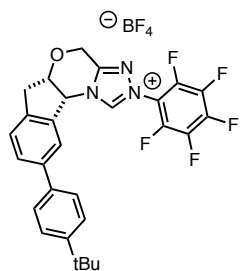
**39c**



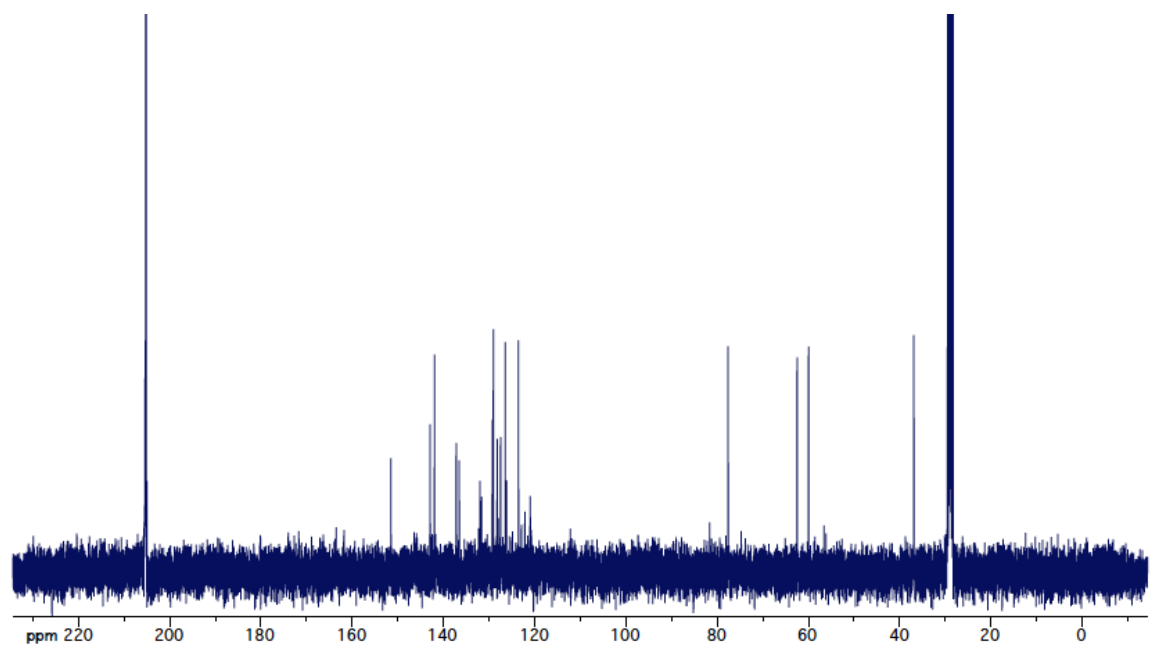
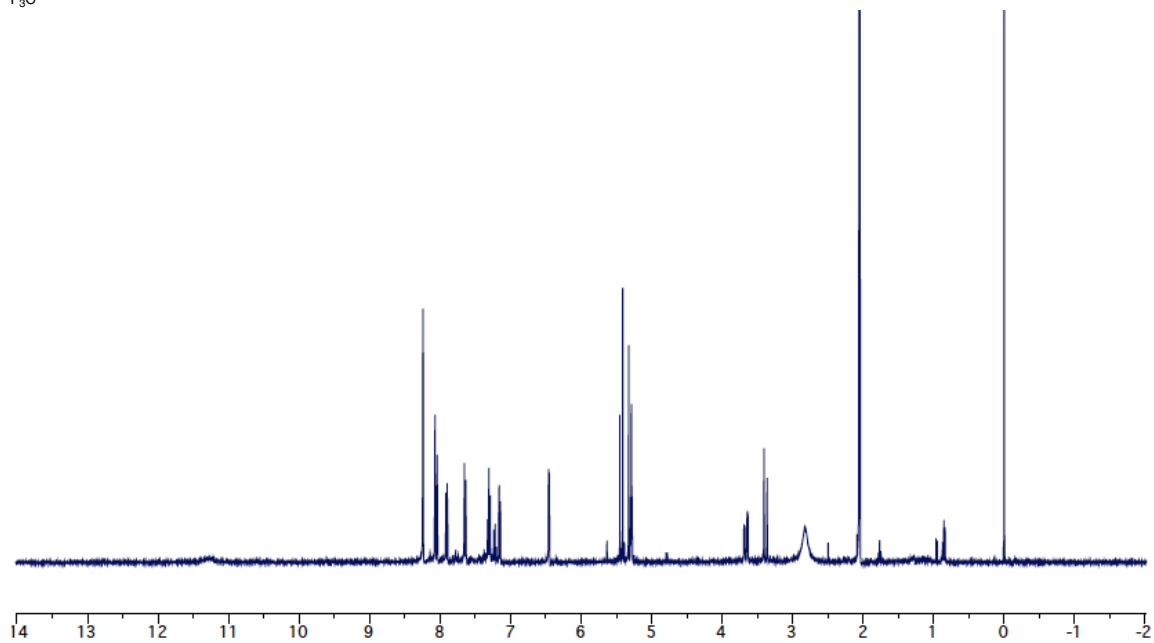
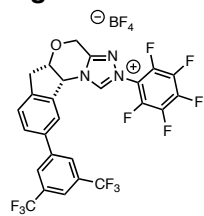
39e



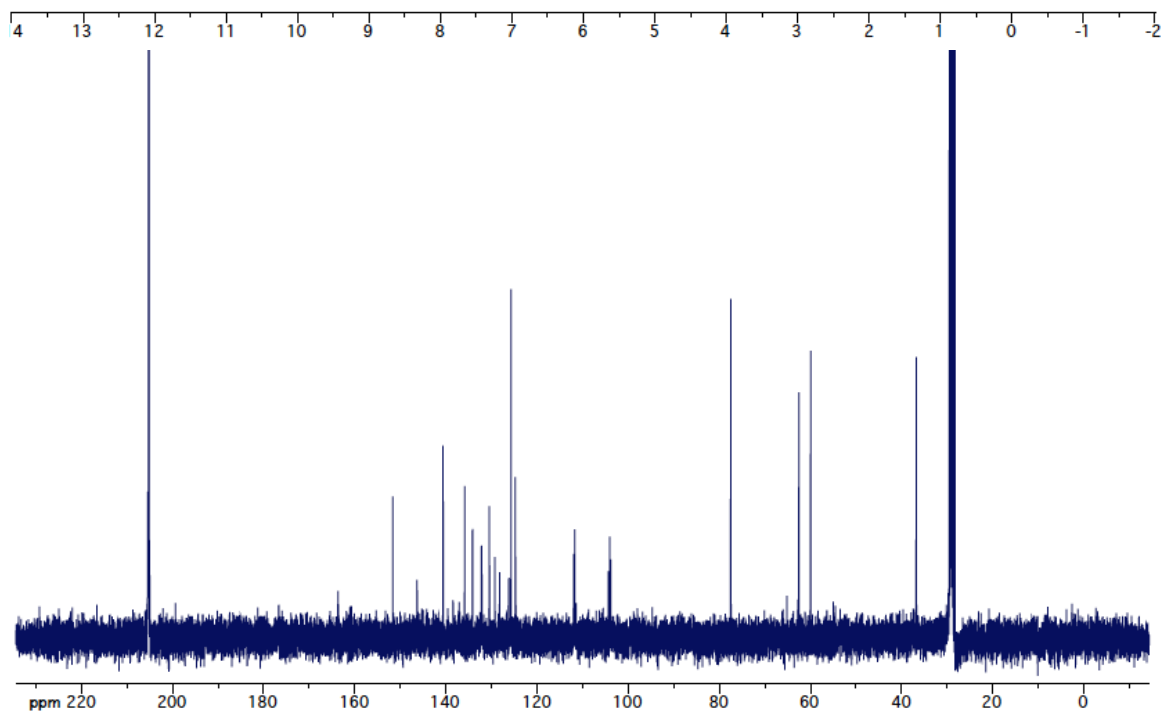
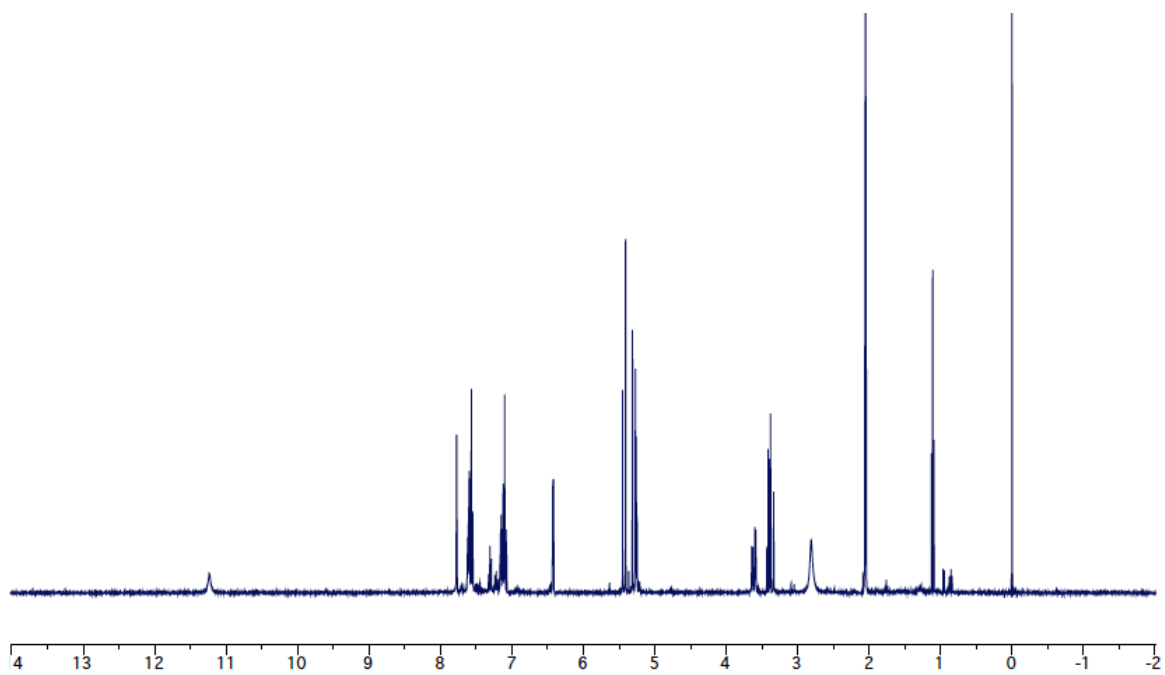
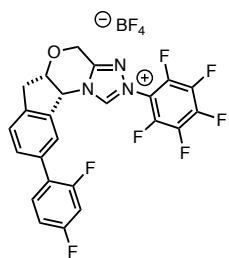
39f

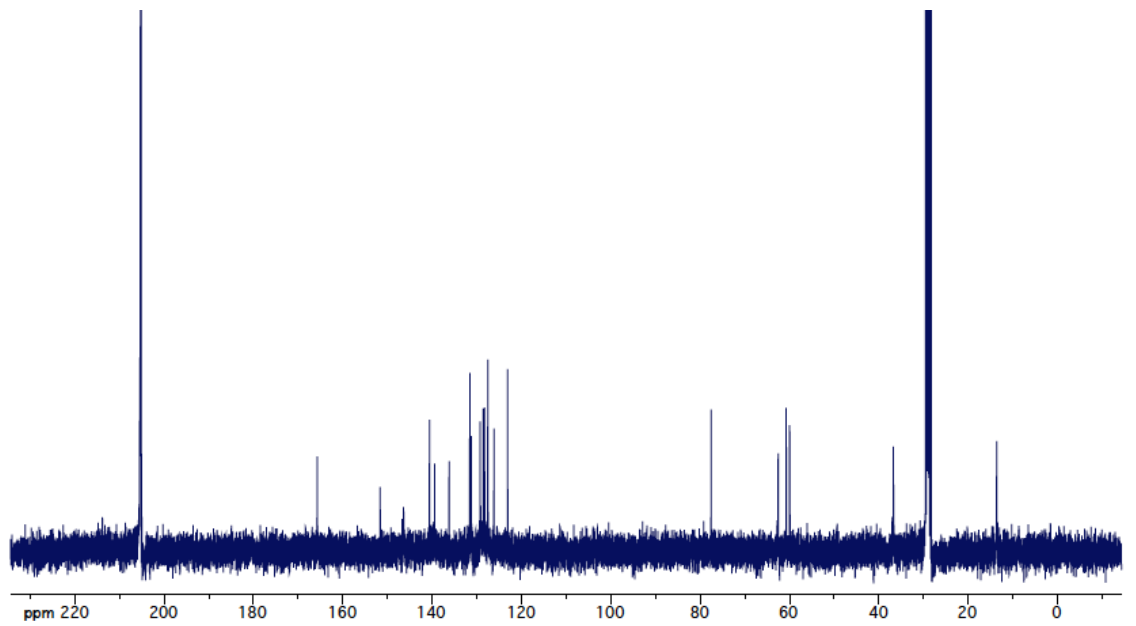
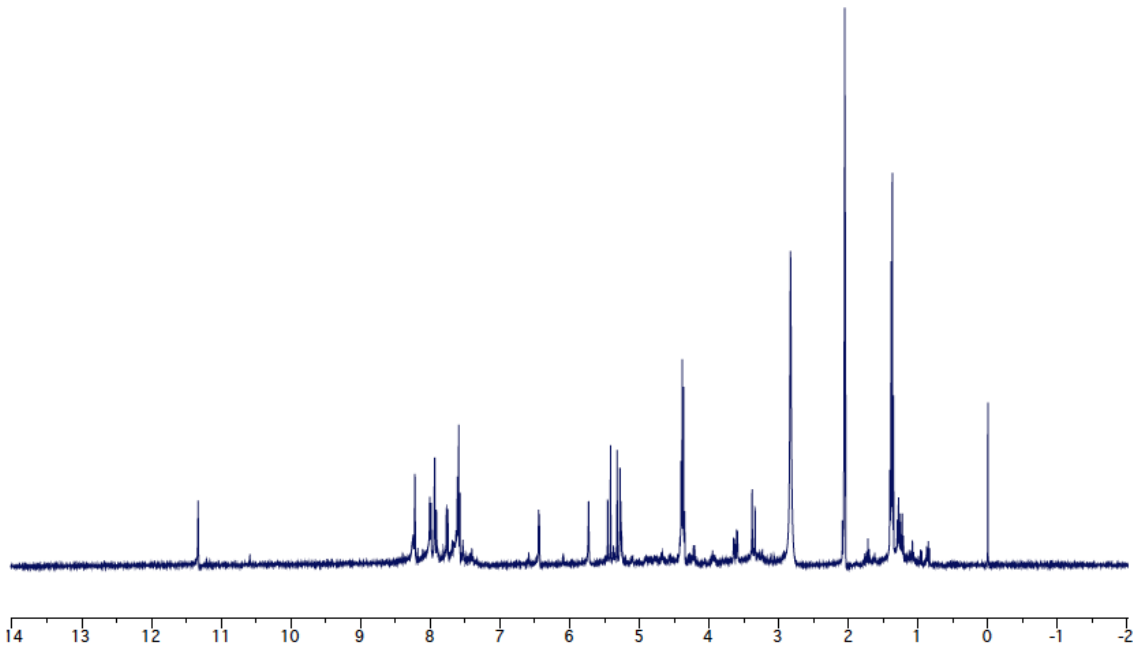
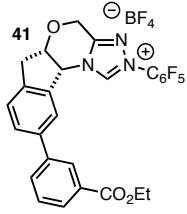


39g



39h



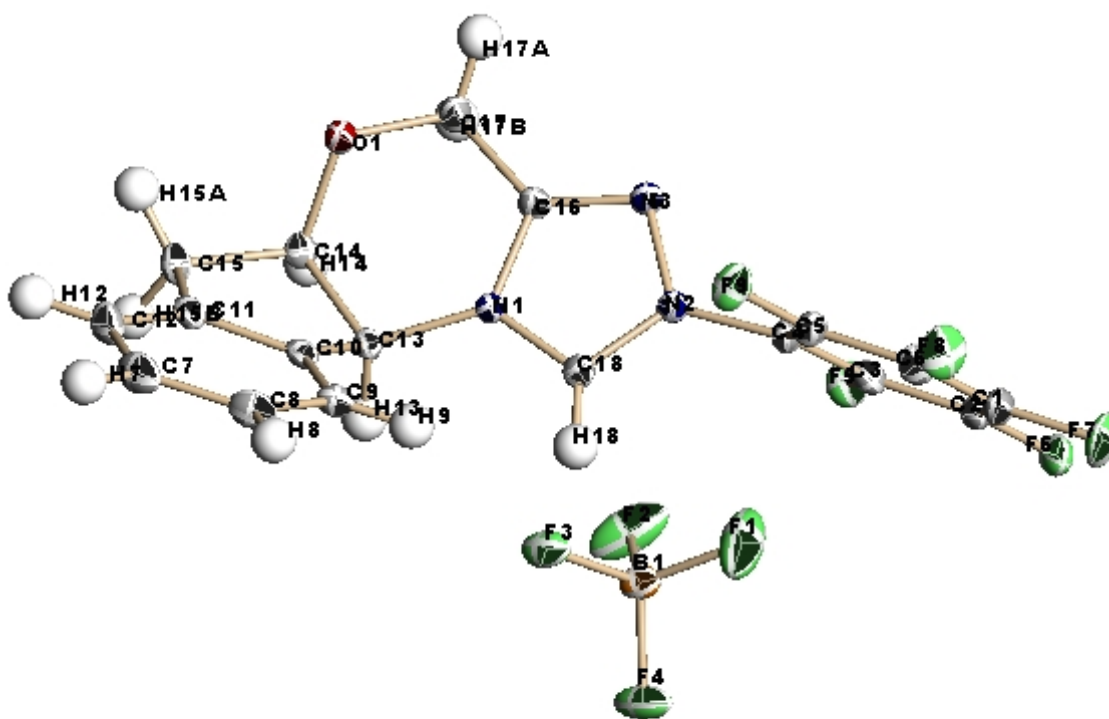


## APPENDIX 5

### X-RAY CRYSTALLOGRAPHY DATA FOR CHAPTER 4

Crystallographic Data for Figure 4.2

X-Ray grade crystals were formed by dissolving the NHC catalyst in minimal Ethyl Acetate and layer with heptane in a 1.5 dram vial. Vial was capped and punctured several times with a syringe needle. The biphasic solution was allowed to evaporate slowly over the course of 3 days until suitable crystals were formed.



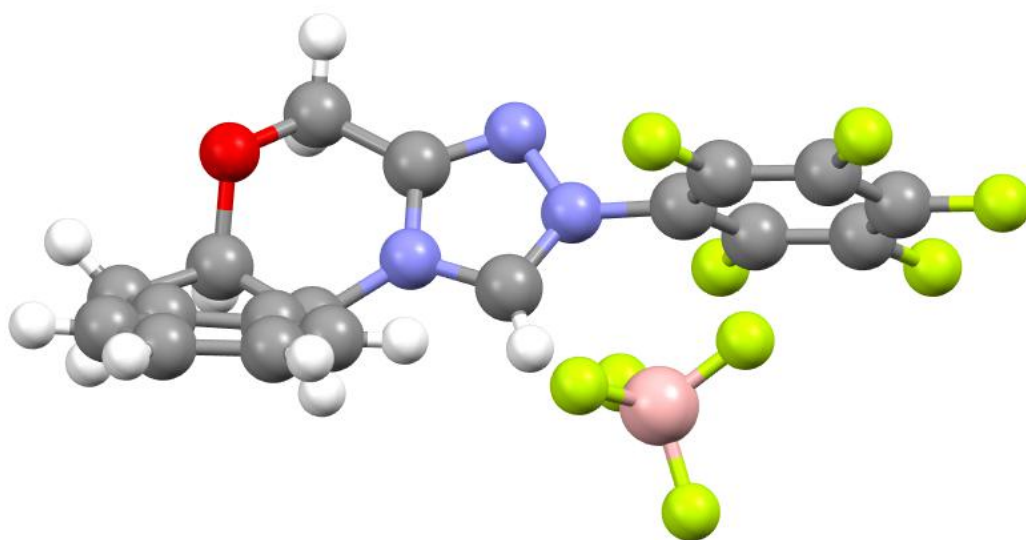


Table 1. Crystal data and structure refinement for Rovi175.

Identification code	Rovi175	
Empirical formula	C <sub>18</sub> H <sub>11</sub> B F <sub>9</sub> N <sub>3</sub> O	
Formula weight	467.11	
Temperature	296(2) K	
Wavelength	0.71073 Å	
Crystal system	Orthorhombic	
Space group	P 21 21 21	
Unit cell dimensions	a = 7.6458(11) Å	a = 90°.
	b = 10.4929(15) Å	b = 90°.
	c = 22.929(3) Å	g = 90°.
Volume	1839.5(5) Å <sup>3</sup>	
Z	4	
Density (calculated)	1.687 Mg/m <sup>3</sup>	
Absorption coefficient	0.169 mm <sup>-1</sup>	
F(000)	936	
Crystal size	0.384 x 0.276 x 0.260 mm <sup>3</sup>	

Theta range for data collection	2.134 to 32.010°.
Index ranges	-9<=h<=10, -13<=k<=14, -34<=l<=23
Reflections collected	27221
Independent reflections	5336 [R(int) = 0.0380]
Completeness to theta = 25.242°	99.9 %
Refinement method	Full-matrix least-squares on F <sup>2</sup>
Data / restraints / parameters	5336 / 0 / 289
Goodness-of-fit on F <sup>2</sup>	1.032
Final R indices [I>2sigma(I)]	R1 = 0.0384, wR2 = 0.0855
R indices (all data)	R1 = 0.0454, wR2 = 0.0897
Absolute structure parameter	0.0(2)
Extinction coefficient	n/a
Largest diff. peak and hole	0.520 and -0.462 e.Å <sup>-3</sup>

Table 2. Atomic coordinates ( $\times 10^4$ ) and equivalent isotropic displacement parameters ( $\text{\AA}^2 \times 10^3$ ) for Rovis175.  $U(\text{eq})$  is defined as one third of the trace of the orthogonalized  $U^{ij}$  tensor.

	x	y	z	$U(\text{eq})$
B(1)	201(3)	4630(2)	8487(1)	19(1)
C(1)	2876(3)	688(2)	9399(1)	24(1)
C(2)	2375(3)	-280(2)	9031(1)	21(1)
C(3)	2565(3)	-128(2)	8439(1)	18(1)
C(4)	3237(3)	1000(2)	8218(1)	16(1)
C(5)	3752(3)	1958(2)	8593(1)	19(1)
C(6)	3578(3)	1803(2)	9184(1)	24(1)
C(7)	2122(3)	6637(2)	5996(1)	26(1)
C(8)	1868(3)	6235(2)	6565(1)	24(1)
C(9)	1886(3)	4944(2)	6704(1)	18(1)
C(10)	2181(2)	4073(2)	6262(1)	15(1)
C(11)	2506(3)	4470(2)	5695(1)	18(1)
C(12)	2464(3)	5757(2)	5558(1)	24(1)
C(13)	2103(2)	2634(2)	6269(1)	14(1)
C(14)	3115(3)	2239(2)	5718(1)	16(1)
C(15)	2819(3)	3349(2)	5299(1)	20(1)
C(16)	4391(3)	1293(2)	6769(1)	16(1)
C(17)	5375(3)	1138(2)	6213(1)	23(1)
C(18)	2257(3)	1958(2)	7311(1)	16(1)
F(1)	1109(3)	4493(2)	9000(1)	62(1)
F(2)	599(3)	3622(2)	8132(1)	53(1)
F(3)	719(2)	5758(1)	8212(1)	28(1)
F(4)	-1581(2)	4653(1)	8600(1)	37(1)
F(5)	2081(2)	-1064(1)	8082(1)	26(1)
F(6)	1699(2)	-1354(1)	9249(1)	29(1)
F(7)	2714(2)	541(2)	9971(1)	36(1)
F(8)	4144(2)	2709(1)	9544(1)	33(1)
F(9)	4439(2)	3026(1)	8382(1)	25(1)
N(1)	2899(2)	2026(2)	6779(1)	13(1)
N(2)	3336(2)	1224(2)	7611(1)	16(1)
N(3)	4715(2)	790(2)	7277(1)	19(1)

O(1)

4954(2)

2186(2)

5843(1)

19(1)

---

Table 3. Bond lengths [ $\text{\AA}$ ] and angles [ $^\circ$ ] for Rovis175.

---

B(1)-F(2)	1.370(3)
B(1)-F(1)	1.375(3)
B(1)-F(4)	1.387(3)
B(1)-F(3)	1.398(3)
C(1)-F(7)	1.327(2)
C(1)-C(2)	1.376(3)
C(1)-C(6)	1.378(3)
C(2)-F(6)	1.336(3)
C(2)-C(3)	1.373(3)
C(3)-F(5)	1.331(3)
C(3)-C(4)	1.386(3)
C(4)-C(5)	1.380(3)
C(4)-N(2)	1.415(2)
C(5)-F(9)	1.329(3)
C(5)-C(6)	1.372(3)
C(6)-F(8)	1.330(3)
C(7)-C(8)	1.384(3)
C(7)-C(12)	1.390(3)
C(8)-C(9)	1.393(3)
C(9)-C(10)	1.383(3)
C(10)-C(11)	1.388(3)
C(10)-C(13)	1.511(3)
C(11)-C(12)	1.387(3)
C(11)-C(15)	1.504(3)
C(13)-N(1)	1.463(2)
C(13)-C(14)	1.538(3)
C(14)-O(1)	1.436(2)
C(14)-C(15)	1.526(3)
C(16)-N(3)	1.302(3)
C(16)-N(1)	1.376(3)
C(16)-C(17)	1.489(3)
C(17)-O(1)	1.426(2)
C(18)-N(1)	1.318(2)
C(18)-N(2)	1.321(3)

N(2)-N(3)	1.381(2)
F(2)-B(1)-F(1)	108.4(2)
F(2)-B(1)-F(4)	110.1(2)
F(1)-B(1)-F(4)	109.74(19)
F(2)-B(1)-F(3)	108.84(18)
F(1)-B(1)-F(3)	109.4(2)
F(4)-B(1)-F(3)	110.36(19)
F(7)-C(1)-C(2)	119.7(2)
F(7)-C(1)-C(6)	119.2(2)
C(2)-C(1)-C(6)	121.11(19)
F(6)-C(2)-C(3)	120.6(2)
F(6)-C(2)-C(1)	120.05(19)
C(3)-C(2)-C(1)	119.4(2)
F(5)-C(3)-C(2)	119.5(2)
F(5)-C(3)-C(4)	120.55(18)
C(2)-C(3)-C(4)	120.0(2)
C(5)-C(4)-C(3)	120.05(18)
C(5)-C(4)-N(2)	118.44(18)
C(3)-C(4)-N(2)	121.44(18)
F(9)-C(5)-C(6)	119.8(2)
F(9)-C(5)-C(4)	120.11(18)
C(6)-C(5)-C(4)	120.1(2)
F(8)-C(6)-C(5)	119.8(2)
F(8)-C(6)-C(1)	120.78(19)
C(5)-C(6)-C(1)	119.4(2)
C(8)-C(7)-C(12)	120.4(2)
C(7)-C(8)-C(9)	120.7(2)
C(10)-C(9)-C(8)	118.46(19)
C(9)-C(10)-C(11)	121.16(19)
C(9)-C(10)-C(13)	130.22(18)
C(11)-C(10)-C(13)	108.49(17)
C(12)-C(11)-C(10)	120.0(2)
C(12)-C(11)-C(15)	128.96(19)
C(10)-C(11)-C(15)	110.99(18)
C(11)-C(12)-C(7)	119.2(2)

N(1)-C(13)-C(10)	115.31(16)
N(1)-C(13)-C(14)	109.21(15)
C(10)-C(13)-C(14)	103.91(16)
O(1)-C(14)-C(15)	107.45(16)
O(1)-C(14)-C(13)	109.85(15)
C(15)-C(14)-C(13)	103.68(16)
C(11)-C(15)-C(14)	103.97(16)
N(3)-C(16)-N(1)	111.70(17)
N(3)-C(16)-C(17)	128.69(18)
N(1)-C(16)-C(17)	119.59(17)
O(1)-C(17)-C(16)	108.15(17)
N(1)-C(18)-N(2)	106.33(17)
C(18)-N(1)-C(16)	107.06(16)
C(18)-N(1)-C(13)	127.48(17)
C(16)-N(1)-C(13)	125.12(16)
C(18)-N(2)-N(3)	112.36(16)
C(18)-N(2)-C(4)	125.17(17)
N(3)-N(2)-C(4)	122.15(16)
C(16)-N(3)-N(2)	102.54(16)
C(17)-O(1)-C(14)	111.66(16)

---

Symmetry transformations used to generate equivalent atoms:

Table 4. Anisotropic displacement parameters ( $\text{\AA}^2 \times 10^3$ ) for Rovis175. The anisotropic displacement factor exponent takes the form:  $-2p^2[ h^2 a^*2U^{11} + \dots + 2 h k a^* b^* U^{12} ]$

	U <sup>11</sup>	U <sup>22</sup>	U <sup>33</sup>	U <sup>23</sup>	U <sup>13</sup>	U <sup>12</sup>
B(1)	18(1)	16(1)	24(1)	-2(1)	4(1)	1(1)
C(1)	22(1)	35(1)	15(1)	6(1)	3(1)	8(1)
C(2)	16(1)	25(1)	23(1)	12(1)	1(1)	2(1)
C(3)	16(1)	20(1)	19(1)	3(1)	-2(1)	2(1)
C(4)	16(1)	19(1)	14(1)	4(1)	1(1)	4(1)
C(5)	20(1)	18(1)	18(1)	2(1)	3(1)	4(1)
C(6)	28(1)	27(1)	16(1)	-3(1)	1(1)	7(1)
C(7)	24(1)	16(1)	38(1)	6(1)	-1(1)	2(1)
C(8)	22(1)	18(1)	32(1)	-5(1)	-1(1)	3(1)
C(9)	16(1)	18(1)	20(1)	-1(1)	0(1)	2(1)
C(10)	12(1)	15(1)	18(1)	2(1)	-3(1)	1(1)
C(11)	15(1)	18(1)	19(1)	2(1)	-3(1)	0(1)
C(12)	25(1)	21(1)	26(1)	9(1)	-2(1)	1(1)
C(13)	14(1)	15(1)	13(1)	2(1)	-2(1)	0(1)
C(14)	19(1)	17(1)	14(1)	-1(1)	-2(1)	0(1)
C(15)	23(1)	22(1)	13(1)	1(1)	-4(1)	0(1)
C(16)	16(1)	17(1)	16(1)	1(1)	1(1)	4(1)
C(17)	24(1)	28(1)	16(1)	5(1)	5(1)	10(1)
C(18)	17(1)	14(1)	17(1)	2(1)	1(1)	2(1)
F(1)	54(1)	96(2)	36(1)	26(1)	-16(1)	-38(1)
F(2)	63(1)	25(1)	70(1)	-20(1)	39(1)	-9(1)
F(3)	21(1)	18(1)	44(1)	7(1)	7(1)	0(1)
F(4)	19(1)	22(1)	68(1)	13(1)	13(1)	3(1)
F(5)	29(1)	22(1)	28(1)	1(1)	-4(1)	-3(1)
F(6)	23(1)	32(1)	32(1)	19(1)	0(1)	-2(1)
F(7)	46(1)	48(1)	15(1)	9(1)	5(1)	4(1)
F(8)	45(1)	34(1)	19(1)	-10(1)	1(1)	6(1)
F(9)	35(1)	16(1)	24(1)	1(1)	5(1)	-2(1)
N(1)	13(1)	14(1)	13(1)	1(1)	0(1)	1(1)
N(2)	17(1)	16(1)	15(1)	2(1)	3(1)	4(1)
N(3)	18(1)	22(1)	17(1)	2(1)	3(1)	6(1)

O(1)      18(1)      24(1)      16(1)      4(1)      3(1)      5(1)

---



## Aza-MBH Yield

